# Wnt signalling and the differentiation of otic progenitors from human embryonic stem cells

Darrell Barrott

Thesis submitted for the degree of Doctor of Philosophy

Department of Biomedical Science

The University of Sheffield

September 2014

**ACKNOWLEDGMENTS**

First and foremost I would like to thank my supervisor, Professor Marcelo Rivolta, for providing me with the opportunity to carry out my PhD in his laboratory. He must be thanked for all the support and encouragement he has given to me over the last four years, and for all the last minute advice and guidance on making sure I actually submitted it on time! It has been an honour to have had the opportunity to work alongside him.

The undertaking of this PhD has been made all the more bearable by the fantastic members of the Rivolta laboratory family. Each member, past and present, has offered me great help in pushing me towards this conclusion, and I cannot thank them enough. I would like to specifically acknowledge Johanna Thurlow for teaching me all there is to know about looking after stem cells, and training me up on most of the techniques I have (hopefully!) now got to grips with. A very special shout out has to go to Sarah Jacob for allowing me to use some of her data, and for generally being my best buddy over these years. And of course, for sharing my love for all things cake! I would also like to thank Paul Gokhale for scanning numerous In Cell plates for me and answering my many inane questions, and Sarah Boddy for helping me with the analysis.

Extra special thanks goes to Adrian for showing such patience with me throughout this PhD, particularly throughout this writing up phase. I know it has not been easy! Your motivation for me to succeed is endless, and you have no doubt helped shape this experience.

I would like to dedicate this thesis to my Mum, who has had to put up with my numerous mood swings and general negative attitude far too many times over these four years! Your love and support has always been there, and you have continuously strived to ensure my happiness in everything I do.

Lastly, I would like to say a big thank you to the bright lights of Las Vegas for providing me with solace during the particularly rough times! Viva Las Vegas!

**CONTENTS**

**FIGURES**

**TABLES**

**ABBREVIATIONS**

AFP: Alpha-fetoprotein

ANOVA: Analysis of variance

APC: Adenomatous polyposis coli

ATOH1: atonal homolog 1

BDNF: Brain-derived neurotrophic factor

BIO: 6-bromoindirubin-3'-oxime

BMP: Bone morphogenetic protein

cDNA: complementary cDNA

DAPI: 4',6-diamidino-2-phenylindole

DFNB: DMEM/F12 with N2 and B27

DLX5: Distal less homeobox 5

DMEM: Dulbecco's Modified Eagle Medium

DMSO: Dimethylsulphoxide

DNA: Deoxyribonucleic acid

dNTP: Deoxyribonucleotide triphosphate

DTT: Dithiothreitol

DVL: Dishevelled

EDTA: Ethylenediaminetetraacetic acid

EGF: Epidermal growth factor

EYA1: Eyes-absent homolog 1

FCS: Fetal calf serum

FGF: Fibroblast growth factor

FOXG1: Forkhead box 1

GFP: Green fluorescent protein

hES: Human embryonic stem

hFASC: Human fetal auditory stem cells

IGF-1: Insulin-like growth factor-1

iPS: Induced pluripotent stem

IWR-1: Inhibitor of Wnt Response-1

LB: Luria Bertani

MEF: Mouse embryonic fibroblast

MEOX1: Mesenchyme homeobox 1

MSC: Mesenchymal stem cell

MYO7A: Myosin VIIa

NEUROG1: Neurogenin-1

NOP: Nasal and otic placode

NT-3: Neurotrophin-3

OEP: Otic epithelial progenitor

OEPD: Otic-epibranchial precursor domain

ONP: Otic neural progenitor

OSCFM: Otic stem cell full medium

PAX: Paired box

PBS: Phosphate buffered saline

PBST: PBS with 0.1% Triton X-100

QPCR: Quantitative Polymerase Chain Reaction

RNA: ribonucleic acid

RPM: Revolutions per minute

Shh: Sonic hedgehog

SIX1: SIX homeobox 1

SOX2: Sex-determining region Y-box 2

SLC17A7: Solute carrier family 17

SSEA: Stage specific embryonic antigen

SYP: Synaptophysin

**ABSTRACT**

Deafness is a major sensory disorder affecting an enormous number of people worldwide. Loss of the auditory hair cells and their associated spiral ganglion neurons in the cochlea causes the vast majority of hearing loss cases. Therapies currently available are unable to address the root cause of the impairment, and as such are limited in their effectiveness. The field of regenerative medicine is emerging as a viable option for restoring and repairing lost or damaged cells in the inner ear.

Human embryonic stem cells have been previously used to generate otic progenitors by employing ligands involved in otic placode induction, FGF 3 and FGF 10. Canonical Wnt signalling is known to play a major role in the expansion of the otic placode. In this work, I have manipulated the canonical Wnt signalling pathway in combination with FGF and explored their effect on otic progenitor differentiation. An initial period of FGF signalling combined with canonical Wnt inhibition was required to promote an ectodermal identity in the differentiating human embryonic stem cells, with a concomitant increase in the expression of otic markers. Following this, a phase of canonical Wnt activation with an attenuated FGF signal further expanded the proportion of otic progenitors, substantially more so than in the standard FGF based protocol. The progenitors derived from this more efficient, developmentally informed protocol also possessed the ability to further differentiate into hair cell-like cells and in particular, auditory neurons. Reporter lines were also generated in order to monitor otic and hair cell differentiation in real time and visualise the effects of manipulating the canonical Wnt signalling pathway with molecular compounds.

This work involved the development of an updated *in vitro* protocol capable of readily and efficiently inducing the differentiation of otic progenitors from human embryonic stem cells. This could be beneficial in the development of potential cell-based therapies for deafness.

# *Chapter 1*

# CHAPTER 1: INTRODUCTION

## *1.1 Anatomy of the human auditory system and its function*

Hearing is one of the five main senses, and can be described as the ability to perceive auditory sound information. In humans this perception of auditory information takes place within the ear. A basic schematic diagram of the anatomy of the human auditory system is shown in Figure 1.1. It is comprised of outer, middle and inner ear structures, all of which play a crucial role in the perception of hearing. Sound pressure waves enter the ear by initially being funnelled through the outer ear and along the external meatus towards the structures of the middle ear. The vibrations produced from the entering sound are transmitted to the ear drum, or tympanic membrane, causing the ossicles of the middle ear (malleus, incus, and stapes) to transfer the acoustic vibrations through to the main organ of the inner ear, the cochlea. The human cochlea is a coiled hollow tube divided into three chambers, referred to as the scala vestibuli, scala media and scala tympani. A cross-section through the chambers of the cochlea is schematically illustrated in Figure 1.2. The chambers of the cochlea are filled with sodium-rich perilymph (scala vestibuli, scala tympani) or potassium-rich endolymph (scala media). The difference in ionic composition of the three chambers generates an electrical and chemical gradient within the cochlea, which aids in the mechanotransduction of the sound waves into electrical energy (Cristobal and Oghalai, 2008; Kim et al., 2011).

Housed in the scala media is the organ of Corti, the main sensory epithelium of the cochlea. Comprised of a single row of inner hair cells and three rows of outer hair cells (Figure 1.2), they are highly specialised epithelial cells and act to convert sound energy into an electrical signal that is then relayed to the brain for hearing perception. Each hair cell responds to a different detection of vibration, setting up a tonotopic gradient from base to apex of the cochlea. The tectorial membrane responds to the pressure variations induced by sound energy in the endolymph of the scala media, and the vibrations are passed into the hair cells where electrical impulses are generated and relayed to the afferent sensory neurons (Wan et al., 2013). The embryological development of sensory hair cells and the various other cell types found within the

organ of Corti will be discussed later in this chapter. In the adult ear there are approximately 15,000 to 20,000 hair cells per cochlea. Once induced and matured, sensory hair cells become post-mitotically inactive and do not replicate, nor repair (Baumgartner and Harper, 2003). As such, damage to the hair cells via a variety of different mechanisms results in permanent, irreversible loss in mammals. Avian species have demonstrated an ability to regenerate damaged or lost hair cells in the basilar papilla (the avian equivalent of the mammalian cochlea).

**Figure 1.1: Schematic diagram of the anatomy of the human auditory system.** The major components of the outer, middle and inner ear are highlighted. Image adapted from Patel and Groppo (2010).

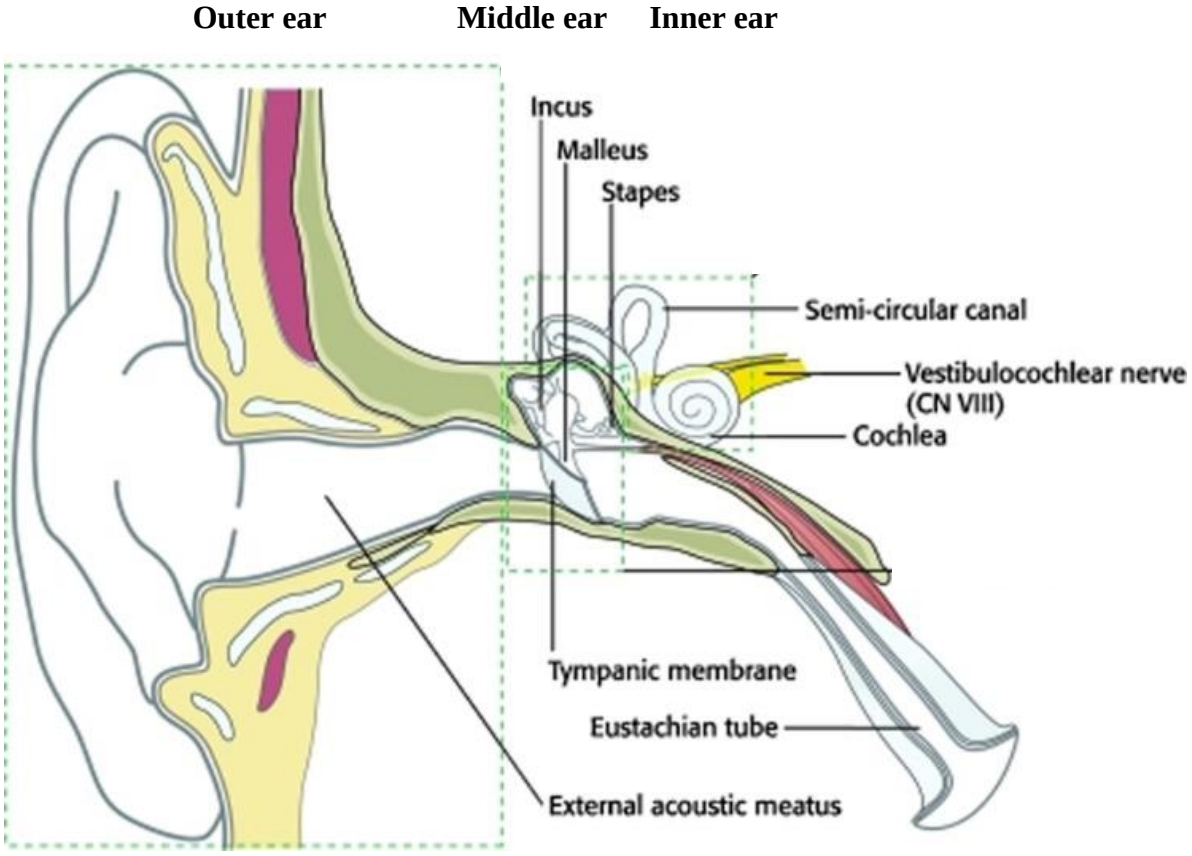

**Figure 1.2: A schematic cross-section through the human cochlea.** The three main chambers (scala vestibuli, scala media, and scala tympani) are highlighted. SV: stria vascularis; IHC: inner hair cells; OHC: outer hair cells; AN: auditory nerve; BM: basilar membrane. Image adapted from Cristobal and Oghalai (2008).

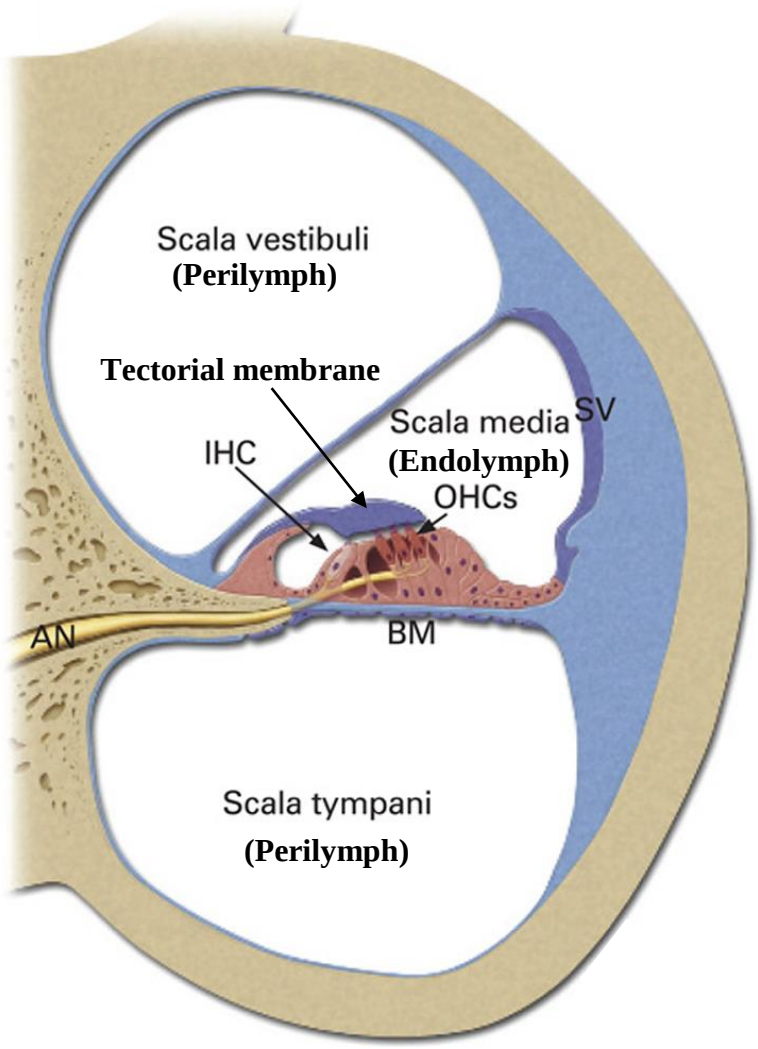

## *1.2 Deafness and hearing impairment*

Hearing impairment of some form currently affects over 10 million people in the UK alone, which is approximately one in six of the UK population (Action on Hearing Loss, 2014). Worldwide this figure is believed to be over 300 million people affected. As the population ages this figure is expected to rise substantially in the coming years. Hearing impairment can be as a result of a number of factors, and defects in any part of the auditory system can be responsible. Obstructions to the external meatus or middle ear, such as from infections or cerumen build-up, or perforation of the tympanic membrane are known as causes of conductive hearing loss. These cases are quite usually mild, easily treatable, and reversible.

Accounting for the vast majority of the cases of deafness or hearing impairment is sensorineural hearing loss (SNHL). SNHL is produced primarily by the damage to and subsequent loss of the sensory hair cells of the organ of Corti, usually with consequent degeneration of the spiral ganglion neurons. Common causes of SNHL include noise-induced trauma, use of ototoxic drugs, aging, and genetic disorders.

### *1.2.1 Noise-induced hearing loss*

Noise-induced hearing loss occurs as a result of prolonged and repeated expose to high intensity sound. Emerging in recent years is the implication of reactive oxygen species as a causal factor in noise-induced hearing loss. One of the first studies to report this was carried out in guinea pigs. Prolonged exposure (three hours) to sound of 120 decibels (dB) resulted in the presence of reactive oxygen species, detectable after just five minutes following noise exposure (Yamane et al., 1995). In mice, reactive oxygen species are detectable after just 1 hour of intense noise, and this level was found to be at least four-fold above the non-exposed animals (Ohlemiller et al., 1999). This early appearance of reactive oxygen species was shown to remain within the cells of the organ of Corti for a number of hours after noise exposure, without decline. Similarly a study conducted by Hu et al. (2002) in the chinchilla reported that the three rows of outer hair cells in the organ of Corti are particularly susceptible to reactive oxygen

species damage, via the induction of apoptotic pathways. Following one hour of 110 dB noise, the nuclei of the outer hair cells was found to be morphologically typical of cells undergoing apoptosis (condensed, fragmented nuclei) and caspase-3, a marker of apoptosis, was detected. Interestingly the induction of the apoptotic pathways remained in the outer hair cells for up to three days following the one hour noise exposure period.

As a result of these findings the administration of anti-oxidant compounds has been extensively tested as a potential preventative therapy for noise-induced hearing loss. Anti-oxidants such as glutathione (Ohinata et al., 2000), ascorbic acid (Heinrich et al., 2008), and N-acetylcysteine (Kopke et al., 2007) have been demonstrated to reduce the severity of noise-induced hearing loss as a result of reactive oxygen species significantly when administered prior to noise exposure.

### *1.2.2 Exposure to ototoxic drugs*

Aminoglycosides (for example neomycin, gentamicin, streptomycin) are a group of antibiotics, commonly used primarily in developing countries. They are also often used in the treatment of chronic pulmonary infections of cystic fibrosis patients (Davies et al., 2007), and in some cases of difficult to treat urinary tract infections (Greer et al., 2008). Ototoxicity of these type of antibiotics is believed to be a result of induced apoptosis, particularly in the outer hair cells. Suzuki et al. (2008) investigated the time course of apoptosis in the guinea pig induced by administration of intratympanic gentamicin. As in noise-induced hearing loss it was found that reactive oxygen species are the cause of the increase in apoptosis. Evidence of outer hair cell apoptosis was apparent at just 12 hours post-administration, with the severity increasing until 48 hours. Cisplatin, a commonly used chemotherapeutic in various forms of cancer has also previously been shown to have ototoxic side effects. As with the aminoglycosides reactive oxygen species-induced apoptosis is believed to be the major cause of hair cell damage (Dehne et al., 2001).

### *1.2.3 Aging and congenital causes of sensorineural hearing loss*

Throughout the years of life, genetic predispositions and various environmental causes (including smoking, exposure to loud noises, and administration of ototoxic drugs) all contribute to age related SNHL. SNHL is the major sensory disorder reported in the elderly (Fujimoto and Yamasoba, 2014), and is thought to affect over half of the over 65 year old population in the United States (Gopinath et al., 2009). Once again oxidative stress and mitochondrial dysfunction have been implicated as causative factors. A study carried out in the senescence-accelerated mouse prone 8 (SAMP8) model (Menardo et al., 2012) demonstrated that these mice have deficient levels of antioxidants, increased production of reactive oxygen species and resulting apoptosis in the hair cells of the organ of Corti.

Approximately 50% of all congenital cases of hearing loss are of a genetic cause, and mutations in a large number of different genes have already been identified (Duman and Tekin, 2012). Mutations in the *GJB2* gene are considered to be the major genetic dysfunction associated with SNHL. *GJB2* encodes for connexin 26, a component of gap junctions which play a role in connecting all of the different cell types together in the organ of Corti (Kikuchi et al., 2000). Mutations in this gene result in inefficient potassium ion cycling within the endolymph; a requirement for effective sensory transduction. Mutations in genes associated with cellular organisation (*MYO3A*, *MYO6*, *MYO15A*) and neuronal transmission (*OTOF*) have also been identified. Another of the major genetic causes is Usher syndrome (Reiners et al., 2006) which is also known to be the most frequent cause of combined deafness and blindness. This is caused in part by mutations in a number of key markers found in the hair cells of the inner ear and the retina, for example *MYO7A*.

The tectorial membrane (Figure 1.2) has connected attachments to the distal tips of the outer hair cells in the normal inner ear. Vibrational movements of the tectorial membrane as a result of sound induced pressure waves cause displacement of the outer hair cell tips, generating the mechanoreceptor-induced electrical signals. Genetic defects within the tectorial membrane, therefore, may also lead to cases of deafness. One of the major protein components of the tectorial membrane is α-tectorin, encoded by the *TECTA* gene (Alasti et al., 2008). Various mouse knockout studies (Legan et

al., 2000; Legan et al., 2005; Xia et al., 2010) have demonstrated that disruption to the α-tectorin protein results in a shortened tectorial membrane that becomes detached from the underlying outer hair cells of the organ of Corti, resulting in a decreased ability of the outer hair cells to act as cochlear amplifiers.

In addition, it is not just the hair cells of the organ of Corti which are responsible for cases of hearing loss when damaged; supporting cells are also gradually being implicated. Damage to the organ of Corti during noise-induced trauma or as a result of ototoxicity from aminoglycoside drugs, leads to degeneration and loss of the various types of supporting cells, with broad implications to hearing. For example, supporting cells are sources of neurotrophic factors which aid in spiral ganglion neuron survival and growth, and as such, damage to these cell types can potentially lead to neuronal death and receding.

The stria vascularis (Figure 1.2) is another contributor to age-related hearing loss cases. The endolymph potential within the cochlea is generated as a result of potassium ion release from the hair cells of the organ of Corti (Hibino and Kurachi, 2006). Potassium ions are circulated from the hair cells, via the perilymph, to the endolymph of the scala media through the stria vascularis. The *KCNJ10* gene encodes for an inward rectifier potassium channel known as Kir4.1 (Chen and Zhao, 2014) and is the only potassium inward rectifier channel found within the stria vascularis. Human mutations within the *KCNJ10* gene therefore lead to disruption to the endolymph potential within the cochlea and hearing loss ensues. Patients with mutations within this gene can suffer from EAST syndrome (Thompson et al., 2011), involving epilepsy, ataxia, sensorineural deafness and renal tubulopathy. Further evidence of the importance of the Kir4.1 channel in normal hearing was demonstrated by a *KCNJ10* knockout mouse model (Kofuji et al., 2000). Homozygous knockout mice experienced a loss of endolymphatic potassium ions, and a consequent loss of the endolymph potential, with later degeneration of the spiral ganglion neurons. These effects could be rescued by co-expression of wild type *KCNJ10* (Sala-Rabanal et al., 2010).

### *1.3 Currently available treatments for sensorineural hearing loss*

The therapeutic options currently available for sensorineural hearing loss are very limited, circumscribed to prosthetic devices such as hearing aids and cochlear implants. Hearing aids act by amplifying acoustic signals to make sounds louder and clearer for the wearer. As such they are only suitable for mild hearing impairment and require some degree of functionality in the hair cells and neurons in the inner ear, and intact auditory pathways to the brain. For the more profoundly deaf, as a result of damage or permanent loss of the sensory hair cells, hearing aids are inadequate. Loss of the inner or outer hair cells results in no mechanotransduction of sound pressure waves emanating from the tectorial membrane, and thus the spiral ganglion neurons do not receive any electrical signals to relay to the brain. Cochlear implantations are a potential therapy for patients with this kind of profound hearing loss. Cochlear implants act by providing electrical stimulation to the spiral ganglion neurons, in place of the lost or damaged hair cells. This artificial stimulation therefore can only be beneficial to the patient if spiral ganglion neurons are intact and at a suitable density for relaying the sound information to the higher auditory processes (Lenarz et al., 2013). Unfortunately loss of sensory hair cells on cases of SNHL can sometimes be associated with subsequent receding or loss of the spiral ganglion neurons (Otte et al., 1978; Webster and Webster, 1981), making cochlear implantation an ineffective therapeutic option. In these patients the only viable alternative is the use of the brain stem implant, where an electrode is inserted close to the cochlear nucleus and stimulates the central pathway directly. However this technology is still in its early days and the clinical results thus far are not very satisfactory (Merkus et al., 2014).

Given the current limitations, research is actively looking for new therapeutic alternatives using different systems.

## *1.4 Potential future therapies for hearing impairment*

### *1.4.1 Gene therapy*

Studies investigating potential gene therapy treatments for deafness and hearing impairment are a major source of current research. The connexin 26 (Cx26) encoding gene *GJB2*, accounting for approximately half of all cases of congenital and inherited deafness, is a common target for a possible gene therapeutic strategy. A proof of principle study carried out by Crispino et al. (2011) used bovine adeno-associated viral vectors to successfully deliver recombinant Cx26 protein to *in vitro* explants sourced from Cx26 knockout mice. In a more advanced recent study, adeno-associated viral vectors were utilised for the delivery of Cx26 protein directly to the scala media of conditional *Gjb2* knockout mice *in vivo* (Yu et al., 2014). It was observed that intercellular gap junctions were restored in the supporting cells of the knockout mice, leading to significantly lower levels of cell death within the organ of Corti and a reduction in the loss of associated spiral ganglion neurons.

Transmembrane channel-like proteins 1 and 2 (*TMC1, TMC2*), expressed in both inner and outer hair cells, are known to play a crucial role in normal functional maturation of the hair cells, although the exact method of this functionality is still unknown (Marcotti et al., 2006). Kawashima et al. (2011) reported murine *Tmc1* and *Tmc2* gene expression is associated with mechanotransduction of the hair cells, and targeted deletion of these genes caused a deaf phenotype in the knockout mice. Adenoviral delivery of exogenous TMC proteins were found to be able to restore hair cell mechanotransduction and normal levels of electrophysiology.

For noise- or age-related hearing loss, gene therapy with *ATOH1* (a basic helix-loop-helix transcription factor, crucial and necessary for hair cell induction in the developing organ of Corti) is a promising therapeutic target. Yang et al. (2012) exposed guinea pigs to excessive noise in order to cause trauma to the hair cells of the organ of Corti. One week after noise-induced hearing loss was confirmed, adenoviral vectors were used to deliver an *Atoh1-GFP* (green fluorescent protein) construct to the cochlea. Interestingly *Atoh1* gene-driven GFP expression was not found in any of the hair cells of the damaged organ of Corti, but was found in the supporting cells. Despite this the stereocilia of the hair cells appeared restored, compared to the untreated noise-

damaged cochleae, and great improvements in hearing thresholds were achieved. It is hypothesised that over-expression of *Atoh1* in the supporting cells may have resulted in secretion of trophic factors which induced repair of the hair cells and stereocilia.

Other recent studies involving adenoviral vector delivery of *Atoh1* as a possible therapeutic target include that by Atkinson et al. (2014). In this study viral vectors were used to infect mature guinea pigs with aminoglycoside-damaged cochleae with vectors containing either the *Atoh1* gene alone, or *Atoh1* in combination with neurotrophic factors such as BDNF (brain-derived neurotrophic factor) or NT-3 (neurotrophic factor-3) four days post-deafening. Functional hearing tests were conducted in the animals three weeks post viral infection. It was observed that in the organ of Corti of aminoglycoside treated animals, a significant increase in the number of hair cells was seen following Atoh1 gene therapy, marked by an increase in the number of cells expressing myosinVIIa (a characteristic marker of hair cells). Unfortunately, but interestingly, hearing function in the deafened animals was not recovered following *Atoh1* or *Atoh1* with neurotrophic factor gene therapy.

Lack of recovery of functional hearing with *Atoh1* gene therapy in the guinea pig study highlights the potential pitfalls and limitations of gene therapy within the inner ear. When using a viral vector delivery method it is difficult to be able to target the exact cell type of interest. All of the cells exposed to the viral vectors will have the potential for uptake of the vector, however the rate of uptake will be different between cell types, and not all cells will uptake the vector equally (Chien et al., 2015). Therefore it is possible for viral vector delivery to the organ of Corti to be scattered and lacking a uniform pattern, which has the potential to lead to disorganised gene delivery and a limited functional effect as a consequence. In addition the route of administration of gene therapy may also been a limiting factor for the inner ear. According to Kawamoto et al. (2001) and Praetorius et al. (2003), a cochleostomy approach for gene delivery (a commonly used method of gaining access to the scala media) can itself be associated with a higher incidence of sensorineural hearing loss. Therefore, for gene delivery as a potential future therapy for deafness, methods of minimising the potential damage of the surgical approach must also be investigated simultaneously.

### *1.4.2 Neurotrophic factors*

Neurotrophic factors including BDNF and NT-3 have been previously shown to be expressed in the organ of Corti during development (Pirvola et al., 1994; Wheeler et al., 1994), and also expression the BDNF and NT-3 receptors have been identified in the spiral ganglion neurons (Ernfors et al., 1992; Pirvola et al., 1992). Spiral ganglion neuron loss can be as a result of direct damage to the cells or synapses, or secondary to the loss of support provided by neurotrophic factors, such as BDNF and NT-3. Current opinion on the source of release of these neurotrophic factors is divided; hair cells (Ernfors et al., 1995) or the supporting cells (Zilberstein et al., 2012) of the organ of Corti. Irrespective of the source, spiral ganglion loss as a result of hair cell damage can dramatically reduce the effectiveness and suitability for cochlear implantation, and many studies have been carried out to determine if gene delivery of neurotrophic factors can improve the survivability of the spiral ganglion neurons following hair cell injury. For example, Wise et al. (2010) delivered BDNF or NT-3 in adenoviral vectors to the scala media of guinea pig cochleae damaged by aminoglycoside administration. Spiral ganglion neuron densities were found to be significantly increased with viral vector delivery of the neurotrophic factors compared to untreated damaged cochleae, especially within the basal turn. Connexin 26 null mice (as a result of *Gjb2* gene mutations) have rapid hearing loss throughout the first weeks of life due to the loss of non-sensory cells in the organ of Corti. Loss of the spiral ganglion neurons quickly follows leading to severe hearing impairments. Adenoviral vector delivery of the BDNF gene into the scala media of these connexin 26 deficient mice was able to rescue the spiral ganglion neurons, particularly in the basal turn of the cochleae (Takada et al., 2014).

### *1.4.3 Cell based therapies*

Studies to generate inner ear cell types from stem cell populations for potential transplantation as a treatment for deafness and hearing impairment are becoming a major research focus. Reports have been published on the ability to generate hair cells

*in vitro* from murine embryonic stem cells (Koehler et al., 2013; Li et al., 2003; Oshima et al., 2010). Although providing essential evidence of the ability of *in vitro* derivation of hair cell-like cells, these studies all focus on differentiation of embryonic stem cells via an embryoid body process. As such it can be difficult to efficiently control the differentiation process. Attempts to generate functional otic progenitors from human embryonic stem (hES) cells has also proven promising (Chen et al., 2012). Once derived, otic neural-like progenitors have been shown to have the ability to restore auditory function to deafened gerbils by recolonizing the areas of lost spiral ganglion neurons initially destroyed by oubain treatment.

Bone marrow-derived mesenchymal stem cells (MSCs) are another potential source of a cellular based therapy for deafness. Benefits of the use of bone marrow-derived MSCs over hES cells currently include the ease of accessibility for harvesting of such cells, elimination of potential ethical issues surrounding embryonic stem cells, and the ability to create patient-specific therapeutics. MSCs have also already been used in a number of clinical trials for various purposes, including neuronal and cardiac regeneration (reviewed in Trounson et al., 2011). A study carried out Boddy et al. (2012) demonstrated how conditioned media from the culturing of human fetal auditory stem cells (hFASCs) (Chen et al., 2007; Chen et al., 2009) was able to induce the expression of key otic markers such as *PAX2*, *PAX8*, *GATA3* and *SOX2* in human bone marrow-derived MSCs. Not only were markers of the otic placode induced, but sustained culturing of the MSCs in this conditioned media was able to induce markers of the more mature hair cell and auditory neuronal lineages. Canonical Wnt signalling ligands were identified as a component of the hFASC conditioned media, and the inductive role of this on the otic progenitor markers was confirmed by inhibitors of Wnt signalling leading to a reduction in otic marker expression in the MSCs. A complimentary study by Duran-Alonso et al. (2012) has also demonstrated the ability of this cell type to respond to factor such as retinoic acid and epidermal growth factor (EGF) for the induction of hair cell-like markers.

## *1.5 Human pluripotent stem cells*

First derived in 1998 from human blastocysts (Thomson et al., 1998), hES cells have changed the landscape of research into cellular differentiation and disease modelling. *In vitro* they have the capacity to self-renew and be expanded indefinitely, and have the ability to differentiate into the cell types of all three germ layer lineages (pluripotency) if provided with the correct molecular cues. If injected into a mouse the hES cells differentiate and form a teratoma, and will also contribute to a chimeric animal. Gene markers of hES cells include the transcription factors *POU5F1*, *NANOG*, and *SOX2*. hES cells may also be identified by the expression of cell surface markers such as stage-specific embryonic antigen 3 (SSEA3), TRA-1-60 and TRA-1-81 (Schopperle and DeWolf, 2007).

More recent emerging research is being carried out using what has been referred to as human induced pluripotent stem cells (hIPS). The discovery that terminally differentiated fibroblast cells could be reprogrammed back to a stem cell-like state (Takahashi et al., 2007) via viral vector delivery of just four transcription factors (POU5F1, SOX2, KLF-4 and c-MYC), and the resulting hIPS cells having the ability to differentiate into any of the germ layer lineages, dramatically improved the prospect of using human stem cells in a regenerative capacity. It allows for the derivation of patient-specific therapies, rather than having to tackle the difficult challenge of ethical approval of the use of embryonic stem cells, and also potential issues with immune rejection.

Studies have been conducted to highlight the benefits of using hES and hIPS cells as a method of exploring cell-based therapies for many diseases, for example the *in vitro* modelling of spinal muscular atrophy (Ebert et al., 2009), and the therapeutic drug testing for Rett syndrome (Marchetto et al., 2010). To further the development of a potential cell-based therapy for deafness using hES or hIPS cells and to efficiently direct their differentiation towards the otic lineage using developmental cues, it is important to understand the events in which the otic placode and inner ear are derived *in vivo*.

## *1.6 Induction of the otic placode and development of the inner ear*

### *1.6.1 Early embryological development*

One of the earliest commitment decisions that must take place in the developing embryo is germ layer lineage commitment. Endoderm, mesoderm, and ectoderm are the three germ layers and cell types emanating from these lineages go on to differentiate further into cells and tissue types such as the gastrointestinal respiratory tract (endoderm), circulatory system and musculature (mesoderm), and the central and peripheral nervous system and skin (ectoderm). This acquisition of the three germ layers in mammals takes place via a process known as gastrulation, and the formation of the primitive streak. Cells in the epiblast layer of the early developing embryo undergo an epithelial to mesenchymal transition and ingress through the primitive streak to form the precursors of mesoderm and endoderm (Williams et al., 2012). It is known that cells which do not undergo ingression through the primitive streak adopt an ectodermal fate (Quinlan et al., 1995; Tam et al., 1997), which later becomes subdivided into neural and non-neural ectoderm.

### *1.6.2 The pre-placodal region develops in the ectoderm*

All of the craniofacial placodes (including the ear, eye and olfactory system) initially arise from a horse shoe-shaped region of the ectoderm, commonly referred to as the pre-placodal region (PPR), and is schematically illustrated in Figure 1.3. Following on from the events of gastrulation the ectoderm is segregated into the neural ectoderm and non-neural ectoderm. Fibroblast growth factor (FGF) signalling has been demonstrated to be crucial for the initiation of neural ectoderm, whereas bone morphogenetic protein (BMP) and Wnt signalling have been implicated in promoting non-neural ectoderm differentiation (Levine and Brivanlou, 2007; Rogers et al., 2009). Precursors which will later form cells of each distinct placode region and the neural

crest are initially intermingled throughout a region between the neural and non-neural ectoderm, referred to as the neural border region. Studies in the chick, mouse and *Xenopus* have highlighted a number of transcription factors marking this border region, including members of the Dlx, Pax, and FoxI families (Hong and Saint-Jeannet, 2007; Yang et al., 1998).

Members of the Six (1 and 4), Eya (1 and 2), Dlx and Dach transcription factor families are believed to be the key characteristic markers of the PPR, and remain present within the placodes after their induction (Brugmann and Moody, 2005). Six1 has been shown to be the master regulator of the induction of the PPR, as deletion of this transcription factor results in the downregulation of other PPR-associated transcription factors such as Eya1 (Brugmann et al., 2004). Defects in the inner ear and the olfactory system are an additional consequence of deletion of Six1 in the mouse, emphasising the key regulatory role of the Six family members in sensory organ development (Zheng et al., 2003; Zou et al., 2004). In humans mutations in the *EYA1* gene lead to the onset of Branchio-Oto-Renal Syndrome, where the mutation inhibits the ability of EYA1 to complex with SIX1, resulting in symptoms such as renal disease and hearing loss (Kumar et al., 1997).

The signalling pathways involved in PPR induction include the concerted combination of FGF, BMP and Wnt activity, and the mode of interaction of these three pathways was elegantly demonstrated by Litsiou et al. (2005). In this study the role of head mesoderm in supplying some of the PPR inductive factors to naïve ectoderm was highlighted, as ablation of the underlying mesoderm caused a loss of expression of *Six4* and *Eya2* in chick studies. Markers associated with other regions of the ectoderm, including *Sox3* and *Pax7*, were unaffected by the mesoderm ablation. This study also reported that an attenuation of both the Wnt and BMP signalling pathways is required for PPR marker expression, and alongside active FGF signalling, this combination can promote PPR identity in naïve ectoderm, at least in the chick.

Prior to segregation and specification of each placode, evidence suggests that all PPR precursors are initially specified as lens, with FGF signalling acting repressively to promote the switch from lens to other placodal fates (Bailey et al., 2006). Additionally it has been proposed by Martin and Groves (2006) that all precursors of the various placodes must adopt a pre-placodal fate as an initial step in placode induction.

**Figure 1.3: Schematic diagram of the pre-placodal region (PPR) of the developing ectoderm.** The horse shoe-shaped PPR is subsequently molecularly divided into regions which will go on to form each of the craniofacial placodes. Image adapted from Cvekl and Duncan (2007).

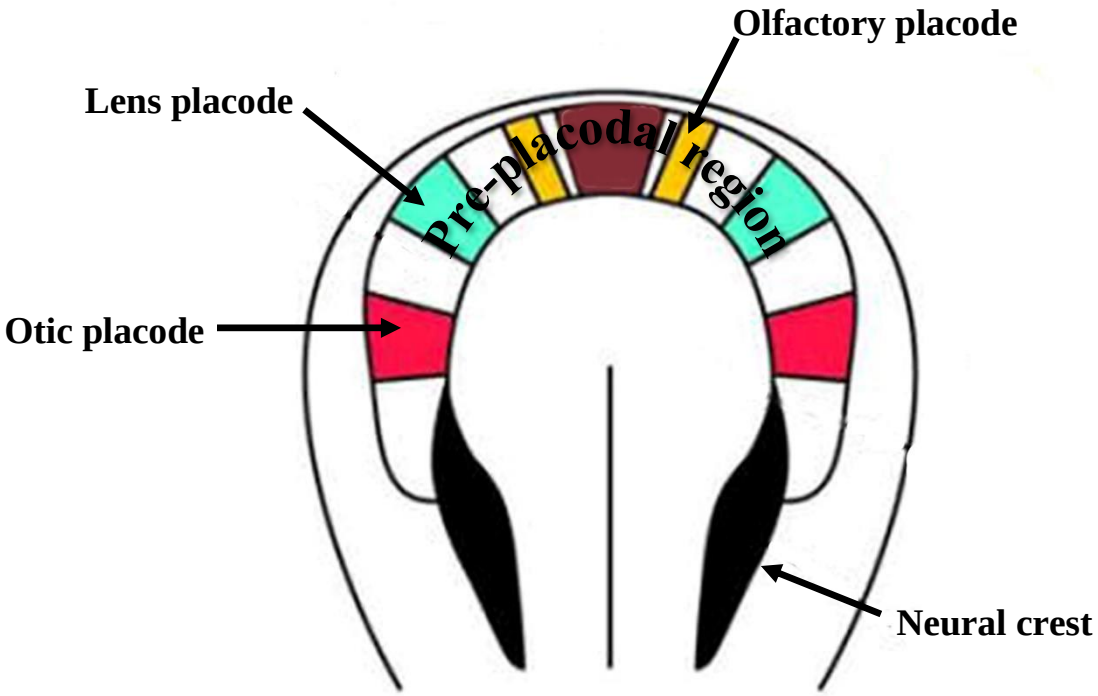

### *1.6.3 Induction of the otic placode*

The exquisite structures of the auditory and vestibular systems of the human ear, as shown schematically in Figures 1.1 and 1.2, all arise from the cells in a simple patch of thickened surface ectoderm known as the otic placode. Many key studies have been conducted to ascertain the events taking place in the developing embryo to induce the otic placode from the pre-placodal region.

Proceeding the induction of the PPR is the formation of a common region containing the precursors of both the otic and the epibranchial placodal cells, referred to as the otic-epibranchial precursor domain (OEPD). FGF signalling is one of the major promoters of the OEPD identity. Previously it was believed that the induction of the otic and epibranchial placodes were separate distinguishable events. More recent evidence however has suggested that these two placodes as part of the OEPD region both arise from a Pax2-positive region of the non-neural ectoderm (Streit, 2002; Sun et al., 2007). Studies have revealed the underlying mesoderm and hindbrain as sources of FGF signalling for OEPD induction (Freter et al., 2008; Liu et al., 2003; Wright and Mansour, 2003). The inductive FGF ligands appear to be species-dependent, with FGF 3 and FGF 8 common to all species, with FGF 10 and FGF 19 specific to the mouse and chick, respectively. Evidence from knockout mutant mice of various FGF ligands strengthens the roles of FGFs in OEPD formation. Ablation of FGFs leads to the loss of Pax2 expression with subsequently small or even a complete failure in the formation of otic vesicles (Alvarez et al., 2003; Wright and Mansour, 2003). The importance of Pax2 expression has also been shown in knockout studies (Sehgal et al., 2008; Torres et al., 1996), with consequent defective generation of inner ear structures. Loss of Pax8 appears to have little effect on the morphology of the structures of the mature inner ear, yet Pax8 deficient mice have profound hearing loss (Christ et al., 2004). Double mutant mice for both Pax2 and Pax8 (Bouchard et al., 2010) have severe early morphological defects, and the inner ear development is halted at the otocyst stage.

After the OEPD region is induced it is required to be segregated into the otic and epibranchial placodal regions, and canonical Wnt signalling is a crucial mediator of this segregation. Indeed a number of Wnt ligands are expressed in the hindbrain region

surrounding the OEPD (Ohyama et al., 2006; Park and Saint-Jeannet, 2008). Freter et al. (2008) have demonstrated that canonical Wnt signalling has little or no effect on the induction of the OEPD region in studies in the chick, but instead functions to enhance the otic placode development following FGF signalling. Intriguingly, it was found that unless Fgf 3 and Fgf 19 signalling is attenuated the presence of canonical Wnt signalling does not allow the otic placode to differentiate, causing an expansion instead of the epibranchial placode, as demarcated by an widening of epibranchial associated *Foxi2* expression. Adding further evidence of a synergistic role of FGF and canonical Wnt signalling, Urness et al. (2010) reported expression of Wnt 8a in the mouse is dependent on FGF signalling, due to a reduction in its expression in the Fgf 3/Fgf 10 knockout mouse. Complementing this was the finding that loss of the FGF antagonists *Sprouty1* and *Sprouty2* in the mouse leads to an increase in Wnt 8a expression and consequently, an increase in the size of the otic placode region at the expense of the *Foxi2*-positive epibranchial placode.

A diagrammatical summary of the interaction of the FGF and canonical Wnt pathways can be seen in Figure 1.4. It must be noted however that the FGF and canonical Wnt signalling pathways are not the only pathways implicated in otic placode development. Nevertheless the main focus of this work is to investigate whether the links between FGF and canonical Wnt signalling on the *in vivo* induction of the otic placode can be utilised *in vitro* during hES cell differentiation.

**Figure 1.4: Schematic of the otic-epibranchial precursor domain (OEPD) and signalling pathways associated.** The inductive effect of FGFs emanating from the neural tube and mesoderm on canonical Wnt signalling aids in the expansion of the otic partition of the OEPD, at the expense of the epibranchial placode. Image adapted from Chen and Streit (2013).

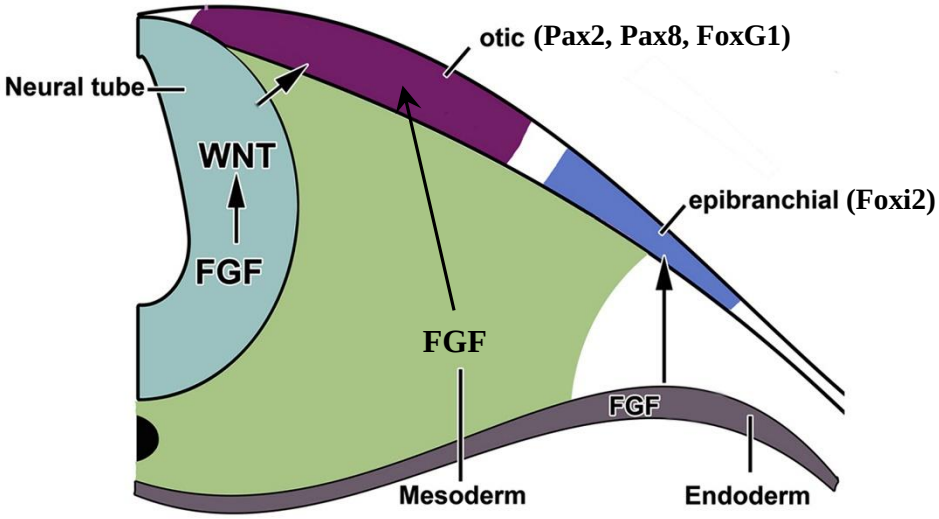

## *1.7 The canonical Wnt signalling pathway*

In basic terms Wnt signalling can be divided into two broad pathways: canonical and non-canonical. Arguably the canonical Wnt signalling pathway is the most established and understood aspect of Wnt signalling, and is the pathway investigated as part of this work. Therefore the mechanisms and modes of action of the canonical Wnt signalling pathway will be the main focus.

The members of the canonical Wnt signalling pathway play a major role in a number of essential processes during development of the embryo. These processes include cell differentiation, cell fate determination and cell proliferation (Macdonald et al., 2009). β-catenin and its regulation is the main method of action of the canonical Wnt signalling pathway. If β-catenin is translocated to the nucleus it will activate the transcription of a number of Wnt target genes. However in the absence of any Wnt signalling, or if Wnt signalling is inhibited, β-catenin is flagged for proteasomal degradation, preventing Wnt target gene expression. A basic schematic representation of canonical Wnt signalling is presented in Figure 1.5.

For Wnt signalling to function secreted Wnt ligands must act through extracellular receptors on the target cell surface. There are 19 members of the Wnt family and 10 of its Frizzled receptors in the human genome. Alongside the Frizzled receptors canonical Wnt signalling also requires the presence of low-density-lipoprotein related protein receptors, or LRPs, in particular LRP5 and LRP6 in order to be able to transduce Wnt signals (He et al., 2004; Tamai et al., 2000). The major activity of the LRP5/6 co-receptor transmembrane protein receptors is to bind Axin (Liu et al., 2003), which is part of the β-catenin degradation complex. This degradation complex is comprised of an Axin scaffolding protein, glycogen synthase kinase 3 (GSK), casein kinase I (CKI), and adenomatous polyposis coli (APC, a tumour suppressor) (Scott and Brann, 2013). When Wnt ligands bind to the Frizzled and the LRP5/6 co-receptor, Dishevelled (Dvl) is recruited and LRP6 becomes phosphorylated. This phosphorylation promotes Axin to bind to the transmembrane receptors, resulting in the inactivation of the β-catenin degradation complex. As such β-catenin in the cytosol is stabilised and can subsequently be translocated to the nucleus, where it binds to TCF/LEF (T-cell factor/Lymphoid enhancer factor) domains and promotes Wnt target

gene transcription (Arce et al., 2006). Conversely if Wnt signalling ligands are absent, LRP6 is not phosphorylated, Axin is not recruited to the membrane receptors and thus the β-catenin degradation complex is free to phosphorylate β-catenin and cause its ubiquitination and consequent degradation by the proteasome.

**Figure 1.5: Schematic of the canonical Wnt signalling pathway.** In the absence of Wnt ligands cytosolic β-catenin is flagged for proteasomal degradation to prevent activation of Wnt target genes in the nucleus. Conversely the β-catenin degradation complex is interrupted in the presence of Wnt ligands, promoting abundant cytosolic β-catenin accumulation, and subsequent translocation to the nucleus. Image adapted from Scott and Brann (2013).

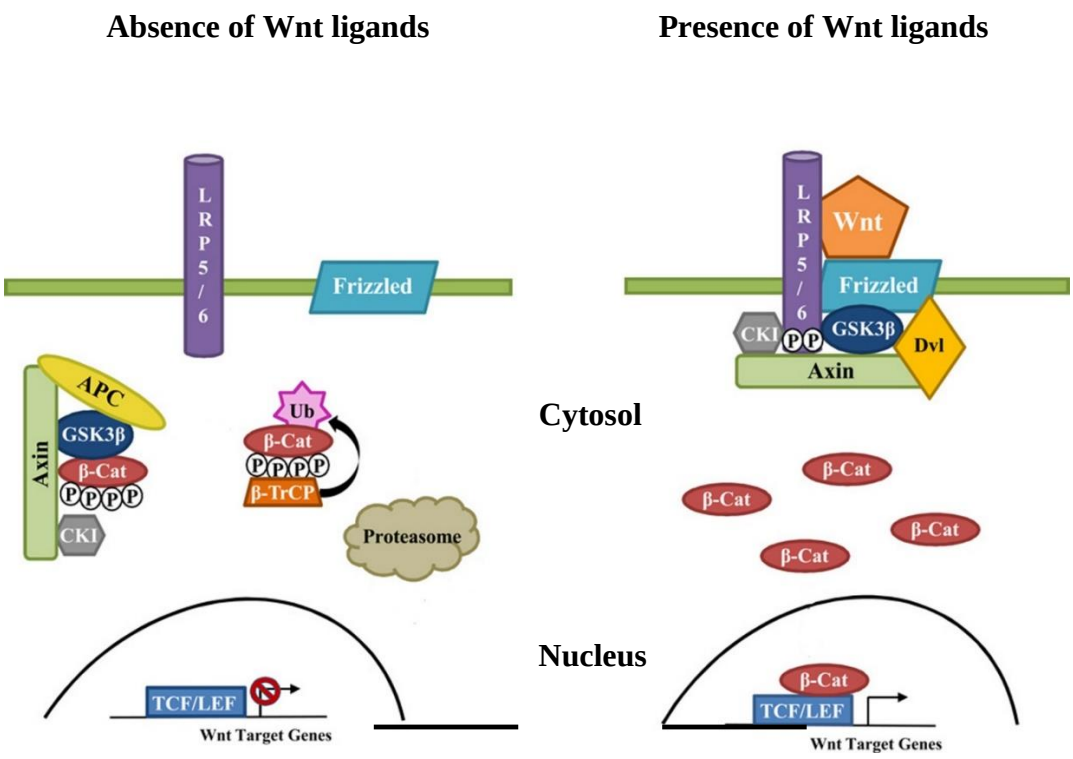

### *1.7.1 Canonical Wnt signalling within the developing cochlea*

Previously within this chapter the role of canonical Wnt signalling in the induction of the otic placode has been discussed. Extensive research on this early inductive role has been carried out, but canonical Wnt signalling is also thought to be implicated in further maturation of the cochlea, and this role has been less well characterised. In an attempt to address this, Jacques et al. (2012) identified a possible dual role for canonical Wnt signalling in the cochlea. Firstly canonical Wnt signalling was established to still be active, albeit at a low level, within the developing cochlea, as shown via a *TCF/LEF:H2B-GFP* reporter mouse. Activation of the canonical Wnt signalling pathway by exposing organ of Corti explants to lithium chloride (LiCl, a GSK3 inhibitor) caused an increase in proliferation, an expansion of Sox2-positive cells and also an increase in the number of hair cells. Conversely, inhibition of canonical Wnt signalling with inhibitor-of-Wnt-response-1-endo (IWR-1-endo) reduced proliferation, and decreased the number of Sox2-positive cells and hair cells within the explants.

Adding further evidence of the role of canonical Wnt signalling in the mature cochlea was the study conducted by Shi et al. (2014). Temporal disruption of β-catenin was shown to inhibit Atoh1 expression resulting in loss of hair cells *in vivo*, yet inhibition of β-catenin following induction of hair cells did not cause a phenotypic change. These findings suggest the role of canonical Wnt signalling is to induce the initial formation of sensory hairs in the organ of Corti, but it is not required for hair cell maintenance or survival.

### *1.7.2 Potential for regeneration within the organ of Corti*

Despite the knowledge that the post-mitotic sensory epithelium of the organ of Corti is quiescent, a number of studies have highlighted potential proliferative capacity and even the ability to generate hair cells in the mammalian cochlea (Oshima et al., 2007; White et al., 2006), although the mechanisms for these findings were not apparent. Both Chai et al. (2012) and Shi et al. (2012) attempted to ascertain which cell types in

the organ of Corti featured this ability to recover proliferation ability. The findings of both studies identified leucine-rich repeat-containing G-protein coupled receptor 5 (Lgr5) expressing cells in the mature mouse cochlea, and it was demonstrated that these cells are the most likely candidates to impart regenerative capacity. Lgr5 has been previously described as an adult stem cell marker, found in the highly proliferative areas of the intestinal crypts, stomach and hair follicles (Barker et al., 2007; Barker and Clevers, 2010). Lgr5 expression in the cochlea was found in a small number of supporting cells, and most interestingly, overexpression of canonical Wnt activity via stabilised β-catenin caused the Lgr5-positive cells to re-enter the cell cycle and proliferate. Direct differentiation of the Lgr5-positive cells into myosinVIIa-positive hair cells as a consequence of overactive canonical Wnt signalling was also observed in both studies, suggesting that Wnt signalling is able to induce both proliferation and differentiation in these Lgr5-positive cells. Overactive canonical Wnt signalling inducing hair cell differentiation has previously been demonstrated in avians (Stevens et al., 2003). The exact mechanisms of these actions are still to be fully determined but as canonical Wnt signalling has already been shown to act upstream of Atoh1 (Shi et al., 2010), the ability to upregulate Atoh1 expression is an obvious feature to be investigated further.

### *1.8 Generation of otic progenitors from hES stem cells – a step towards a stem cell therapy for deafness*

In the Rivolta laboratory an established protocol has been derived to drive the differentiation of hES cells into otic placodal-like progenitors (Chen et al., 2012). A basic schematic representation of this differentiation protocol is represented in Figure 1.6, and detailed steps are highlighted in Chapter 2. Based on the ligands known to play a crucial role in the induction of the otic placode from the ectoderm *in vivo*, FGF 3 and FGF 10, a 12 day differentiation period results in the generation of cells expressing combinations of characteristic otic markers, including *PAX2*, *PAX8*, *FOXG1* and *SOX2*. Approximately 15 – 20% of these cells express high levels of these otic marker combinations and it is this population that is believed to represent

the otic progenitors. Amongst a number of cellular and colony morphologies, two morphologies of interest are generated: epithelial-like progenitors and neural-like progenitors. These are referred to as otic epithelial progenitors (OEPs) and otic neural progenitors (ONPs), respectively. Subsequently the OEPs can be further differentiated into hair cell-like cells and, to a lesser extent auditory neuronal-like cells. The ONPs however are restricted in their differentiation capacity to only have the ability to differentiate into auditory neuronal-like cells. Moreover, and most crucially, ONPs transplanted into a gerbil model of neuropathy have shown the ability to engraft, further differentiate into auditory neurons, and significantly improve hearing thresholds by approximately 46% on average.

These results highlight the potential benefits of using hES and hIPS cells to pursue a cell-based therapy for deafness.

**Figure 1.6: Standard protocol schematic used to differentiate hES cells into otic progenitors *in vitro*.**

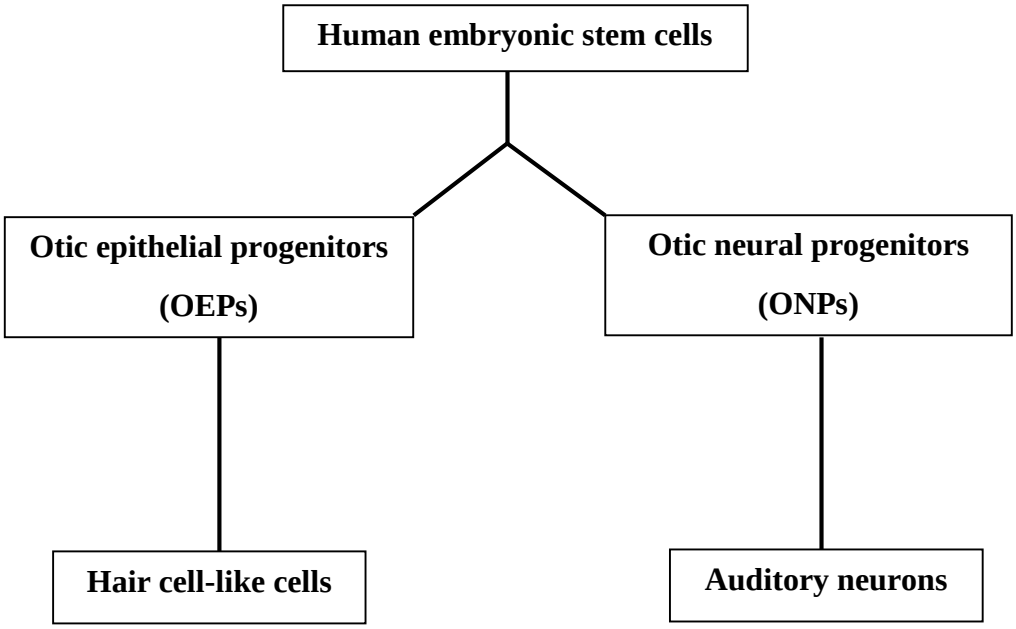

## *1.9 Aims*

The ultimate aim of this work is to build upon the already established FGF 3 and FGF 10 based otic differentiation protocol by investigating the effects of manipulating the canonical Wnt signalling pathway in combination with the standard otic *in vitro* differentiation protocol. Differentiation of hES cells with FGF 3 and FGF 10 ligands produces otic progenitor cells with approximately 20% efficiency. Increasing this efficiency, and making the current methodology more robust would be invaluable for further research into regenerative strategies for deafness. Simultaneously the ability to monitor the induction of otic progenitors by generation of a hES reporter cell line will allow for real-time visualisation of the dynamics of otic differentiation, and provide an additional readout for the impact of manipulating various signalling pathways on otic induction *in vitro*.

Thus the broad aims of this work are as follows:

- Generation of an *in vitro* hES reporter line to monitor otic induction using *SOX2* enhancer sequences which show activity solely in the nasal and otic placodes *in vivo*
- Investigation of the effects of canonical Wnt signalling manipulation on germ layer differentiation of hES cells *in vitro*
- Determination of the impact of canonical Wnt signalling manipulation in synergy with FGF signalling on induction of pre-placodal identity and otic placodal progenitor differentiation from hES cells
- Exploration of the downstream differentiation capacity of the canonical Wnt signalling-manipulated otic progenitors into hair cell-like cells and auditory neurons.

# *Chapter 2*

# CHAPTER 2: MATERIALS AND METHODS

## *2.1 In vitro mammalian cell culture*

### *2.1.1 Human embryonic stem cell maintenance medium*

All human embryonic stem (hES) cell lines used in this study (H14S9, Shef 1 and Shef3) were cultured under the exact same conditions. Cells were maintained in hES cell maintenance medium which comprised of Knockout DMEM (Gibco), 20% Knockout Serum Replacement (Gibco), 1 mM GlutaMAX (Gibco), 1x MEM non-essential amino acids (Gibco), 0.1 mM 2-mercaptoethanol (Gibco), and 4 ng/ml basic FGF (R&D Systems). hES cell maintenance media was replenished daily and the cells were routinely passaged every five to seven days or when the culture reached approximately 80 – 85% confluency, and were maintained usually on mitotically-inactivated mouse embryonic fibroblast (MEF) feeder cells.

### *2.1.2 Mouse embryonic fibroblasts*

Mouse embryos (E13.5) were decapitated and eviscerated, followed by dissociation by trypsinisation, and the cells were cultured in DMEM (Sigma) containing 20% fetal calf serum (FCS) (Gibco) to bulk. MEF cells were then mitotically-inactivated using 10 µg/ml Mitomycin-C (Sigma). Stocks of inactivated MEF cells were then frozen and placed into liquid nitrogen stores for routine usage over a period of several weeks.

Tissue culture vessels were coated with EmbryoMax 0.1% Gelatin Solution (Millipore) for one hour prior to use. Cryogenic vials of MEF cells were quickly thawed in a 37 °C water bath, transferred to a 15 ml centrifuge tube containing DMEM with 10% FCS, centrifuged at 1000 rpm for five minutes, and cell pellet resuspended in 1 ml of DMEM with 10% FCS. Cells were counted using the TC20 Automated Cell Counter (Bio-Rad) and seeded into the previously gelatin coated culture vessels at a density of approximately $2.5x10^4$ cells/$cm^2$, and maintained at 37 °C with 10% $CO_2$.

### *2.1.3 Routine passaging of human embryonic stem cells*

When the hES cells reached 80 – 85% confluency (usually between five and seven days) the expended culture media was removed, and 1 ml of 1 mg/ml collagenase type IV solution (in DMEM) (Gibco) was added and the cells were incubated for six to 12 minutes to allow time for the hES colony edges to begin lifting away from the underlying layer of MEF feeder cells. The collagenase solution was then removed and replaced with 2 ml fresh hES maintenance medium. Using a 1 ml fine tip Pasteur pipette under light microscopy good quality hES cell colonies, with defined borders and minimal areas of differentiation, were scraped in order to divide the colonies into smaller segments. Any areas of differentiation were avoided, and minimal scraping of MEF cells to avoid carry over into the new culture vessel. The smaller segments of hES colonies were then transferred into a freshly prepared MEF feeder vessel and maintained for the following days at 37 °C with 5% $CO_2$.

### *2.1.4 Maintenance of human embryonic stem cells in a MEF feeder free environment*

For the derivation and maintenance of hES reporter lines, MEF feeder free conditions were routinely used. In place of an inactivated MEF feeder layer, Growth Factor-Reduced Matrigel (BD Biosciences) was used. Matrigel was initially diluted 1:2 in Knockout DMEM and aliquots were frozen for later use. When required, aliquots were thawed at 4 °C and further diluted 1:15 in Knockout DMEM to give a final dilution of 1:30 from the stock solution. Using pre-chilled pipettes the diluted matrigel solution was added to the culture vessel (approximately 1 ml per T12.5 flask) and incubated for 30 minutes at 37 °C to allow the matrigel layer to set and coat the vessel with a thin layer of gel. Serum-free medium is used in combination with matrigel, and this work involved the use of mTeSR1 maintenance medium (STEMCELL Technologies). This was supplied as a Basal Medium and 1x Supplement. Aliquots were frozen for later use. hES cells maintained in this culture system were passaged using the same method as described previously for use with inactivated MEF cells. Prior to receiving the small hES colony segments, the excess matrigel was aspirated

from the culture vessel. Cells were maintained at 37 °C with 5% $CO_2$ and were passaged every five to seven days.

### *2.1.5 Maintenance of mouse and human fetal auditory stem cells*

Both mouse and human fetal auditory stem cells (FASCs) were maintained in Otic Stem Cell Full Medium (OSCFM) which comprised of DMEM/F12 (Gibco) supplemented with N2/B27, with 20 ng/ml basic fibroblast growth factor (basic FGF) (Peprotech), 50 ng/ml insulin-like growth factor-1 (IGF-1) (R&D Systems), and 20 ng/ml epidermal growth factor (EGF) (R&D Systems). Mouse and human FASCs were grown on culture vessels previously coated with EmbryoMax 0.1% Gelatin Solution. Cells were passaged when 75 – 80% confluent by either enzymatic dissociation with very mild trypsin-EDTA (ethylenediaminetetraacetic acid) (0.00625% in Hanks Balanced Salt Solution (Sigma)), or using Enzyme Free Dissociation Solution (Millipore). Using enzyme free or very mild trypsin dissociation methods were carried out to avoid potential neuralisation of the FASCs.

## *2.2 In vitro differentiation experiments*

### *2.2.1 Otic progenitor derivation from human embryonic stem cells*

At least four hours (typically overnight) prior to setting up differentiation of hES cells into otic progenitors, culture vessels were coated with mouse laminin I (Cultrex). Mouse laminin I was prepared by diluting the stock to a working concentration of 2.5 $\mu g/cm^2$ in ice cold phosphate buffered saline (PBS) (Sigma) and 1.5 ml was used to coat T12.5 culture flasks. Polymerisation of the laminin was carried out at 37 °C. Undifferentiated hES colonies were assessed for their good quality and any differentiated patches or high density MEF feeder cell areas were removed. The hES culture was then washed twice with Hanks Balanced Salt Solution, and the cells were then trypsinised for up to five minutes with 0.025% Trypsin-EDTA at 37 °C. Once the hES cells were dissociated into a suspension of single cells, they were transferred

to a centrifuge tube containing pre-warmed 0.5 mg/ml Soybean Trypsin Inhibitor Solution (Gibco), diluted in DMEM. The cells in the trypsin inhibitor solution were subsequently centrifuged at 1000 rpm for five minutes, the cell pellet was resuspended in 1 ml of DFNB (DMEM/F12 with N2 and B27 supplements), and then passed through a 100 µM sieve strainer to remove any large clumps of cells. Cell counts were performed in triplicate using the TC20 Automated Cell Counter, and a 10 µl sample of cells was diluted 1:2 in Trypan Blue (Bio-Rad) to determine cell viability following the trypsinisation process. Triplicate counts were averaged and cells were seeded into the previously laminin coated flasks or dishes at a typical density of $8x10^3/cm^2$. Differentiating hES cells were seeded and maintained in either the control DFNB media, or DFNB supplemented with FGF 3 and FGF 10 (50 ng/ml, R&D Systems) for basic otic progenitor differentiation experiments. Differentiation experiments were carried out for 12 days and media was replenished every 2 days.

### *2.2.2 Manual enrichment of otic progenitor morphologies*

Two colony morphologies of interest begin to appear within the differentiating hES cultures approximately three to four days into the differentiation process, surrounded by extraneous cell types. These two morphologies are cells with an epithelioid island morphology (referred to as otic epithelial progenitors, or OEPs) and cells with a more neural-like appearance (referred to as the otic neural progenitors, or ONPs). To enrich for a particular colony type of interest (dependent on the downstream experiments), currently the extraneous cell types are manually scraped away using a sterile plastic Pasteur pipette under light microscopy, leaving behind only the cell morphologies of interest.

### *2.2.3 Further expansion and differentiation of otic progenitors in vitro*

At the end of the 12 day differentiation period manually enriched otic progenitors could be further expanded for a finite number of passages if transferred into gelatin

coated flasks and maintained in OSCFM. Mildly diluted Trypsin-EDTA (0.00625%) or Enzyme Free Dissociation Solution is used to gently dissociate the progenitors for transfer, and to avoid potential triggering of further differentiation.

OEPs have previously been shown to be able to further differentiate into hair cell-like cells, whereas ONPs have the capacity to be pushed to differentiate into auditory neurons. For hair cell-like differentiation, manually purified OEPs at the end of the 12 day differentiation period were washed with Hanks Balanced Salt Solution, trypsinised with 0.00625% Trypsin-EDTA, transferred to a centrifuge tube containing 0.5 mg/ml Soybean Trypsin Inhibitor and centrifuged at 1000 rpm for five minutes. The cell pellet is resuspended in 1 ml of DFNB, sieved through a 100 µM strainer and counted. OEPs were then seeded into previously gelatin coated culture vessels containing hair cell induction media at a density of $1x10^4/cm^2$. This media is comprised of DFNB supplemented with $10^{-6}$ M all-*trans* retinoic acid and 20 ng/ml EGF, and is used to induce the differentiation of hair cell-like cells over a 14 day differentiation period.

The further differentiation of ONPs was carried out by washing the manually enriched cells twice with Hanks Balanced Salt Solution, dissociating with 0.125% Trypsin, transferring to a centrifuge tube containing 0.5 mg/ml Soybean Trypsin Inhibitor Solution and centrifuging at 1000 rpm for five minutes. Cell pellets were resuspended in 1 ml DFNB and sieved through a 100 µM cell strainer and counted. ONPs were then seeded at a density of $4x10^3/cm^2$ into gelatin coated flasks containing DFNB supplemented with 20 ng/ml basic FGF and 500 ng/ml Sonic hedgehog C24II (R&D Systems) (the C24II mutation enhances its potency). On day 4 of differentiation the media is replaced with DFNB containing 20 ng/ml basic FGF, 500 ng/ml Sonic hedgehog C24II, 10 ng/ml neurotrophic factor-3 (NT-3, Peprotech) and 10 ng/ml brain-derived neurotrophic factor (BDNF, Peprotech). On day 6 through to day 12 Sonic hedgehog supplementation is removed (DFNB with basic FGF, NT-3 and BDNF only).

## *2.3 Transfection techniques*

### *2.3.1 Generation of human embryonic stem cell reporter lines by electroporation*

The process of the preparation of plasmid DNA for transfection into hES cells is described in the following section (2.4). Electroporation of plasmid DNA into the hES cells in order to generate stably transfected reporter lines was carried out in a serum and feeder free culture system. Undifferentiated hES colonies were trypsinised with 0.025% Trypsin-EDTA for five minutes, transferred into a centrifuge tube containing an equal volume of Soybean Trypsin Inhibitor, then centrifuged for five minutes at 1000 rpm. The cell pellet was then resuspended in 5 ml of PBS to wash and a 10 µl sample was collected for counting, and then the cells were centrifuged again. The pellet was resuspended in Ingenio Electroporation Solution (Mirus Bio) at a concentration of $2.5x10^6$ cells/ml and divided into 250 µl aliquots containing approximately $6.25x10^5$ cells/aliquot. 10 µg of plasmid DNA (pEGFP-1 NOP-SOX2, pEGFP-1 Atoh1nGFP, or pCAG EGFP control) was added to each aliquot, gently mixed and transferred to a 4 mm gap electroporation cuvette. The ECM830 Electroporator (BTX) was set up to pulse the cells with two pulses of 240 volts for 10 milliseconds, with a 100 millisecond interval between the pulses. 500 µl of pre-warmed mTeSR1 was added to the cuvette to collect the electroporated cells, and this was transferred to matrigel coated (section 2.1.4) 60 mm dishes containing warm mTeSR1. Y-27632 (ROCK-inhibitor, Sigma) was added to the dishes at a concentration of 10 µg/ml to aid the survival of the single hES cells. 24 hours later the media was replaced to remove dead cells. Beginning at 48 hours post-electroporation, the antibiotic G418 was added at 20 µg/ml to begin to select for stably transfected cells. The pCAG EGFP electroporated cells quickly died as this plasmid vector does not confer resistance to G418. After approximately 21 days of G418 selection, hES colonies were able to be picked and transferred into new culture vessels for further analysis and expansion. Where possible these hES clones were maintained on matrigel as the G418 antibiotic would kill the MEF feeder cells. Due to the high running costs of this serum and feeder free culture system, hES clones were routinely passaged onto MEF feeder cells without G418 supplementation prior to setting up differentiation experiments. Every few weeks hES clones on MEF feeders were

transitioned back onto matrigel to receive G418 treatment to ensure the plasmid integration was not lost.

### *2.3.2 Transient transfections by lipofection*

The otic progenitors and mouse and human FASCs were found to be too sensitive to electroporation, and so lipofection was carried out as an alternative. For this method cells were required to be freshly seeded into wells of a culture plate 24 hours pre-transfection. Lipofection was done using Lipofectamine with PLUS reagent (Life Technologies). Per transfection a 1.5 ml Eppendorf tube containing 1 ml of Opti-MEM (Gibco) was mixed with 500 ng of plasmid DNA and 0.5 µl of PLUS reagent. This mixture was mixed gently by vortexing and incubated for 15 minutes at room temperature. 1 µl of Lipofectamine LTX was then added, gently mixed and incubated for one hour at room temperature to allow the formation of lipid:DNA complexes. The 1 ml solution was then added directly to the cell types of interest and transfection was allowed to take place for six hours. Following this the media was removed, gently washed with Hanks Balanced Salt Solution and replenished with fresh media. The transfection was then usually visualised 24 hours later.

## *2.4 Plasmid DNA preparation*

### *2.4.1 Restriction digests of plasmid DNA*

For the generation of the H14S9 NOP-SOX2 and H14S9 Atoh1nGFP reporter cell lines the pEGFP-1 vector (Clontech) was used for the delivery of the plasmid DNA to the hES cells. For the mNOP-1/2x4 enhancer tandem Sac I and Xba I (New England Biolabs) were used to enzymatically digest both the phspEGFPver2 plasmid containing the NOP-SOX2 enhancer sequences and the pEGFP-1 vector. Bgl II and BsrG I were used for the Atoh1nGFP-containing plasmid (J2XnGFP) and the pEGFP-1 vector. Restriction digests for both reporters were carried out in the same way as follows. 1 µg of plasmid DNA (preparation described in section 2.4.4) was

enzymatically digested with 1 µl of each restriction enzyme in a total reaction of 50 µl, containing 1x NEBuffer 3. The restriction digest took place over 1 hour at 37 °C. A 20 minute heat inactivation step at 65 °C was carried out to prevent further digestion. The digestions were run in a gel electrophoresis tank for approximately 1 hour at low voltage using a 0.8% low melting agarose gel (Sigma) in order to separate out the enhancer sequences from their original vectors, and also to prepare the pEGFP-1 vector. Ethidium bromide was added to the agarose gels to enable the visualisation of the plasmid DNA digests on a UV transilluminator (SYNGENE) to aid in manually dissecting out each fragment.

### *2.4.2 Purification of plasmid DNA and ligation*

Ethanol precipitation of the plasmid DNA fragments was then carried out to purify and concentrate the DNA for ligation. For a typical 50 µl digestion 5 µl of 3 M sodium acetate and 150 µl of ice cold 100% ethanol were added to the digested DNA in a 1.5 ml Eppendorf tube and incubated at -80 °C for at least one hour. Following this step the Eppendorf tube is centrifuged at maximum speed (approximately 14,500 rpm) for 30 minutes. The supernatant is then removed and replaced with 200 µl of ice cold 70% ethanol before centrifugation at maximum speed for five minutes. The supernatant is then carefully removed and the DNA pellet allowed to air dry. Approximately 10 – 20 µl molecular grade water is then added to resuspend the DNA pellet. Quantification of plasmid DNA was carried out using the Nanodrop 1000 spectrometry platform (Thermo Fisher Scientific).

The pEGFP-1 vector backbone plasmid DNA and the enhancer sequences were then ligated together to form the plasmid constructs which were transfected into the H14S9 hES cells in section 2.3. Ligation reactions were performed with T4 DNA Ligase (New England Biolabs) as follows. Using a 1:3 vector:insert ratio plasmid DNA was added to 2 µl T4 DNA Ligase Buffer and made up to 19 µl with molecular grade water. 1 µl of T4 DNA Ligase was added and the mixture was incubated at 16 °C overnight. Heat inactivation at 65 °C for 15 minutes was then carried out and ethanol precipitation performed to purify and concentrate the plasmid DNA.

### *2.4.3 Electroporation of plasmid DNA and bacterial propagation*

In order to create a stock of pEGFP-1 NOP-SOX2 and pEGFP-1 Atoh1nGFP plasmid DNA bacterial culture is required. XL1-Blue MRF (Minus Restriction) (Strategene) strain of electrocompetent bacteria were utilised for this. 50 µl aliquots of XL1-Blue MRF cells were thawed on ice, and 1 µl of the plasmid DNA of interest was added to the cells and gently pipetted to mix. The bacteria/DNA mix was transferred to a pre-chilled 1 mm gap electroporation cuvette, and placed into the ECM830 Electroporator (BTX). A single pulse of 500 volts with a pulse length of eight milliseconds was applied to the cells. The cells were then quickly transferred into 1 ml of pre-warmed SOC medium (Super Optimal Broth with Catabolite Repression) (Sigma) and incubated at 37 °C with 250 rpm shaking. After this 100 µl of bacterial culture was plated and spread onto LB agar plates (Luria-Bertani) containing 25 µg/ml kanamycin (the pEGFP-1 vector confers resistance to kanamycin) and incubated at 37 °C overnight. Bacterial colonies were subsequently picked and inoculated into 15 ml of LB broth containing 25 µg/ml kanamycin and left in a shaking 37 °C incubator overnight. This provided an adequate culture for plasmid DNA preparation.

### *2.4.4 Plasmid DNA preparation for transfection into human embryonic stem cells*

From a bacterial liquid culture it is then necessary to extract and purify the plasmid DNA in order to use it for transfection into mammalian cells. This process was done using the Plasmid Midi Prep Kit (Qiagen) and following the manufacturers' protocol. In brief, the bacterial cultures were centrifuged at 6000g for 15 minutes at 4 °C to pellet the cells. The pellet is then resuspended in lysis buffers to destroy the bacterial cell walls and organelles. The lysate is then precipitated and centrifuged for 30 minutes at 20,000g at 4 °C to separate the solid material from the plasmid DNA contained within the supernatant. The supernatant is centrifuged a second time for 15 minutes and is applied to a Qiagen-100 tip column. The plasmid DNA binds to the column and washing steps are carried out to eliminate any trace of protein or genomic

DNA contamination. The plasmid DNA is then eluted from the column and an ethanol precipitation was carried out to purify and concentrate.

### *2.5 Quantitative real-time PCR (QPCR) analysis*

#### *2.5.1 RNA extraction and cDNA synthesis*

Extraction of total RNA was carried out using the RNeasy Micro Kit (Qiagen), following the manufacturers' guidelines. At the end of differentiation experiments cells were washed twice gently with PBS, lysed using the RLT buffer, and precipitated using 70% molecular grade ethanol. The RNA solution was then passed through the supplied Micro columns to bind the RNA and allow for washing steps. Digestion of genomic DNA was carried out on the column using DNase I (Qiagen), and RNA was eluted from the column using molecular grade water. Quantification of the yield of RNA was done using the Nanodrop 1000 platform.

For the conversion to complementary DNA (cDNA) 1.5 µg of RNA (wherever possible) was used. In a 12 µl reaction RNA was first primed for reverse transcription using 1 µl oligo-dT (Promega) and incubated for five minutes at 65 °C. Following this step 4 µl of First Strand Buffer (Life Technologies), 1 µl 0.1 M dithiothreitol (DTT) (Life Technologies), 1 µl RNasin Plus RNase Inhibitor (Promega), 1 µl 100 mM dNTPs (Bioline), 0.5 µl RNase free water, and 0.5 µl Superscript Reverse Trnscriptase III (Life Technologies) was added before incubating for 90 mins at 50 °C. A heat inactivation step was carried out at 70 °C for 15 minutes.

#### *2.5.2 QPCR Primers*

Forward and reverse primers for QPCR analysis were originally designed by using the software PerlPrimer or Primer BLAST (NCBI). Product lengths were ensured to be approximately 200 base pairs or less to remain efficient in QPCR analysis. In the case of *POU4F1*, *SYP* and *SLC17A7*, these primers were found from carrying out literature searches. Primer stocks were resuspended in molecular grade water at a final stock

concentration of 100 mM, and diluted to 5 µM working stocks. Table 2.1 shows the list of all QPCR primers used throughout this study. cDNA from embryoid body differentiation experiments (Sarah Jacob Eshtan, Johanna Thurlow) were used as positive controls for primer testing and determination of optimal annealing temperatures. The presence of a clean melt curve and product detectable by gel electrophoresis confirmed the suitability of a particular primer pair.

**Table 2.1: Primers used in QPCR analysis.** F: Forward primer; R: Reverse primer

| GENE | PRIMER SEQUENCE | AMPLICON LENGTH |
|---|---|---|
| *AFP* | F: CTT GTG AAG CAA AAG CCA CA<br>R: CCC TCT TCA GCA AAG CAG AC | 122 |
| *DLX5* | F: CCC TAC CAG TAT CAG TAT CAC<br>R: GTC ACT TCT TTC TCT GGC TG | 155 |
| *EYA1* | F: GTT CAT CTG GGA CTT GGA<br>R: GCT TAG GTC CTG TCC GTT | 229 |
| *FOXG1* | F: CTA AAT AGT GAC TGC TTC GCC A<br>R: TTT AGG TTG TTC TCA AGG TCT G | 135 |
| *FOXI2* | F: TGA CGC TCA GCC AGA TCT AC<br>R: CCT TTA CCT GGG TCG TCC T | 151 |
| *GATA6* | F: AAT ACT TCC CCC ACA ACA CAA<br>R: CTC TCC CGC ACC AGT CAT | 69 |
| *MEOX1* | F: AAA TCA TCC AGG CGG AGA A<br>R: AAG GCC GTC CTC TCC TTG | 95 |
| *NANOG* | F: CTC AGC CTC CAG CAG ATG C<br>R: TAG ATT TCA TTC TCT GGT TCT GG | 94 |
| *NESTIN* | F:TCC AGG AAC GGA AAA TCA AG<br>R: GCC TCC TCA TCC CCT ACT TC | 120 |
| *PAX2* | F: CTT TAA GAG ATG TGT CTG AGG G<br>R: CCT GTT CTG ATT TGA TGT GCT | 186 |
| *PAX8* | F: CTT GGC AGG TAC TAC GAG AC<br>R: GCA AAC ATG GTA GGG TTC TG | 128 |
| *POU4F1* | F: CGT ACC ACA CGA TGA ACA GC<br>R: AGG AGA TGT GGT CCA GCA GA | 123 |
| *POU4F3* | F: CCC GGT GCT GCA AGA ACC CA<br>R: GGC GTC GGG CTT GAA CGG AT | 196 |
| *POU5F1* | F: AGC GAA CCA GTA TCG AGA AC<br>R: TTA CAG AAC CAC ACT CGG AC | 142 |
| *RPLPO* | F: GAA GGC TGT GGT GCT GAT GG<br>R: CGG GAT ATG AGG CAG CAG TT | 103 |
| *SLC17A7* | F: TGG GTT TCT GCA TCA GCT TTG<br>R: TGT ACT GTT GTT GAC CAT GGA TAC G | 74 |
| *SOX2* | F: CCC AGC AGA CTT CAC ATG T<br>R: CCT CCC ATT TCC CTC GTT TT | 151 |
| *SYP* | F: GCA GTG GGT CTT TGC CAT CTT<br>R: TGA GGG CAC TCT CCG TCT TG | 101 |
| *T* | F: AAC TCC TTG CAT AAG TAT GAG CC<br>R: TTT AAG AGC TGT GAT CTC CTC GT | 141 |

### *2.5.3 SYBR Green*

QPCR reactions were carried out using SYBR Green JumpStart Reaction Mix (Sigma). Each sample was represented in triplicate within the QPCR plate. A mastermix comprising of 32 µl SYBR Green JumpStart Mix, 24 µl molecular grade water, 6.4 µl of a forward and reverse primer mix (0.5 µM final concentration), and 1.6 µl of cDNA was split into the three triplicate wells with 20 µl each. Negative control wells containing water in the place of cDNA were run alongside each reaction.

The basic protocol for each QPCR reaction was as follows. An initial denaturation step at 94 °C for five minutes, then 40 cycles of 94 °C for 30 seconds, an primer pair-dependent optimal annealing temperature for up to one minute, then an extension phase at 72 °C for one minute. A final extension phase at 72 °C for 10 minutes concluded each reaction. Reactions were done using the iCycler IQ Real-Time PCR machine.

The Delta Delta Ct method developed by Livak and Schmittgen (2001) was used to quantitate and present QPCR data analysis. The gene encoding for a ribosomal protein, *RPLPO*, was used as the calibrator gene to determine the value of the Delta Cts (the housekeeping reference gene). For ascertaining the Delta Delta Cts the values of gene expression were compared as relative to that of the baseline control condition DFNB.

## *2.6 Immunocytochemistry and image analysis*

For the detection of protein expression cells were immunolabelled with a combination of antibodies. Following differentiation experiments, cells were washed once with PBS and 4% paraformaldehyde was used for 15 minutes to fix the cells. Paraformaldehyde was rinsed off with PBS and the cells were then washed three times for five minutes each with PBS containing 0.1% Triton X-100 (PBST) to permeabilise the cell membranes. Non-specific binding sites were then blocked for one hour with

PBST supplemented with 5% donkey serum (Sigma), followed by three further washes with PBST for five minutes each. Primary antibody combinations were diluted in PBST with 5% donkey serum, applied to the cells and incubated overnight at 4 °C. The next day three five minutes washes with PBST were done to remove unbound primary antibodies. Secondary antibodies were diluted in PBST with 5% donkey serum and applied to the cells for one hour at room temperature. Three five minute washes with PBS followed before applying DAPI diluted 1:100 in PBS to counterstain the nuclei. Table 2.2 lists the primary and secondary antibodies used in the experiments presented in this work.

Images were taken either manually using the EVOS FL Cell Imaging System (Life Technologies) or automatically using the In Cell Analyser 1000 platform (GE Healthcare). For manual counting, cells were compared against secondary antibody-only control staining and positivity was recorded if staining appeared brighter than the secondary antibody-only. For the In Cell Analyser platform, cells were differentiated in 24 well (Vision Plate 24, 4titude) glass bottomed plates (previously laminin coated as with plastic culture vessels) and images were taken at x20 magnification. 250 images per well were taken and analysed using the Developer Toolbox software. To ensure of the reliability of the assay, nuclei were initially identified by DAPI staining and nuclear segmentation was carried out to allow the software to automatically identify the nucleus. Nuclear segmentation was subjected to further post-processing tools (such as erosion and sieving) to increase the accuracy of nuclear identification. For testing of the segregation protocols, nuclei stained with DAPI in control wells were counted manually by eye at 20x magnification and this was compared against the automated nuclei count. This process of segmentation provided a nuclear mask which was then applied to the green and red channels to determine the level of fluorescence intensity within. As all of the primary antibodies used for In Cell Analyser analysis were nuclear markers this allowed for ease of fluorescent detection within the area demarcated by the nucleus. Primary antibody titrations (coupled with the secondary antibody) were carried out previously in order to determine a minimum and maximum fluorescence intensity detectable by the Developer Toolbox software. For each secondary antibody, a secondary antibody-only well was also included to allow the software to recognise background levels of fluorescence.

Once the fluorescence intensity values had been determined from the images, analysis was carried out to determine the positive cells. If the fluorescent intensity of a cell was higher than the 99$^{th}$ percentile value of each secondary antibody-only wells (for green and red) then it was considered double positive. Once the percentage of positive cells was determined a more stringent threshold was applied. This threshold identified highly double positive cells if the fluorescent intensity of that cell was higher than the 75$^{th}$ percentile value of the positive cells in the FGF condition.

**Table 2.2: Primary and secondary antibodies for immunolabelling.**

| | ANTIBODY (MANUFACTURER, PRODUCT CODE) | HOST SPECIES | WORKING CONCENTRATION |
|---|---|---|---|
| PRIMARY ANTIBODIES | ATOH1 (Abcam, AB105497) | Rabbit polyclonal | 1:100 |
| | B-TUBULIN III (Covance, MMS-435P) | Mouse monoclonal | 1:100 |
| | FOXG1 (Abcam, 18259) | Rabbit polyclonal | 1:100 |
| | MYO7A (Proteus, 25-6790) | Rabbit polyclonal | 1:100 |
| | NEUROFILAMENT 200 (Sigma, N4142) | Rabbit polyclonal | 1:100 |
| | NKAα3 (Santa Cruz, 16052) | Goat polyclonal | 1:75 |
| | PAX2 (Abcam, 38738) | Rabbit polyclonal | 1:100 |
| | PAX6 (DSHB) | Mouse monoclonal | 1:100 |
| | PAX8 (Abcam, 13611) | Goat polyclonal | 1:100 |
| | POU4F1 (Millipore, AB5945) | Rabbit polyclonal | 1:100 |
| | POU4F3 (Santa Cruz, 81980) | Mouse polyclonal | 1:100 |
| | SOX2 (Millipore, AB5603) | Rabbit polyclonal | 1:100 |
| SECONDARY ANTIBODIES | Alexa 568 anti-goat (Life Technologies, A11057) | Donkey polyclonal | 1:250 |
| | Alexa 488 anti-goat (Life Technologies, A11055) | Donkey polyclonal | 1:250 |
| | Alexa 568 anti-mouse (Life Technologies, A10037) | Donkey polyclonal | 1:250 |
| | Alexa 488 anti-mouse (Life Technologies, A21202) | Donkey polyclonal | 1:250 |
| | Alexa 568 anti-rabbit (Life Technologies, A10042) | Donkey polyclonal | 1:250 |
| | Alexa 488 anti-rabbit (Life Technologies, A21206) | Donkey polyclonal | 1:250 |

### *2.7 Statistical analysis*

All QPCR data were statistically analysed as multiple sets using a one way analysis of variance (ANOVA) approach, with Bonferroni's multiple comparison applied post-test. For In Cell Analyser statistical analysis, a chi-squared test with Yates' continuity correction was applied. In all figures bar charts represent the mean and error bars denote standard deviation of the mean.

# *Chapter 3*

# CHAPTER 3: GENERATION OF HUMAN EMBRYONIC STEM CELL REPORTER LINES TO MONITOR OTIC PROGENITOR INDUCTION AND HAIR CELL DIFFERENTIATION

## 3.1 Introduction

### *3.1.1 Human embryonic stem cells*

Since the initial derivation of a number of human embryonic stem (hES) cell lines in 1998 (Thomson et al., 1998), advances in the knowledge of their capabilities has grown significantly. The ability to direct the differentiation of hES cells towards a desired fate lineage has been the subject of a vast amount of recent and current research. Efficiently directing their differentiation has a number of advantages, including the study of organogenesis (Narayanan et al., 2013), providing a platform for disease modelling and toxicity testing (Sharma et al., 2013), and perhaps most excitingly, generating mature cell types for clinical trials and future cellular based therapies and regenerative medicine.

### *3.1.2 Fluorescent reporter lines and gene delivery systems*

Technologies in the genetic modification of hES stem cells have also rapidly expanded in recent years, most notably in the form of generating cell type-specific promoter-driven fluorescent reporter lines (reviewed in Giudice and Trounson 2008). The purpose of these is to be able to monitor the differentiation of hES cells into the desired derivative in real time microscopy, without having to use traditional destructive techniques such as immunocytochemistry or RT-PCR to determine gene expression. Fluorescent reporter lines have also proved invaluable in high-throughput screening assays to rapidly identify molecules capable of manipulating differentiation towards a particular lineage. As an example of this, a study conducted by Willems et al. (2011) involved using expression of a fluorescent reporter gene driven by the cardiac-specific

MYH6 promoter as a rapid high-throughput screen for testing 550 small molecules to identify new candidates for promoting hES cell-derived cardiomyocyte differentiation. In addition differentiated fluorescent progeny of such reporter lines have been easily isolated and expanded for further study and testing for a future use in a cellular replacement capacity (Huber et al., 2007; Ovchinnikov et al., 2014; Szebényi et al., 2014). Fluorescent reporter lines used in this area of research have helped to increase knowledge of the processes involved in lineage differentiation, and have the potential to speed up the process of using human pluripotent stem cells as a source for cellular based regenerative medicine.

Numerous techniques have been developed to create fluorescent reporter lines in hES cells, such as random integration of transgenes, or targeted gene knock-ins (by homologous recombination). A study conducted by Xue et al. (2009) generated a targeted neuroglial reporter from a hES cell line, whereby one allele of *Olig2* (a transcription factor important in neuro- and gliogenesis) was replaced by an EGFP reporter cassette by homologous recombination. This allowed the researchers to monitor and track *Olig2* expression during hES cell neural differentiation. Random integrations of transgenes is another method used to create hES reporter lines. Noisa et al. (2010) carried out a random integration transfection of the H1 (WiCell) hES cell line with a plasmid vector containing the second intron of the human nestin gene enhancer, a minimal TK promoter and an EGFP reporter sequence. The resultant transfected cell line showed an upregulation of EGFP reporter expression when the cells were differentiated *in vitro* toward a neuroepithelial lineage. Recently, newer, more sophisticated methods of creating reporters such as transcription activator-like effector nucleases (TALENs) and clustered regularly interspaced short palindromic repeats (CRISPR) (Xue et al., 2014) are beginning to emerge.

### *3.1.3 Otic placode-specific Sox2 enhancer sequences for generating a human embryonic stem cell reporter line*

The *SOX* gene family in mammals contains approximately 20 different genes with important roles during embryonic development and maturation. These genes encode for related transcription factors comprising an approximately 80 amino acid DNA-

binding region known as a High Mobility Group box (HMG-box) (Collignon et al., 1996). *SOX2* (sex determining region Y)-box 2 is one such member of the *SOX* family, and is known to be one of the key transcription factors essential for hES cell pluripotency, along with *OCT4* and *NANOG* (Adachi et al., 2010). It is also implicated in marking various stages of neural and sensory development.

An enhancer sequence can be defined as *cis*-acting regulatory DNA elements that can act to upregulate the transcription of a target gene or genes important for differentiation and development (Plank and Dean, 2014). Uchikawa et al. (2003) analysed a wide genomic region (approximately 50 kilobases) surrounding the *SOX2* locus in developing chicken embryos in order to find corresponding extragenic enhancer sequences. These anticipated enhancer sequences were electroporated into stage 4 embryos and activity was monitored using an EGFP reporter system. Despite *SOX2* being thought to have a pan-neural expression pattern in early neural and sensory placodal development, this study found eight enhancer sequences governing *SOX2* expression with distinct spatio-temporal specificities. Two of these enhancers, NOP-1 and NOP-2, were identified as having restricted activity solely in the developing nasal and otic placodes, suggestive of a similar developmental regulation of these placodes by *SOX2*. These enhancer sequences were also found to be highly conserved between mouse and human (81 and 83% respectively for NOP-1, 77 and 85% respectively for NOP-2). Later studies complemented the otic specificity of the NOP-1 and NOP-2 enhancers, such as that conducted by Kiernan et al. (2005). Mouse mutants light coat and circling (*Lcc*) and yellow submarine (*Ysb*) were studied to assess the effects of their complex chromosomal rearrangements and deletions in the vicinity of *Sox2* on chromosome 3 on the development of sensory regions of the inner ear. The otocysts of these mutant mice, with particular severity in the *Lcc* mutant, lack *Sox2* expression whereas expression in the neural tube and other expected areas was normal. This is suggestive of the regulatory enhancer sequences NOP-1 and NOP-2 being disrupted or translocated leading to loss of otic-specific *Sox2* expression and subsequent impact on normal inner ear development. Another study found the epigenetic status of these *Sox2* enhancers directly affected self-renewal ability of stem cells derived from the post-natal organ of Corti. Inactivation by sequence-specific methylation of NOP-1 and NOP-2 enhancer sequences led to a reduction in self-renewal capabilities (Waldhaus et al., 2012). These studies combined offer further

validation of the specificity of the NOP-1 and NOP-2 enhancers and are therefore potential candidates for use in generating an otic placode differentiation reporter system.

### *3.1.4 Human fetal auditory stem cells as a readout for otic placode-specific enhancer activity*

9-week-old to 11-week-old human fetal cochleae have previously been used to isolate a population of multipotent human fetal auditory stem cells (hFASCs) (Chen et al., 2007 and Chen et al., 2009). These cells (believed to be equivalent to stage E11.5-13.5 in the mouse) were found to express characteristic otic progenitor markers (*SOX2*, *GATA3*), and also typical markers associated with stem cell pluripotency (*OCT4*, *NANOG*, *REX1*) and could be maintained in an undifferentiated state for a number of passages. It was also highlighted that these cells, when exposed to specific molecular triggers, could readily differentiate into the more mature cell types of the inner ear; auditory neurons (as shown by expression of neuronal markers such as *NEUROFILAMENT 200*, *NEUROGI*, *POU4F1*) and hair cells (expressing *ATOH1*, *POU4F3*, *MYO7A*). As the human fetal auditory stem cells express the progenitor marker *SOX2* throughout their undifferentiated state, it was thought that they could be used as a positive control for determining the efficiency and activity of the otic placode-specific *SOX2* enhancer sequences, prior to generating a hES cell reporter line.

### *3.1.5 An Atoh1 enhancer sequence and its potential as an auditory hair cell differentiation reporter system in human embryonic stem cells*

Atoh1 (Cath1, Math1 and Hath1 in chicken, mouse and human respectively) is a transcription factor with a basic helix-loop-helix structural motif, and plays a crucial

role in many pro-neural and non-neural differentiation events throughout embryonic development (Mulvaney and Dabdoub, 2012). For example, Atoh1 expression and activity is known to have a key involvement in the differentiation of secretory cells of the intestinal tract, initiation of the differentiation of neurons, and also mechanoreceptors such as the auditory hair cells of the inner ear.

In the developing inner ear, Atoh1 expression has been shown in several studies to be essential for the induction of hair cell development. Math1 mutant mice experience early postnatal lethality (Ben-Arie et al., 1997), and their cochlear and vestibular epithelia are devoid of any detectable hair cells. Hair cell-specific markers, such as calretinin and myosin VI, are also undetectable immunologically, supporting the requirement of Math1 in the generation of inner ear hair cells (Bermingham et al., 1999).

A 1.4 kilobase Math1 enhancer sequence has been previously identified (Helms et al., 2000) which has been shown to be sufficient in driving reporter gene expression in a number of Math1 expressing domains, and is a highly conserved sequence between mouse and human. Lumpkin et al. (2003) were then able to generate transgenic mouse strains using a GFP-expressing reporter construct with a nuclear localising signal (Math1/nGFP). This allowed for the study of Math1 enhancer activity *in vivo*, using the nuclear localising signal to concentrate the GFP for transcription factor co-immunolabelling. From the *in vivo* studies it was found that the Math1/nGFP reporter was able to accurately depict Math1 expression in the developing hair cells of the auditory and vestibular systems. Consequently, the Math1/nGFP enhancer reporter could be utilised as a method of monitoring hair cell differentiation from otic progenitors derived from hES cells *in vitro*.

Until now, we do not have a system that will allow us to monitor otic differentiation in real time. Having cells that will report on the generation of progenitors, as well as on the generation of the sensory lineages could prove a powerful tool not only to expand our understanding of cell fate determination and commitment, but also for the screening of molecules that would facilitate the production of these cell types. In this regard, the regulatory sequences for *SOX2* and *ATOH1* could be highly useful.

### *3.1.6 General objectives of the chapter*

The general aims of this chapter will be to generate hES cell reporter lines that will allow us to monitor the generation of otic progenitors and, eventually, of sensory hair cells by using otic-*SOX2* specific enhancers and *ATOH1* regulatory sequences. Working towards this aim, initially the investigation and characterisation of the expression of the otic placode-specific SOX2 enhancers (NOP-1 and NOP-2) and the *ATOH1* enhancer via transient transfections, and to assess their suitability for use in a hES cell reporter line system. Optimal methodologies for transient and stable transfections will also be determined. Stable lines will then be characterized and studied in detail.

## 3.2 Results

### *3.2.1 Transient transfection of mFASCs, hFASCs and hES cell-derived otic progenitors*

It was important to characterise the expression activity of the NOP-1 and NOP-2 enhancer sequences in the mFASCs, hFASCs and hES cell-derived otic progenitors in order to assess their suitability for later generating a hES cell reporter line. A transient transfection approach was taken to determine the enhancer activity in these populations.

To successfully carry out transient transfections it was necessary to optimise the transfection methodology itself. The plasmid pCAG-GFP was introduced into the cell types of interest (mFASCs, hFASCs, and H14S9 hES cell-derived otic progenitors) by electroporation or lipofection. pCAG is a hybrid construct comprising of the cytomegalovirus enhancer fused to the chicken beta-actin promoter and is commonly used to drive constitutive expression of high levels of a transgene of interest. For electroporation cells were required to be typsinised into a single cell suspension before the introduction of plasmid DNA, followed by seeding them into wells of a 48 well plate. In contrast, for lipofection cells were seeded into wells of a 48 well plate 24 hours prior to transfection with Lipofectamine LTX and PLUS reagent solution (Life Technologies). Further details of the two transfection methods used can be found in Chapter 2.

All attempts to transfect the different cell populations via electroporation resulted in very poor cell viability. A range of pCAG-GFP plasmid concentrations (from 250 ng to 1 µg) and electroporation parameters (Chapter 2) were tested but cell survival 24 hours post transfection was very poor and no visible GFP expression could be detected by fluorescent microscopy. For lipofection, it was important to investigate whether the presence or absence of serum in the culture media during transfection would affect cell survival and/or transfection efficiency. The cell types of interest in this chapter are routinely maintained in serum-free based media (OSCFM, see Chapter 2). 24 hours following lipofection with 500 ng of plasmid DNA the number of GFP positive

cells were counted and expressed as a mean percentage of the total number of cells per field of view, as shown in Figure 3.1. As anticipated (Brunette et al., 1992; Ross and Hui, 1999) the efficiency of lipofection, denoted by a higher percentage of GFP positive cells, was greater when the transfection was carried out in serum-free culture media compared to being in the presence of serum, as the presence of serum throughout lipofection has previously been shown to be inhibitory. This was found to be consistent across all cell types investigated (mFASCs 23.6% ± 6.2% and 3.1% ± 1.4%; hFASCs 26.0% ± 5.6% and 2.8% ± 1.6%; H14S9 otic progenitors 30.5% ± 9.1% and 3.8% ± 1.2% respectively). Subsequently, all transient transfections using these cell types were carried out via lipofection in a serum-free environment.

**Figure 3.1: Transfection efficiency of pCAG-GFP using Lipofectamine LTX in mFASCs, hFASCs and H14S9 otic progenitors.** GFP positive cells counted 24 hours post transfection using fluorescent microscopy and presented as the mean percentage of GFP positive cells per field of view (10x magnification). Error bars denote mean and standard deviation of all fields of view counted.

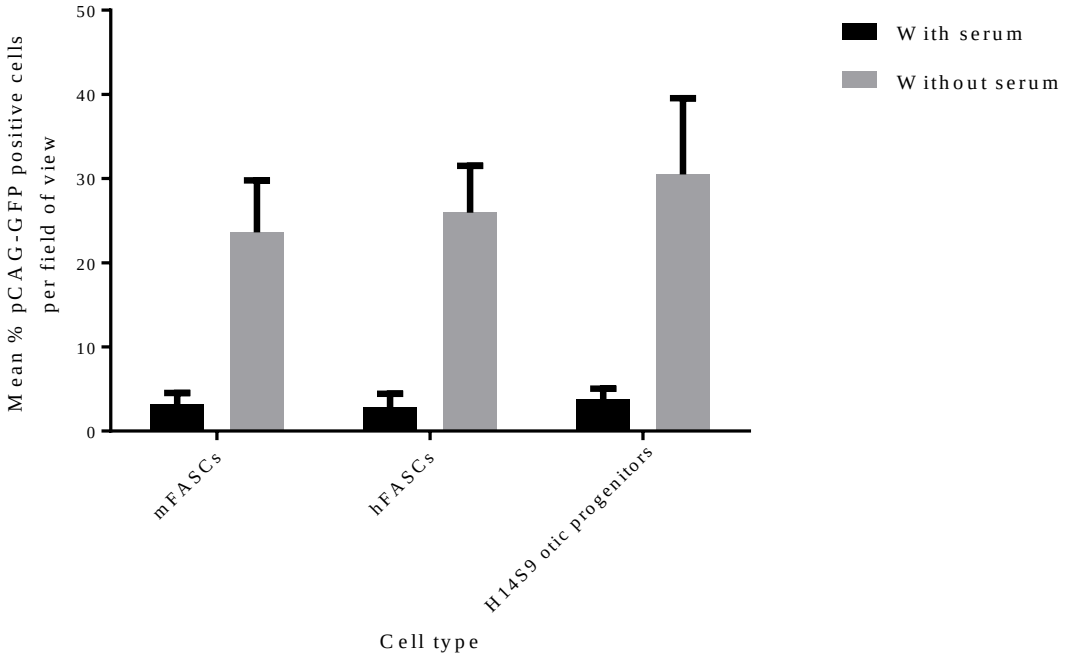

### *3.2.2 Otic placode-specific SOX2 enhancer sequences are active in mFASCs, hFASCs, and human embryonic stem cell derived otic progenitors*

In an attempt to determine the level of activity of the NOP-1 and NOP-2 *SOX2* enhancer sequences (Uchikawa et al., 2003) in different cell populations, a transient transfection approach was taken. Plasmid vectors containing the chicken (referred to here as cNOP-1 and cNOP-2) or a tetrameric form of the mouse (mNOP-1/2x4) enhancer sequences upstream of a GFP reporter were a kind gift from the Kondoh laboratory, where these enhancer sequences were initially identified. Plasmid preparations of these enhancers were carried out as previously described in Chapter 2. Briefly, XL1-Blue MRF electrocompetent bacteria were transformed via electroporation and cultured in Luria broth containing ampicillin antibiotic to select for successfully transformed bacteria. Plasmid Mini Kit (Qiagen) was used to prepare and purify the plasmid DNA. To ensure the plasmid DNA contained the correct enhancer sequences, restriction enzyme mapping was carried out.

Upon purification of the enhancer sequence plasmid DNA, transient transfections were carried out in mFASCs, hFASCs and H14S9 hES cell-derived otic progenitors (at day 6 and day 12 of the otic differentiation protocol) using Lipofectamine LTX and PLUS reagent in serum-free media. 24 hours post transfection the number of GFP positive cells were counted and a percentage of the total number of cells per field of view was calculated. The mean percentages were then normalised to the pCAG-GFP control for each cell type and are represented in Figure 3.2. It was found that the mNOP-1/2x4 enhancer sequence was detectably expressed in a very high percentage of all of the transfectable cells in mFASCs (100%), hFASCs (93.2%) and day 12 H14S9 otic progenitors (89.5%). The individual cNOP-1 and cNOP-2 enhancer sequences had lower levels of expression in all the cell types overall, but were consistent in expression between mFASCs and hFASCs (34.6% and 25.5% in mFASCs, 32.8% and 34.8% in hFASCs, respectively). In the H14S9 otic progenitors investigated at day 6 of the otic differentiation protocol the expression of cNOP-1 and cNOP-2 was visibly undetectable. However a very low expression (8.3%) of cNOP-1 was detected in the day 12 H14S9 otic progenitors.

**Figure 3.2: Transient transfection of NOP1/2 enhancer sequences in mFASCs, hFASCs and H14S9 otic progenitors.** Mean percentages of GFP expressing cells are presented as normalised from the pCAG-GFP control of each cell type. Error bars denote mean and standard deviation of all fields of view counted (at 10x magnification). Statistical significance determined by one way ANOVA with Bonferroni's multiple comparison post-test. ns = no significant difference. ****$P$<0.0001.

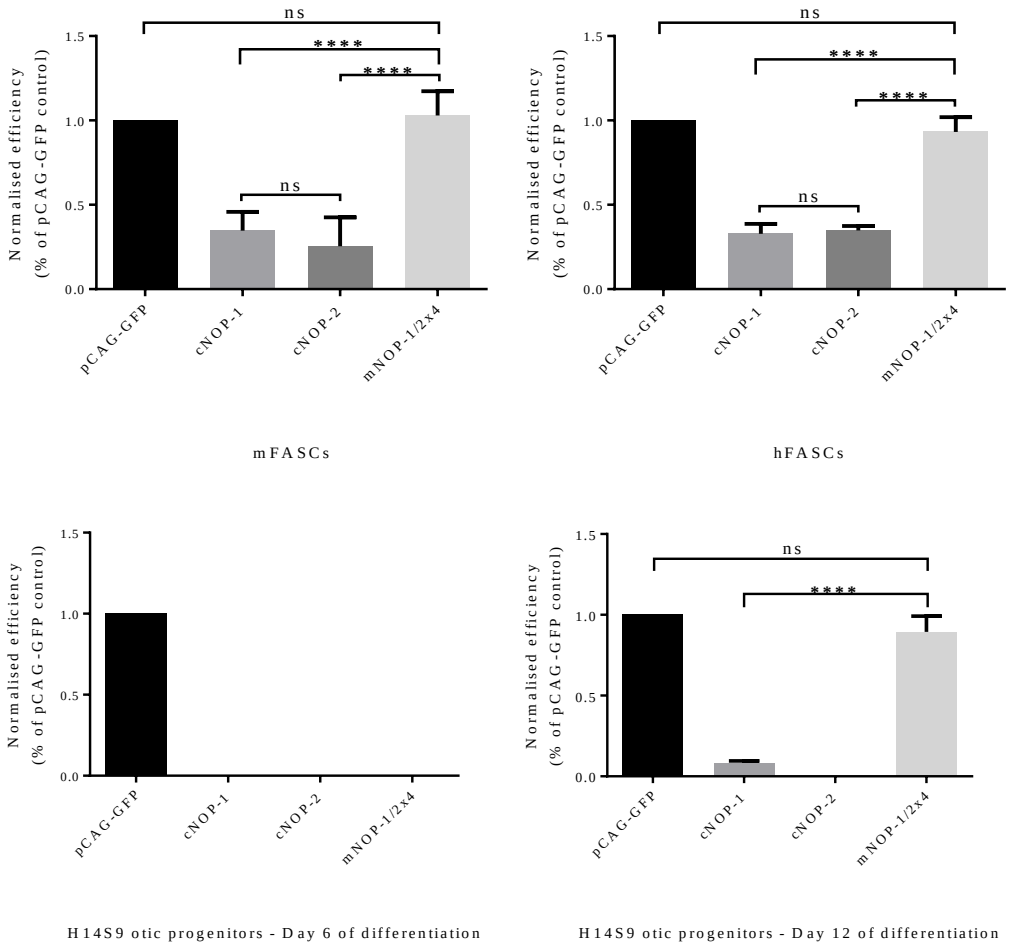

### *3.2.3 Using otic placode-specific Sox2 enhancer sequences to generate a stably transfected human embryonic stem cell reporter line to monitor otic differentiation in vitro*

The murine tetrameric form of the nasal and otic placode-specific *SOX2* enhancer sequences (mNOP-1/2x4) was chosen to generate a stably transfected hES cell reporter line. The tetrameric form of the enhancer visibly boosted the brightness of the GFP expression during the transient transfections of the cell types discussed previously, when compared to the GFP brightness produced from the single cNOP-1 or cNOP-2 enhancers. H14S9 was chosen as the parental cell line, with pEGFP-1 as the plasmid vector of choice as it features a selectable marker (G418 antibiotic resistance conferred via a neomycin resistance cassette) which is required to select for stably transfected cells, and has been successfully employed previously in the generation of stable hES cell reporter lines (Lenka et al., 2002; Noisa et al., 2010). Detailed information on the generation of the reporter plasmid construct can be found in Chapter 2. Briefly, the mNOP-1/2x4 enhancer tandem along with the heat shock protein 68 (hsp68) minimal promoter and EGFP sequence was enzymatically digested from the phspEGFPver2 plasmid and ligated into the pEGFP-1 vector. From here on this nasal and otic placode-specific *SOX2* plasmid reporter construct will be referred to as pEGFP-1 NOP-SOX2.

Once the plasmid reporter construct was generated it was transfected into the H14S9 parental hES cell line. As with the transient transfections discussed earlier in this chapter, it was important to determine the optimal transfection conditions and methodology for the hES cells (details in Chapter 2). Electroporation and lipofection were tested, with the plasmid reporter construct either being linearised (with the restriction endonuclease enzyme ApaLI) or circular. As a stably transfected cell line was required, it was important to transfect the hES cells in a single cell state in order to permit clonogenicity. Once the reporter plasmid was transfected into the cells, G418 antibiotic was required to be added to the hES culture media in order to select for successfully transfected colonies. Because of this, transfected cells had to be maintained in feeder-free conditions (matrigel as a matrix and mTeSR1 as a maintenance medium) due to the sensitivity of the mouse feeders to the G418 antibiotic. A kill curve experiment was carried out (Figure 3.3) using the parental

H14S9 cell line to determine the optimal concentration of G418 to use for this selection. A kill curve may be defined as the concentration of G418 antibiotic that kills all of the parental H14S9 cells within five days of treatment. A range of concentrations were tested (0 – 500 µg/ml) and as demonstrated in Figure 3.3 the optimal concentration was found to be 20 µg/ml G418. During optimisation of the transfection methodology, H14S9 hES cells were electroporated or lipofected with 10 µg linearised or circular pEGFP-1 NOP-SOX2 reporter plasmid DNA. After an initial recovery period of 48 hours post transfection, transfected cells were maintained in mTeSR1 medium with the supplementation of 20 µg/ml G418 antibiotic for a further 21 days. At the end of this time period, the lipofected hES cells did not produce any colonies from linearised or circular plasmid DNA transfection. Two poorly defined colonies had formed from electroporation of the circular plasmid DNA, in contrast to 12 colonies from linearised plasmid DNA electroporation. These 12 colonies were individually picked and expanded to generate a frozen bank prior to testing reporter activity during the *in vitro* otic differentiation protocol. The reporter line will henceforth be referred to as H14S9 NOP-SOX2.

An important aspect of the H14S9 NOP-SOX2 reporter line is that the clones are morphologically comparable to the H14S9 cell line (Figure 3.4A). In addition, there is no difference in the relative expression of the pluripotency genes (OCT4, SOX2 and NANOG) between the parental H14S9 and the H14S9 NOP-SOX2 reporter line (Sarah Jacob-Eshtan, unpublished data, Appendix 1). Interestingly, some of the H14S9 NOP-SOX2 reporter colonies in the undifferentiated state have a low level of GFP expression. This is not a phenomenon featured in all undifferentiated colonies, and where it is present it has a tendency to be found towards the peripheral edges of the colonies (Figure 3.4B). This heterogeneous, low level of expression has been explored in a parallel work by Sarah Jacob Eshtan.

**Figure 3.3: Kill curve experiment of H14S9 hES cells with G418 antibiotic**. Cells were maintained in a 12 well plate format on a matrigel matrix in mTeSR1 medium supplemented with 0, 20, 50, 100, 200 or 500 µg/ml G418 antibiotic. The number of cells were counted every 24 hours for five consecutive days. 20 µg/ml G418 antibiotic killed all parental H14S9 hES cells by day 5 of treatment and so this concentration was used to select for successfully transfected cells.

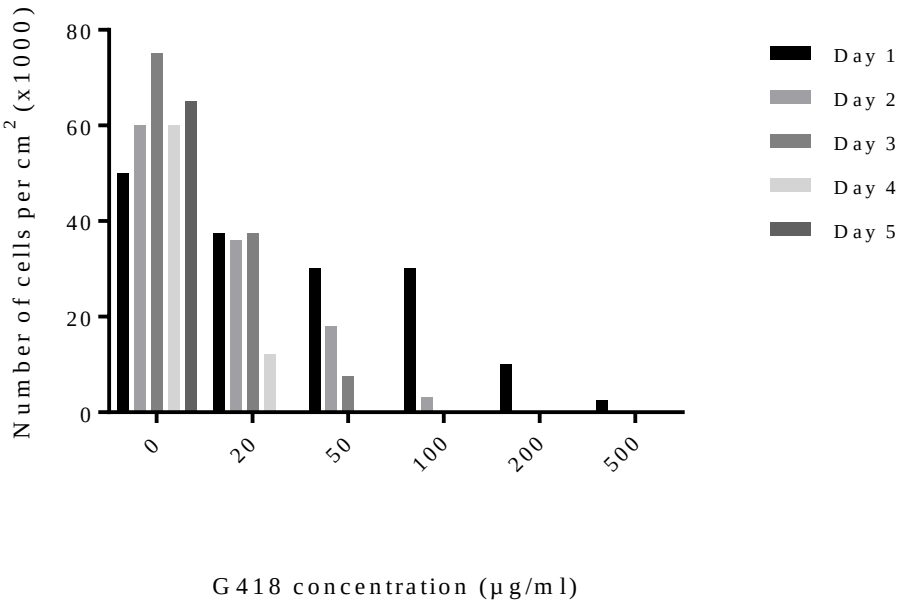

**Figure 3.4A: Micrographs of the H14S9 and H14S9 NOP-SOX2 hES cell lines**. Phase images show that the H14S9 NOP-SOX2 reporter line is morphologically similar to its parental H14S9 cell line. 4x magnification. Scale bars are 1000 µm. **Figure 3.4B: Micrographs of the H14S9 NOP-SOX2 reporter line expressing GFP**. GFP-expressing cells can be seen in some undifferentiated colonies, typically concentrated towards the outer perimeter of the colonies. 10x magnification. Scale bars are 400 µm.

**3.4A**

H14S9 H14S9 NOP-SOX2

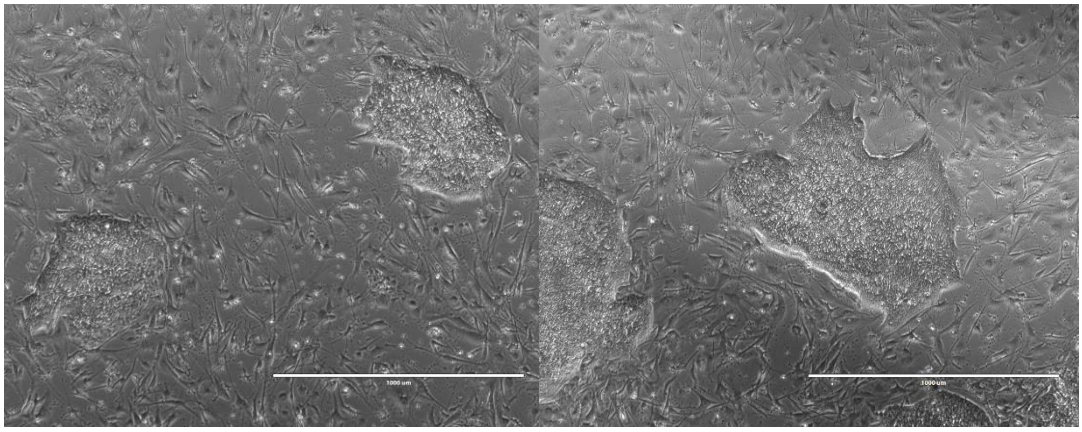

**3.4B**

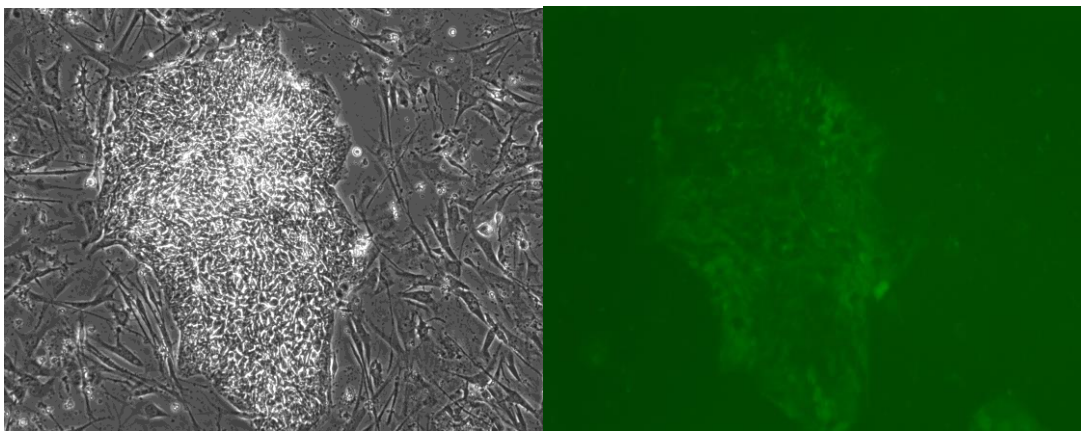

### *3.2.4 Parental H14S9 and H14S9 NOP-SOX2 reporter line activity during in vitro otic differentiation*

As described in detail in Chapter 2, through the supplementation of basal DFNB (DMEM, F12, N2 and B27) media with the key signalling ligands FGF 3 and FGF 10, undifferentiated hES cells can be induced to differentiate into progenitors of the otic lineage. Amongst various extraneous cell types, two predominant cell types of interest are produced during the 12 day differentiation process; epithelioid-like cells (referred to as otic epithelial progenitors, or OEPs) and neural-like cells (referred to as otic neural progenitors, or ONPs). These two progenitor populations are morphologically distinct, but share a common gene expression profile. *PAX8* (paired box 8), *PAX2* (paired box 2), *FOXG1* (forkhead box G1) and *SOX2* (sex determining region Y-box 2) are characteristic markers of otic progenitors. Previously published work in the laboratory (Chen et al., 2012) has demonstrated that a large proportion of the differentiated cells (approximately 78% and above) induced by FGF 3 and FGF 10 signalling co-express combinations of the aforementioned otic markers. Imaging and relative fluorescence intensity data was generated using the In Cell Analyzer 1000 automated microscopy platform (GE Life Sciences). When a stringent threshold of the 75$^{th}$ intensity percentile was applied, a smaller proportion (approximately 15% to 20%) of these cells were found to co-express high levels of otic marker combinations in the FGF medium condition compared to the DFNB control, and these high expressing cells are believed to be the true population of otic progenitors.

Differentiation experiments using the parental H14S9 hES cells were carried out (as detailed in Chapter 2) using control DFNB or with DFNB medium supplemented with FGF 3 and FGF 10 (referred to from here on as FGF medium). Cells were differentiated for 12 days and were immunolabelled with the primary antibody combinations SOX2/PAX8, SOX2/PAX2 and SOX2/FOXG1 and analysed using the In Cell Analyzer 1000 (representative experiment in Figure 3.5A with results of three repeat experiments displayed in Figure 3.5A'). A cell is considered to be positive for a particular antibody labelling if the fluorescence intensity value is higher than the 99$^{th}$ percentile threshold intensity of the secondary antibody-only control. The 75$^{th}$ fluorescence intensity percentile was then applied to determine the proportion of the brightest immunolabelled cells. Parallel differentiation experiments were set up in

order to determine the activity of the H14S9 NOP-SOX2 hES reporter line and to ensure of its usefulness and reliability as an *in vitro* assay for otic induction. At the end of the 12 day differentiation period, the percentage of NOP-SOX2 GFP expressing cells was determined (Figure 3.5B). Cells were also fixed, immunolabelled with PAX8, PAX2 or FOXG1 primary antibodies with Alexa 568 secondary antibodies, and imaged on the In Cell Analyzer 1000 platform. The number of positive cells co-expressing otic markers with NOP-SOX2 reporter GFP were ascertained. Results from three repeat experiments are represented in Figure 3.5B'). It is also important to note that across the three replicate experiments very small numbers of cells were positive for NOP-SOX2 GFP with negative antibody staining for PAX2 (based on the $99^{th}$ percentile) (0.1% ± 0.02%), PAX8 (0.17% ± 0.07%) or FOXG1 (0.28% ± 0.04%).

Consistent with the previously published data (Chen et al., 2012) the percentage of highly double positive cells in the parental H14S9 was overall greater in the FGF treated condition compared to the baseline DFNB condition for all antibody combinations investigated. 15.7% ± 1.9% of the cells expressed high levels of SOX2 and PAX8 ($SOX2^{hi}PAX8^{hi}$) in the FGF condition compared to 5.9% ± 4.6% in the DFNB condition, 20.7% ± 1.2% in FGF compared to 11.7% ± 3.4% in DFNB were found to be $SOX2^{hi}PAX2^{hi}$, and 25.7% ± 3% in FGF compared to 9.6% ± 2.3% in DFNB for $SOX2^{hi}FOXG1^{hi}$ (Figure 3.5A and 3.5A').

31.0% ± 10.8% of NOP-SOX2 GFP positive cells were found at the end of the 12 day protocol in the DFNB condition compared to 42.7% ± 9.7% in FGF medium (n=4 experiments, Figure 3.5B). A greater percentage of NOP-SOX2 GFP reporter expression co-staining with other key otic markers was found in the FGF treated condition compared to the DFNB control (19.6% ± 0.5% and 10% ± 3.7% for NOP-SOX2/PAX8, 23.6% ± 1.3% and 13.3% ± 1.1% for NOP-SOX2/PAX2, and 22.2% ± 1.8% and 11.7% ± 2.4% for NOP-SOX2/FOXG1 respectively) (Figure 3.5B').

**Figure 3.5A**: **Parental H14S9 hES cells differentiated for 12 days in DFNB or FGF medium.** Representative experiment displayed below. Experiments ran in parallel to those in Figure 3.5B. Scatterplots for immunolabelling with SOX2/PAX8 (green/red), SOX2/PAX2 (green/red) and SOX2/FOXG1 (green/red). Fluorescence intensity of each antibody is displayed on each axis. The scatter plots are coloured according to two different intensity thresholds: 99th percentile points of fluorescent intensity in the secondary antibody only control, and 75$^{th}$ percentile points of fluorescent intensity seen in the FGF condition labelling. Grey: intensity below 99$^{th}$ percentile. Green: intensity above the 99$^{th}$ percentile for the green (SOX2) but not red channel (PAX8, PAX2 or FOXG1). Red: intensity above the 99$^{th}$ percentile in the red channel but not green channel. Purple: cells are double positive, intensity above the 99$^{th}$ percentile in both channels. Black: cells are highly double positive, intensity is above the FGF 75$^{th}$ percentile in both channels.

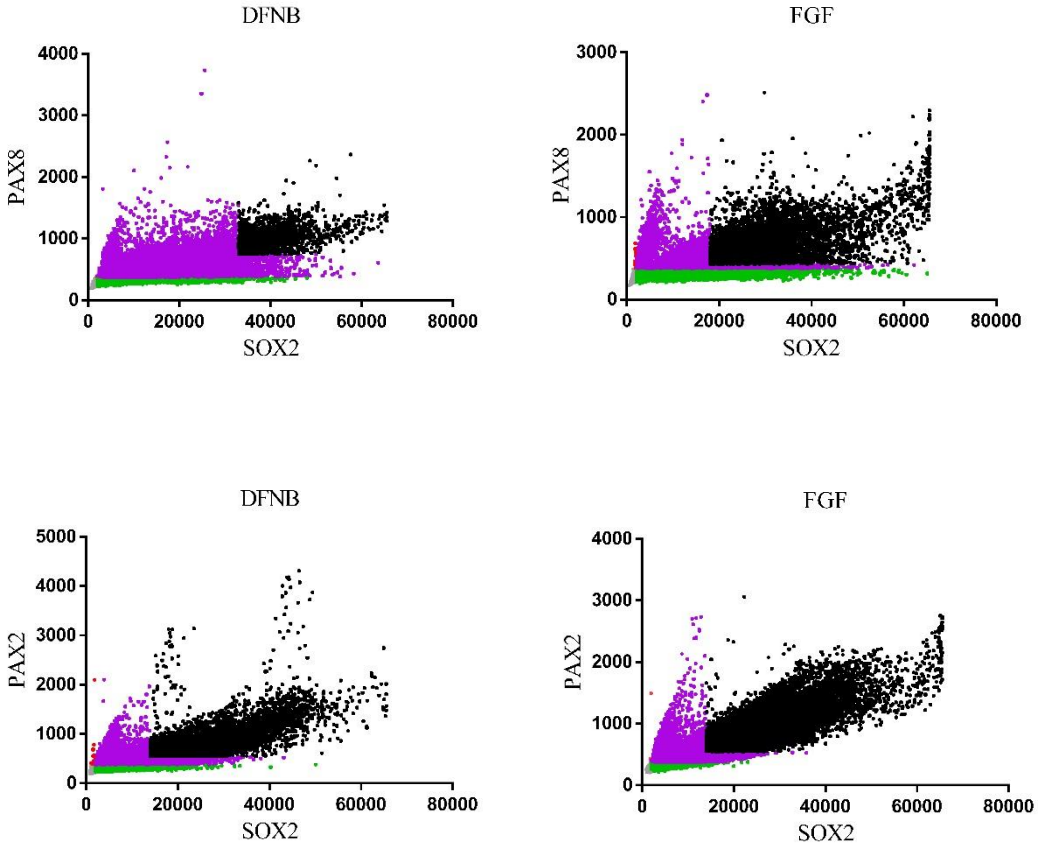

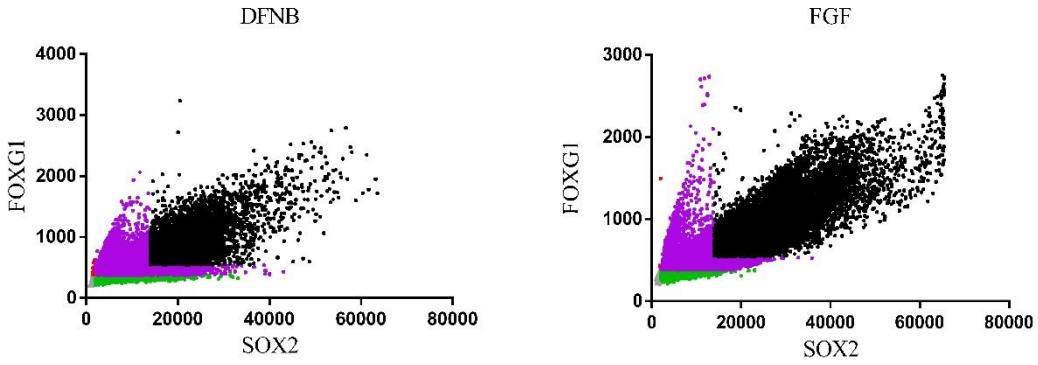


**Figure 3.5A': Parental H14S9 hES cells differentiated for 12 days in DFNB or FGF medium**. Bar charts show the percentage of highly double positive cells (with a threshold intensity above the 75$^{th}$ percentile) in each condition for the antibody combinations SOX2$^{hi}$/PAX8$^{hi}$, SOX2$^{hi}$/PAX2$^{hi}$, and SOX2$^{hi}$/FOXG1$^{hi}$. The results are presented as three experimental replicates combined. Error bars denote mean and standard deviation. Statistical significance was determined using Chi-square with Yates' continuity correction. ****$P$<0.0001.

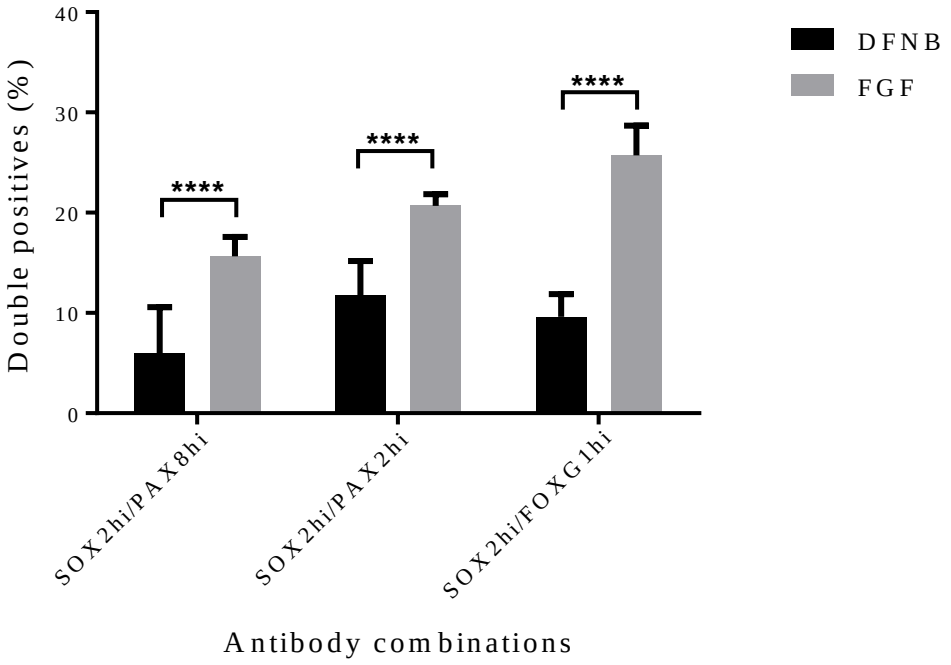

**Figure 3.5B: GFP expression in NOP-SOX2 differentiated cells.** H14S9 NOP-SOX2 reporter cells were differentiated in DFNB or FGF medium for 12 days. GFP positive cells per field of view were counted and presented below as a mean percentage of the total number of cells per field. Error bars denote mean and standard deviation. Using an unpaired t-test the differences between the means from DFNB and FGF medium are not statistically significant (n=4).

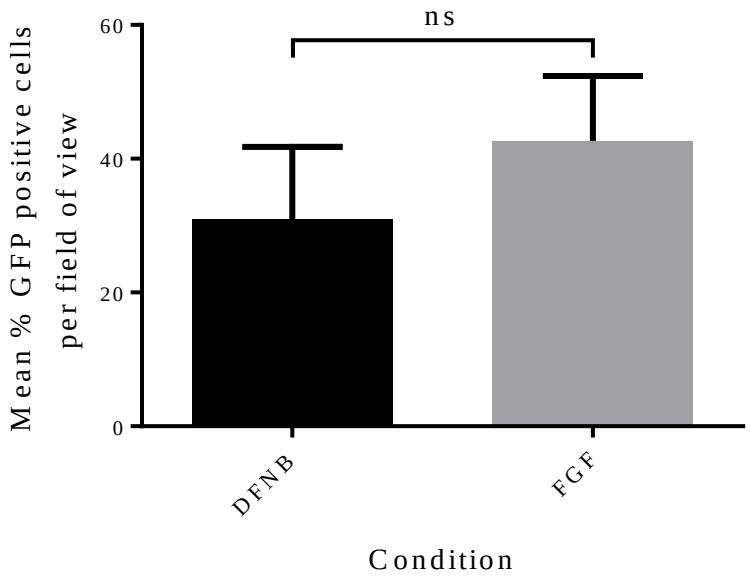

**Figure 3.5B': Co-staining of H14S9 NOP-SOX2 differentiated reporter cells.** Cells were immunolabelled with PAX8, PAX2 or FOXG1 primary antibodies, and the percentage of double positive cells (primary antibody and NOP-SOX2 GFP) is shown below (n=3). Error bars denote mean and standard deviation. Statistical significance was determined using Chi-square with Yates' continuity correction. **P*<0.05, *****P*<0.0001.

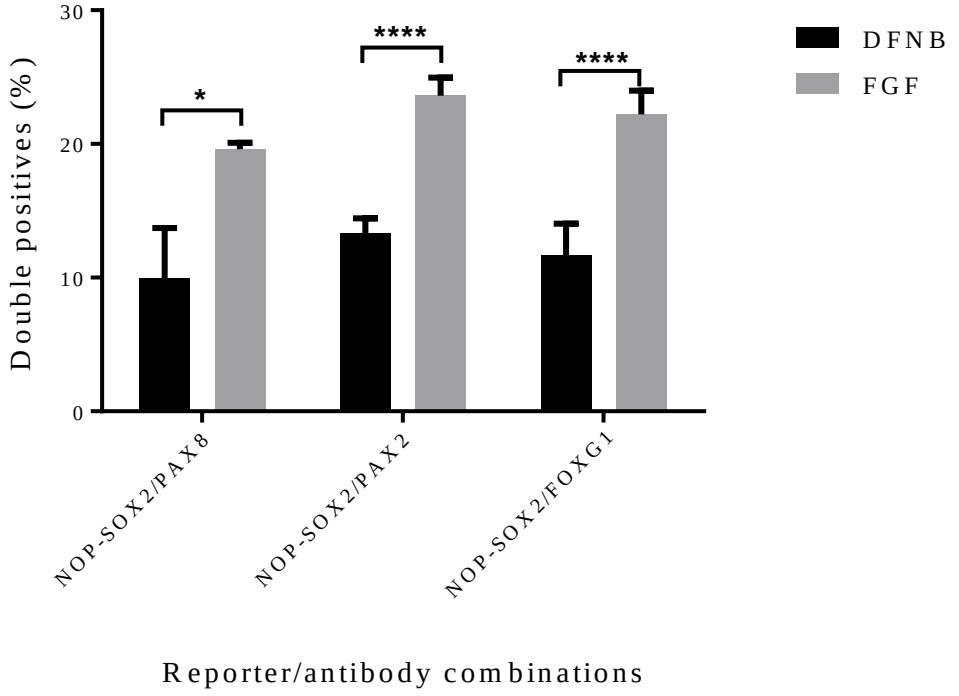

### *3.2.5 Cellular morphology and reporter expression in H14S9 NOP-SOX2 otic differentiation*

As mentioned previously in this chapter, when hES cells are subjected to our *in vitro* otic differentiation protocol a number of different cell morphologies are produced. Two of these morphologies are of particular interest; otic epithelial progenitors (OEPs) and otic neural progenitors (ONPs). As well as their morphological distinctions, the downstream applications and differentiation capacities of OEPs and ONPs are also discrete. The OEPs have been previously shown to have a capability to further differentiate into hair cell-like cells, whereas the ONPs can readily differentiate into the more mature sensory auditory neurons (Chen et al., 2012). A purified culture of either OEPs or ONPs is required in order to further differentiate them. Currently, the methodology in the laboratory for the purification of a particular cell type of interest is to manually clean the differentiating cultures. Usually beginning at day four to six of the 12 day differentiation protocol, unwanted cell morphologies are scraped away using a sterile plastic Pasteur pipette, and the remaining cell type of interest may then be expanded. There are a number of disadvantages to this current technique of cell purification. It can be labour intensive, prone to subjective bias, and there is no way to determine whether the cells being selected are truly otic in nature based on morphology alone. Recent research in the laboratory has sought to look for more reliable methods of selecting for the cell types of interest, including identifying cell surface markers to sort via flow cytometry. Unfortunately this research has had very limited success so far.

The H14S9 NOP-SOX2 reporter line can be utilised to provide greater insight into our *in vitro* otic differentiation protocol by offering more detail on the cell morphologies produced during differentiation in relation to the reporter GFP expression. Differentiating H14S9 NOP-SOX2 cells were monitored throughout the 12 day protocol and the emerging colonies were noted for both their morphology (OEP, ONP or ‘other’) and GFP expression status (positive or negative) (Table 3.1). Illustrative examples are shown in Figure 3.6.

**Table 3.1: Colony morphology and NOP-SOX2 GFP expression in a typical experiment.** The total number of colonies per field (10 fields counted in total) were counted using phase microscopy at day 12 of otic differentiation. Colonies were then noted for their GFP expression status (positive or negative).

| Colony type | GFP positive | GFP negative | Total | GFP positive (%) |
|---|---|---|---|---|
| **OEP** | 9 | 7 | 16 | 56.3 |
| **ONP** | 7 | 11 | 21 | 33.3 |
| **Other** | 4 | 13 | 17 | 23.5 |

**Figure 3.6: OEP and ONP colonies can be NOP-SOX2 GFP positive or negative.** Illustrative examples of day 12 progenitors differentiated with FGF medium. 4x magnification. Scale bar is 1000 μm.

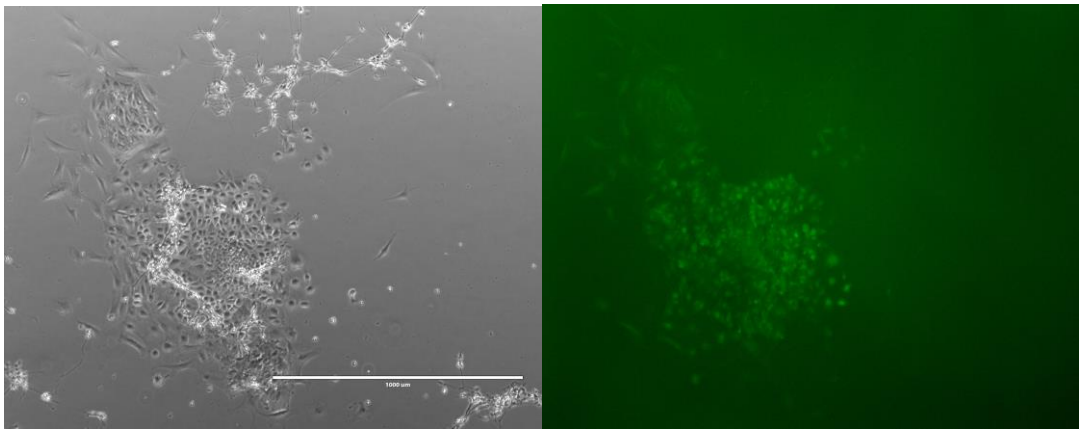

### *3.2.6 Pax6 expression can be used as a marker of nasal placode progenitors*

OEP and ONP colonies (and other colony morphologies) formed from the H14S9 NOP-SOX2 hES reporter line during the otic differentiation protocol vary in their level of GFP expression (3.2.5). As the *SOX2* enhancer sequence used to create the reporter line has been shown to display activity in both the nasal and otic placodes in developing chick and mouse embryos (Uchikawa et al., 2003), it was important to attempt to distinguish NOP-SOX2 reporter expression in the hES cell-derived progenitors as being either nasal or otic. *PAX6* expression has been used in previous research as a marker for nasal placodal progenitors, and is known to be restricted from the maturing progenitors of the otic placode during development (Bhattacharyya and Bronner-Fraser 2008; Grindley et al., 1995; Lleras-Forero et al., 2013).

In order to assess this H14S9 NOP-SOX2 hES cells were differentiated in either baseline DFNB or FGF medium for the standard 12 day otic differentiation protocol. Differentiating progenitors were fixed at day 12 of the protocol and immunolabelled with a monoclonal PAX6 primary antibody using standard laboratory protocol (see Chapter 2 for details) and image analysis was carried out using the In Cell Analyzer 1000 platform. Figure 3.7 displays the percentage of NOP-SOX2 GFP/PAX6 double positive cells from both DFNB and FGF differentiation conditions. It was observed that 50.13% ± 8.50% of the differentiated cells in the DFNB condition were double positive for NOP-SOX2 GFP and PAX6, compared to 27.92% ± 4.70% in the FGF treated condition.

**Figure 3.7: PAX6 expression in H14S9 NOP-SOX2 reporter differentiated for 12 days in DFNB or FGF medium**. Cells were co-labelled with a monoclonal PAX6 antibody and the percentage double positive cells (NOP-SOX2 GFP with PAX6 antibody staining) is presented. Error bars denote mean and standard deviation. Statistical significance was determined using Chi-square with Yates' continuity correction (n=2). **P*<0.05.

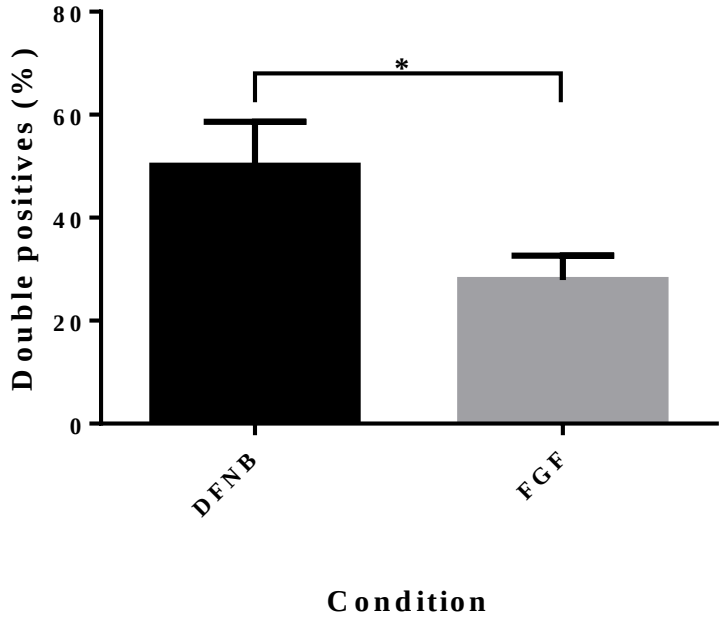

### *3.3 Using an Atoh1 enhancer sequence to generate an Atoh1-reporting hES reporter cell line*

The 1.4 kilobase Atoh1 (Math1) enhancer sequence identified by the research of Helms et al. (2000) coupled to a nuclear localising signal sequence has been shown to be sufficient to function as an Atoh1 reporter. Its patterns of expression during *in vivo* development are found in Atoh1 domains such as Merkel cells of the skin, granular cell progenitors in the immature cerebellum, and hair cells of the cochlear and vestibular systems of the developing inner ear (Lumpkin et al., 2003). Expression was not solely restricted to Atoh1 domains, however, as some off target areas of expression were observed. Nevertheless, having a hES cell reporter line which could be used to monitor the expression of Atoh1 during *in vitro* hair cell differentiation would be very valuable, especially as Atoh1 is believed to be the earliest determinant of hair cell fate (Bodson et al., 2010; Hongmiao et al., 2014).

The Atoh1 enhancer sequence and nuclear localising signal was originally housed in the J2XnGFP plasmid (Jane Johnson, TX, USA), containing a minimal beta globin promoter sequence but lacking a selectable marker. As for the NOP-SOX2 reporter line, pEGFP-1 (Clontech) was chosen as the vector vehicle for generating a stably transfected hES reporter line. H14S9 was again used as the hES cell line of choice, as this particular cell line has repeatedly proved to be the most efficient at inducing OEP colony morphology (OEPs rather ONPs have the capacity to be further differentiated into hair cell-like cells *in vitro* in our laboratory).

The J2XnGFP plasmid construct was enzymatically digested to extract an approximately 2.5 kilobase plasmid sequence containing the minimal beta globin promoter, Atoh1 enhancer, nuclear localising signal and the EGFP sequence, and this was ligated into the pEGFP-1 vector. Plasmid DNA preparations were carried out using XL1-Blue MRF bacteria as previously described in Chapter 2. The plasmid construct will be referred to from here on as pEGFP-1 Atoh1nGFP.

The murine neuroblastoma cell line Neuro2a has been used in many previous studies investigating and manipulating Atoh1 expression and activity (Flora et al., 2009; Jeon et al., 2011; Klisch et al., 2011; Shi et al., 2010), and so acted as a control for testing

the J2XnGFP and pEGFP-1 Atoh1nGFP plasmid constructs. As in section 3.2.3, lipofection with Lipofectamine LTX and PLUS reagent (Life Technologies) was used to transiently transfect the Neuro2a cells with pCAG-GFP plasmid in order to determine the transfection efficiency. 53.5% ± 8.1% (mean ± standard deviation, n=2) of the Neuro2a cells were GFP positive 24 hours following transfection. This efficiency was then used to normalise the transient transfection efficiency of the J2XnGFP and pEGFP-1 Atoh1nGFP plasmid constructs. Illustrative images are displayed in Figure 3.8A and normalised data is shown in Figure 3.8B. A similar mean transfection percentage was observed between the parental J2XnGFP plasmid and the pEGFP-1 Atoh1nGFP construct (12.9% ± 2.8% and 15.2% ± 2.1% respectively). This result provided confidence in the efficiency and suitability of utilising the pEGFP-1 Atoh1nGFP plasmid construct to generate an Atoh1 reporting hES cell reporter line.

**Figure 3.8A: Transient transfections of J2XnGFP and pEGFP-1 Atoh1nGFP plasmid constructs in Neuro2a cells**. Images were taken at 10x magnification 24 hours post transfection (n=2). Illustrative example images are displayed below.

BRIGHTFIELD J2XnGFP

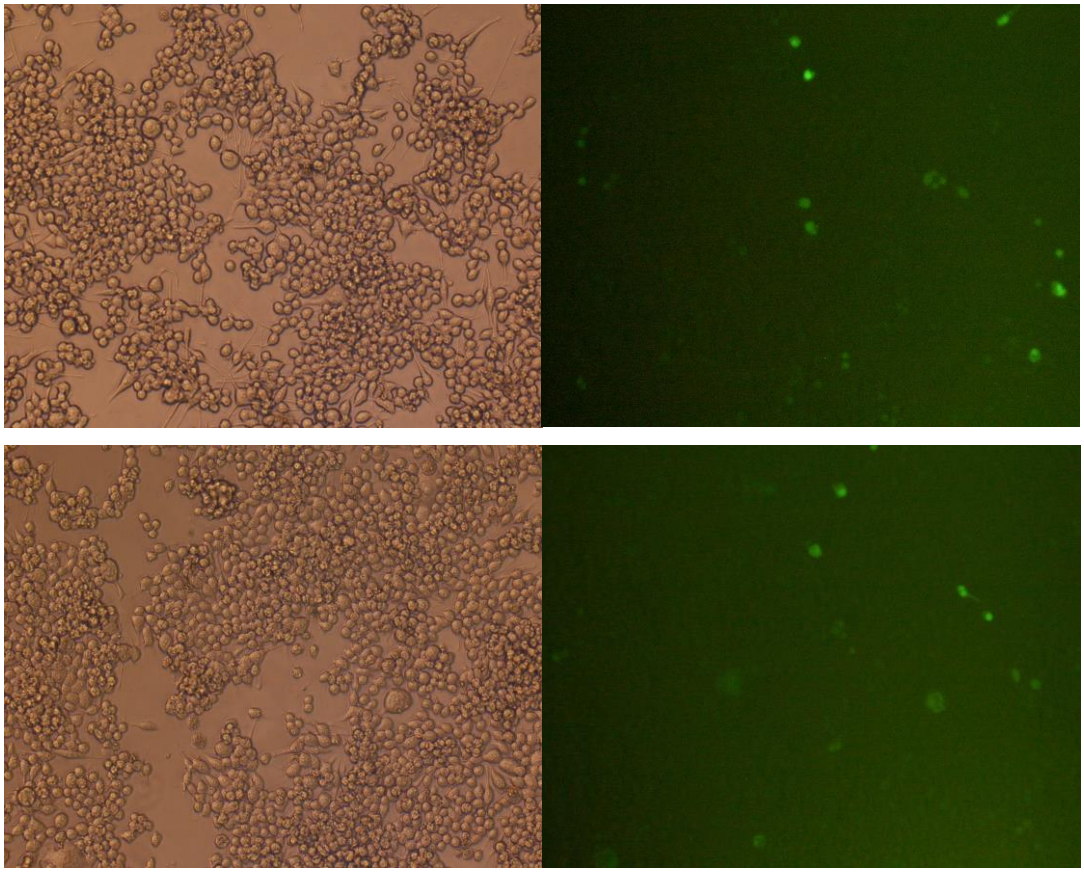

BRIGHTFIELD pEGFP-1 Atoh1nGFP

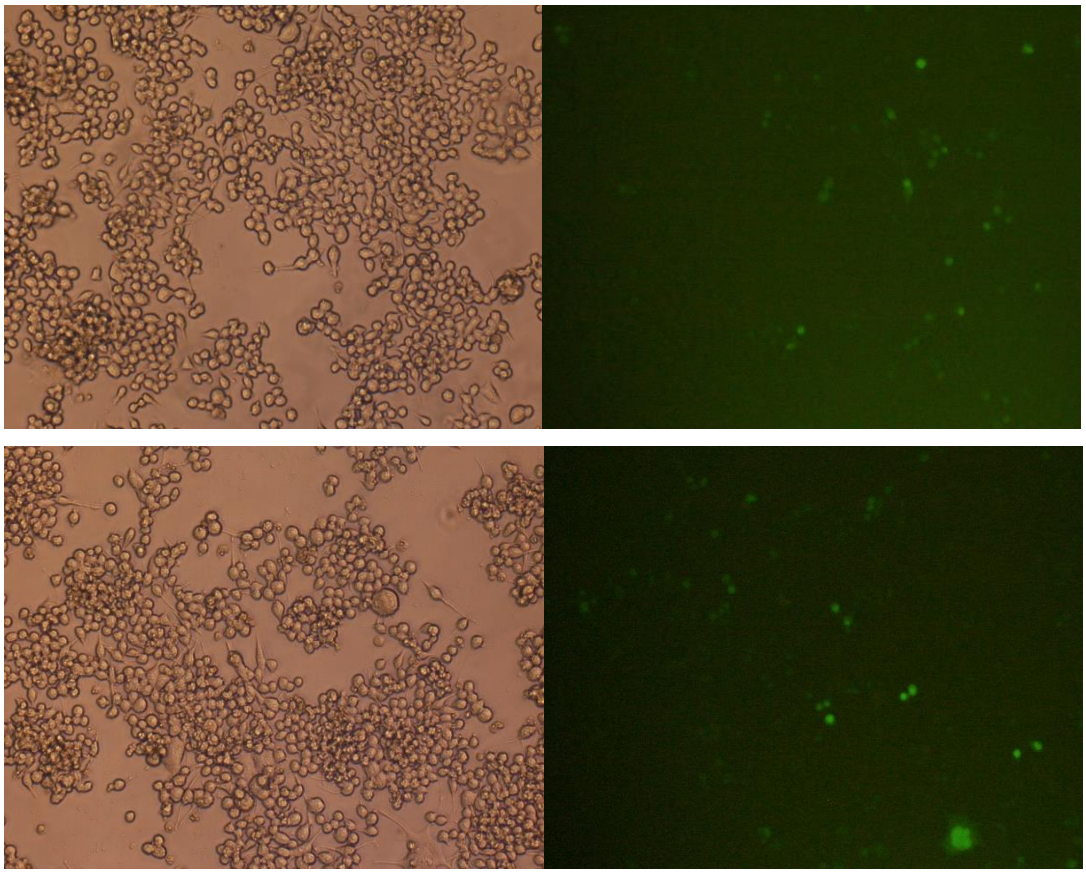

**Figure 3.8B: Transient transfections of J2XnGFP and pEGFP-1 Atoh1nGFP plasmid constructs in Neuro2a cells**. Mean percentages of GFP expressing cells are presented as normalised from the pCAG-GFP control of each cell type. Error bars denote mean and standard deviation of all fields of view counted (at 10x magnification). Statistical significance determined by one way ANOVA with Bonferroni's multiple comparison post-test. ns = no significant difference.

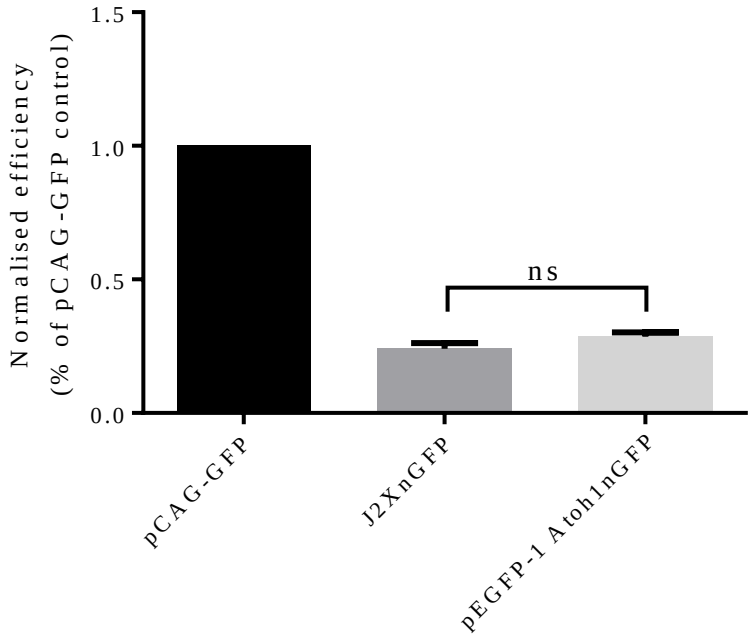

For generating the stably transfected Atoh1 hES reporter cell line, the same transfection parameters optimised for the H14S9 NOP-SOX2 reporter line were used (as pEGFP-1 was the vector of choice used for both reporter plasmid constructs). As a reminder, 10 μg of ApaLI-linearised pEGFP-1 Atoh1nGFP plasmid DNA was electroporated into a H14S9 single cell suspension and plated onto growth factor reduced matrigel. After a 48 hour recovery period 20 μg/ml G418 antibiotic (as determined by the H14S9 kill curve experiment, Figure 3.3) was introduced into the maintenance media for a further 21 days to select for transfected clones. From here on the stably transfected reporter cell line will be referred to as H14S9 Atoh1nGFP. The stably transfected reporter line is morphologically similar to the H14S9 parental cell line (Figure 3.9A). In a similar finding to that of the H14S9 NOP-SOX2 reporter line, some GFP expression could be seen in the undifferentiated state (Figure 3.9B), especially concentrated around towards the edges of the colonies. Not all H14S9 Atoh1nGFP undifferentiated colonies contained GFP-expressing cells.

**Figure 3.9A: Micrographs of the H14S9 and H14S9 Atoh1nGFP hES cell lines**. Phase images show that the H14S9 Atoh1nGFP reporter line is morphologically similar to its parental H14S9 cell line. 4x magnification. Scale bars are 1000 μm. **Figure 3.9B: Micrographs of H14S9 Atoh1nGFP reporter line**. GFP-expressing cells can be seen in some undifferentiated colonies, typically concentrated towards the outer perimeter of the colonies. 10x magnification. Scale bars are 400 μm.

**3.9A: H14S9 and H14S9 Atoh1nGFP are morphologically indistinct**

H14S9 H14S9 Atoh1nGFP

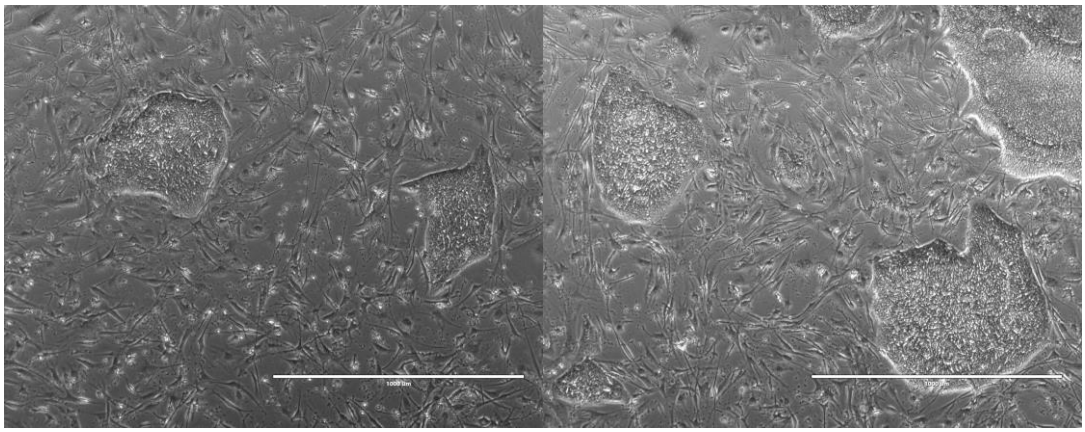

**3.9B: H14S9 Atoh1nGFP features GFP expression in some undifferentiated colonies**

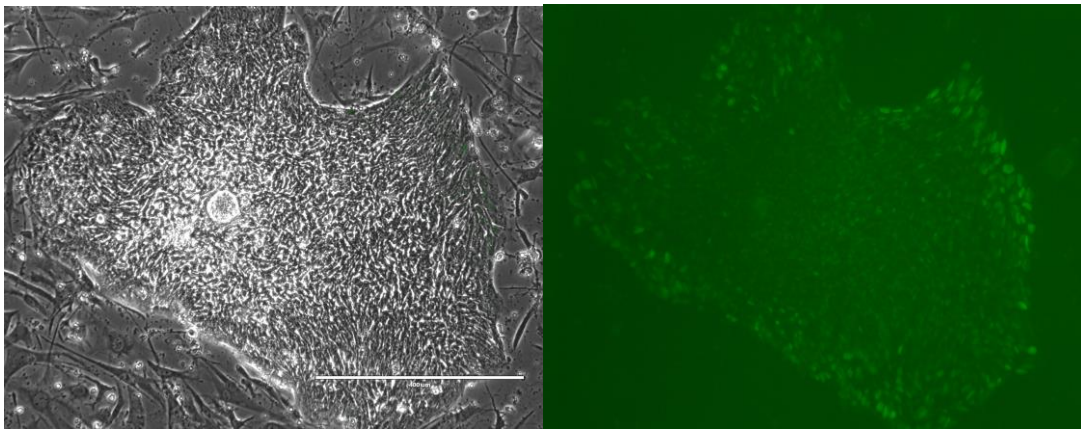

### *3.3.1 H14S9 Atoh1nGFP reporter line activity during in vitro otic differentiation*

Experiments were set up in order to ascertain how the H14S9 Atoh1nGFP reporter behaves throughout the first phase of otic differentiation. Cells were maintained in DFNB or FGF medium for the standard 12 day protocol and GFP expression was monitored. The mean percentage of GFP positive cells counted at the end of the 12 day protocol is displayed in Figure 3.10 showing no statistically significant difference in Atoh1nGFP expression between DFNB and FGF medium (22.4% ± 19.7% for DFNB and 24.4% ± 16.7% in the FGF condition).

**Figure 3.10: H14S9 Atoh1nGFP reporter cells differentiated for 12 days in DFNB or FGF medium**. GFP positive cells per field of view were counted and presented below as a mean percentage of the total number of cells per field. Error bars denote mean and standard deviation. Statistical significance was determined using Unpaired t-test (n=2). ns = no significant difference.

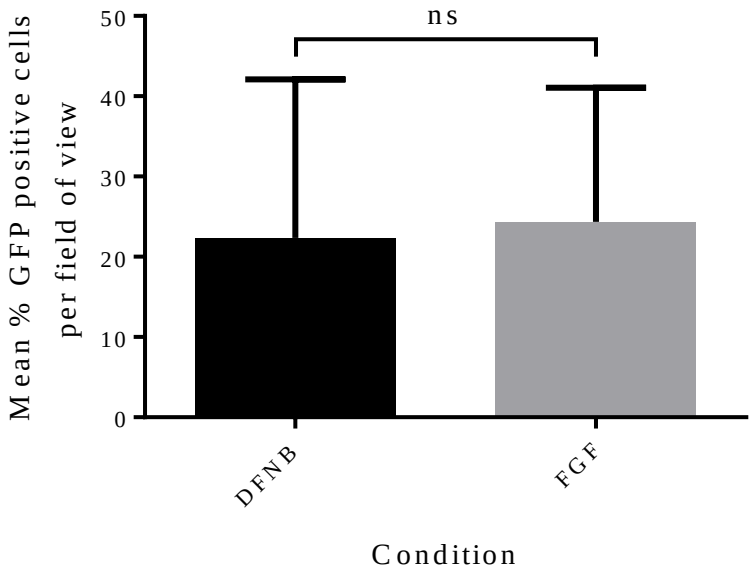

## 3.3 Discussion

### *3.3.1 Reporter line generation to monitor otic differentiation and hair cell induction in vitro*

To date there has been no information published regarding the generation of human otic placode specific reporter cell line, and only one published study based on reporting the later hair cell differentiation from hES cells (Ronaghi et al., 2014). Other studies of tracking otic development have been carried out in mice and zebrafish, and tend to be based on the use of non-otic specific genes and proteins. For example, a few studies have looked at *Pax3* expression and its contribution to the developing otic placode and otic vesicle (Freyer et al., 2011; Kim et al., 2014; Sandell et al., 2014). Despite its acknowledged importance in normal inner ear development (*Pax3* null mice have severe inner ear morphology malformations) *Pax3* expression is not exclusive to the inner ear, and is classically used in reporting on neural crest cell differentiation and migration (Wang et al., 2008). Similarly, a recent study by Economou et al. (2013) identified a 1.4 kilobase minimal enhancer sequence that was used to create an *Fgf 10* reporter system in the mouse. Expression of *Fgf 10* has been found to play a crucial role in otic placode induction, yet is also involved in the development of other tissues such as the limb buds and lungs (Itoh and Ohta, 2014). Therefore, despite such reporters displaying potential benefits to the further understanding of otic development in *in vivo* models, their lack of otic exclusivity does not make them the most ideal candidates for creating a human embryonic stem cell *in vitro* reporter line.

Using enhancer sequences which convey otic placode specificity are therefore a much more desirable reporter system to utilise. The *SOX2* enhancer sequences (NOP-1 and NOP-2) originally identified by Uchikawa et al. (2003) were found to show reporter activity solely in the developing otic and nasal placodes of developing chick embryos.

Following transient transfection of the NOP-1 and NOP-2 enhancer sequences into human fetal cochlea-derived auditory stem cells (hFASCs) initially isolated by Chen et al. (2007) we observed a very high percentage of the transfectable cells (up to 100%

in some cases) expressing tetrameric enhancer driven GFP (Figure 3.2). This was an anticipated finding as the hFASCs are obviously otic in origin and have previously been shown to express *SOX2* throughout their undifferentiated state. The high level of enhancer driven GFP expression was also noted upon transiently transfecting otic progenitors differentiated directly from hES cells. Taking these results into account provided us with the confidence that using these otic placode enhancer sequences to generate a hES cell reporter line would be most beneficial and informative as an *in vitro* assay to monitor otic differentiation.

The H14S9 NOP-SOX2 reporter line created was found to be morphologically indistinct from its parental cell line and expression of pluripotency genes was also similar between the two lines, ensuring the reporter line still behaved akin to its non-genetically modified parental hES cell line. One particular point of interest to note was the fact that low levels of GFP expression could be visually detected in some, but not all, of the H14S9 NOP-SOX2 colonies in their undifferentiated state, typically towards the outer periphery of the colonies (Figure 3.4B). This phenomenon has also been seen in other hES reporter lines, such as the ones generated by Lenka et al. (2002) and Noisa et al. (2010). In these studies, human nestin enhancer sequences were used to generate reporter lines, also with pEGFP-1 as the vector vehicle for stable transfections. Despite nestin being known to be a neural stem cell and neuroectoderm marker (King et al., 2009) low levels of nestin enhancer driven GFP expression were detected in the undifferentiated hES colonies. The GFP expression increased in fluorescent intensity upon neural differentiation and later became confined to neural progenitors. GFP expression in the undifferentiated hES state could be indicative of neural lineage commitment or priming bias occurring prior to the onset of neural differentiation. In the H14S9 NOP-SOX2 case this could suggest that the low level of GFP expression is indicative of early otic or nasal placode differentiation bias in the hES undifferentiated state. Ongoing work in the laboratory (Sarah Jacob-Eshtan, PhD Thesis) has found that the H14S9 NOP-SOX2 reporter cell line features subpopulations within the undifferentiated state which are GFP+/SSEA3+ and GFP+/SSEA3- (Stage Specific Embryonic Antigen-3). SSEA3 is a cell surface antigen used widely as an undifferentiated pluripotent stem cell marker (Draper et al., 2002). Therefore populations of undifferentiated H14S9 NOP-SOX2 hES cells which are positive for enhancer driven GFP with or without SSEA3 could indicate a priming

bias for otic or nasal placode differentiation. Indeed, these population of cells when put through our otic differentiation protocol yield a greater propensity to differentiate into otic progenitors, as characterised by upregulation of *PAX2*, *PAX8* and *FOXG1* when compared to GFP-/SSEA3+ or GFP-/SSEA3- hES cells.

It should be noted however that the method in which this reporter line was generated has some limitations. Non-targeted transfection of plasmid DNA leads to a random insertion of the transgenes without the possibility of controlling for the site of integration. This lack of control can lead to a number of potential problems. For example disruption of DNA sequences at the site of integration which may alter the phenotype of the cell or its downstream differentiation capacity, increasing the gene copy number, and the exogenous transgene sequence may itself be truncated or rearranged leading to a loss of normal expression patterns (Adamson et al., 2011). Linearising the plasmid construct prior to transfection as done here can reduce the chances of the sequence being rearranged, however. More sophisticated approaches (such as homologous recombination, CRISPR, and TALEN) could have been favourable, but due to the time required to optimise such new and emerging techniques we decided to begin exploring this topic by employing a more established random integration transgene method.

### *3.3.2 H14S9 and the H14S9 NOP-SOX2 reporter line respond to our otic differentiation protocol*

The importance of FGF 3 and FGF 10 on the induction of the otic placode first came about through the elegant study by Wright and Mansour (2003) in which it was found that Fgf 3 and Fgf 10 mouse mutants fail to form otic vesicles and have aberrant otic marker gene expression patterns. These findings led to the development of our *in vitro* otic differentiation protocol. Differentiation of hES cells leading to the induction of otic progenitors with upregulation of the characteristic otic placode markers *PAX2*, *PAX8*, *FOXG1* and *SOX2* following induction by the ligands FGF 3 and FGF 10 has previously been demonstrated in our laboratory by the work of Chen et al. (2012) in a number of different hES cell lines, and has been corroborated in this study with H14S9 (Figures 3.5A and 3.5A'). Using a stringent fluorescent intensity threshold a range of

approximately 15% to 25% of the cells differentiated in FGF medium were considered to be highly expressive of a combination of otic markers and this population is believed to represent the otic progenitors. In the control DFNB condition a significantly lower amount of otic marker co-expression was observed, demonstrating that FGF 3 and FGF 10 is required for induction of otic gene expression.

Analysis of H14S9 NOP-SOX2 differentiation showed there was no significant difference between the mean percentage of NOP-SOX2 GFP positive cells in the control DFNB and FGF conditions (Figure 3.5B). However a difference between the DFNB and FGF conditions became apparent when looking at the NOP-SOX2 GFP expression co-stained with an otic marker antibody. It was then observed that a range of approximately 20% to 25% of the NOP-SOX2 differentiated cells co-stained with the otic markers *PAX2*, *PAX8* and *FOXG1* when cultured in FGF medium, compared to approximately 10% to 13% co-staining in the control DFNB condition (Figure 3.5B').

Considering these data together suggests that the co-expression of NOP-SOX2 enhancer driven GFP with *PAX2*, *PAX8* and *FOXG1* antibody staining denotes the true otic progenitors within the differentiated population, and these progenitors are represented by the highly otic marker expressing cells differentiated from the parental H14S9 line. As such this data helps to validate the methodology of using a stringent fluorescent intensity threshold to identify otic progenitors differentiated from human pluripotent stem cells.

The H14S9 Atoh1nGFP hES reporter was also generated using the transgene approach. This line has the potential to be used as an *in vitro* hair cell differentiation reporter. Although Atoh1 is not exclusive to the inner ear, it is however one of the first and most crucial genes expressed during hair cell induction (Mulvaney and Dabdoub, 2012), and thus is a good candidate for a hES cell reporter system. Certainly the enhancer sequence in this study has also been used by Ronaghi et al. (2014) for a similar purpose, albeit for a 3D embryoid body-based differentiation study contrasted to our monolayer system approach. As with H14S9 NOP-SOX2 low level Atoh1nGFP enhancer driven GFP expression can be seen in some undifferentiated hES colonies (Figure 3.9B).

### *3.3.3 Pax6 expression marks nasal placode progenitors*

Displayed in Figure 3.5B the mean percentage of NOP-SOX2 GFP expressing cells was not significantly different between the control DFNB and FGF conditions. Moreover the enhancer driven GFP expressing cells represented a fairly large proportion of the differentiated cells at the end of the 12 day protocol (means of approximately 31% in DFNB and 42.7% in FGF), with a smaller fraction of the GFP expressing cells also co-staining for the other characteristic otic markers, *PAX2*, *PAX8* and *FOXG1*. Due to the NOP-SOX2 enhancers also being active within the developing nasal placode, it is possible that the proportion of GFP expressing cells which do not co-stain with other otic markers could be progenitors of the nasal placode. The importance of the expression of *PAX2* and *PAX8* in the developing otic placode has been well characterised in a number of different species (Alvarez et al., 2003; Wright and Mansour, 2003) and importantly they have also been shown to be excluded from the developing nasal placode (Streit, 2007). *FOXG1* expression is also implicated in otic placode induction (Duncan and Fritzsch, 2013) but also plays a key role in nasal placode induction (Duggan et al., 2008).

A characteristic marker for nasal placode progenitors is *PAX6*. A study in the chick conducted by Bailey et al. (2006) demonstrated that all craniofacial placodal progenitors are initially specified as *Pax6*-expressing lens, and this default lens state is progressively restricted by various signalling molecules to give rise to distinct placodal regions. Fgf 8 signalling was shown to be necessary and sufficient to confine *Pax6* expression to the nasal placode (*Pax6* expression continues in the developing lens tissue also), excluded from the otic placode. When comparing the expression of NOP-SOX2-driven GFP co-labelling with a PAX6 antibody, it was observed that approximately half of the NOP-SOX2 positive cells in the control DFNB condition co-express PAX6, in contrast to approximately 27% of the NOP-SOX2 positive cells in the FGF treated condition. These results imply that treatment with the FGF ligands shifts the differentiating cells away from adopting a nasal placode progenitor fate, and more towards becoming otic progenitors. In addition, as the default state of the craniofacial placodes is believed to PAX6-positive lens, it is possible that the

supplementation of the otic inducing FGF ligands may have played a role in restricting the default lens state to allow for otic placodal differentiation to take place.

With the generation of a hES reporter lines, they will allow us to monitor differentiation in real time and will also provide a tool for visualising the effects of using compounds to improve the efficiency of the *in vitro* differentiation protocols.

# *Chapter 4*

# CHAPTER 4: MANIPULATION OF WNT SIGNALLING DURING HUMAN EMBRYONIC STEM CELL DIFFERENTIATION: EFFECT ON OTIC MARKER AND GERM LAYER GENE EXPRESSION

## 4.1 Introduction

### *4.1.1 Germ layer commitment in early development of the embryo*

A crucial event in the early developing embryo is the process of gastrulation in which the three distinctive germ layers (ectoderm, mesoderm and endoderm) are specified by the precise coordination of various morphogenic signals and gradients. Gastrulation occurs post-implantation in which stage the embryo is composed of mainly epiblast cells, a pluripotent derivative of the inner cell mass. The *in vitro* derivation of mouse epiblast cells (Brons et al., 2007; Tesar et al., 2007) demonstrated that these epiblast cells retain some characteristic markers of mouse embryonic stem cells (*Oct4* and *Nanog*, but not *Rex1*) but do not form chimeric animals when transplanted into a pre-implantation inner cell mass. It is from these epiblast cells that a key process of gastrulation occurs; the formation of the primitive streak. In this posterior positioned structure, epiblast cells migrate and undergo an epithelial to mesenchymal transition and give rise to mesoderm and endoderm progenitor cell types (Tsakiridis et al., 2014). Epiblast cells positioned anteriorly do not migrate through the primitive streak and instead differentiate into neuroectoderm and surface ectoderm lineages (Cajal et al., 2012; Lawson 1999). In combination, anterior-posterior axis formation of the embryo is established.

### *4.1.2 Wnt signalling is essential in gastrulation and primitive streak formation in vivo*

There has been an abundance of research into the early events of embryonic development leading to the commitment of ectoderm, mesoderm and endoderm lineage differentiation from pluripotent epiblast cells. Canonical Wnt signalling has

extensively been shown to play a major role in not only the initiation of gastrulation but also the formation of the primitive streak and coordination of axis patterning.

Expression of the main effector of the canonical Wnt signalling pathway (see Chapter 1), β-catenin, has been identified in epiblast cells that later go on to establish the primitive streak (Mohamed et al., 2004). Moreover, a hypomorphic Apc (adenomatous polyposis coli, a component of the β-catenin degradation complex) allele was generated in the mouse (Ishikawa et al., 2003), leading to approximately 80% attenuation of Apc expression. This led to increased β-catenin activity and as a result, the more anterior ectodermal structures were truncated with concomitant expansion of mesodermal and endodermal structures.

Additional support of the role of canonical Wnt signalling in induction of gastrulation events was a study conducted by Huelsken et al. (2000) in which β-catenin-null mouse embryos were generated and found to have impaired axis specification with a lack of mesoderm or endoderm structure formation, but normal ectodermal development. Mice deficient in Wnt3, a canonical pathway ligand, also fail to produce mesodermal structures and lack a primitive streak, with little effect on ectoderm (Liu et al., 1999). The generation of ectoderm-derived neural crest cells has also been shown to require an inhibition of canonical Wnt signals (Steventon and Mayor 2012). These studies highlight the strong role of Wnt signalling in the promotion of mesoderm and endoderm differentiation, and thus could be a potential candidate to target for improving ectodermal differentiation *in vitro*.

### *4.1.3 In vitro ES cell differentiation of primitive streak-like cells mimics events in vivo*

Directing the differentiation of hES cells *in vitro* towards cell types of a particular lineage is a major area of research focus currently. Identifying signalling pathways implicated in lineage commitment from knockout and overexpression studies *in vivo* has allowed researchers to manipulate these pathways in pluripotent stem cell differentiation to enhance progenitor induction for further study.

A study carried out by Lindsley et al. (2006) demonstrated that the *in vivo* activity of canonical Wnt signalling is mirrored in *in vitro* differentiation of mouse ES cells.

Canonical Wnt ligands such as Wnt3 and Wnt8a are expressed in the early mouse embryo prior to primitive streak formation (Kemp et al., 2005) and were also found to have peak expression during early *in vitro* mouse ES cell differentiation. With the addition of the canonical Wnt signalling inhibitor Dickkopf 1 during the first four days of mouse ES cell differentiation, genes associated with primitive streak and mesodermal induction (including *T/Brachyury*) were expressed at a significantly lower level than the cells untreated, emphasising the early role of Wnt signalling in mesoderm and endoderm differentiation. Corroborating this early timing for Wnt signalling, Turner et al. (2014) developed a *Brachyury*:GFP mouse ES cell reporter line. GFP expression was increased within three to four days of the addition of CHIR99021, a canonical Wnt signalling activator. Also using mouse ES cells, an elegant study by ten Berge et al. (2008) utilised an Axin2 lacZ reporter line to generate *in vitro* embryoid bodies, 3D structures formed from the aggregation of undifferentiated ES cells which undergo self-directed differentiation. Upon treating these embryoid bodies early in differentiation with canonical Wnt inhibitors Dickkopf 1 or Fz8CRD, lacZ reporter expression was either delayed (with Dickkopf 1) or abolished altogether (with Fz8CRD). Moreover, the lacZ reporter expression in the embryoid bodies was markedly expanded with the addition of exogenous Wnt3a ligand.

The role of Wnt signalling in gastrulation events has also been advantageous to *in vitro* hES cell differentiation studies. For example Lian et al. (2013) were able to dramatically increase cardiac progenitor differentiation from hES cells from approximately 1% in an embryoid body-based assay, to approximately 30 % to 90 % if the hES cells were pretreated with a canonical Wnt activator such as CHIR99021 or BIO to induce a more primitive streak-like fate.

### *4.1.4 General objectives of the chapter*

Since Wnt activation is necessary for primitive streak formation and generation of mesoderm and endoderm, it has been demonstrated that Wnt inhibition will prevent these fates and enhance the production of ectoderm. I therefore hypothesised that this would facilitate in the generation of otic placodal progenitor cells. As such, the aims

of this chapter are to begin investigating if manipulation of the canonical Wnt signalling pathway can improve the efficiency of our standard otic differentiation protocol. The effect of canonical Wnt inhibition and activation in the presence of FGF 3 and FGF 10 in our standard otic differentiation protocol will be ascertained, and the outcome of canonical Wnt manipulation on the gene expression of characteristic otic markers and markers of germ layer differentiation will be assessed. Moreover, timing of Wnt manipulation in our differentiation protocol will be investigated.

## 4.2 Results

### *4.2.1 Canonical Wnt signalling inhibition in combination with FGF 3 and FGF 10 upregulates otic marker gene expression*

The various roles of the canonical Wnt signalling pathway in controlling lineage specification (endoderm, mesoderm, and ectoderm) during embryogenesis have been fairly well characterised (Blauwkamp et al., 2012; Loh et al., 2014; Sokol, 2011). For example, the inhibition of canonical Wnt signalling to promote ectodermal lineage differentiation has been extensively researched in both mouse (Verani et al., 2007) and human (Nicoleau et al., 2013) embryonic stem cell differentiation studies. Despite this it was important to ascertain the effect of inhibiting canonical Wnt signalling during our standard otic differentiation protocol, to determine the outcome of *in vitro* otic and lineage differentiation when Wnt signalling inhibition is carried out in the presence of FGF 3 and FGF 10 ligands.

Two small molecule inhibitors of the canonical Wnt signalling pathway were facilitated by Neusentis (Pfizer, Cambridge, UK); PF-01441479 and PF-1404058, referred to from here on as PF-1 and PF-2, respectively. Alongside these small molecules a commercially available canonical Wnt inhibitor (Inhibitor of Wnt Response-1-endo, IWR-1-endo, Calbiochem) was also tested. Little information was known regarding the molecular activity of PF-1 and PF-2, whereas IWR-1-endo has been more extensively used for Wnt manipulation in human pluripotent stem cell differentiation studies (Bengoa-Vergniory et al., 2014; Hudson et al., 2012; Karakikes et al., 2014). IWR-1-endo mode of action is to stabilise Axin2, a component of the β-catenin destruction complex leading to proteasome-mediated proteolysis of phosphorylated β-catenin (Chen et al., 2009).

The decision was made to initially explore the effect of the Wnt inhibitors in the backdrop of our current differentiation protocol, which includes FGF 3 and FGF 10 supplementation from the outset. Experiments were carried out to determine the effect of canonical Wnt inhibition on the differentiation of otic progenitors in FGF medium (standard concentration of 50 ng/ml for both FGF 3 and FGF 10) and obtain an optimal

working concentration. PF-1, PF-2 or IWR-1-endo were present from day 0 of differentiation (day 0 refers to the initial seeding of the hES cells into differentiation conditions) and were maintained throughout the 12 day protocol. At the end of the differentiation protocol RNA was extracted and relative quantification of *PAX2*, *PAX8*, and *FOXG1* gene expression was carried out by quantitative real time PCR (QPCR) using SYBR Green (Sigma Aldrich). Delta Cts were calculated against the large ribosomal protein RPLPO housekeeping gene, and Delta Delta Ct values were compared against the levels expressed by cells differentiated in the control DFNB medium (Livak and Schmittgen, 2001). Figure 4.1 displays the responses to PF-1, PF-2 and IWR-1-endo and the effect on the gene expression of *PAX2*, *PAX8* and *FOXG1* in the H14S9 hES cell line. Dimethyl sulfoxide (DMSO) was the vehicle for all small molecule compounds. A vehicle only control was added to FGF medium to ascertain the effects of DMSO. It was observed that DMSO added to the standard FGF differentiation medium did not significantly affect expression of any of the otic markers investigated. This provides confidence that it is the small molecule compound itself exerting an effect on gene expression, and not the carrier vehicle. While treatment with each of the compounds showed an upregulation of the otic markers tested, they appeared to behave in slightly different ways. PF-1 for example appeared to reach a saturation point of otic upregulation at 50 nM, as higher doses did not elicit as good a response with *PAX2* and *PAX8*. 50 nM PF-1, 1 µM PF-2 and 10 µM IWR-1-endo were chosen for future experiments, as these concentrations overall led to a more robust and reproducible upregulation of *PAX2*, *PAX8* and *FOXG1*. The optimal concentration of IWR-1-endo agrees with published findings in human stem cell studies (Chen et al., 2009; Hudson et al., 2012). 5 µM PF-2 and 20 µM IWR-1-endo were also tested but these concentrations caused massive cell death in the cultures.

**Figure 4.1: Responses to PF-1 (A), PF-2 (B) and IWR-1-endo (C), present throughout the 12 day protocol, on the gene expression of *PAX2, PAX8,* and *FOXG1* in the H14S9 hES cell line, seeded at 8x10$^3$ cells/cm$^2$.** Compounds were reconstituted in the vehicle DMSO and a vehicle only control was also included. Bar charts denote mean and standard deviation of gene expression relative to that of the DFNB control condition (n=2 independent experiments). Statistical significance was determined by one way ANOVA with Bonferroni's multiple comparison post-test. ns = no significant difference. **P*<0.05, ***P*< 0.01, *****P*<0.0001.

(A)

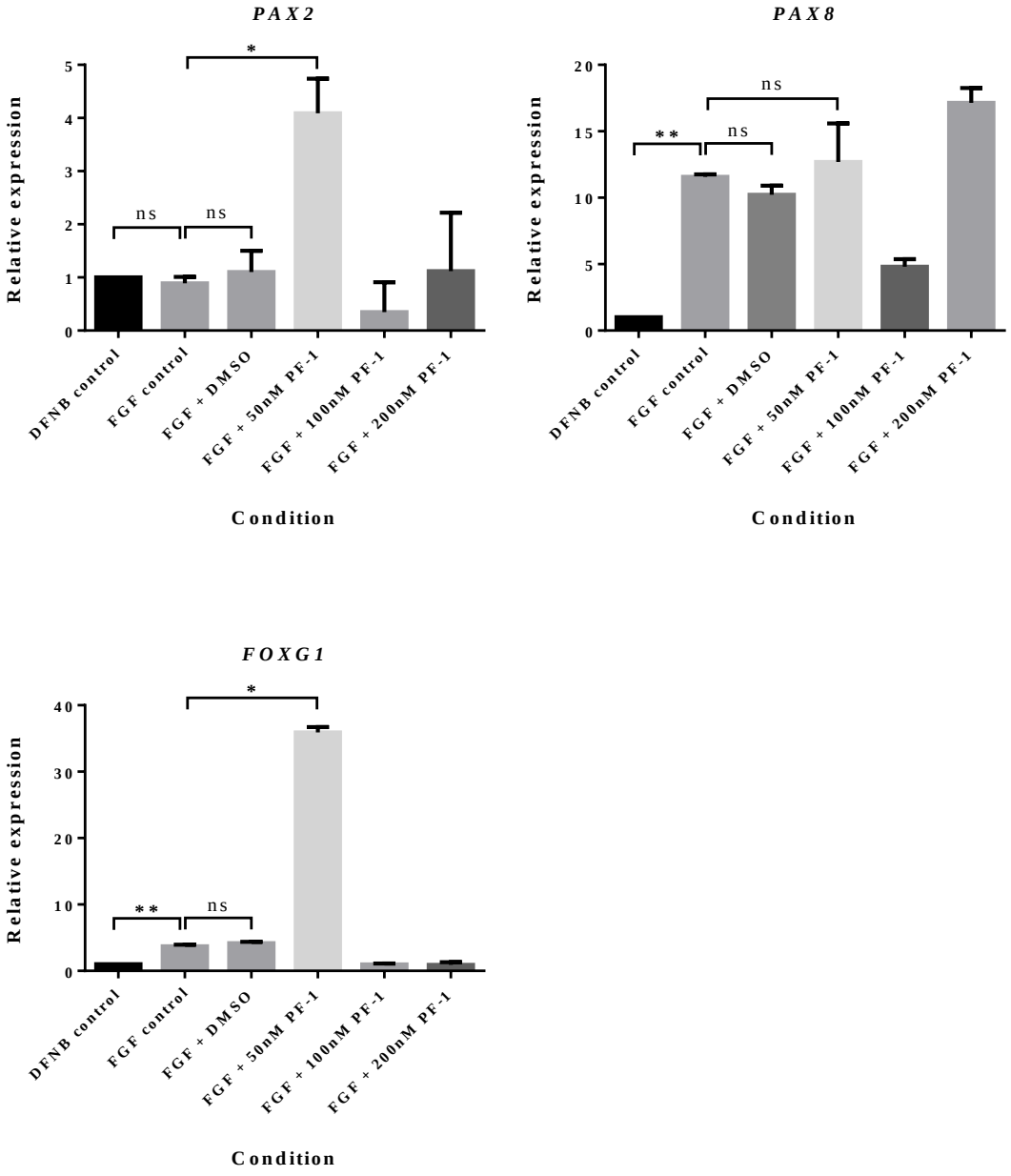

(B)

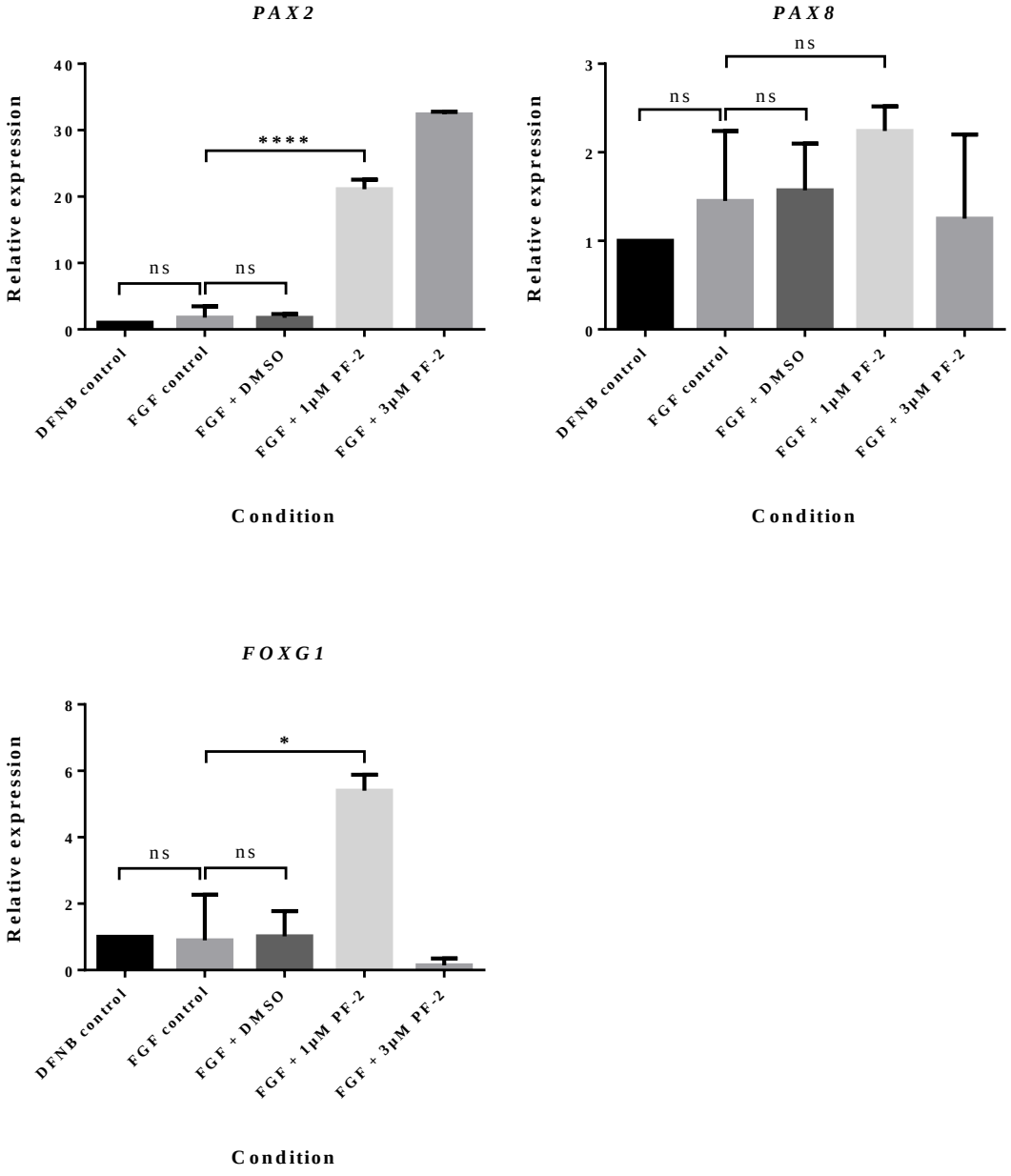
PAX2
Relative expression
40
30
20
10
0
ns
ns
****
DFNB control
FGF control
FGF + DMSO
FGF + 1μM PF-2
FGF + 3μM PF-2
Condition
PAX8
Relative expression
3
2
1
0
ns
ns
ns
DFNB control
FGF control
FGF + DMSO
FGF + 1μM PF-2
FGF + 3μM PF-2
Condition
FOXG1
Relative expression
8
6
4
2
0
ns
ns
*
DFNB control
FGF control
FGF + DMSO
FGF + 1μM PF-2
FGF + 3μM PF-2
Condition

(C)

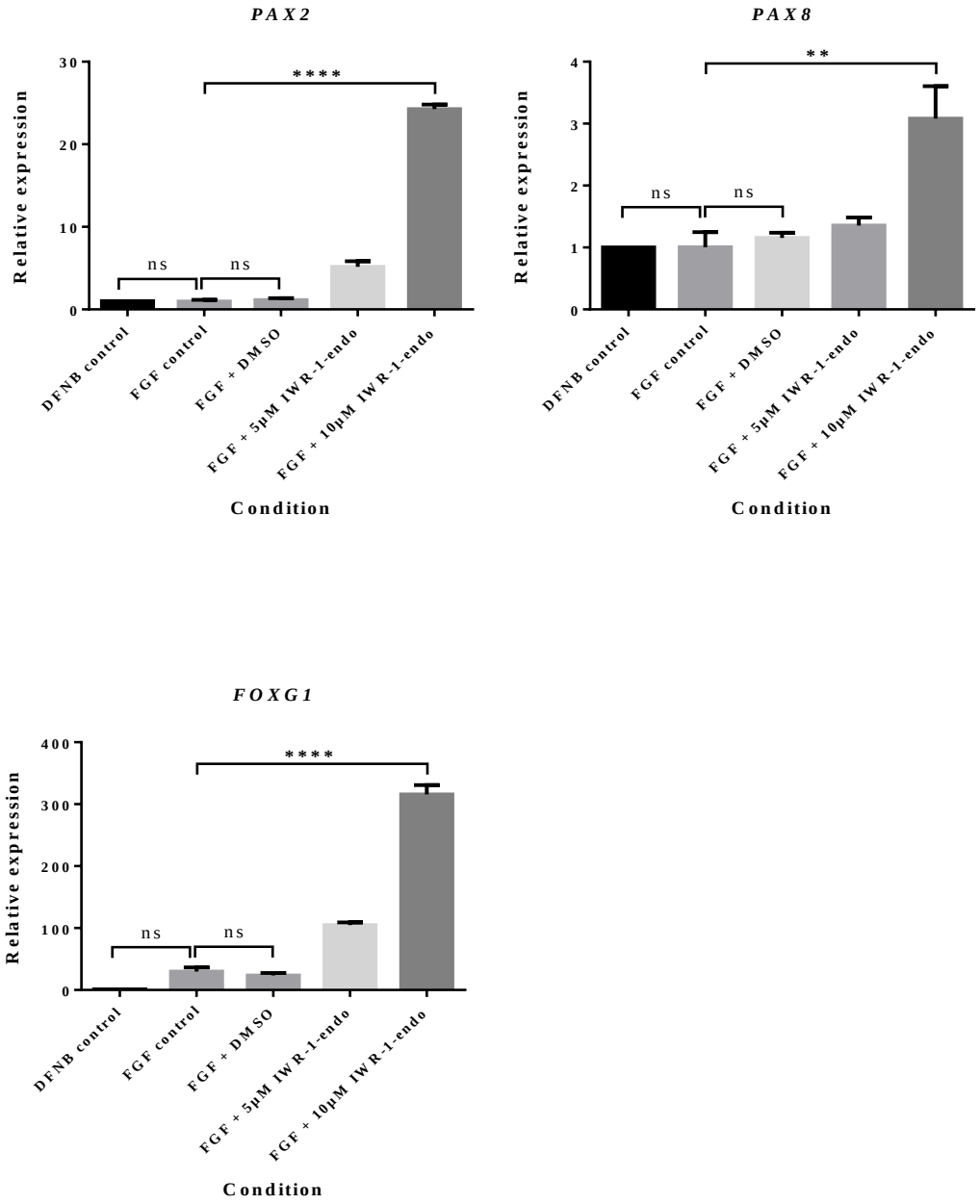
PAX2
Relative expression
30
20
10
0
****
ns
ns
DFNB control
FGF control
FGF + DMSO
FGF + 5μM IWR-1-endo
FGF + 10μM IWR-1-endo
Condition
PAX8
Relative expression
4
3
2
1
0
**
ns
ns
DFNB control
FGF control
FGF + DMSO
FGF + 5μM IWR-1-endo
FGF + 10μM IWR-1-endo
Condition
FOXG1
Relative expression
400
300
200
100
0
****
ns
ns
DFNB control
FGF control
FGF + DMSO
FGF + 5μM IWR-1-endo
FGF + 10μM IWR-1-endo
Condition

### *4.2.2 Canonical Wnt inhibition in combination with FGF 3 and FGF 10 upregulates gene expression of ectodermal markers, but disrupts gene expression of endodermal and mesodermal markers*

The effect of disrupting canonical Wnt signalling with various small molecule inhibitors present throughout the full 12 days of our otic differentiation protocol giving rise to an upregulation of the characteristic otic markers led to the investigation of the expression of genes associated with lineage differentiation. It was anticipated that our standard FGF differentiation protocol would drive the differentiating hES cells towards an ectodermal fate (as the otic placode is ectodermal in origin). The effect on endoderm and mesoderm differentiation in the FGF condition has not been addressed, and the consequence of combining FGF treatment with canonical Wnt signalling manipulation on lineage differentiation has also not been investigated in our system.

With the H14S9 hES cell line, 12 day otic differentiation experiments were carried out in control DFNB, FGF, or FGF with 50 nM PF-1, 1 µM PF-2 or 10 µM IWR-1-endo supplemented medium. Gene expression of the three germ layer lineages relative to the baseline DFNB condition were quantified by QPCR. Two gene markers for each germ layer were investigated; *PAX6* and *NESTIN* (ectoderm), *T* and *MEOX1* (mesoderm), and *AFP* and *GATA6* (endoderm) (Figure 4.2).

It was interesting to observe that compared to the DFNB baseline condition, our standard FGF medium led to the upregulation of genes associated with all three germ layers. It was anticipated that the addition of FGF 3 and FGF 10 would induce ectodermal differentiation but have no effect of mesoderm and endoderm differentiation. This was not the case however. Significant upregulation of the ectoderm genes *PAX6* and *NESTIN* was observed in the FGF condition as expected, yet significant upregulation of mesoderm and endoderm markers was also observed in the FGF condition. When the FGF medium was supplemented with the canonical Wnt inhibitors PF-1, PF-2 and IWR-1-endo ectodermal differentiation was enhanced further over the FGF condition, particularly *PAX6*. However, the gene expression of mesoderm and endoderm markers was significantly reduced compared to the FGF condition. This downregulation effect was seen with the supplementation of all three canonical Wnt inhibitors (especially IWR-1-endo) in FGF medium for *T*, *MEOX1*, and

*GATA6*. Only supplementation with IWR-1-endo could cause significant downregulation of *AFP* however.

Following a loss of function/gain of function paradigm an experiment was done to determine the effect of activating canonical Wnt signalling throughout the 12 days of otic differentiation. The small molecule compound BIO (6-bromoindirubin-3'-oxime, Tocris) is a potent inhibitor of GSK-3β kinase, a component of the β-catenin degradation complex. Inhibition of GSK-3β kinase activity disrupts the proteolytic breakdown of β-catenin and so Wnt activity is sustained (Meijer et al., 2003). BIO is well established in the literature and has been used to investigate survival and proliferation of hES cells and also lineage differentiation studies (Dravid et al., 2005; Tseng et al., 2006). BIO was tested at a concentration of 2 μM (Chuang et al., 2010). Figure 4.3 shows the effect on the gene expression of otic markers *PAX2*, *PAX8* and *FOXG1* (A), and also markers of ectoderm, mesoderm and endoderm lineage differentiation (B). In contrast to inhibiting canonical Wnt signalling throughout the 12 day protocol, activating canonical Wnt signalling throughout appears to downregulate gene expression of the otic and ectoderm markers, with upregulation of markers of mesoderm and endoderm.

**Figure 4.2: Gene expression of markers associated with ectoderm (A), mesoderm (B) and endoderm (C) lineage differentiation following a 12 day differentiation protocol with H14S9 hES cells, seeded at 8x10$^3$ cells/cm$^2$. Small molecule compounds were present throughout the protocol from the initial day of seeding**. Gene expression is presented as relative to that of the DFNB baseline control. Bar charts denote mean and standard deviation of gene expression relative to that of the DFNB control condition (n=3 independent experiments). Statistical significance was determined by one way ANOVA with Bonferroni's multiple comparison post-test. ns = no significant difference. **P*<0.05, ***P*<0.01, ****P*<0.001.

(A)

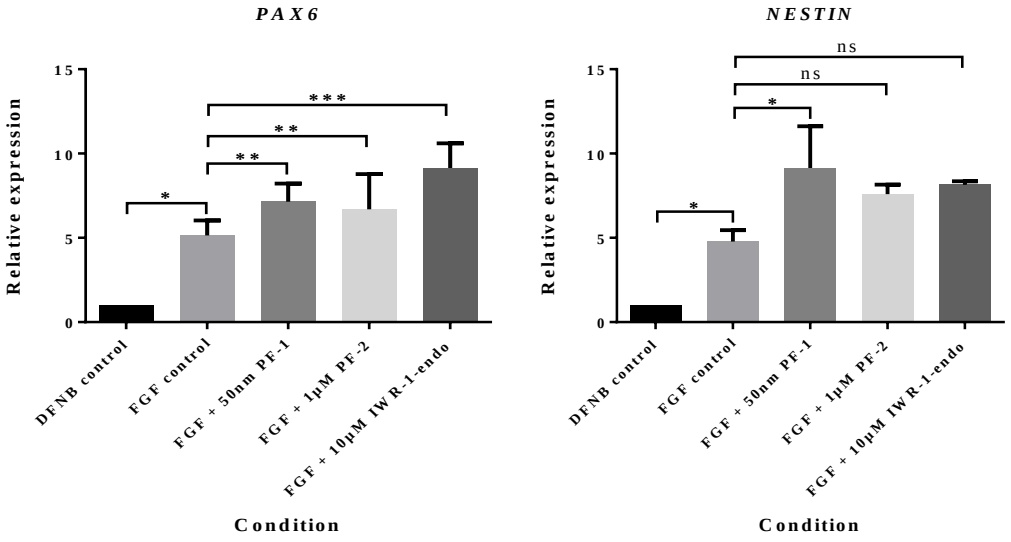


(B)

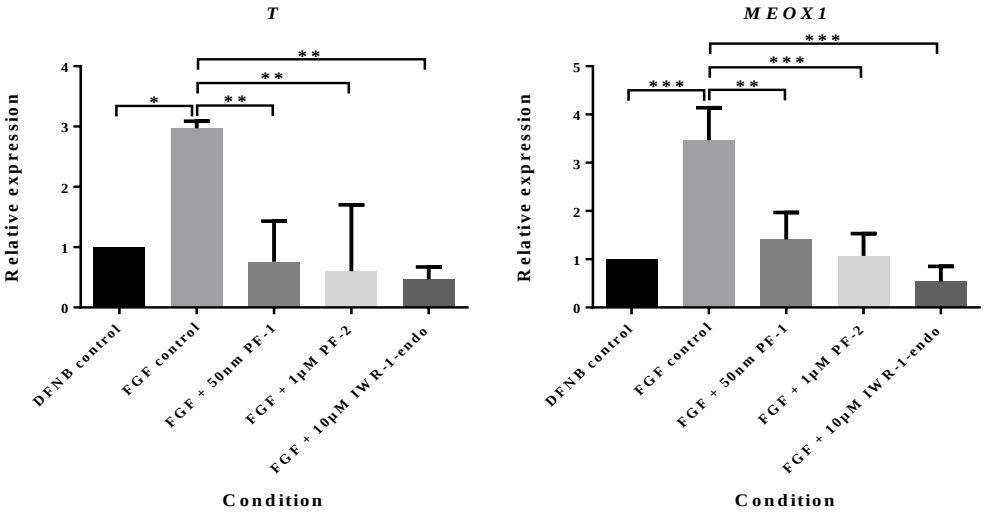

(C)

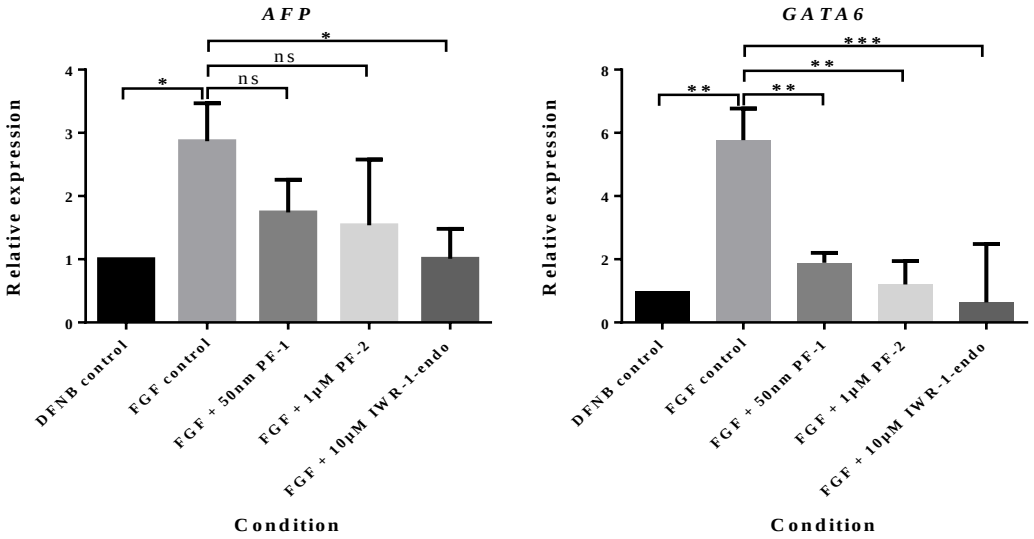
AFP
Relative expression
0
1
2
3
4
*
ns
ns
*
DFNB control
FGF control
FGF + 50nm PF-1
FGF + 1μM PF-2
FGF + 10μM IWR-1-endo
Condition
GATA6
Relative expression
0
2
4
6
8
**
**
**
***
DFNB control
FGF control
FGF + 50nm PF-1
FGF + 1μM PF-2
FGF + 10μM IWR-1-endo
Condition

**Figure 4.3: Gene expression of otic markers *PAX2*, *PAX8* and *FOXG1* (A) and markers of ectoderm (*PAX6*, *NESTIN*), mesoderm (*T*, *MEOX1*) and endoderm (*AFP*, *GATA6*) (B) following a 12 day differentiation protocol with H14S9 hES cells, seeded at 8x10$^3$ cells/cm$^2$. BIO was supplemented into FGF medium and maintained throughout.** Gene expression is presented as relative to that of the DFNB baseline control. One experiment was carried out and so statistical significance cannot be determined.

(A)

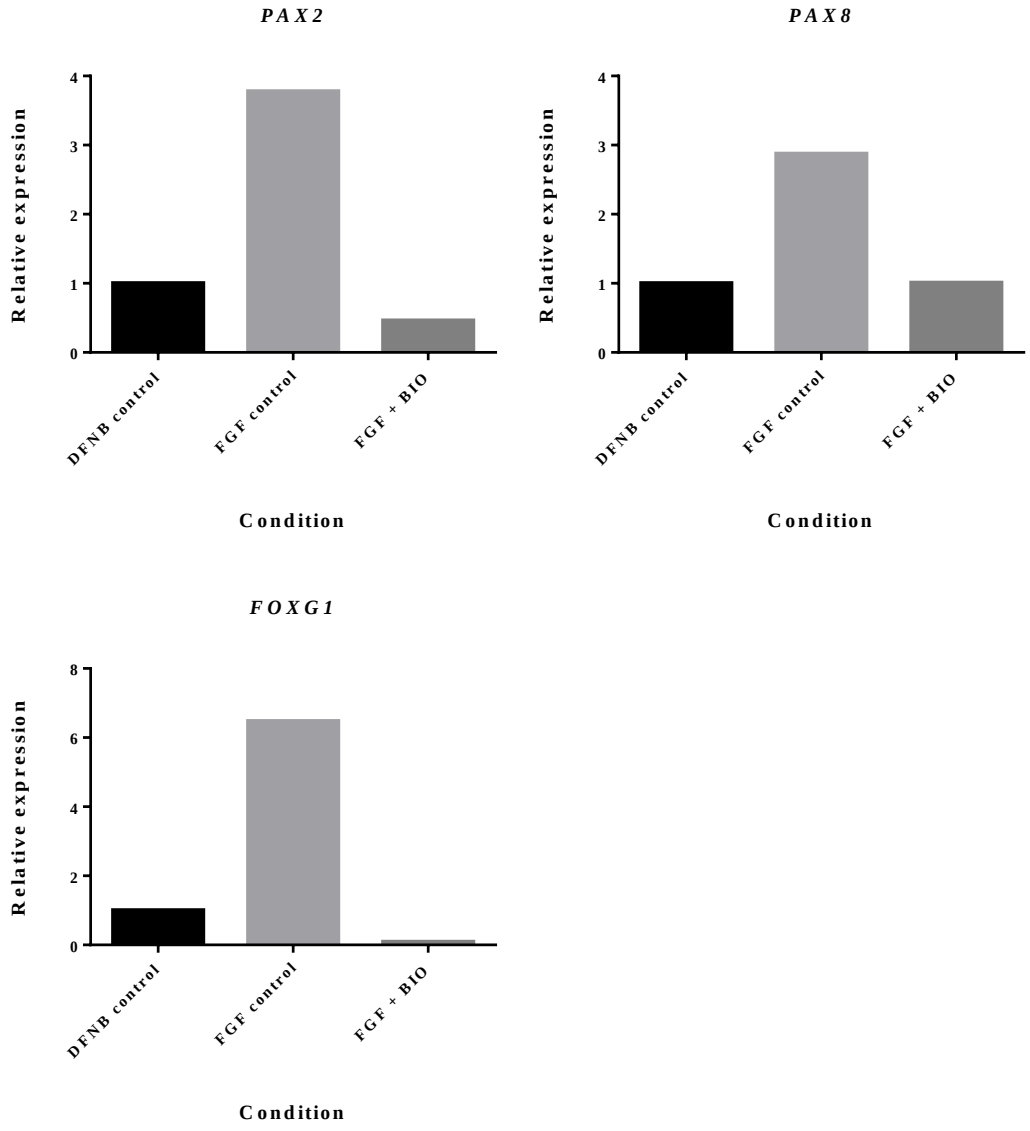

(B)

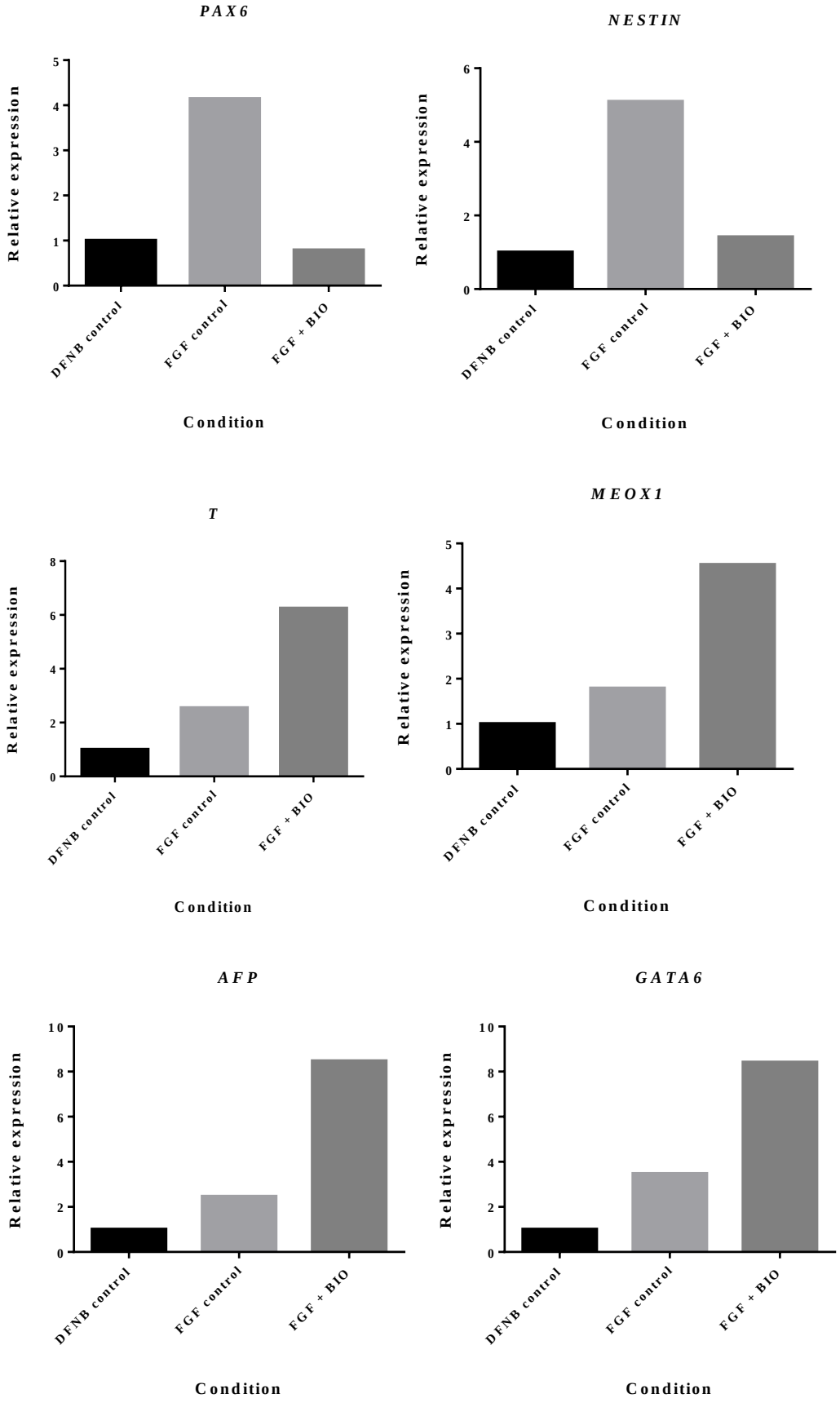
PAX6
Relative expression
0
1
2
3
4
5
DFNB control
FGF control
FGF + BIO
Condition
NESTIN
Relative expression
0
2
4
6
DFNB control
FGF control
FGF + BIO
Condition
T
Relative expression
0
2
4
6
8
DFNB control
FGF control
FGF + BIO
Condition
MEOX1
Relative expression
0
1
2
3
4
5
DFNB control
FGF control
FGF + BIO
Condition
AFP
Relative expression
0
2
4
6
8
10
DFNB control
FGF control
FGF + BIO
Condition
GATA6
Relative expression
0
2
4
6
8
10
DFNB control
FGF control
FGF + BIO
Condition

### *4.2.3 Timing of canonical Wnt inhibition is critical for upregulation of otic marker gene expression*

Previous experiments in this chapter have involved supplementing the FGF medium with one of three canonical Wnt inhibitor compounds and maintaining this supplementation throughout the full 12 day protocol, leading to upregulation of the gene expression of the characteristic otic markers. Since timing and sequence of developmental signals is critical to drive a particular process, it was important to determine whether it is necessary for canonical Wnt signalling to be inhibited from the very start of *in vitro* otic differentiation in order for it to have its upregulatory effect. Figure 4.4 shows the effect of supplementing the FGF medium with canonical Wnt inhibitors from day 4 of the otic differentiation protocol on gene expression of *PAX2, PAX8* and *FOXG1*, and Figure 4.5 displays the outcome on the ectoderm (A), mesoderm (B) and endoderm (C) germ layer marker gene expression.

It was observed that inhibiting canonical Wnt signalling with any of the three small molecule compounds from day 4 of the standard 12 day otic differentiation protocol did not lead to an upregulation of the otic markers or ectodermal lineage markers compared to the FGF condition, as seen when canonical Wnt was inhibited from the start of the differentiation protocol. Conversely gene expression of mesoderm and endoderm markers, previously seen to be significantly downregulated upon canonical Wnt inhibition from the start of differentiation, was significantly upregulated with the supplementation of at least one of the small molecule compounds from day 4 of differentiation. This is suggesting the initiation of canonical Wnt signalling inhibition must take place from the start of hES cell differentiation in order for it to have a positive effect on upregulating gene expression of otic specific markers.

**Figure 4.4: Gene expression of otic markers *PAX2*, *PAX8* and *FOXG1* following a 12 day differentiation protocol with H14S9 hES cells, seeded at 8x10$^3$ cells/cm$^2$. Canonical Wnt inhibitors were supplemented into the media on day 4 and maintained until day 12**. Gene expression is presented as relative to that of the DFNB baseline control. Bar charts denote mean and standard deviation of gene expression relative to that of the DFNB control condition (n=3 independent experiments). Statistical significance was determined by one way ANOVA with Bonferroni's multiple comparison post-test. ns = no significant difference. **P*<0.05, ***P*<0.01, *****P*<0.0001.

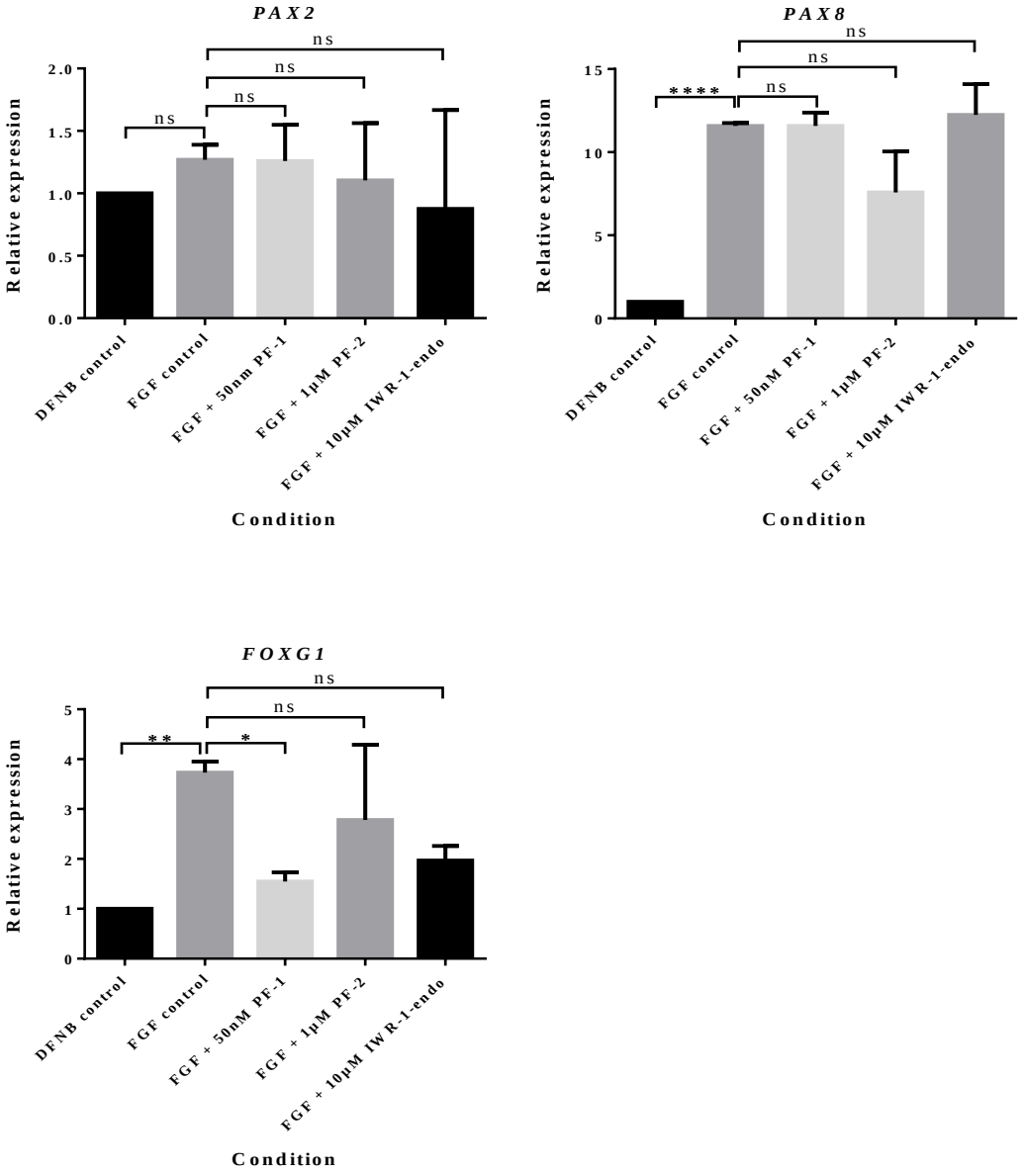

**Figure 4.5: Gene expression of markers associated with ectoderm (A), mesoderm (B) and endoderm (C) lineage differentiation following 12 day differentiation with H14S9 hES cells, seeded at 8x10$^3$ cells/cm$^2$. Canonical Wnt inhibitors were supplemented into the media from day 4 and maintained throughout to day 12**. Gene expression is presented as relative to that of the DFNB baseline control. Bar charts denote mean and standard deviation of gene expression relative to that of the DFNB control condition (n=3 independent experiments). Statistical significance was determined by one way ANOVA with Bonferroni's multiple comparison post-test. ns = no significant difference. **P*<0.05, ***P*<0.01, ****P*<0.001, *****P*<0.0001.

(A)

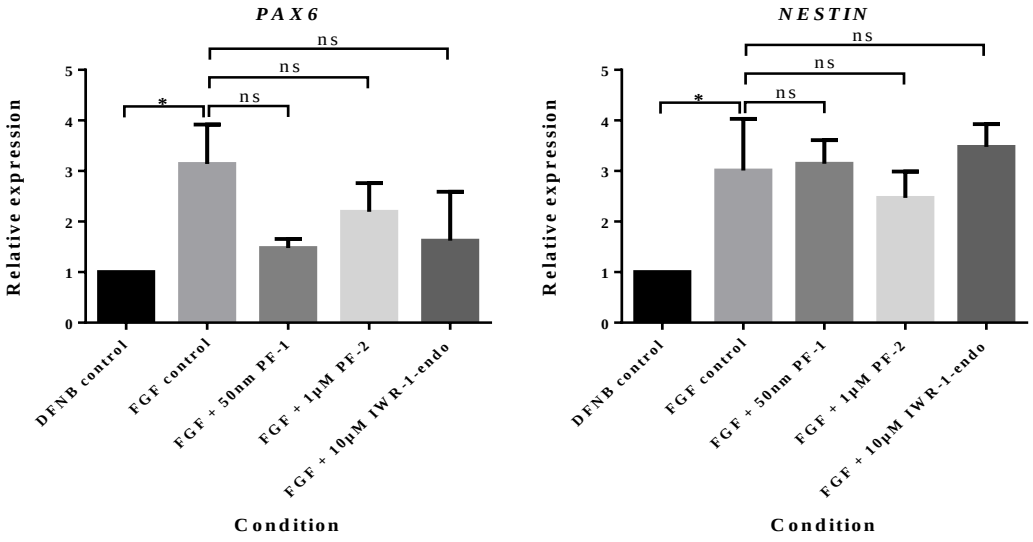


(B)

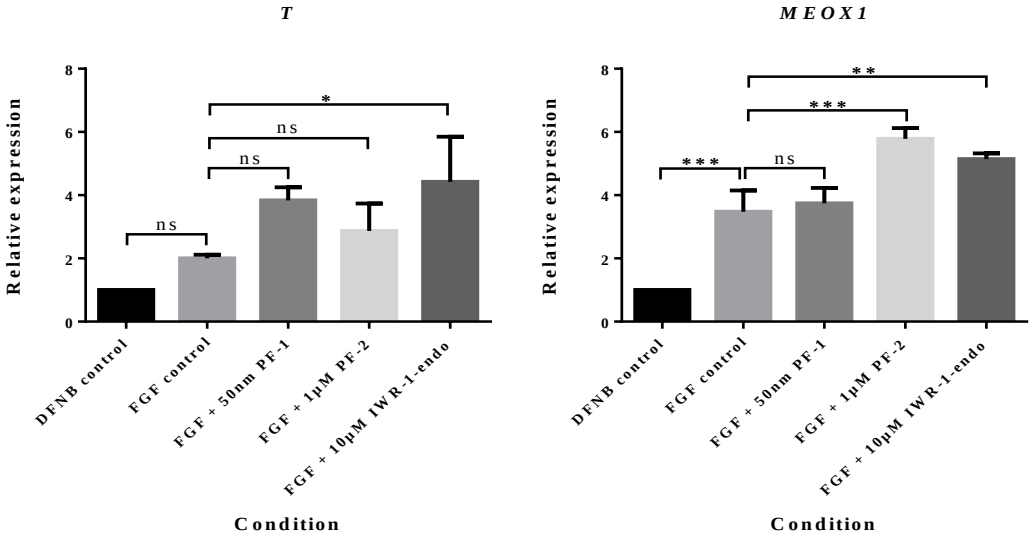

(C)

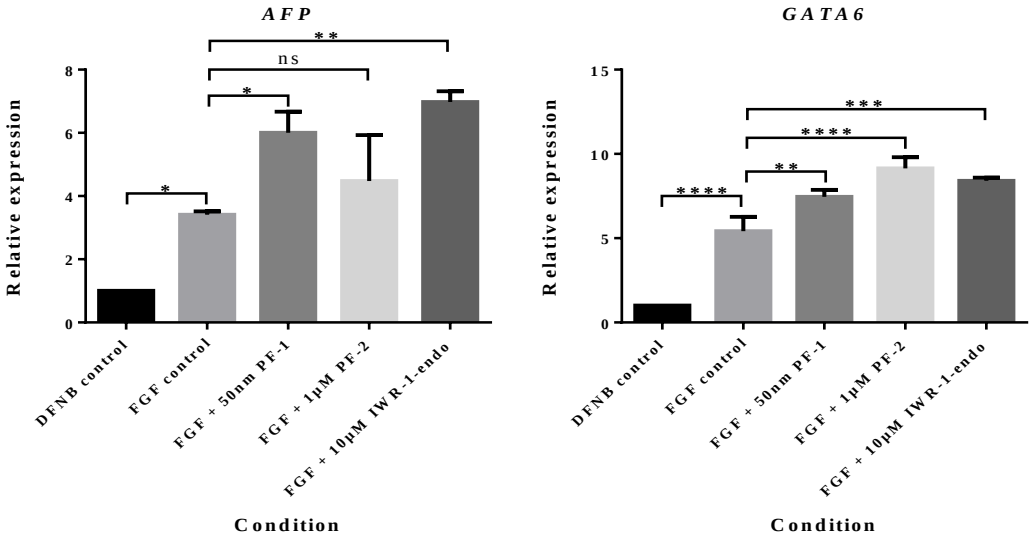
AFP
Relative expression
Condition
DFNB control
FGF control
FGF + 50nm PF-1
FGF + 1μM PF-2
FGF + 10μM IWR-1-endo
ns
GATA6
Relative expression
Condition

### *4.2.4 Canonical Wnt signalling inhibition in combination with FGF 3 and FGF 10 is not required for the duration of otic differentiation in vitro*

This chapter has thus far demonstrated that inhibition of canonical Wnt signalling must occur from the very start of *in vitro* otic differentiation in order to promote gene expression of ectodermal lineage markers and upregulation of gene expression of the key otic markers, *PAX2*, *PAX8* and *FOXG1*. Concomitantly a downregulation of mesoderm and endoderm marker gene expression is also observed when canonical Wnt signalling is present for the full 12 days of the protocol. These effects are essentially reversed when inhibition takes place from day 4.

Further investigating the timing of canonical Wnt inhibition it was important to address whether inhibition is required throughout the whole 12 day differentiation protocol to have an upregulatory effect on otic marker gene expression. Experiments were set up to inhibit canonical Wnt signalling for different lengths of time. In combination with FGF medium, Wnt inhibition took place from day 0 to day 4, day 0 to day 6, or day 0 to day 8. Differentiating cells were maintained in FGF medium only following day 4, 6 or 8, respectively until day 12. Day 0 to day 12 inhibition was also included as shown in previous figures. At the end of day 12, RNA was extracted and reverse transcribed. Subsequent gene expression of *PAX2*, *PAX8* and *FOXG1* was then quantified relative to the DFNB baseline condition, and is shown in Figure 4.6. As the effects on gene expression of PF-1, PF-2 and IWR-1-endo were similar in all experiments carried out previously, and with IWR-1-endo being commercially available and well established in the literature, all future experiments were carried using IWR-1-endo as the canonical Wnt inhibitor of choice.

Inhibiting canonical Wnt signalling with IWR-1-endo from day 0 to day 4 or day 0 to day 6 did not significantly alter gene expression of *PAX2*, *PAX8* or *FOXG1* from that of FGF medium alone. Significant upregulation of the otic markers was only found between the standard FGF medium and FGF with canonical Wnt inhibition from day 0 to 8 or day 0 to 12. Moreover, there was no significant difference on otic marker gene expression between inhibiting Wnt signalling from day 0 to day 8 or throughout the whole 12 day differentiation protocol (for *PAX2* and *PAX8*. *FOXG1* gene expression was significantly higher with 12 days of canonical Wnt inhibition in

contrast to eight days however). Therefore canonical Wnt inhibition is required from the initiation of hES differentiation, and must be maintained for at least eight days to elicit an upregulatory response of the key otic marker gene expression.

**Figure 4.6: Gene expression of otic markers *PAX2*, *PAX8* and *FOXG1* following a 12 day differentiation protocol with H14S9 hES cells, seeded at 8x10$^3$ cells/cm$^2$. IWR-1-endo was supplemented at day 0 and maintained to day 4, day 6, day 8 or day 12.** Gene expression is presented as relative to that of the DFNB baseline control. Bar charts denote mean and standard deviation of gene expression relative to that of the DFNB control condition (n=3 independent experiments). Statistical significance was determined by one way ANOVA with Bonferroni's multiple comparison post-test. ns = no significant difference. **P*<0.05, ****P*<0.001, *****P*<0.0001.

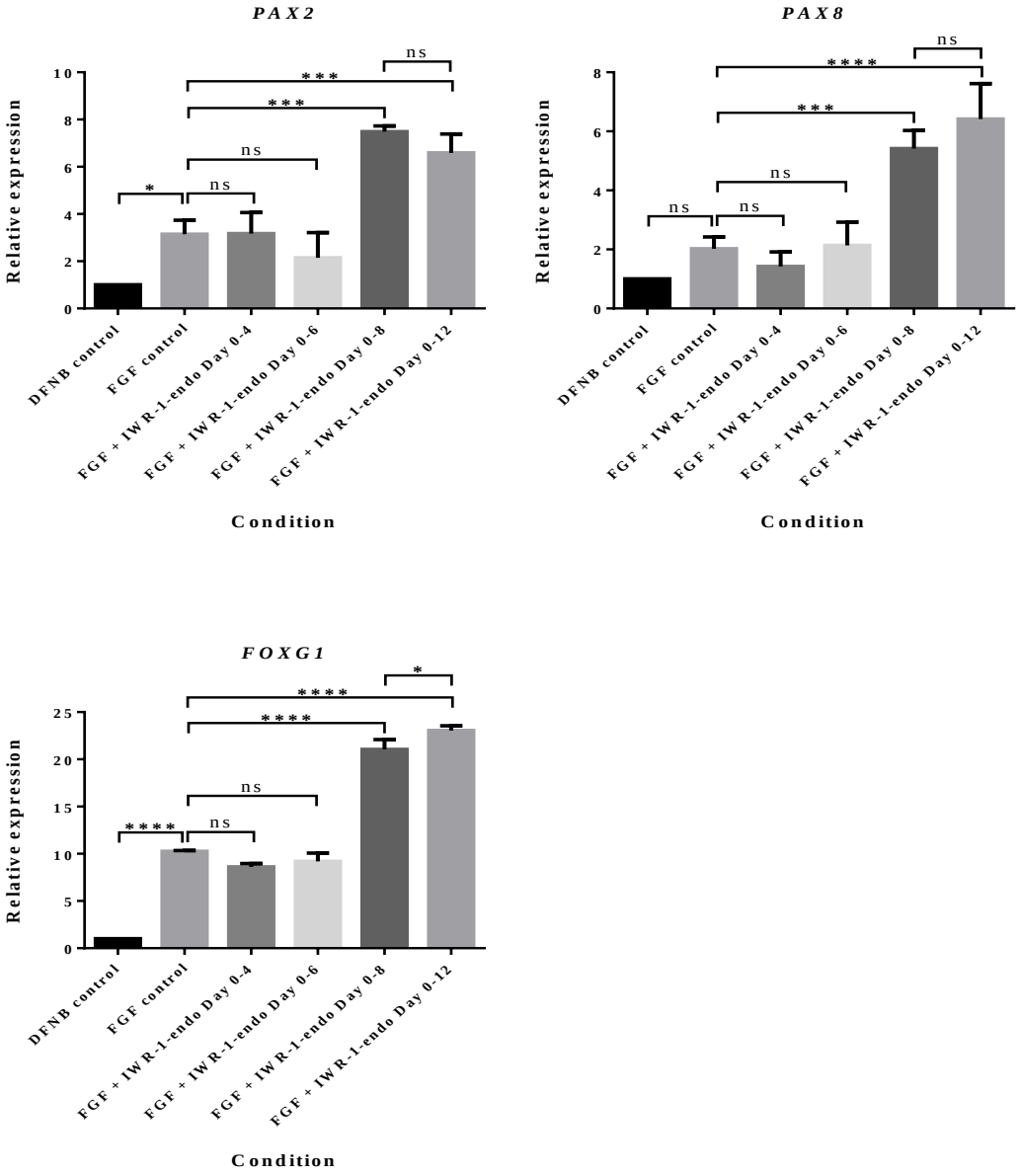

## 4.3 Discussion

### *4.3.1 Manipulation of the canonical Wnt signalling pathway alters otic and germ layer differentiation*

It was observed that inhibiting the canonical Wnt signalling pathway throughout the 12 day otic differentiation protocol with a variety of small molecule compounds overall caused an upregulation of otic and ectodermal marker gene expression, with a concomitant downregulation of markers of mesodermal and endodermal differentiation. Conversely, a 12 day activation of the canonical Wnt signalling pathway provided a *vice versa* effect; upregulation of mesodermal and endodermal marker gene expression, with loss of otic and ectodermal gene expression. Inhibition of canonical Wnt signalling enhancing ectodermal differentiation at the expense of mesoderm and endoderm is a well-established finding *in vitro* and *in vivo* (Arkell et al., 2013). Gadue et al. (2006) looked at the manipulation of the canonical Wnt signalling in an embryoid body study from a *Foxa2:GFP* (marker of the endoderm germ layer lineage) murine embryonic stem cell reporter line. Canonical Wnt signalling inhibition with Dickkopf1 throughout the embryoid body differentiation period led to a decrease in *Foxa2*-driven GFP expression and further loss of primitive streak-like differentiation. Even within inner ear research early Wnt inhibition has been used to drive differentiating mouse embryonic and induced pluripotent stem cells into a more ectodermal fate to enhance otic differentiation. Oshima et al. (2010), also using an embryoid body protocol, inhibited Wnt signalling with Dickkopf1 to push the differentiating cells away from taking on a mesodermal or endodermal lineage, and enhancing ectodermal differentiation. The use of a three dimensional approach to induce otic differentiation are emerging as new methodologies to generate otic progenitor cells and the more differentiated cell types, such as sensory hair cell-like cells in studies in the mouse. Similar success with human embryonic stem cells has yet to be reported.

### *4.3.2 Timing of canonical Wnt signalling inhibition is crucial for upregulation of otic gene expression*

The upregulation of the otic and ectoderm marker gene expression was found to only occur if canonical Wnt signalling is inhibited from the very start of the otic differentiation protocol, and this enhancement of gene expression was absent if inhibition took place four days into the protocol. This is consistent with the role of Wnt signalling in early gastrulation. Canonical Wnt signalling having stage specific roles has also been demonstrated in numerous other systems. A rich area of research utilising Wnt modulation is the *in vitro* differentiation of cardiac progenitors from embryonic stem cells. Paige et al. (2010) highlighted the different outcomes of activating or inhibiting canonical Wnt signalling early in hES differentiation into cardiac progenitors. Inhibition of canonical Wnt signalling from the start of differentiation was found to suppress the expression of mesodermal and early cardiac progenitor genes, yet the gene expression of these markers were unaffected or even enhanced when canonical Wnt inhibition took place from four days into the differentiation protocol. Similarly, a study (Ueno et al., 2007) used heat-shock-inducible Dickkopf1 and Wnt 8a transgenic zebrafish lines to ascertain the effects of inhibition and activation of canonical Wnt signalling on mesoderm and subsequent cardiac differentiation *in vivo*, respectively. Mesodermal differentiation was reduced in the Dickkopf1 transgenic line, and expanded in the Wnt 8a line when the zebrafish embryos were subjected to heat shock early. Opposing effects were encountered when heat shock was applied later into development. Mouse embryonic stem cells lines have also been shown to have similar timing requirements of canonical Wnt modulation (Kwon et al., 2007), whereby inhibiting signalling three days into embryoid body differentiation had no effect on mesodermal and cardiac progenitor induction. The findings of these studies combined suggest that canonical Wnt signalling is tightly controlled and regulated and the effect of manipulation is time and stage specific, indicative of a bi-phasic role in germ layer differentiation and organogenesis.

From the multitude of studies carried out to ascertain the role of canonical Wnt signalling in generating progenitors of various lineages *in vitro*, and with the

awareness of the key functions of canonical Wnt signalling in inner ear development *in vivo* (Chapter 1), it was of apparent interest to investigate Wnt manipulation within our hES cell otic differentiation protocol. The data presented in this chapter suggests a model in which inhibition of canonical Wnt signalling from the start of otic differentiation leads to a downregulation of mesoderm and endoderm lineage gene expression, with a concomitant upregulation of ectodermal differentiation. This expansion of ectoderm then allows the supplemented FGF 3 and FGF 10 ligands to induce progenitors with an upregulated gene expression of the characteristic otic markers. This positive effect on otic differentiation is lost if canonical Wnt is not inhibited until four days into the protocol, suggesting that once early mesodermal and/or endodermal lineage differentiation has taken place the cells become committed to these lineages, at the expense of ectodermal and subsequent otic progenitor induction.

With the increasing knowledge of the bi-phasic roles of canonical Wnt signalling during embryonic development, it is possible that further manipulation of the Wnt signalling pathway could enhance the efficiency of *in vitro* otic differentiation to provide a more developmentally informed protocol.

# *Chapter 5*

# CHAPTER 5: FURTHER FINE TUNING OF *IN VITRO* OTIC DIFFERENTIATION VIA WNT SIGNALLING MANIPULATION

## 5.1 Introduction

### *5.1.1 FGF signalling is required for the induction of the pre-placodal region and otic placode*

The results of Chapter 4 highlighted the ability to direct the differentiation of hES cells away from adopting a mesodermal or endodermal fate, and taking on a more ectodermal identity. This was achieved by a combination of FGF 3 and FGF 10 signalling in conjunction with inhibition of canonical Wnt signalling. It was hypothesised that gastrulation-like events during *in vitro* hES differentiation were blocked by the inhibition of canonical Wnt signalling, and in combination with FGF signalling, ectoderm (and subsequently otic placode) differentiation was upregulated. It has been shown in many *in vivo* studies that following the early embryonic process of gastrulation the ectoderm is roughly divided into two sections; the neural and non-neural ectoderm, with a wide intermediate area of overlap between these two subdivisions (Fernandez-Garre et al., 2002; Lawson, 1999). The neural ectoderm will give rise to structures such as the neural plate, neural tube and neural crest, whereas the non-neural ectoderm division will differentiate into epidermis. The area of overlap between these two divisions, sometimes referred to as the neural plate border, contains all the cells that will give rise to the future placodes. Within this area members of the Six and Eya transcription factor families are upregulated, specifically Six1, Six4, Eya1 and Eya2 (Kobayashi et al., 2000; Schlosser and Ahrens, 2004), and placodal precursors become concentrated here in a region referred to as the pre-placodal region (PPR) (Chapter 1). FGF signalling has been implicated as having a necessary direct role in the induction of the PPR via its effect on the expression of the Six and Eya transcription factors. Studies conducted in chick (Litsiou et al., 2005) and *Xenopus* (Ahrens and Schlosser, 2005) have identified FGF 8 knockdown or inhibition as a causative factor in abolishing PPR induction.

Of particular interest to our laboratory is the formation of the otic-epibranchial placode domain (OEPD), or pre-otic field. The OEPD has been identified as a region of Pax2-positive progenitor cells within the maturing PPR (Sun et al., 2007) which contains a mixture of cells which will later give rise to both the otic and epibranchial placodes, and also cells of the epidermis (Ohyama and Groves, 2004). FGF signalling is believed to play a major role in the induction of the OEPD, by posteriorising the expression of members of the Dlx family of transcription factors to form an area of the PPR known as the posterior placode area (PPA). In the PPA FGF signalling promotes Pax8 and Pax2 expression to initiate otic placode formation. It is believed that cells in the PPA receiving prolonged FGF signalling activity take on an epibranchial fate, whereas attenuated FGF signalling with concomitant canonical Wnt signalling activity from the adjacent neural tube pushes the cells of the PPA to segregate and adopt an otic phenotype (Freter et al., 2008).

The identification of the members of the FGF signalling pathways associated with otic placode induction have been well characterised, and there are known species differences. Studies carried out in the mouse have identified a role for neural Fgf 3 and mesodermal Fgf 10. The classic study conducted by Wright and Mansour (2003) demonstrated the severe decrease in size, or complete lack, of otic vesicle formation in Fgf 3 and Fgf 10 mouse mutants. Later studies in both mouse and chick have identified a crucial role for Fgf 8 in otic placode formation. Ladher et al. (2005) identified Fgf 8 expression in the mouse prospective otic placode and also within the underlying mesenchyme and endoderm, and mice mutant for Fgf8 were found to have reduced expression of Fgf 10, suggesting Fgf 8 is a key regulator of Fgf 10 expression. Therefore the role of Fgf 8 in the otic placode induction is indirect, acting by controlling the expression of Fgf 10. Similarly in the chick, endoderm was determined to be the source of expression of Fgf 8, a crucial inducer for the expression of Fgf 19 (Fgf 3 and Fgf 19 are believed to be both necessary and sufficient for otic placode induction in the chick). In zebrafish injection of Fgf 3 and Fgf 8 morpholinos are able to prevent the formation and development of otocysts (Maroon et al., 2002).

### *5.1.2 Role of canonical Wnt signalling in otic placode initiation and expansion*

The role of FGF signalling in the induction of the otic placode has been extensively established. However the function of canonical Wnt signalling is less well characterised to date. One of the earliest studies elucidating a role for Wnt signalling in the development of the inner ear was carried out by Ladher et al. (2000). Using *Xenopus* embryos, hindbrain-derived Wnt 8c was identified as being able to induce the expression of known otic placode markers such as *Pax2*, *Dlx5* and *Soho1* when exposed to uncommitted presumptive otic ectoderm, but only when exposed in combination with Fgf 19. Later studies such as that conducted by Urness et al. (2010) further expanded on the role of canonical Wnt signalling in the otic placode induction. Using Fgf 3 and Fgf 10 double mutant mice, microarray analysis was undertaken to determine the expression patterns of various otic and ectodermal genes compared to wild type animals. Wnt 8a was found to be significantly downregulated in the double mouse mutants, but its expression appeared normal in Fgf 10 mutants and Fgf 3 heterozygote mutants, suggesting Fgf 3 plays a direct or indirect role in inducing and maintaining the expression of Wnt 8a. *Foxi2* was also found to be downregulated in the Fgf 3 and Fgf 10 double mutant mice, a similar effect to the inhibition of canonical Wnt signalling in the pre-otic field in the mouse (Ohyama and Groves, 2004). Thus it was concluded in this study that the role of Wnt signalling in otic placode induction is to act in synergy with FGF signalling, to specify and maintain the otic placode, and to restrict the positioning of the otic placode to the dorsal ectoderm. Following on from this Vendrell et al. (2013) supported the findings of Urness et al. (2010) and also demonstrated how the absence of Wnt 8a in mutant mice did not affect the initiation of the otic placode, but delayed the onset of the expression of key otic markers. Similarly absent Wnt 8a expression in zebrafish does not abolish otic placode induction, but leads to embryos featuring otocysts of reduced size (Phillips et al., 2004).

Strengthening the hypothesis that the role of canonical Wnt signalling is to coordinate the positioning and restricting the size of the otic placode, rather than a direct involvement in its induction was a study by Ohyama et al. (2006). Using TCF/Lef (Chapter 1) reporter mice it was found that canonical Wnt signalling is active in a

subset of the Pax2-positive cells of the pre-otic field. Conditional inactivation of β-catenin in this Pax2-positive region lead to the upregulation of the epidermal marker Foxi2, with an expansion of Foxi2-positive epidermal cells at the expense of Foxi2-negative otic cells. Activation of β-catenin provided the opposing result; an expansion of the otic placode, with a reduction in size of the epidermal region. A schematic of this is shown in Figure 5.1.

**Figure 5.1: Schematic representation of the effect of canonical Wnt signalling on the otic placode and surrounding epidermis.** Image adapted from the PhD thesis of Sarah Jacob Eshtan. The otic placode is shown in the exaggerated area coloured green. On the left shows the effect on the otic placode if canonical Wnt signalling is inhibited leading to otic restriction. The right side shows the effect of canonical Wnt activation expanding the region of the otic placode at the expense of the Foxi2 positive epidermis.

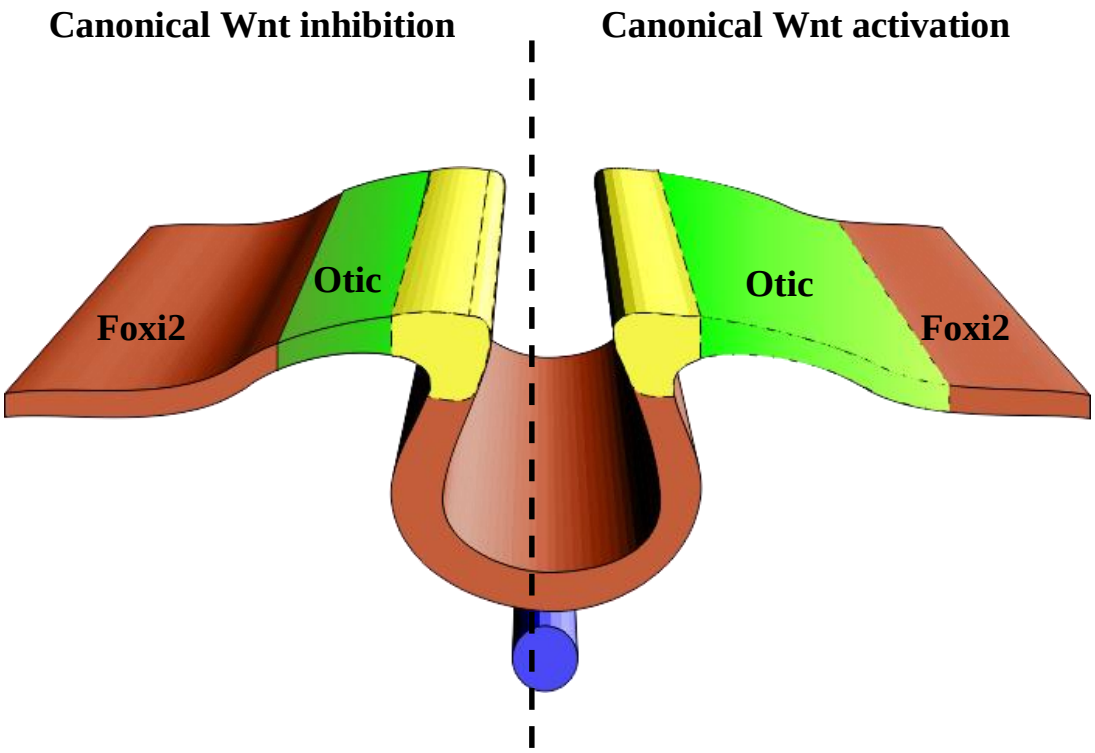

### *5.1.3 General objectives of the chapter*

The results of Chapter 4 have demonstrated the ability to push the differentiating hES cells into adopting a more ectodermal identity which in turn impacts positively on the expression of the key characteristic otic markers. Expanding upon this further by synchronising FGF signalling with manipulation of canonical Wnt signalling may help in further improving the efficiency of directing the differentiation of hES cells into otic progenitors *in vitro*. To date there are no established protocols using hES cells for otic differentiation in such a developmentally-informed manner.

The effect of additional canonical Wnt signalling manipulation will be investigated later into the differentiation protocol, following on from the period of canonical Wnt inhibition highlighted in Chapter 4. Gene expression of the classic otic markers will be investigated, alongside the expression of characteristic PPR and epidermal markers.

## 5.2 Results

### *5.2.1 Canonical Wnt signalling activation late in otic differentiation in the presence of FGF signalling leads to loss of otic marker gene expression*

The results in the previous chapter demonstrated that inhibition of canonical Wnt signalling enhanced the induction of ectodermal fate and subsequent expression of otic genes when inhibition was carried out from the start of the otic differentiation protocol. In addition canonical Wnt signalling needed to be inhibited for at least eight days to have this upregulatory effect on the ectodermal and otic marker gene expression. Inhibition of canonical Wnt signalling from day four of the protocol showed a downregulation or loss of ectodermal and otic gene expression, with differentiation favouring a more mesodermal and endodermal fate.

Taking these data into account it was hypothesised that the increase in ectodermal differentiation with canonical Wnt inhibition was permissive for the FGF 3 and FGF 10 supplemented ligands to induce the otic fate. The role of Wnt signalling in otic placode development is less well characterised than the role of FGF signalling (Freyer and Morrow, 2010; Jacques et al., 2012; Vendrell et al., 2013), but activation of the canonical pathway is believed to be involved in the expansion of the otic placode size once it has been induced (Ohyama et al., 2006). Therefore it was of most interest to determine if the otic marker gene expression could be enhanced further by incorporating a period of canonical Wnt activation into the differentiation protocol.

Otic differentiation experiments were set up comprising of a phase of canonical Wnt inhibition for eight days with 10 µM IWR-1-endo, then a switch to activation with 2 µM BIO for the remaining four days of the protocol. FGF 3 and FGF 10 ligands were supplemented throughout the full 12 days of differentiation. From here on this modified protocol will be referred to as Modified Protocol 1. Standard DFNB and FGF conditions were also included. At the end of the differentiation period RNA was extracted, converted to cDNA and gene expression analysis was carried out by QPCR. The DFNB baseline condition was used as the reference calibrator. For ease of understanding Figure 5.2 shows a schematic representation of Modified Protocol 1 (A)

and the relative gene expression of the otic markers *PAX2*, *PAX8*, *FOXG1* and *SOX2* (A').

**Figure 5.2: Schematic representation of Modified Protocol 1 (A). Gene expression of otic markers *PAX2, PAX8, FOXG1* and *SOX2* following a 12 day differentiation protocol with H14S9 hES cells, seeded at 8x10$^3$ cells/cm$^2$ (A').** Canonical Wnt inhibition was via 10 µM IWR-1-endo and activation via 2 µM BIO. FGF 3 and FGF 10 ligands were supplemented at 50 ng/ml. Gene expression is presented as relative to that of the DFNB baseline control. Bar charts denote mean and standard deviation of gene expression relative to that of the DFNB control condition (n=3 independent experiments). Statistical significance was determined by one way ANOVA with Bonferroni's multiple comparison post-test. ns = no significant difference. **P*<0.05, ***P*<0.01, ****P*<0.001, *****P*<0.0001.

(A)

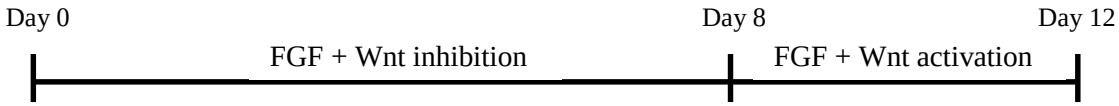


(A')

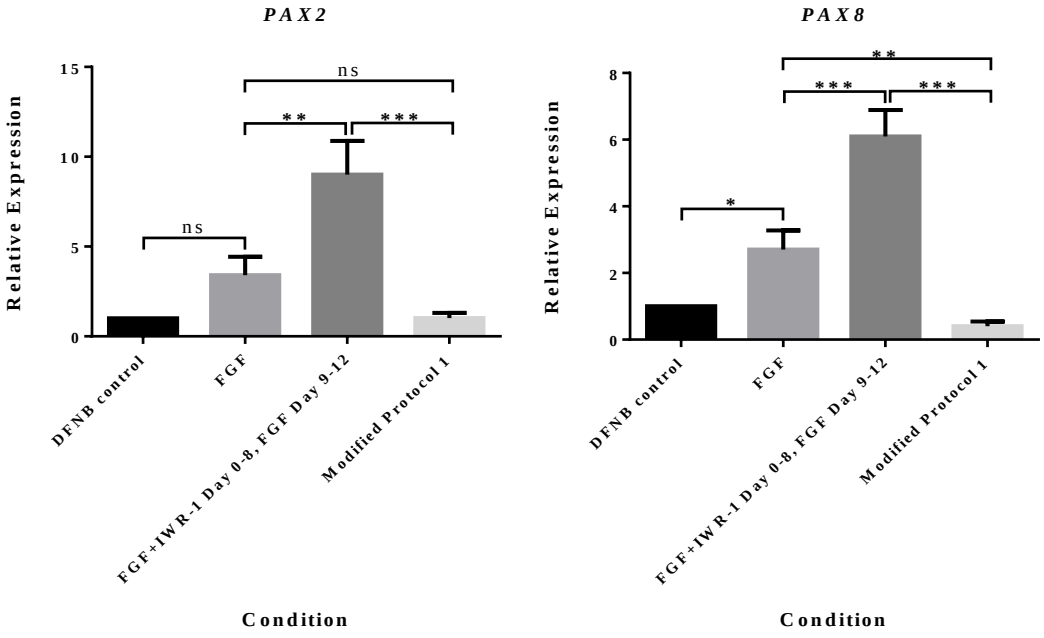

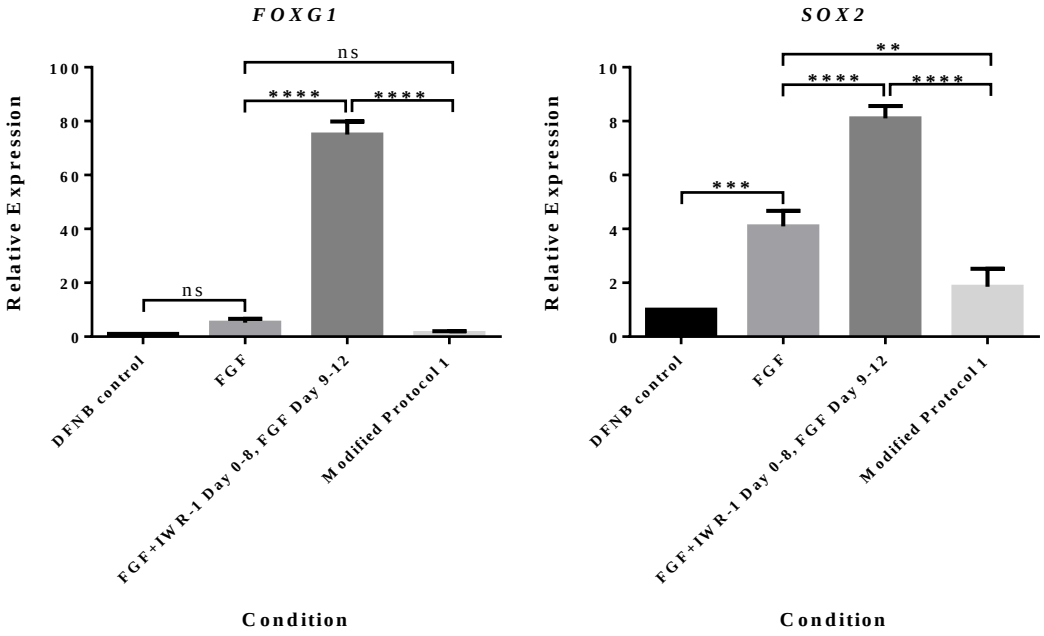
FOXG1
Relative Expression
100
80
60
40
20
0
ns
ns
****
****
DFNB control
FGF
FGF+IWR-1 Day 0-8, FGF Day 9-12
Modified Protocol 1
Condition
SOX2
Relative Expression
10
8
6
4
2
0
**
****
****
***
DFNB control
FGF
FGF+IWR-1 Day 0-8, FGF Day 9-12
Modified Protocol 1
Condition

Unexpectedly the combination of FGF ligands and canonical Wnt activation during the last four days of the manipulated otic differentiation protocol (Modified Protocol 1) caused a highly statistically significant downregulation of all otic marker gene expression investigated compared to the previous eight day Wnt inhibition protocol (Figure 4.6). In addition, in the case of *PAX2* and *FOXG1* there was no significant difference in the gene expression between the standard FGF and Modified Protocol 1. Aware of the published data on the role of canonical Wnt signalling in otic placode expansion, these results were surprising. However the work of Freter et al. (2008) has proposed an inhibitory role of continuous FGF signalling during otic placode maturation and expansion when canonical Wnt signalling is active. In this study in the chick it was demonstrated that an attenuation of *Fgf 3* and *Fgf 19* signalling is required for otic commitment once the otic placode has been established.

### *5.2.2 Canonical Wnt activation with removal of supplemented FGF ligands in late otic differentiation leads to upregulation of PAX2, PAX8 and FOXG1, with a loss of SOX2 expression*

In light of the data shown by Freter et al. (2008) another alteration to the Wnt manipulation protocol was tested. This protocol involved the initial eight day period of FGF 3 and FGF 10 ligand supplementation with canonical Wnt signalling inhibition with IWR-1-endo. For the remaining four days canonical Wnt activation was carried out with BIO in the DFNB basal medium. FGF 3 and FGF 10 were not supplemented into the medium during these last four days of the protocol (featured in Modified Protocol 1). This alternate protocol will be referred to from here on as Modified Protocol 2, and is schematically represented in Figure 5.3A. As with previous experiments, RNA was extracted at the end of the 12 day differentiation protocol and QPCR analysis was carried out to determine gene expression levels of the characteristic otic markers, as displayed in Figure 5.3A'.

The effect of Modified Protocol 2 on the gene expression of *PAX2, PAX8* and *FOXG1* was positive, leading to a significant upregulation of these otic markers when compared to the FGF and initial eight day Wnt inhibition protocol. Therefore in this case the removal of FGF 3 and FGF 10 ligand supplementation during the canonical

Wnt activation phase was beneficial for the differentiation and gene expression of these markers. However a striking feature of this modified protocol is the highly significant downregulation of the gene expression of *SOX2*. In the Modified Protocol 1 experiment (Figure 5.2A') with canonical Wnt activation and FGF 3 and FGF 10 ligand supplementation, *SOX2* gene expression was downregulated alongside the other otic markers investigated. *SOX2* gene expression was also downregulated during the final four days of Modified Protocol 2 (Figure 5.3A'), when canonical Wnt activation takes place with no concomitant FGF ligand supplementation. These experiments, performed side by side, suggested that FGF signalling during the final four days of the modified protocols was required at a particular level in order for otic differentiation to progress. Maintaining FGF 3 and FGF 10 at the standard 50 ng/ml concentration throughout the phase of canonical Wnt activation with BIO appeared to be inhibitory to the gene expression of *PAX2*, *PAX8*, *FOXG1* and *SOX2* (Figure 5.3A'). However, removing supplemented FGF 3 and FGF 10 ligands from the differentiation media during canonical Wnt activation (Figure 5.2A') appeared to have an upregulatory effect on *PAX2, PAX8* and *FOXG1* gene expression, but was still detrimental for expression of *SOX2*. It could consequently be hypothesised that a "Goldilocks" effect of FGF signalling was taking place in otic differentiation; too little was inhibitory, and too much was inhibitory for *SOX2* expression, a key regulator of downstream development of the inner ear structures.

As Modified Protocol 2 appeared to be the most efficient protocol in the upregulation of the majority of the otic marker gene expression, this protocol was looked at in greater detail. To determine if the loss of *SOX2* gene expression (and also the upregulation of the other otic markers) is just at the level of RNA, it was important to also investigate protein expression. Analysis of the protein expression was done using the In Cell Analyser 1000 platform. Differentiation experiments were carried out with H14S9 hES cells subjected to DFNB, FGF and the Modified Protocol 2 conditions. Following the 12 day differentiation period cells were immunolabelled with the following combinations of primary antibodies (a representative experiment is displayed in Figure 5.4): PAX2/PAX8 (A), FOXG1/PAX8 (B) and SOX2/PAX8 (C). Results of three independent repeat experiments are shown in Figure 5.4A'. As featured in Chapter 3, the In Cell Analyser platform was used to determine the percentage of highly co-expressing cells believed to represent the true otic progenitor

population with the differentiating cultures. Cells were deemed to be highly co-expressive of the otic marker antibody combinations if their fluorescent intensity threshold was above the $75^{th}$ percentile set within the FGF condition.

**Figure 5.3: Schematic representation of Modified Protocol 2 (A). Gene expression of otic markers *PAX2*, *PAX8*, *FOXG1* and *SOX2* following a 12 day differentiation protocol with H14S9 hES cells, seeded at 8x10$^3$ cells/cm$^2$ (A').** Canonical Wnt inhibition was via 10 µM IWR-1-endo and activation via 2 µM BIO. FGF 3 and FGF 10 ligands were supplemented at 50 ng/ml. Gene expression is presented as relative to that of the DFNB baseline control. Bar charts denote mean and standard deviation of gene expression relative to that of the DFNB control condition (n=3 independent experiments). Statistical significance was determined by one way ANOVA with Bonferroni's multiple comparison post-test. ns = no significant difference. **P*<0.05, ***P*<0.01, ****P*<0.001, *****P*<0.0001.

(A)

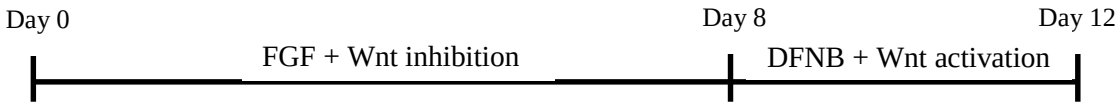


(A')

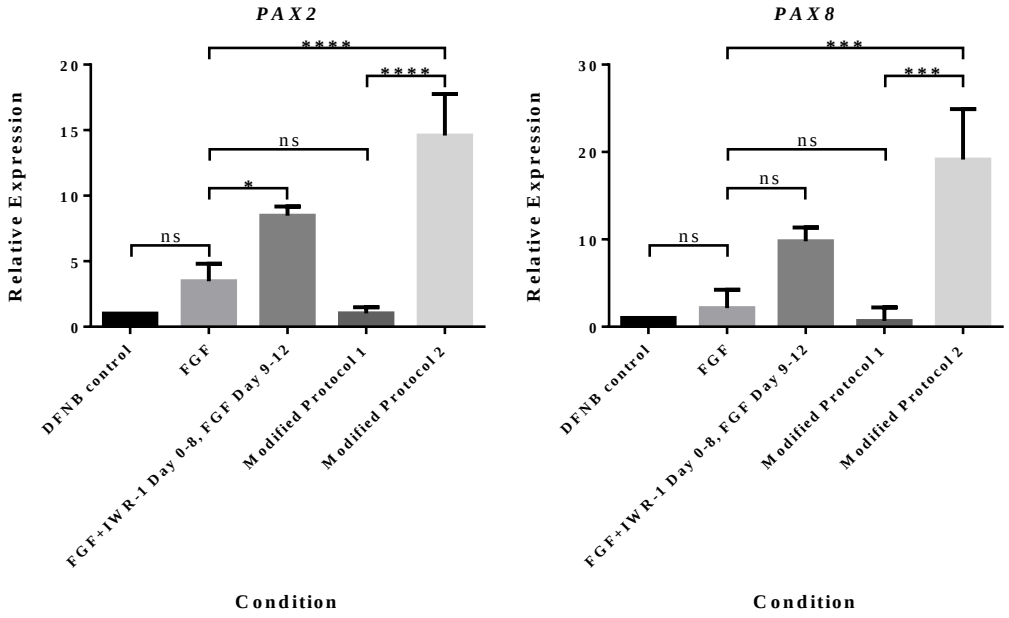

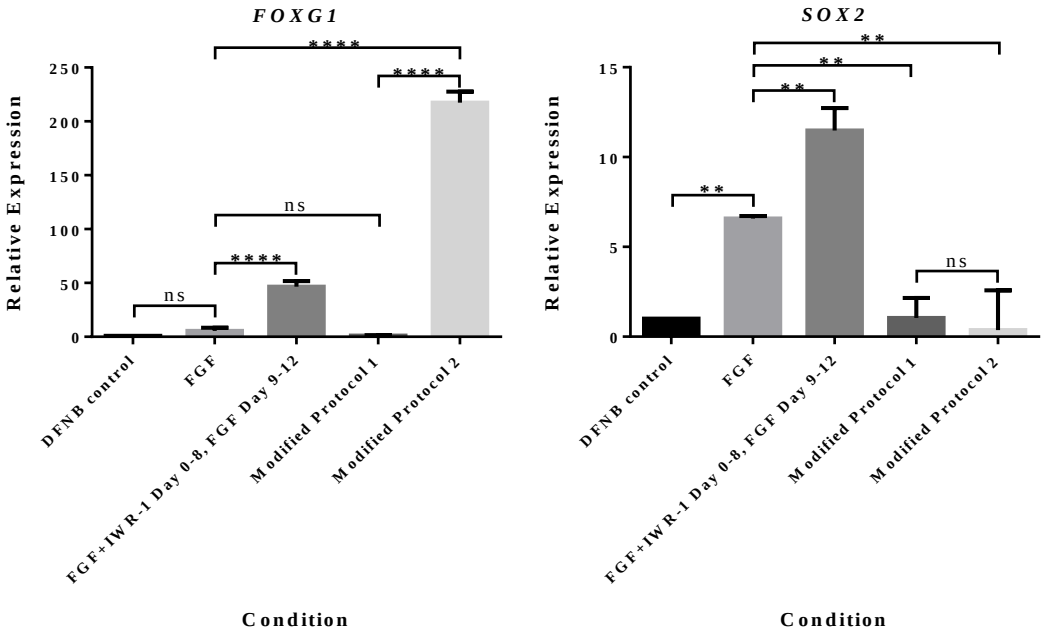
FOXG1
Relative Expression
250
200
150
100
50
0
****
****
ns
****
ns
DFNB control
FGF
FGF+IWR-1 Day 0-8, FGF Day 9-12
Modified Protocol 1
Modified Protocol 2
Condition
SOX2
Relative Expression
15
10
5
0
**
**
**
**
ns
DFNB control
FGF
FGF+IWR-1 Day 0-8, FGF Day 9-12
Modified Protocol 1
Modified Protocol 2
Condition

**Figure 5.4**: **H14S9 hES cells differentiated for 12 days in DFNB, FGF or subjected to Modified Protocol 2.** Representative experiment displayed below. Scatterplots for immunolabelling with (A) PAX2/PAX8 (green/red), (B) FOXG1/PAX8 (green/red) and (C) SOX2/PAX8 (green/red). Fluorescence intensity of each antibody is displayed on each axis. The scatter plots are coloured according to two different intensity thresholds: 99th percentile points of fluorescent intensity in the secondary antibody only control, and 75$^{th}$ percentile points of fluorescent intensity seen in the FGF condition labelling. Grey: intensity below 99$^{th}$ percentile. Green: intensity above the 99$^{th}$ percentile for the green (PAX2, FOXG1, SOX2) but not red channel (PAX8). Red: intensity above the 99$^{th}$ percentile in the red channel but not green channel. Purple: cells are double positive, intensity above the 99$^{th}$ percentile in both channels. Black: cells are highly double positive, intensity is above the FGF 75$^{th}$ percentile in both channels.

(A)

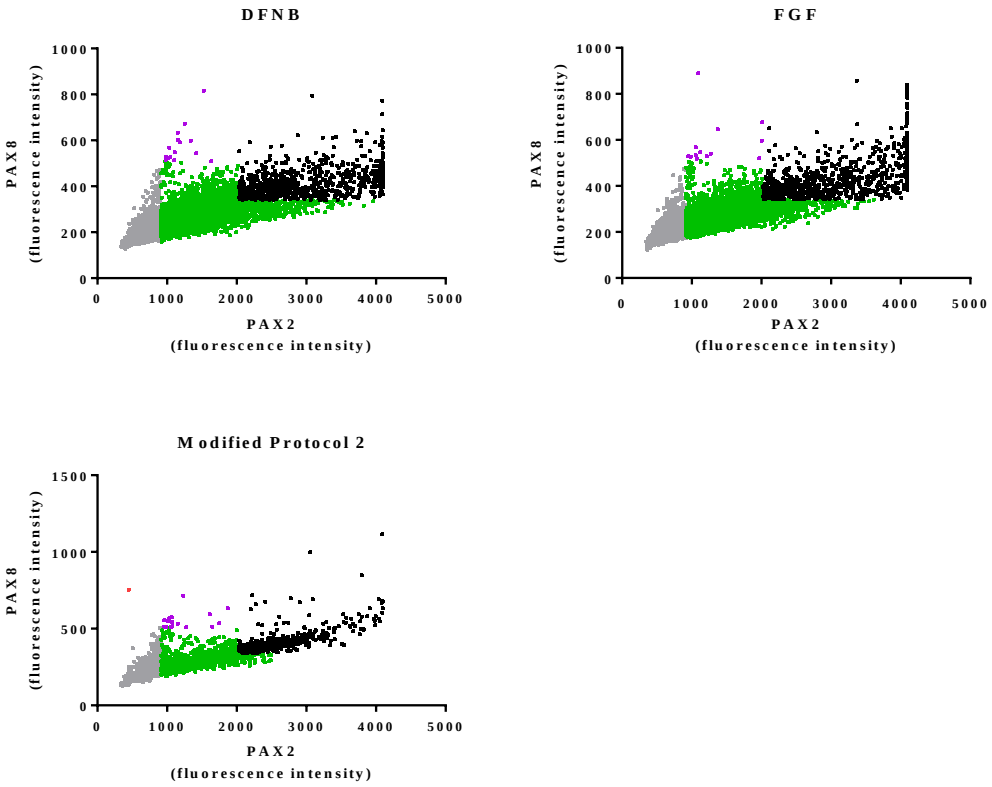

(B)

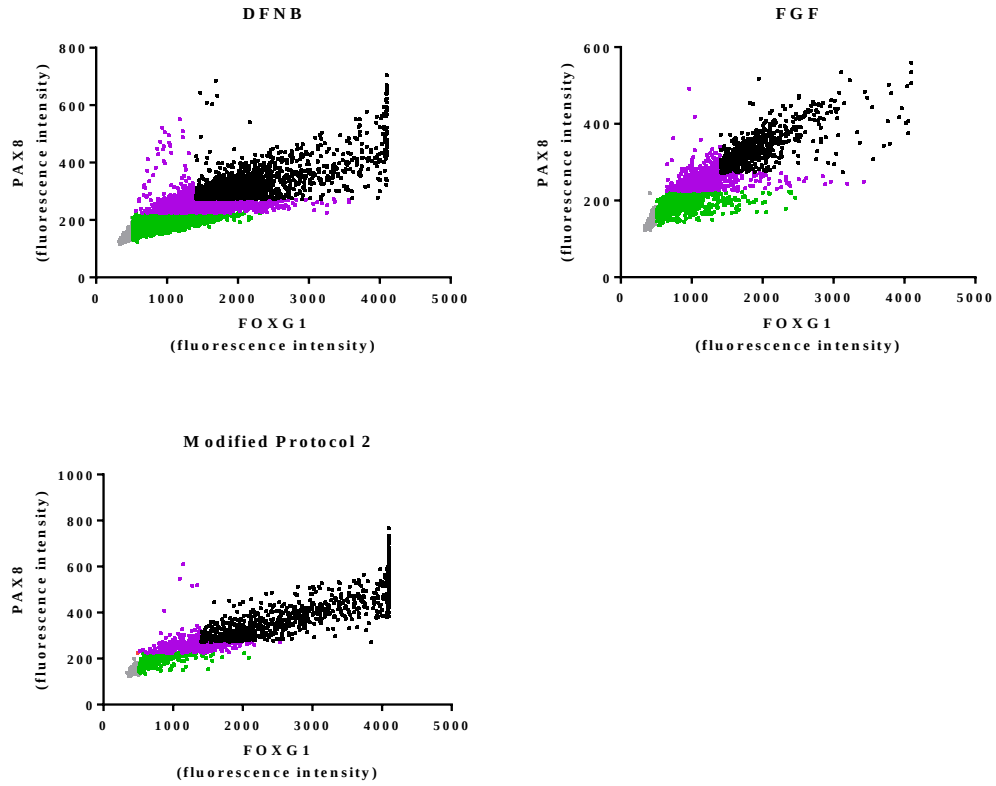
DFNB
PAX8 (fluorescence intensity)
FOXG1 (fluorescence intensity)
FGF
PAX8 (fluorescence intensity)
FOXG1 (fluorescence intensity)
Modified Protocol 2
PAX8 (fluorescence intensity)
FOXG1 (fluorescence intensity)

(C)

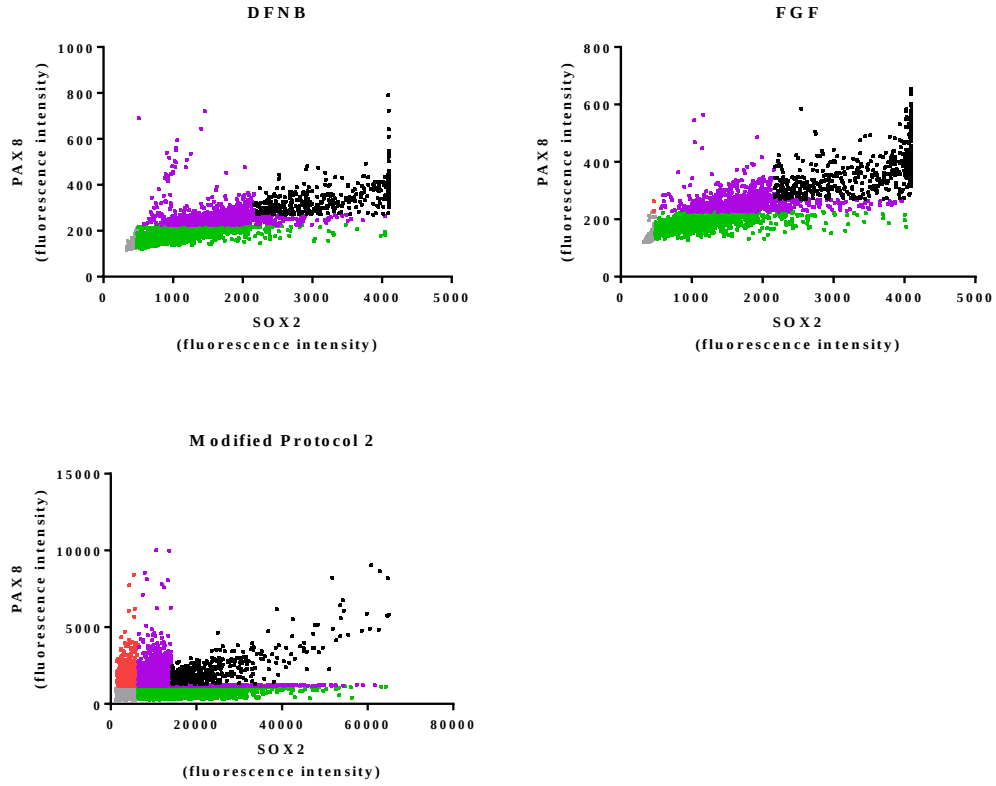
DFNB
PAX8 (fluorescence intensity)
SOX2 (fluorescence intensity)
FGF
PAX8 (fluorescence intensity)
SOX2 (fluorescence intensity)
Modified Protocol 2
PAX8 (fluorescence intensity)
SOX2 (fluorescence intensity)

**Figure 5.4A': H14S9 hES cells differentiated for 12 days in DFNB, FGF or subjected to Modified Protocol 2**. Bar charts show the percentage of highly double positive cells (with a threshold intensity above the 75$^{th}$ percentile) in each condition for the antibody combinations PAX2$^{hi}$/PAX8$^{hi}$, FOXG1$^{hi}$/PAX8$^{hi}$, and SOX2$^{hi}$/PAX8$^{hi}$. The results are presented as the mean of three experimental replicates combined. Error bars denote mean and standard deviation. Statistical significance was determined using Chi-square with Yates' continuity correction. ***$P$<0.001, ****$P$<0.0001.

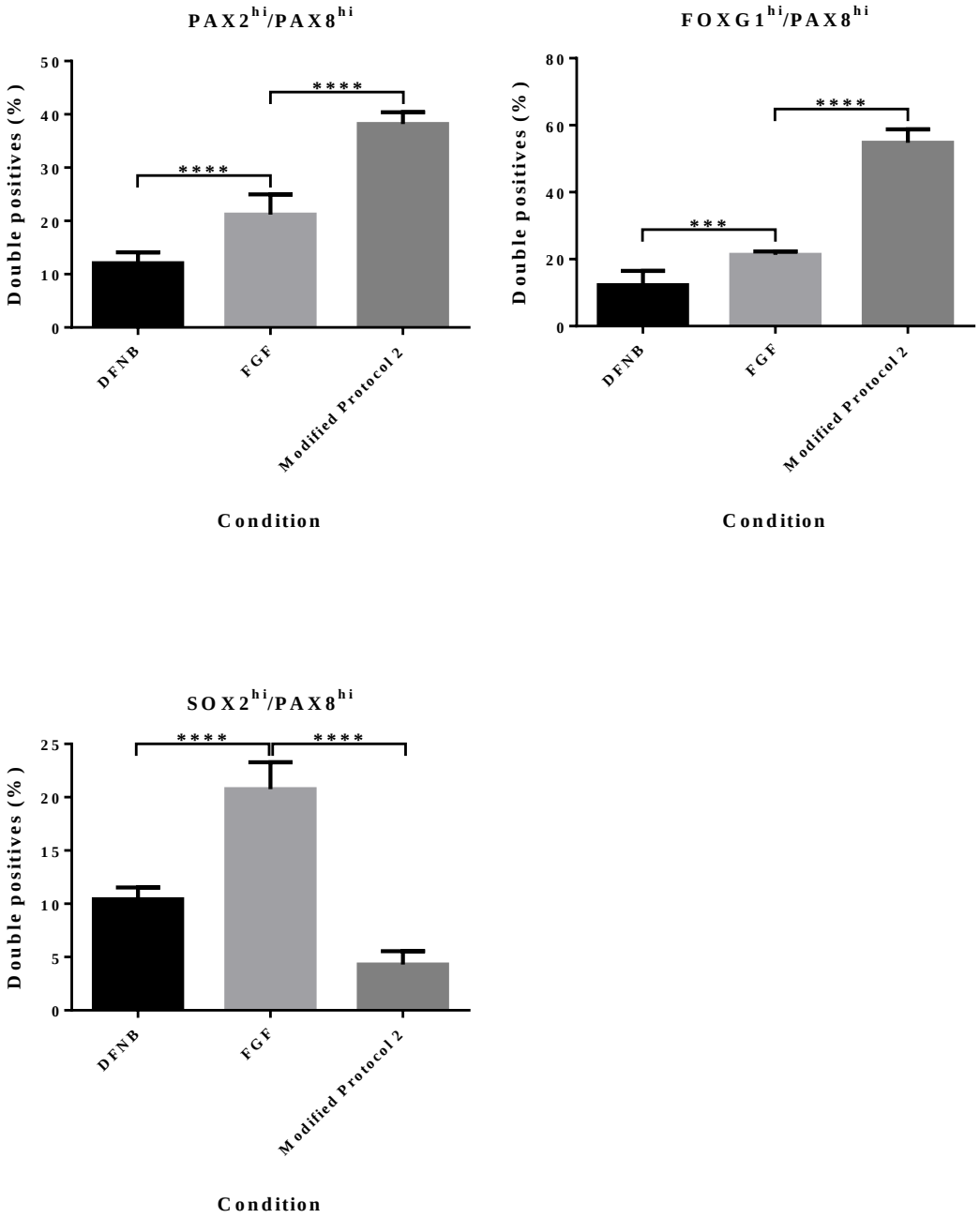

The results of the three independent experiments presented in Figure 5.4A' once again show a statistically significant upregulation of otic marker protein expression between the baseline DFNB control and the FGF treated conditions, as shown previously in Chapter 3 (Figure 3.5A'). The percentage of highly double positive cells for the DFNB, FGF and Modified Protocol 2 conditions respectively for each pair of antibodies used were as follows: PAX2/PAX8: 12.08% ± 2.02%, 21.20% ± 3.78%, and 38.17% ± 2.21%; FOXG1/PAX8: 12.21% ± 4.27%, 21.31% ± 0.97%, and 54.75% ± 4.03%; SOX2/PAX8: 10.41% ± 1.1%, 20.76% ± 2.53%, and 4.30% ± 1.25%. By looking at these results it was apparent that the difference in gene expression levels between the DFNB, FGF and Modified Protocol 2 conditions as shown by QPCR (Figure 5.3) was also demonstrated in the percentage of highly double positive cells for each otic marker antibody combination. Compared to our standard FGF differentiation protocol Modified Protocol 2 appeared to generate a significantly higher proportion of differentiated otic progenitors which highly express the characteristic otic markers PAX2, PAX8 and FOXG1, both at the RNA and protein levels. SOX2 RNA and protein expression, however, was significantly downregulated when the hES cells were subjected to Modified Protocol 2.

Subsequently, for further confirmation of the effect of Modified Protocol 2 on the expression of SOX2, differentiation experiments were set up using the H14S9 NOP-SOX2 reporter line. Reporter line cells were differentiated for 12 days in DFNB, FGF or Modified Protocol 2 conditions, followed by immunolabelling with PAX2, PAX8 or FOXG1 antibodies. The percentage of differentiated cells co-expressing the otic markers with NOP-SOX2 enhancer driven GFP from all three conditions tested are displayed in Figure 5.5. Following the 12 day differentiation period, the percentage of cells co-expressing an otic marker alongside NOP-SOX2 enhancer driven GFP from each of the tested conditions (DFNB, FGF and Modified Protocol 2 respectively) was observed as follows: NOP-SOX2/PAX2: 10.55% ± 1.22%, 21.88% ± 2.02% and 3.83% ±1.14%; NOP-SOX2/PAX8: 11.58% ± 1.56%, 21.25% ± 2.51%, and 4.62% ± 1.78%; NOP-SOX2/FOXG1: 13.18% ± 1.70%, 25.46% ± 3.53%, and 3.52% ± 1.51%. As with the antibody immunolabelling in Figure 5.4A and 5.4A' co-expression of any of the otic markers with the NOP-SOX2 GFP was significantly lower when the reporter hES cells were differentiated in Modified Protocol 2, compared to the DFNB baseline and the standard FGF condition. It can be concluded that the low percentages

seen in Figure 5.5 were as a result of the decreased NOP-SOX2 enhancer reporter activity, and thus SOX2 expression. Expression of PAX2, PAX8 and FOXG1 as seen in Figures 5.3A and 5.3A' was increased during differentiation in Modified Protocol 2 condition and so this also adds weight to the suggestion that it was indeed solely SOX2 expression that was being affected detrimentally in Modified Protocol 2. The consequence of losing SOX2 expression, and its potential impact on downstream applications of further maturation and differentiation of the otic progenitors will be discussed in the section 5.3.

**Figure 5.5: Co-staining of H14S9 NOP-SOX2 reporter cells differentiated for 12 days in DFNB, FGF or Modified Protocol 2 conditions.** Cells were immunolabelled with PAX2, PAX8 or FOXG1 primary antibodies, and the percentage of double positive cells (primary antibody and NOP-SOX2 GFP) is shown below (n=3 independent experiments). Error bars denote mean and standard deviation. Statistical significance was determined using Chi-square with Yates' continuity correction. ****$P$<0.0001.

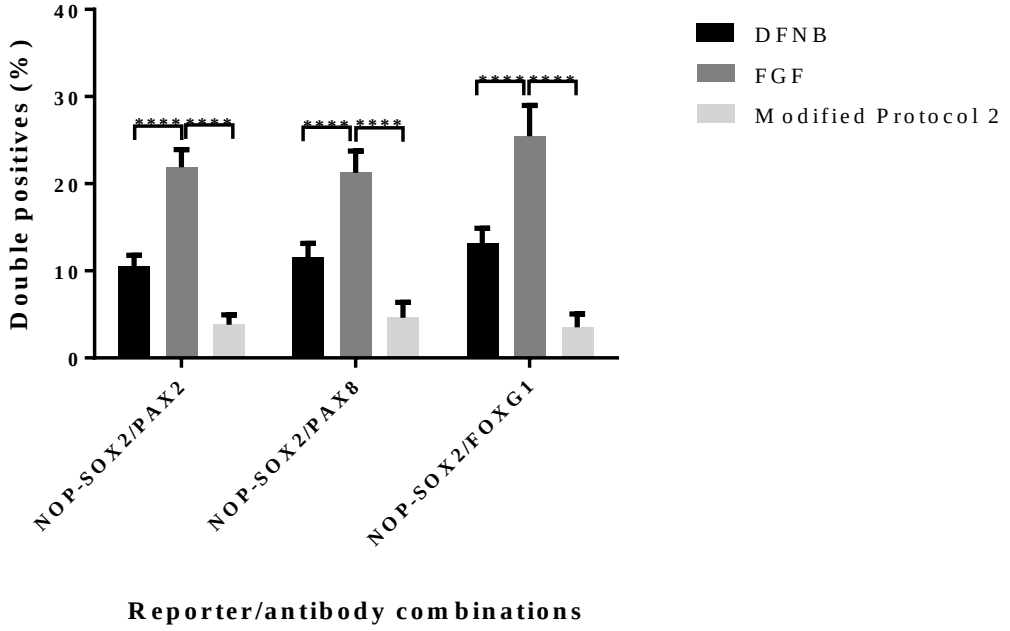

### *5.2.3 FGF ligand supplementation at a lowered dose during canonical Wnt activation in late otic differentiation maintains the upregulation of PAX2, PAX8 and FOXG1, and rescues SOX2 expression*

It has been shown previously in this chapter that in a 12 day differentiation protocol maintaining FGF 3 and FGF 10 ligand supplementation throughout the period of Wnt inhibition (eight days) and subsequent Wnt activation (four days) (Modified Protocol 1) led to a loss or downregulation of gene expression of *PAX2*, *PAX8*, *FOXG1* and *SOX2* (Figures 5.2A and 5.2A'). An alternative version of the protocol was tested in which FGF 3 and FGF 10 ligands were not supplemented into the media during the four day period of canonical Wnt activation (Modified Protocol 2). From this alternate protocol it was observed that gene expression of *PAX2*, *PAX8* and *FOXG1* was significantly upregulated compared to the standard FGF or any other modifications of the protocol tested, yet *SOX2* gene expression was significantly downregulated (Figures 5.3A and 5.3A'). Matching the RNA expression these outcomes of Modified Protocol 2 were also observed in otic marker protein expression (Figures 5.4A and 5.4A'), and also upon differentiating the H14S9 NOP-SOX2 reporter cells (Figure 5.5). In summary, maintenance of FGF supplementation during the canonical Wnt activation phase of the protocol had a negative impact on otic differentiation, whereas removal of FGF ligands was beneficial for all otic marker expression except for *SOX2*, suggesting an intermediate level of FGF signalling may be required.

To address the possibility of an intermediate level of FGF signalling requirement to enhance otic differentiation, differentiation experiments were set up as follows. As with the previous incarnations of the protocol, FGF 3 and FGF 10 ligands were supplemented into the basal DFNB medium at a concentration of 50 ng/ml with concomitant canonical Wnt inhibition with IWR-1-endo at 10 µM, with the hES cells differentiating in this condition for eight days. For the final four days of the protocol, cells were maintained in DFNB medium supplemented with the canonical Wnt agonist BIO at a concentration of 2 µM, and FGF 3 and FGF 10 supplemented at 25 ng/ml (half of the concentration used in the standard otic differentiation protocol and previous modifications). This version of the protocol will be referred to as Modified Protocol 3 from here on. A schematic of the protocol is displayed in Figure 5.6A.

Differentiation experiments with Modified Protocol 3 were carried out alongside H14S9 hES cells differentiated in DFNB, FGF or Modified Protocol 2 conditions. QPCR analysis of otic marker gene expression was carried out and the results are displayed in Figure 5.6A'. It was observed that Modified Protocol 3 reproducibly leads to the differentiation of otic progenitors with a significant upregulation of the gene expression of the otic markers *PAX2*, *PAX8*, *FOXG1* and *SOX2*. For *PAX2*, *PAX8* and *FOXG1* the difference in gene expression between Modified Protocol 2 and 3 was not statistically significant, suggesting the expression of these genes became independent of FGF by this stage, and could be sustained with canonical Wnt activation. Moreover, the gene expression of *SOX2* in the Modified Protocol 3 was rescued and significantly increased over the expression observed from Modified Protocol 2. For *SOX2*, this result suggests an intermediate level of FGF signalling must take place during canonical Wnt activation in order to upregulate and maintain its expression. These results were also seen in the Shef3 hES cell line (Appendix 2).

The In Cell Analyser 1000 platform was next used to ascertain whether the rescue of *SOX2* gene expression at the RNA level was mirrored in the protein level via antibody immunolabelling. The standard FGF condition was used as a baseline in these experiments and PAX8 was used as the co-expressing marker. Figure 5.7A displays a representative example of the In Cell Analyser results, with three independent experimental repeats shown in Figure 5.7A'. Across the repeat experiments the differentiating cells in the FGF condition were observed to have a typical percentage of highly double positive cells for the otic marker combination of SOX2 and PAX8 as seen in previous experiments (mean of 19.6% ± 2.90%). The percentage of cells highly double positive for this combination of markers from the Modified Protocol 3 condition, however, was found to be a mean of 53.98% ± 4.47%. This is a considerable rescue and increase of SOX2 protein expression when compared with Modified Protocol 2 (Figure 5.4A'), and is consistent with the upregulation of *SOX2* gene expression seen in Figure 5.6 by QPCR analysis. Representative images from the In Cell Analyser are shown in Figure 5.7B.

Additionally H14S9 NOP-SOX2 reporter hES cells were also differentiated in both the FGF and Modified Protocol 3 conditions and PAX2, PAX8 and FOXG1 otic marker expression co-labelling with the NOP-SOX2 enhancer driven GFP was investigated. Three experiments were carried out and are displayed in Figure 5.8. In

agreement with the antibody immunolabelling in Figure 5.7, NOP-SOX2 enhancer driven GFP co-labelling with PAX2, PAX8 and FOXG1 was significantly increased when the cells were differentiated in Modified Protocol 3 compared to the standard FGF protocol (Figure 5.8), and is in contrast to the outcome of Modified Protocol 2 on NOP-SOX2 enhancer activity (Figure 5.5). The mean percentage of NOP-SOX2 GFP positive cells with highly positive otic marker antibody immunolabelling for FGF and Modified Protocol 3 respectively were observed as follows: NOP-SOX2/PAX2: 19.59% ± 3.31% and 55.79% ± 7.90%; NOP-SOX2/PAX8: 16.94% ± 1.82% and 52.31% ± 5.07%; NOP-SOX2/FOXG1: 22.04% ± 2.14% and 59.83% ± 6.73%.

**Figure 5.6: Schematic representation of Modified Protocol 3 (A). Gene expression of otic markers *PAX2, PAX8, FOXG1* and *SOX2* following a 12 day differentiation protocol with H14S9 hES cells, seeded at 8x10$^3$ cells/cm$^2$ (A').** Canonical Wnt inhibition was via 10 µM IWR-1-endo and activation via 2 µM BIO. FGF 3 and FGF 10 ligands were supplemented at 50 ng/ml or 25 ng/ml where appropriate. Gene expression is presented as relative to that of the DFNB baseline control. Bar charts denote mean and standard deviation of gene expression relative to that of the DFNB control condition (n=3 independent experiments). Statistical significance was determined by one way ANOVA with Bonferroni's multiple comparison post-test. ns = no significant difference. **P*<0.05, ****P*<0.001, *****P*<0.0001.

(A)

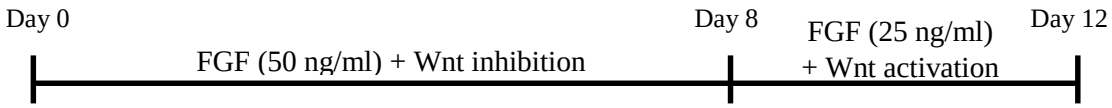


(A')

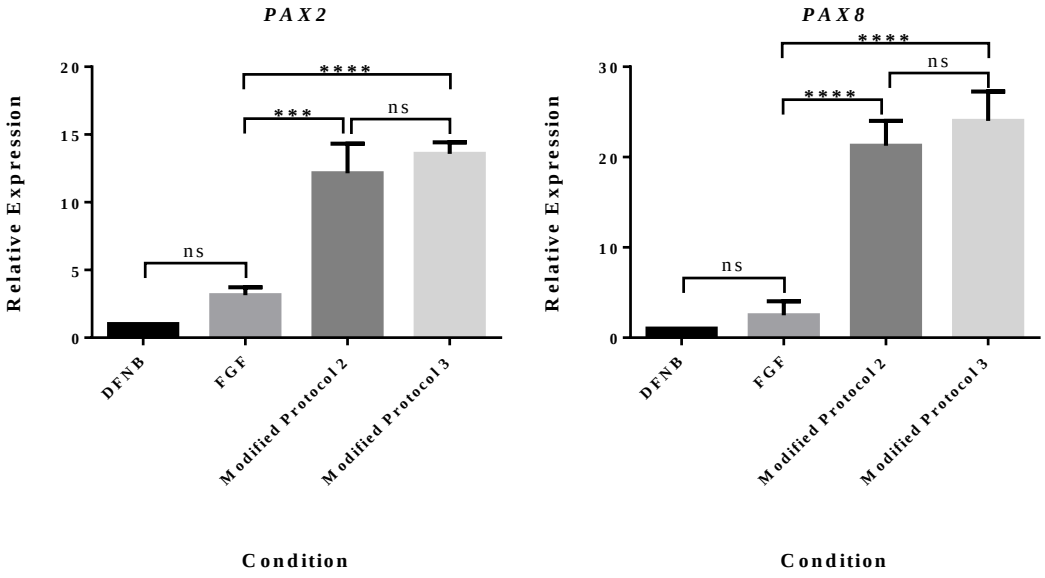

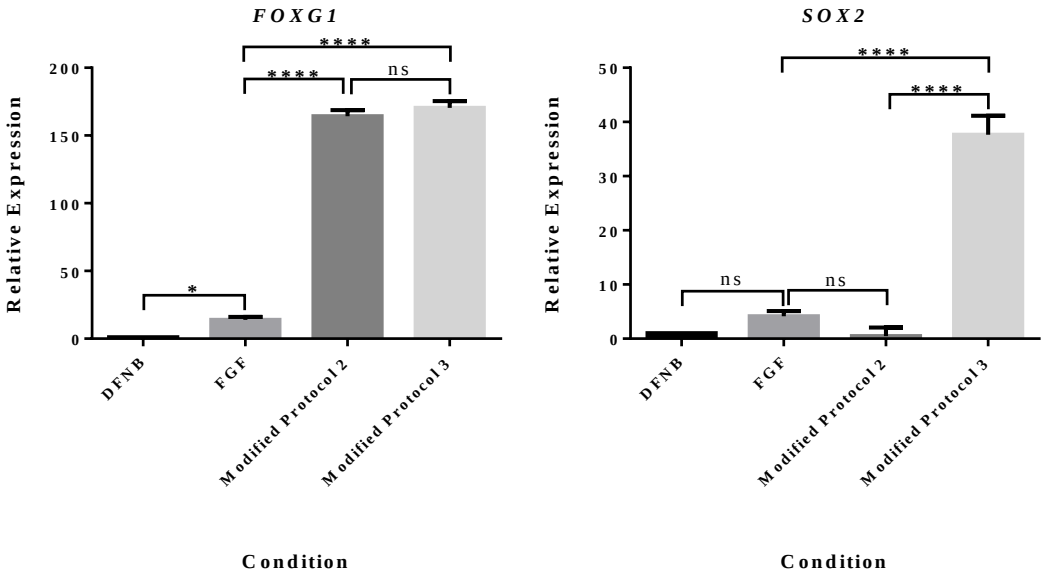
FOXG1
Relative Expression
200
150
100
50
0
****
****
ns
*
DFNB
FGF
Modified Protocol 2
Modified Protocol 3
Condition
SOX2
Relative Expression
50
40
30
20
10
0
****
****
ns
ns
DFNB
FGF
Modified Protocol 2
Modified Protocol 3
Condition

**Figure 5.7A**: **H14S9 hES cells differentiated for 12 days in FGF or subjected to the Modified Protocol 3.** Representative experiment displayed below. Scatterplots for immunolabelling with SOX2/PAX8 (green/red). Fluorescence intensity of each antibody is displayed on each axis. The scatter plots are coloured according to two different intensity thresholds: 99th percentile points of fluorescent intensity in the secondary antibody only control, and 75$^{th}$ percentile points of fluorescent intensity seen in the FGF condition labelling. Grey: intensity below 99$^{th}$ percentile. Green: intensity above the 99$^{th}$ percentile for the green (SOX2) but not red channel (PAX8). Red: intensity above the 99$^{th}$ percentile in the red channel but not green channel. Purple: cells are double positive, intensity above the 99$^{th}$ percentile in both channels. Black: cells are highly double positive, intensity is above the FGF 75$^{th}$ percentile in both channels.

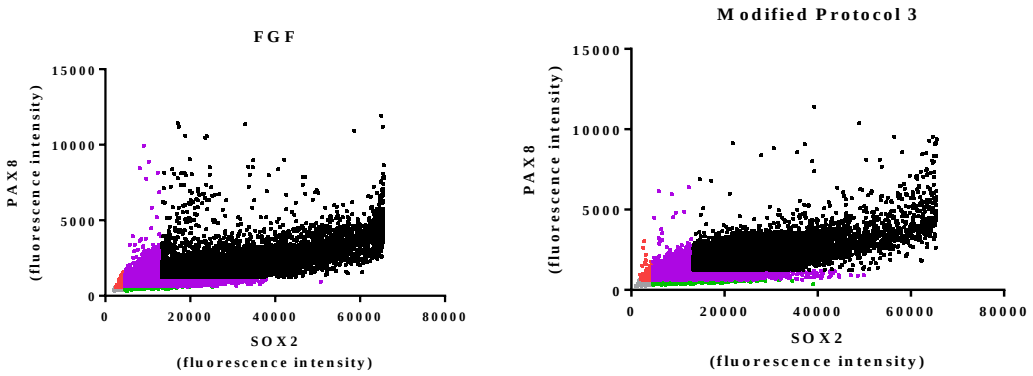

**Figure 5.7A': H14S9 hES cells differentiated for 12 days in FGF or subjected to Modified Protocol 3**. Bar charts show the percentage of highly double positive cells (with a threshold intensity above the 75$^{th}$ percentile) in each condition for the antibody combination SOX2$^{hi}$/PAX8$^{hi}$. The results are presented as the mean of three experimental replicates combined. Error bars denote mean and standard deviation. Statistical significance was determined using Chi-square with Yates' continuity correction. ****$P$<0.0001.

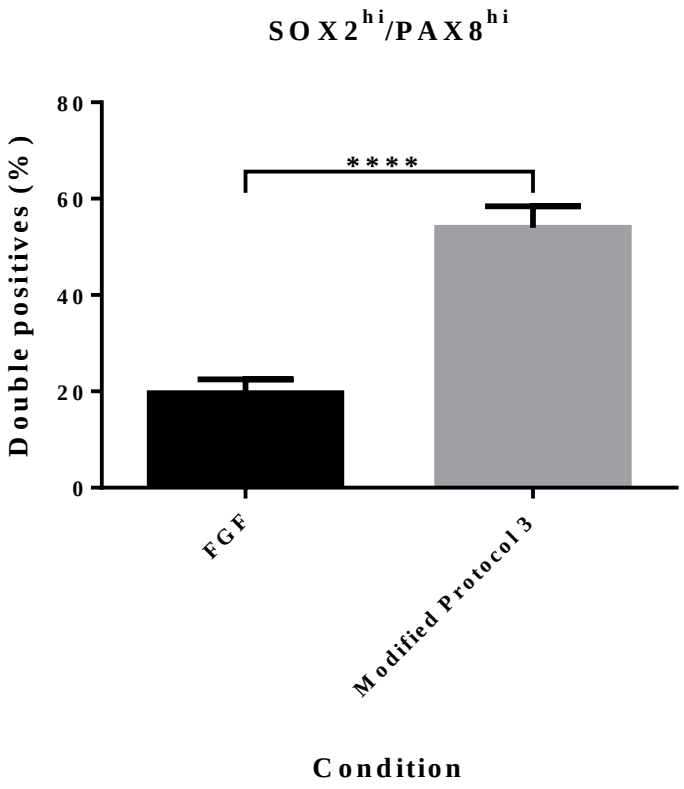

**Figure 5.7B: Representative In Cell Analyser images.** x20 magnification images visually highlighting the difference in fluorescence intensity between the FGF and Modified Protocol 3 differentiation conditions on SOX2/PAX8 labelling.

**FGF**

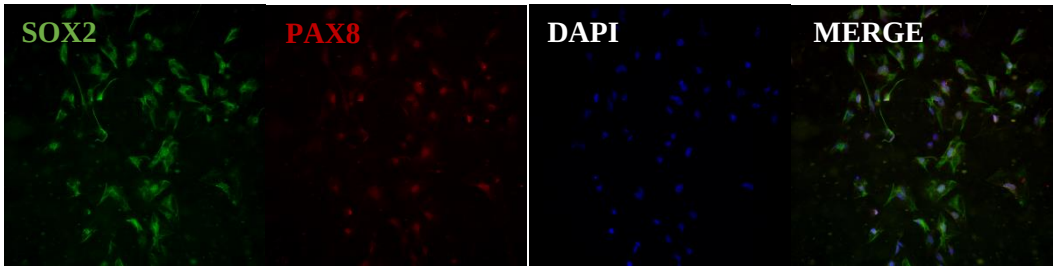


**Modified Protocol 3**

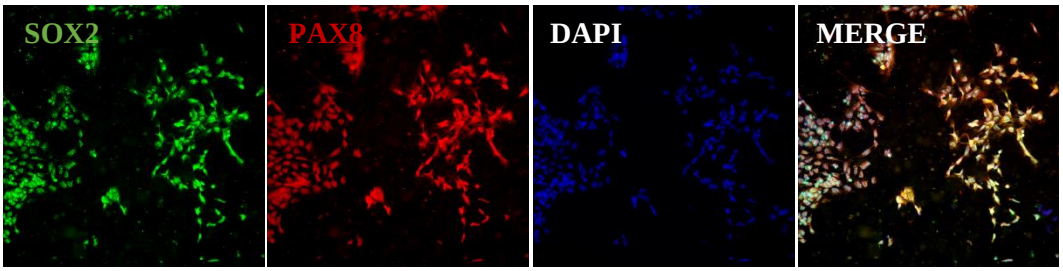

**Figure 5.8: Co-staining of H14S9 NOP-SOX2 reporter cells differentiated for 12 days in FGF or Modified Protocol 3 conditions.** Cells were immunolabelled with PAX2, PAX8 or FOXG1 primary antibodies, and the percentage of double positive cells (primary antibody and NOP-SOX2 GFP) is shown below (n=3 independent experiments). Error bars denote mean and standard deviation. Statistical significance was determined using Chi-square with Yates' continuity correction. ****$P$<0.0001.

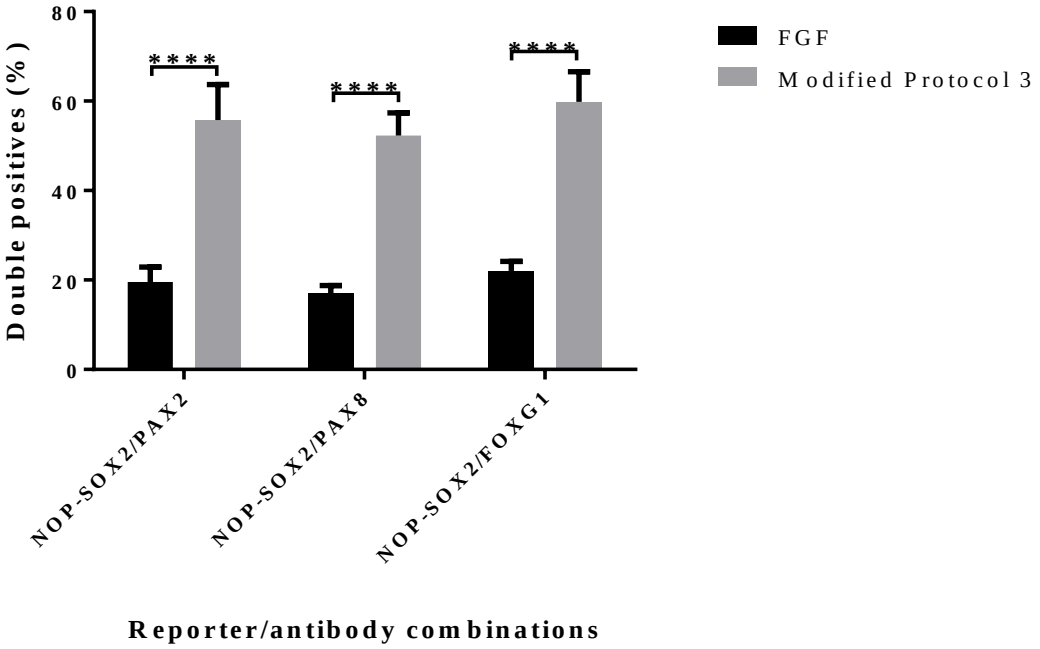

### *5.2.4 Removal of FGF ligand supplementation during the eight day period of canonical Wnt inhibition leads to inconsistent otic differentiation*

In many developmentally informed *in vitro* differentiation protocols using hES cells, researchers have attempted to recapitulate known *in vivo* events. Inner ear and otic placode differentiation *in vitro* is no different. In studies such as those by Koehler et al. (2013), Oshima et al. (2010) and Ronaghi et al. (2014), an attempt to first generate pre-placodal ectoderm is carried out prior to otic placodal differentiation proper. In these studies FGF signalling is not promoted by ligand supplementation in the initial pre-placodal ectoderm differentiation phase. With the knowledge of this, it was important to investigate whether supplementation of FGF 3 and FGF 10 during the first eight day phase of Modified Protocol 3 alongside canonical Wnt inhibition is a requirement for otic differentiation, or if canonical Wnt inhibition alone is sufficient to generate the ectoderm required for otic placodal differentiation to take place. This additional manipulation of the protocol will be referred to as Modified Protocol 4, and is schematically represented in Figure 5.9A. As with the previous modifications three independent replicate experiments were set up to differentiate the H14S9 hES cells in DFNB, FGF, Modified Protocol 3 and Modified Protocol 4 conditions. RNA was extracted following the 12 day differentiation period and QPCR analysis of *PAX2*, *PAX8*, *FOXG1* and *SOX2* gene expression was carried out. The results are displayed in Figure 5.9A'. No statistically significant gene expression differences were observed between the standard FGF condition and Modified Protocol 4, or even between Modified Protocols 3 and 4. This was the case for all otic markers investigated. The large standard deviation in the three independent experiments determining the effect of Modified Protocol 4 was due to the large fluctuations in the gene expression levels observed. One of the three experiments produced an increase in gene expression of all the otic markers tested, higher than that of Modified Protocol 3 (the most efficient protocol thus far). However the following two repeat experiments produced gene expression levels approximately at similar, or even lower, levels than those produced in the standard FGF condition. A possible explanation for this could be that addition and maintenance of FGF 3 and FGF 10 into the culture media during the eight day canonical Wnt inhibition phase is required to stabilise ectodermal

differentiation in our system and will be discussed in section 5.3. As such, Modified Protocol 3 will be used from here on as the preferred method of otic differentiation.

**Figure 5.9: Schematic representation of Modified Protocol 4 (A). Gene expression of otic markers *PAX2*, *PAX8*, *FOXG1* and *SOX2* following a 12 day differentiation protocol with H14S9 hES cells, seeded at 8x10$^3$ cells/cm$^2$ (A').** Canonical Wnt inhibition was via 10 µM IWR-1-endo and activation via 2 µM BIO. FGF 3 and FGF 10 ligands were supplemented at 25 ng/ml. Gene expression is presented as relative to that of the DFNB baseline control. Bar charts denote mean and standard deviation of gene expression relative to that of the DFNB control condition (n=3 independent experiments). Statistical significance was determined by one way ANOVA with Bonferroni's multiple comparison post-test. ns = no significant difference. **P*<0.05, ***P*<0.01, ****P*<0.001.

(A)

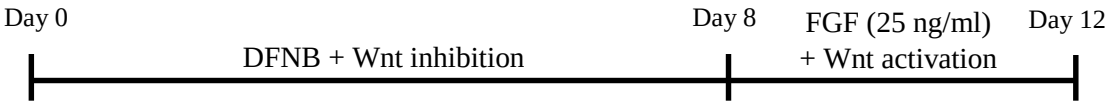


(A')

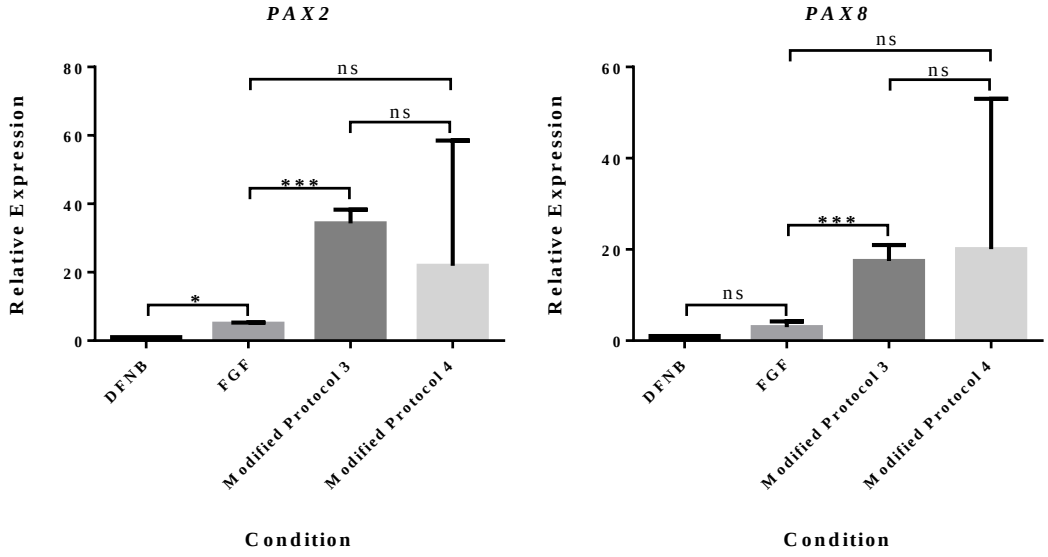

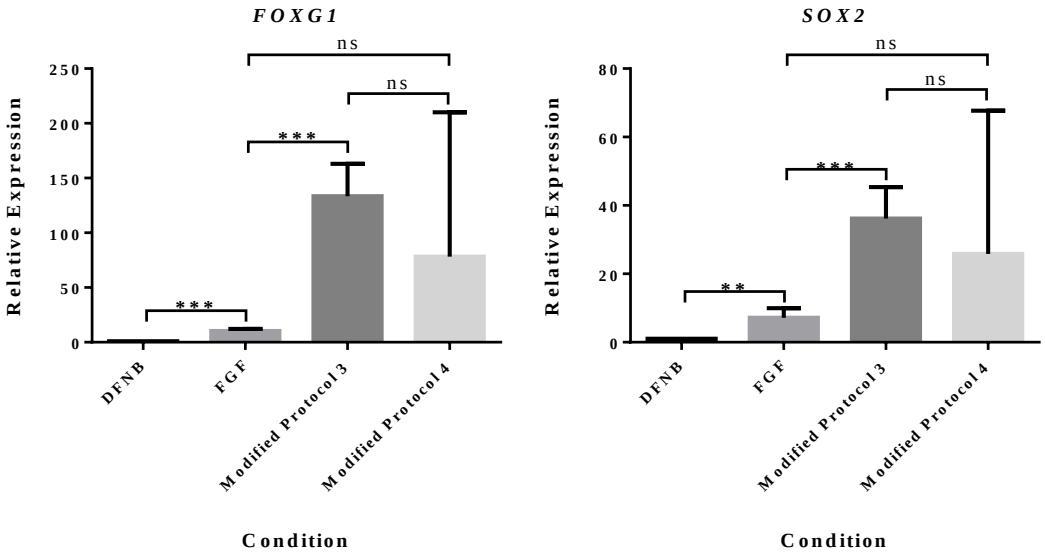
FOXG1
Relative Expression
250
200
150
100
50
0
ns
ns
***
***
DFNB
FGF
Modified Protocol 3
Modified Protocol 4
Condition
SOX2
Relative Expression
80
60
40
20
0
ns
ns
***
**
DFNB
FGF
Modified Protocol 3
Modified Protocol 4
Condition

### *5.2.5 Canonical Wnt manipulation during otic differentiation promotes pre-placodal identity*

Introduced in Chapter 1 and in section 5.1 of this chapter, the otic placode arises from a patch of thickened surface ectoderm in the developing embryo. Prior to otic placode induction a region containing multipotent progenitors which will later differentiate and form cells of all of the craniofacial placodes is induced, known as the pre-placodal region (PPR). Characteristic markers of the PPR include members of the SIX, DLX and EYA gene families. It has been shown previously in this chapter that Modified Protocol 3 leads to a strong upregulation of the otic markers *PAX2, PAX8, FOXG1* and *SOX2* following a 12 day differentiation of hES cells into otic progenitors. This manipulation of the standard FGF protocol can be considered as being more developmentally informed, with basic crucial events of early embryonic development being mimicked *in vitro*. Therefore it was of interest to determine if markers of the PPR are also expressed at key points in the differentiation protocol timeline.

With H14S9 hES cells differentiation experiments were set up to compare the gene expression of *SIX1*, *DLX5* and *EYA1* in DFNB, FGF and Modified Protocol 3 conditions. RNA was extracted from differentiating cells either at day 8 or at the end point of the protocol, day 12. The additional time point of RNA extraction on day 8 was carried out to determine the gene expression of the PPR markers at the end of the phase of canonical Wnt inhibition, prior to the switch to the phase of canonical Wnt activation. A reminder of the components of Modified Protocol 3 is displayed schematically in Figure 5.10A. As shown in Figure 5.10A' gene expression of the PPR markers *SIX1*, *DLX5* and *EYA1* appeared to be slightly upregulated by day 8 of FGF treatment and this level was maintained by day 12 in comparison to the DFNB baseline control condition, although this apparent upregulation was found not to be statistically significant. However the gene expression of all of the PPR markers investigated was significantly upregulated by the end of day 8 of Modified Protocol 3 compared to the standard FGF protocol. This upregulation of gene expression of the PPR markers appeared to be maintained until day 12.

**Figure 5.10: Schematic representation of Modified Protocol 3 (A). Gene expression of PPR markers *SIX1*, *DLX5* and *EYA1* following an 8 or 12 day differentiation protocol with H14S9 hES cells, seeded at 8x10$^3$ cells/cm$^2$ (A').** Canonical Wnt inhibition was via 10 µM IWR-1-endo and activation via 2 µM BIO. FGF 3 and FGF 10 ligands were supplemented at 50 ng/ml days 0-8 and 25 ng/ml thereafter. Gene expression is presented as relative to that of the DFNB baseline control at day 8 or day 12. Bar charts denote mean and standard deviation of gene expression relative to that of the DFNB control condition (n=3 independent experiments). Statistical significance was determined by one way ANOVA with Bonferroni's multiple comparison post-test. ns = no significant difference. **P*<0.05, ***P*<0.01, ****P*<0.001.

(A)

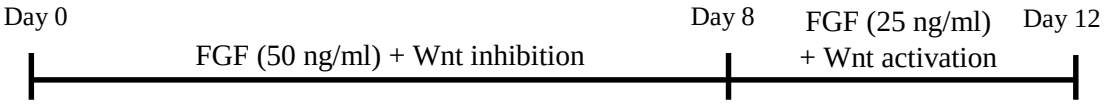


(A')

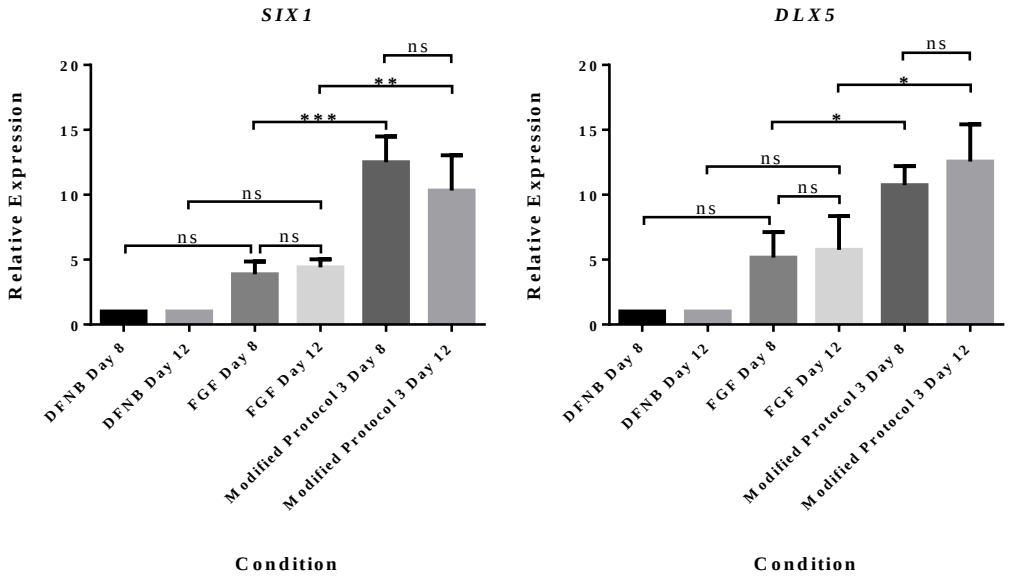

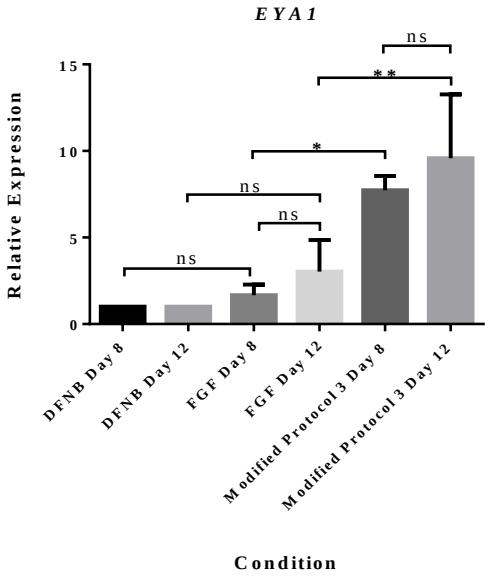
EYA1
Relative Expression
15
10
5
0
ns
**
*
ns
ns
ns
DFNB Day 8
DFNB Day 12
FGF Day 8
FGF Day 12
Modified Protocol 3 Day 8
Modified Protocol 3 Day 12
Condition

### *5.2.6 Canonical Wnt signalling manipulation increases otic differentiation at the expense of epidermis in vitro*

Following the initial induction of the otic placode it is believed that canonical Wnt plays a key role in the expansion of the placode at the expense of the surrounding non-neural ectoderm and epidermis (Jayasena et al., 2008; Ohyama et al., 2006). Foxi2 (Forkhead box I2) has previously been shown, in chicken (Khatri and Groves, 2013) and mouse (Ohyama and Groves, 2004), to initially broadly mark the cranial ectoderm and its expression later becomes excluded from the otic placode, and remains a marker of the epidermis. Using the cDNA samples produced from the experiments displayed in Figure 5.10, *FOXI2* gene expression was determined by QPCR analysis with the purpose of establishing any differences in its expression between the baseline DFNB, FGF and Modified Protocol 3 differentiation conditions. This was determined at both day 8 and day 12 of the protocols, and is represented in Figure 5.11.

As with the PPR markers in Figure 5.10, there appeared to be a slight upregulation of *FOXI2* gene expression in the FGF treated cells compared to be the baseline DFNB condition at both day 8 and at day 12, although this was not a statistically significant difference. There was however a highly significant upregulation of *FOXI2* gene expression in the Modified Protocol 3 treated cells at day 8 of the differentiation period compared to the standard FGF protocol. Moreover, there was no difference in the gene expression of *FOXI2* between FGF and Modified Protocol 3 when comparing the levels observed at day 12 of differentiation. Interestingly it was observed that a highly significant downregulation of *FOXI2* expression occurred between day 8 and day 12 of the Modified Protocol 3 differentiation, suggesting the switch from canonical Wnt inhibition to activation (and presumably the decrease in supplemented FGF 3 and FGF 10 ligands) could be the basis of this downregulation. These results are in agreement with the pattern of FOXI2 expression *in vivo*, where it is initially present in all the cranial ectoderm, to be later excluded from the otic placode.

**Figure 5.11: Gene expression of *FOXI2* following an 8 or 12 day differentiation protocol with H14S9 hES cells, seeded at 8x10$^3$ cells/cm$^2$ (A').** Canonical Wnt inhibition was via 10 µM IWR-1-endo and activation via 2 µM BIO. FGF 3 and FGF 10 ligands were supplemented at 50 ng/ml days 0-8 and 25 ng/ml thereafter. Gene expression is presented as relative to that of the DFNB baseline control at day 8 or day 12. Bar charts denote mean and standard deviation of gene expression relative to that of the DFNB control condition (n=3 independent experiments). Statistical significance was determined by one way ANOVA with Bonferroni's multiple comparison post-test. ns = no significant difference. ****$P$<0.0001.

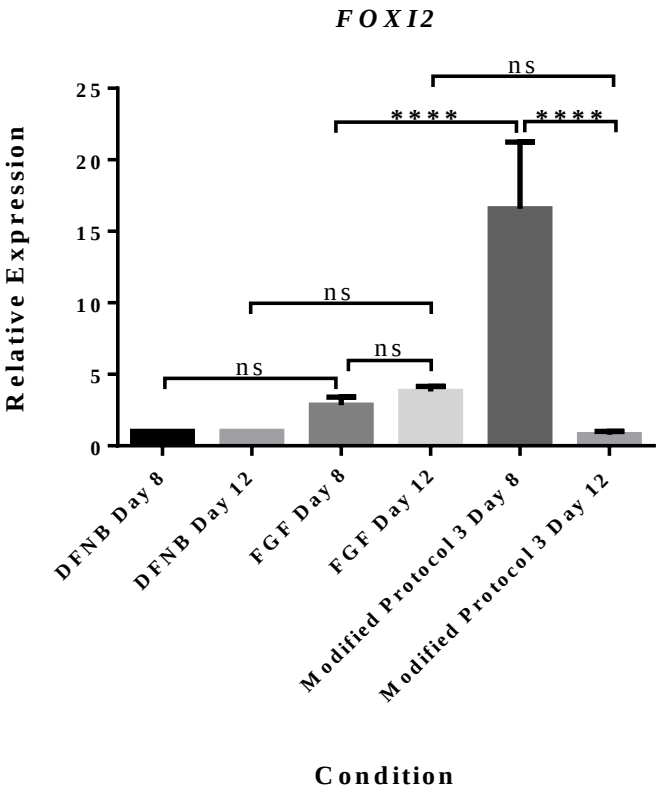

## 5.3 Discussion

### *5.3.1 FGF signalling must be attenuated during late in vitro otic differentiation in the presence of canonical Wnt activation*

In Chapter 4 an eight day period of canonical Wnt signalling inhibition was used in combination with FGF signalling to push the differentiating hES cells into an ectodermal fate, resulting in the upregulation of ectodermal and otic marker gene expression at the expense of markers of the mesoderm and endoderm lineages. This chapter aimed to expand on this by adding a second dimension to the otic differentiation protocol; canonical Wnt activation during the final four days of the protocol. Previous published research in mice has demonstrated a direct role for canonical Wnt signalling in the initiation of otic placode development via the ability of canonical Wnt signalling to expand the otic progenitor population (Ohyama et al., 2006), whereas studies carried out in zebrafish (Phillips et al., 2004) suggest that loss of Wnt signalling does not affect the otic placode formation itself, but delays its onset. In this chapter it was shown that canonical Wnt activation with the small molecule compound BIO in combination with the standard concentration of FGF 3 and FGF 10 ligands (50 ng/ml) during the final four days of differentiation led to a downregulation of the gene expression of the characteristic otic markers, *PAX2*, *PAX8*, *FOXG1* and *SOX2* (Figure 5.2). Moreover, removal of FGF supplementation during this period rescued the expression of *PAX2*, *PAX8* and *FOXG1* and expression levels of these genes were observed to be higher than from the standard FGF protocol or from the protocol used in Chapter 4 (Figures 5.3, 5.4). Gene expression of *SOX2* however was significantly downregulated following the removal of supplemented FGF ligands, and this was also demonstrated by a reduction in the H14S9 NOP-SOX2 reporter activity (Figure 5.5). It was then highlighted that an intermediate level of FGF ligand supplementation (25 ng/ml) was required with canonical Wnt activation in order to rescue the gene expression of SOX2 (Figures 5.6, 5.7).

These findings are similar to key chick *in vivo* findings published by Ladher et al. (2000) and Freter et al. (2008). It was identified that *Fgf 19* and *Fgf 3* from the neuroectoderm and mesoderm in the chick are downregulated early in embryonic

development, prior to the specification of the otic placode and this finding raised the possibility of FGF signalling attenuation as a required event for otic placode differentiation to progress (Ladher et al., 2000). A later study expanded on this theory (Freter et al., 2008) and utilised plasmid constructs constitutively driving *Fgf 19* and *Fgf 3* expression in the chick using the Ef1α promoter system. When electroporated into HH4 (Hamilton and Hamburger) stage chick embryos it was found that expression of *Pax2* in the presumptive OEPD region was much stronger and the region of expression was largely expanded when the two FGF constructs were electroporated simultaneously, compared to single construct electroporation. Conversely short-hairpin interfering RNA (siRNA) used to knockdown *Fgf 19* and *Fgf 3* led to the loss of Pax2 expression and a subsequent reduction in the size of the OEPD region, confirming the necessity of these two FGF ligands on initiation of the otic placode. However when the two FGF plasmid constructs were sustained, *Soho1* and *Nkx5.1* expression (markers present when the otic placode has differentiated and become morphologically visible) was absent or significantly downregulated compared to wild type chick embryos, suggesting that sustained FGF signalling is detrimental for otic placode differentiation. Canonical Wnt signalling inhibition by electroporation of the inhibitor Dickkopf 1 during this time also results in a dramatic loss of the expression of *Soho1* and *Nkx5.1*. Together these results demonstrate the role of canonical Wnt signalling in otic placode specification when FGF signalling has been attenuated.

### *5.3.2 Loss of SOX2 expression with removal of FGF ligands indicates FGF acts upstream of SOX2*

The significant downregulation of *SOX2* expression seen when supplemented FGF is removed (Figures 5.3, 5.4, 5.5) indicates that FGF acts upstream of *SOX2* and may function to directly control its expression. Indeed this is a phenomenon demonstrated in a number of other systems. For example in the differentiation of osteoblasts (Ambrosetti et al., 2008; Mansukhani et al., 2005) FGF signalling has been shown to have an inductive role in *SOX2* expression. Also within the morphogenesis of the stomach forced expression of FGF 10 has been shown to upregulate the expression of *SOX2*. Rescued expression of *SOX2* is crucial in the differentiation of the otic

progenitors *in vitro* as this will impact on the further differentiation of the progenitors into the more mature cell types of the inner ear, as SOX2 is required for the induction of the prosensory regions prior to hair cell and auditory neuronal differentiation (Kiernan et al., 2005).

### *5.3.3 FGF is required with canonical Wnt manipulation to promote pre-placodal identity and otic differentiation*

Published studies have highlighted the roles for FGF signalling in promoting ectodermal differentiation and pre-placodal identity in both *in vitro* (Cohen et al., 2010; Vallier et al., 2009; Zheng et al., 2010) and *in vivo* (Kwon et al., 2010; Litsiou et al., 2005) studies. Nevertheless many recent studies attempting to recapitulate *in vivo* events of embryonic development through to otic placodal identity do not initially supplement differentiation media with exogenous FGF ligands until later in their protocols. One such example is that carried out by Koehler et al. (2013). In this study mouse embryonic stem cells were force aggregated into embryoid bodies and subjected to a scheduled cocktail of various signalling pathway modifiers (BMP agonist, TGF-β inhibitor) to promote non-neural ectoderm and pre-placodal cell identity. FGF signalling by way of FGF 2 was not added until day 4 of differentiation. Similarly the study conducted by Oshima et al. (2010) also used a mouse embryoid body approach to generate otic differentiation. FGF ligands were not supplemented until day 5 in this protocol. Despite this however, it cannot be ruled out that FGF signalling was not taking place in these two protocols. Embryoid bodies (compared to our monolayer approach) feature differentiation of all three germ layers, and although embryoid bodies can be directed to generate cells of a desired germ layer, it is still possible that FGF signalling could be taking place. Additionally in the study by Koehler et al. (2013) Matrigel is used as a component of the differentiation media, which is known to contain a large number of growth factor constituents including FGF2, which may act on pre-placodal and otic differentiation.

Removal of FGF supplementation during the first eight days of differentiation with canonical Wnt inhibition (Modified Protocol 4, Figure 5.9) was tested in order to ascertain if supplemented FGF signalling is required for enhancing otic differentiation.

Inconsistent results were observed. Although the differentiation experiments were all set up at the same starting density, it is entirely plausible that the level of endogenous FGF production likely fluctuates between experiments, and possibly the cells differentiated in the first Modified Protocol 4 experiment may have produced sufficient endogenous FGF signals to induce robust ectodermal differentiation in coordination with canonical Wnt inhibition, an effect lacking in the subsequent replicate experiments. Supplementing the culture media with FGF 3 and FGF 10 during the first phase (Modified Protocol 3) may be acting to stabilise these fluctuations and provide a more consistent differentiation process.

Another interesting finding presented in this chapter is the observation of pre-placodal marker (*SIX1*, *DLX5*, *EYA1*) gene expression being upregulated significantly at day 8 of Modified Protocol 3 (the most consistently efficient differentiation protocol) following a period of FGF 3 and FGF 10 supplementation with canonical Wnt signalling inhibition. This finding has also been implicated in *in vivo* studies in *Xenopus* (Brugmann et al., 2004). In this study the pre-placodal marker *Six1* was found to act as a transcriptional activator of other pre-placodal genes to induce the formation of the PPR. Inhibition of canonical Wnt signalling by either co-expression of a Wnt receptor antagonist (Frzb-1) or expression of a dominant negative form of Wnt 8 was found to robustly upregulate and expand the region of *Six1* expression, which in turn upregulated *Eya1* expression. Comparably in a β-catenin gain of function mouse model Freyer and Morrow (2010) showed that *Six1* (and *Eya1*) were significantly downregulated, reducing the size of the PPR. Upon expression of the pre-placodal markers it is believed that the expression remains in the progenitors of the otic placode (Zou et al., 2004). In the experiments presented in Figure 5.10 it was demonstrated that inhibition of canonical Wnt inhibition through to day 8 of the protocol significantly upregulates gene expression of the markers of the *in vivo* PPR region compared to the standard FGF protocol, and this level of gene expression is maintained through to the end of the protocol on day 12.

### *5.3.4 Epidermal differentiation is expanded with canonical Wnt inhibition and downregulated with canonical Wnt activation*

Figure 5.11 illustrates that along with upregulation of the markers of the PPR region, canonical Wnt inhibition by day 8 of Modified Protocol 3 also gives rise to an increase in the gene expression of the epidermal marker *FOXI2*, with a strong downregulation occurring between day 8 and day 12 when canonical Wnt activation takes place. This change of fate in the epidermal differentiation has previously been reported in mouse (Ohyama et al., 2006) and *Xenopus* (Park and Saint-Jeannet, 2008) *in vivo* studies. In the findings published by Ohyama et al. (2006) canonical Wnt signalling was found to play a role in the decision between adoption of an otic or epidermal fate in the developing OEPD. It was noted that β-catenin inactivation by conditional deletion in the mouse embryo led to the expansion of the epidermal region marked by *Foxi2* expression, akin to canonical Wnt inhibition through to day 8 of Modified Protocol 3. Likewise a constitutively active stable form of β-catenin was found to promote otic placode expansion at the expense of epidermal differentiation and *Foxi2* expression. In the *Xenopus* study E-cadherin expression was used as the marker for epidermal differentiation, and E-cadherin expression was decreased upon canonical Wnt activation with both Wnt 1 and Wnt 8 with a concomitant expansion of the otic placodal expansion of *Pax8*. These observations could be likened to the finding presented in Figure 5.11 in which a significant upregulation of *FOXI2* expression was seen following canonical Wnt inhibition at day 8, which is then lost as canonical Wnt activation occurs through to day 12.

This chapter has demonstrated how the various roles of canonical Wnt signalling established in *in vivo* findings can be utilised to build upon our standard FGF-based *in vitro* otic differentiation protocol to significantly improve the efficiency of otic differentiation from hES cells. The impact of this improved efficiency on the further differentiation of the otic progenitors into the more mature cell types of the inner ear (hair cells and auditory neurons) will be investigated in the next chapter.

# *Chapter 6*

# CHAPTER 6: *IN VITRO* HAIR CELL AND AUDITORY NEURON DIFFERENTIATION FROM FGF AND WNT MANIPULATED OTIC PROGENITORS

## 6.1 Introduction

### *6.1.1 Development of the mature cell types of the inner ear; hair cells and auditory neurons*

Succeeding the initiation and further maturation of the otic placode, morphological changes occur in order to bring about the more mature differentiated structures of the cochlea and inner ear. As discussed in greater detail in Chapter 1, the thickened surface ectoderm housing the otic placode invaginates to form the otic vesicle and otocyst, containing SOX2 positive prosensory regions which go on to develop into structures of both the vestibular and auditory systems. The organ of Corti is the sensory epithelium of the organ of hearing, the cochlea, and contains an exquisite coordination of a number of different cell types. Sensory hair cells, responsible for relaying mechanical sound stimulation into an electrical impulse, are believed to be induced initially by the transcription factor ATOH1 (Chen et al., 2002). ATOH1 is the first detectable marker of hair cell differentiation, and is transiently expressed before being rapidly downregulated (reviewed in Mulvaney and Dabdoub, 2012). It is thought that expression of SOX2 is required for ATOH1 expression, as mice deficient in SOX2 fail to form sensory hair cells as a result of the loss of ATOH1 (Kiernan et al., 2005). ATOH1 is also thought to have an inductive role in the expression of POU4F3 (or BRN3C) (Erkman et al., 1996). POU4F3 has been implicated in the mouse as not being necessary for hair cell induction and proliferation, but important for the further maturation and survival of the hair cells post-mitotically. POU4F3 knockout mice were shown to develop hair cells normally, with expression of other characteristic hair cell markers, yet they do not form the structures of the more mature hair cells, such as the stereocilia bundles (Xiang et al., 2008). Mutations in this gene therefore contribute to some genetic forms of deafness. Likewise the

expression of an additional early key hair cell marker, MYO7A, has also been shown to be important for normal stereocilia bundle structure, organisation and function. The *Myo7a* mouse mutant *Shaker-1* (Gibson et al., 1995) has disorganised stereocilia and consequent disorders of hearing.

Within the anteroventral portion of the developing otocyst, a subset of cells adopt a neuroblast fate and subsequently delaminate from the otocyst, going on to develop the spiral ganglion neurons and cochleovestibular ganglion. For this auditory neuronal differentiation to take place within the developing cochlea, the basic helix-loop-helix transcription factor *NEUROG1* is required (Ma et al., 1998). Notch signalling has been implicated in governing the cell fate decisions of neuronal differentiation by lateral inhibition of neighbouring sensory cells (Morrison et al., 1999). When Notch signalling is inhibited it has been shown in the mouse that cells within the prosensory patch are shifted from an epithelial fate to a more neuronal fate. This has been demonstrated in mouse mutants for *Delta1*, a key mediator of Notch signalling (Brooker et al., 2006) and also in zebrafish studies (Haddon et al., 2008). Knockout of *Delta1* causing loss of Notch-mediated lateral inhibition in the mouse led to a significant increase in the number of cells adopting a neuronal fate, and a consequent increase in the size of the cochleovestibular ganglion.

### *6.1.2 Development of in vitro hair cell and auditory neuron differentiation protocols*

The identification and isolation of human auditory stem cells from the fetal cochlea (Chen et al., 2007; Chen et al., 2009) (hFASCs) provided a model system in which to begin the investigation of *in vitro* differentiation protocols to generate auditory hair cells and neurons. Using the hFASCs it was found that exposure to low concentrations of all-*trans* retinoic acid and epidermal growth factor (EGF) in serum free media (Chapter 2) caused approximately 85 to 90% of the hFASCs to retain their epithelial-like morphology and express key markers of auditory hair cell differentiation such as ATOH1, MYOSIN VIIA and POU4F3. EGF and all-*trans* retinoic acid were chosen as a result of their established roles in the development of the cochlea. The role of

retinoic acid in the developing inner ear has been shown by the work of Kelley et al. (1993). Mouse cochlea explants were used to determine the effects of applying exogenous retinoic acid, and it was reported that a significant increase in the number of hair cells and supporting cells was produced. Retinoic acid receptors have also been previously identified in mouse cochlea studies (Mendelsohn et al., 1991). More recently retinoic acid has been used to aid the differentiation of human bone marrow derived mesenchymal stem cells into hair cells *in vitro* (Boddy et al., 2012; Duran Alonso et al., 2012). EGF has been implicated in hair cell initiation by being involved in the induction of ATOH1, a key initiator of hair cell differentiation (Doetzlhofer et al., 2004), and the EGF receptor has been identified in the developing chick and mouse inner ears (White et al., 2012).

For auditory neuron differentiation from the hFASCs (Chapter 2) it was found that trypsinisation of the cells was required in order to initiate the formation of a bipolar morphology. Differentiating cells were maintained in serum free media with supplemented basic FGF and Sonic hedgehog, followed by the addition of the neurotrophic factors neurotrophin-3 (NT3) and brain-derived neurotrophic factor (BDNF). Neuronal cells resulting from this process were found to express NEUROG1, POU4F1, β-TUBULIN III and NEUROFILAMENT 200. *In vivo* the auditory neurons, or spiral ganglion neurons (SGNs) are responsible for relaying sound information from the sensory hair cells to the brain. SGN precursor development in the embryo is believed to be initially induced in the prosensory patches by upregulation of NEUROG1 (Ma et al., 2000). Later NEUROD is expressed in the mature post-mitotic neurons, and it is thought that NEUROD expression enhances neuronal differentiation via inhibition of non-neural fate (Lawoko-Kerali et al., 2004).

The protocols for differentiating hFASCs into hair cells and auditory neurons have also been tested on otic progenitors derived from hES cells (Chen et al., 2012), with similar results. The ability to reproducibly and efficiently produce hair cell-like cells and auditory neurons *in vitro* has potentially invaluable implications. It could, for example, provide a tool to aid in the identification of factors involved in increasing proliferation, drug screening assays to test potential ototoxic compounds, and even harbours potential for cell-based transplantation into the damaged cochlea.

### *6.1.3 General objectives of the chapter*

In the previous chapters an improved method to produce otic progenitors from hESCs combining manipulation of the Wnt and FGF signalling pathways has been described. In this chapter, the ability of the progenitors generated by this new method to further differentiate into hair cell-like cells and auditory neurons *in vitro,* comparing it to those produced by the former FGF-based protocol, will be explored. This will allow us to determine if the increased efficiency of otic progenitors generated from Modified Protocol 3 is reflected with an increase in efficiency of hair cell and auditory neuronal differentiation.

## 6.2 Results

### *6.2.1 Hair cell differentiation was not enhanced in otic progenitors generated by the manipulation of canonical Wnt signalling*

The differentiation process of generating otic progenitors from hES cells was made more efficient by combining FGF signalling with canonical Wnt signalling manipulation. This improved protocol comprised of an eight day period of FGF 3 and FGF 10 signalling in combination with canonical Wnt signalling inhibition, followed by a four day period of canonical Wnt activation with an attenuated FGF 3 and FGF 10 signalling (Modified Protocol 3, Chapter 5). This more efficient protocol led to the differentiation of otic progenitors with an increase in the expression of the characteristic otic placodal markers, *PAX2*, *PAX8*, *FOXG1* and *SOX2*. Ultimately it was then important to determine if this generation of improved otic progenitors possess a greater capacity to differentiate further into the more mature cells types of the inner ear, such as the hair cells and auditory neurons. This second phase of differentiation is referred to as Phase 2 differentiation.

The *in vitro* hair cell differentiation protocol is described in greater detail in Chapter 2. In brief, during the first phase of otic differentiation, differentiating hES cells were manually purified to generate a pure culture of otic epithelial progenitor (OEP) cells. This was carried out with cells differentiating in the standard FGF condition and also in Modified Protocol 3. At the end of the 12 day differentiation period, the OEPs were lightly trypsinised with dilute trypsin and seeded onto gelatin coated flasks or dishes at a density of $1x10^4/cm^2$. For the following 14 days the OEPs were maintained in DFNB medium supplemented with EGF and all-*trans* retinoic acid. RNA was subsequently extracted, converted to cDNA and QPCR analysis of the gene expression of markers of hair cell differentiation, *POU4F3 (BRN3C)*, *MYO7A* and *ATOH1*, was carried out. OEPs at the end of the first phase of differentiation were also harvested for RNA to determine the gene expression of the hair cell markers prior to undergoing hair cell differentiation. Alternatively cells after hair cell differentiation were fixed in 4% paraformaldehyde and immunolabelled with antibodies against the combinations of POU4F3/ATOH1 and POU4F3/MYO7A. Nuclei were counterstained with 4',6-

diamidino-2-phenylindole (DAPI). QPCR results are displayed in Figure 6.1A. Representative images of the immunolabelling with hair cell markers are displayed in Figure 6.1B, and quantification of this immunolabelling is shown in Figure 6.1B'.

**Figure 6.1A: Gene expression of hair cell markers *POU4F3*, *MYO7A* and *ATOH1* following a 14 day hair cell differentiation protocol. H14S9 OEPs were seeded at $1x10^4/cm^2$.** Hair cell differentiation media consists of DFNB supplemented with 20 ng/ml EGF and $10^{-6}$ molar all-*trans* retinoic acid. Gene expression is presented as relative to that of baseline DFNB control OEPs after 12 days culture. Phase 1 refers to the end of the standard 12 day FGF or Modified Protocol 3 protocol. Phase 2 HC refers to the end of hair cell differentiation. Bar charts denote mean and standard deviation of gene expression relative to that of the DFNB control condition (n=3 independent experiments). Statistical significance was determined by one way ANOVA with Bonferroni's multiple comparison post-test. ns = no significant difference. **P*<0.05, ***P*<0.01.

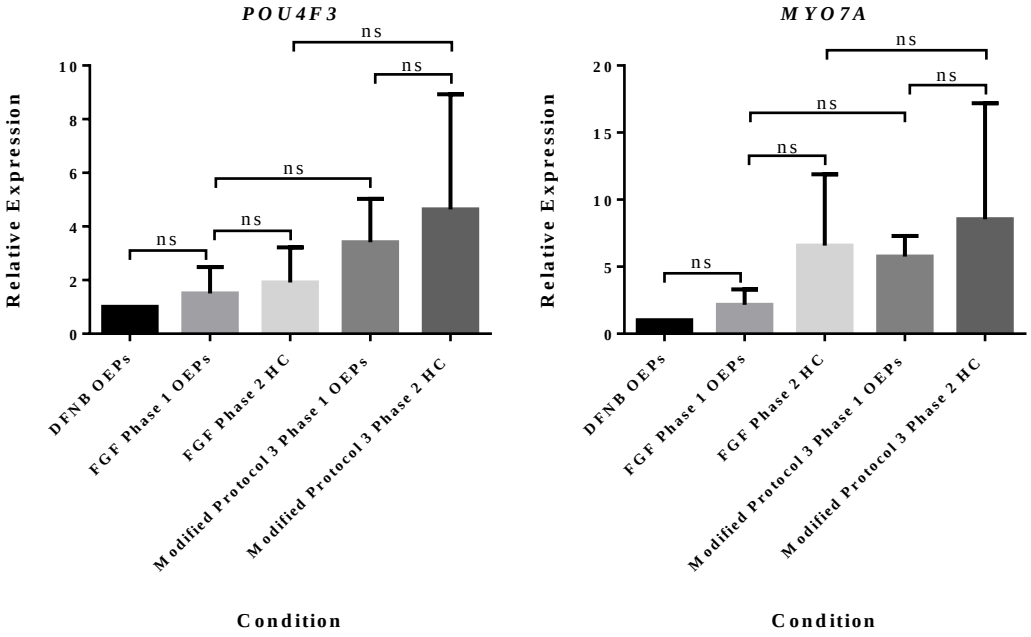

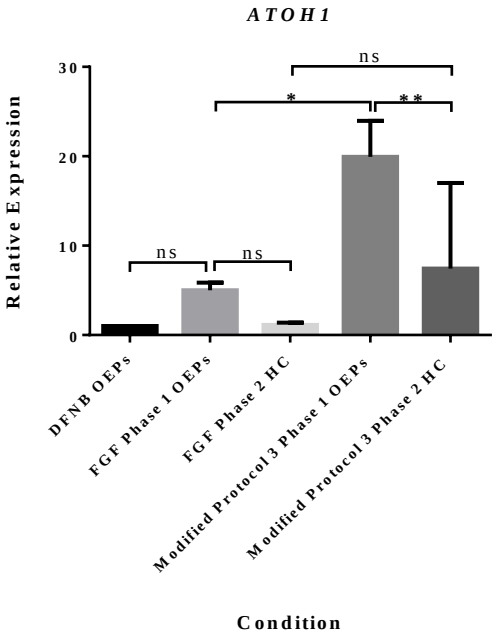
ATOH1
Relative Expression
30
20
10
0
ns
ns
*
**
ns
DFNB OEPs
FGF Phase 1 OEPs
FGF Phase 2 HC
Modified Protocol 3 Phase 1 OEPs
Modified Protocol 3 Phase 2 HC
Condition

**Figure 6.1B: Immunolabelling of OEPs following the 14 day hair cell differentiation protocol. Cells were labelled with a combination of POU4F3 (green) and ATOH1 (red), or POU4F3 (green) and MYO7A (red). Nuclei counterstained with DAPI.** Single representative field of view, 10x magnification**.** Scale bar is 400 µM.

**POU4F3 (green)/ATOH1 (red)**

**FGF** **Modified Protocol 3**

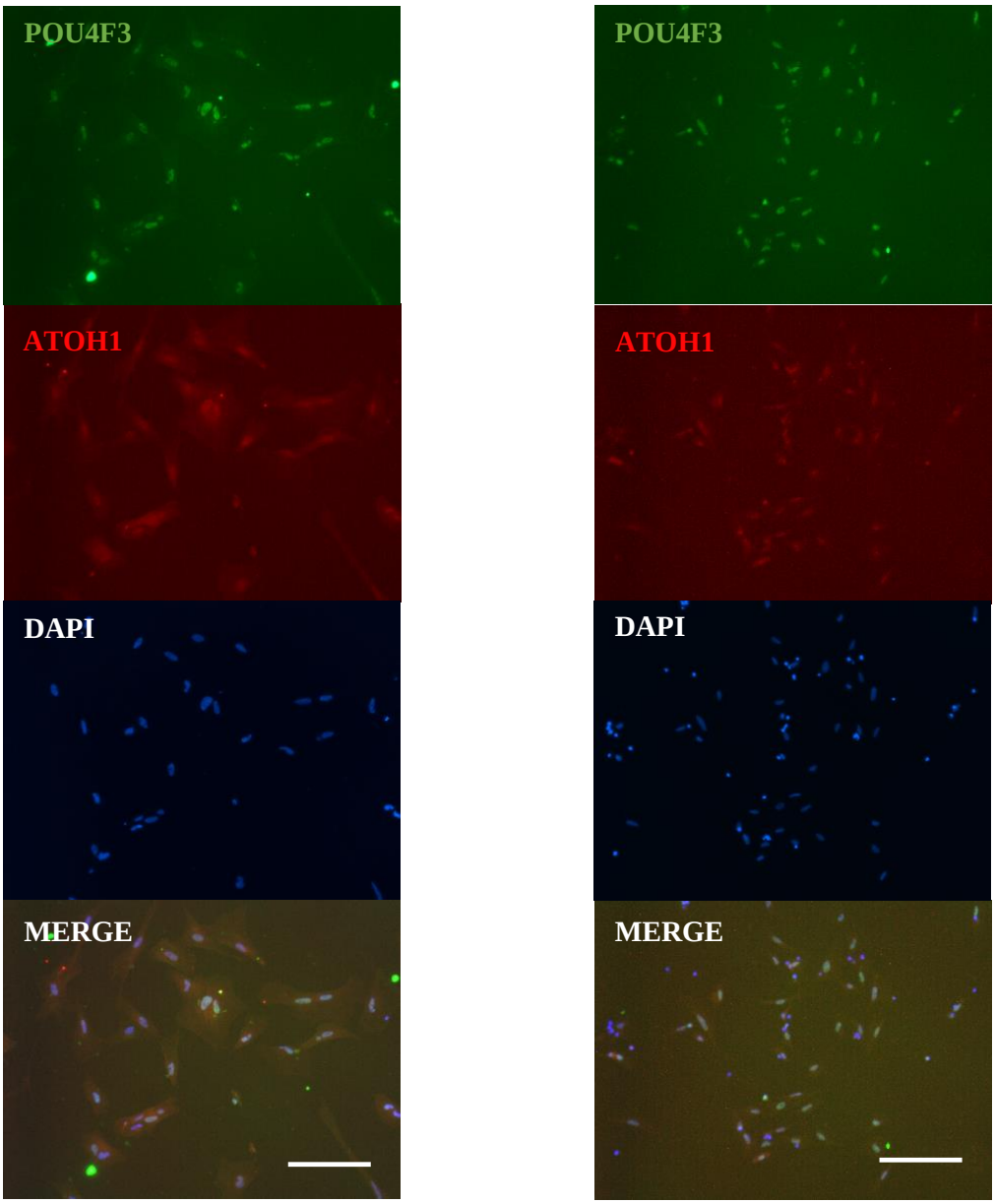

**POU4F3 (green)/MYO7A (red)**

**FGF** **Modified Protocol 3**

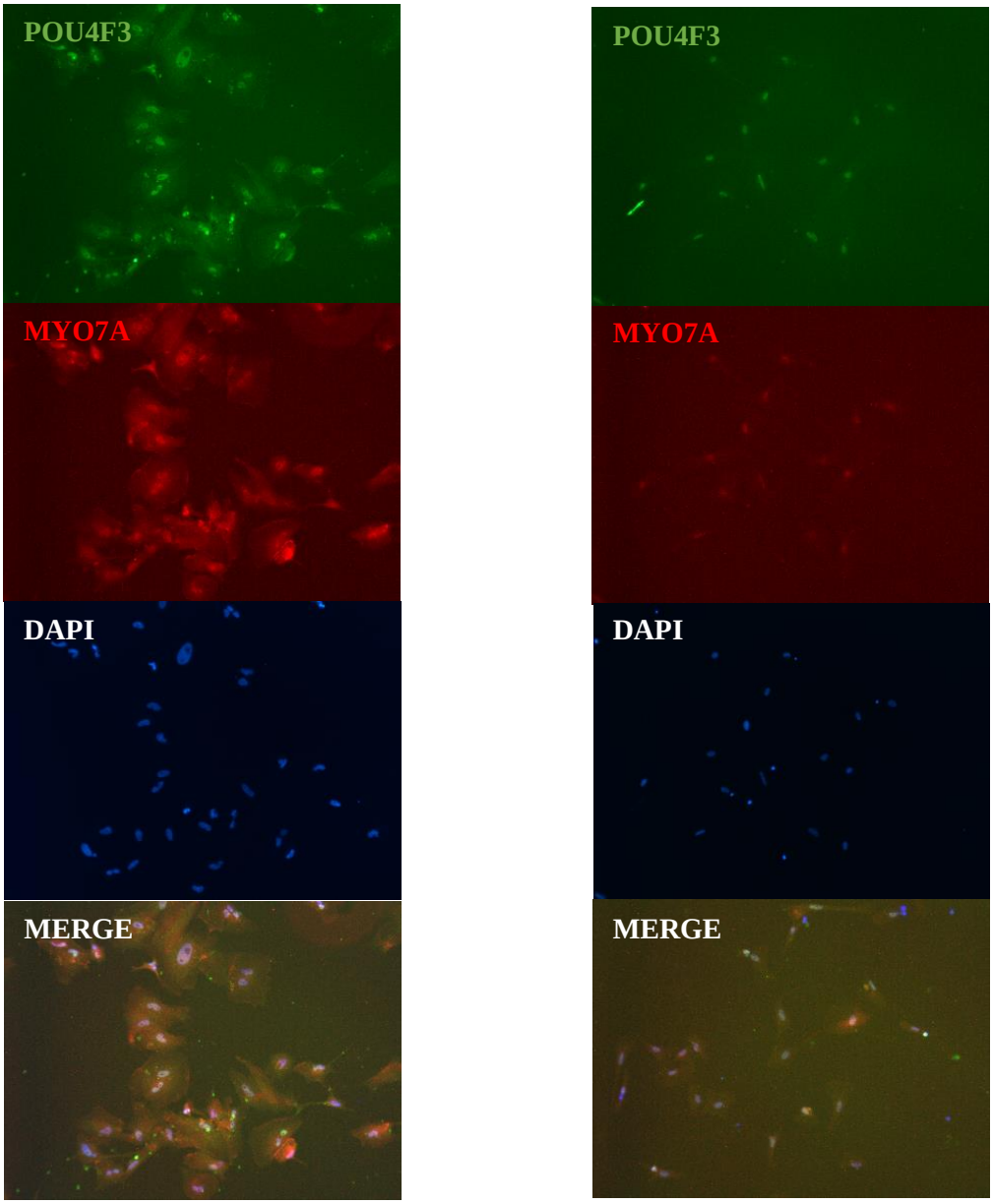

**Figure 6.1B': Quantification of hair cell marker immunolabelling.** Bar charts show the mean percentage of double positive cells labelled with the antibody combinations POU4F3/ATOH1 and POU4F3/MYO7A from n=3 independent experiments. Error bars denote mean and standard deviation. Statistical significance was determined using Chi-square with Yates' continuity correction. ns = no significant difference.

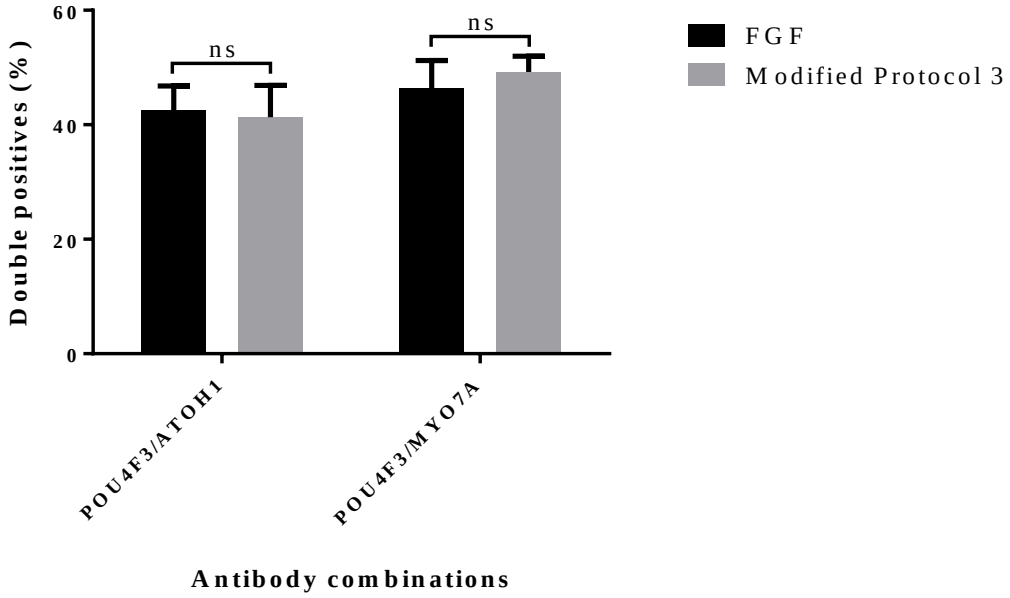

As highlighted in Figure 6.1A, it was observed that there was no significant difference in the gene expression of *POU4F3* and *MYO7A* between any of the conditions investigated. In one of the three independent experiments carried out (Appendix 3) there was a substantial upregulation of the gene expression of all three hair cell markers investigated, however the following two replicate experiments did not produce this upregulation. Significant differences were however observed with the gene expression of *ATOH1* in some conditions investigated. The OEPs generated from the Modified Protocol 3 differentiation protocol had significantly higher *ATOH1* gene expression than the OEPs produced from the standard FGF condition, prior to further differentiation. Moreover there was a significant downregulation of *ATOH1* gene expression after the Modified Protocol 3 OEPs were differentiated for 14 days in hair cell media, compared to the expression in their progenitor state. With the FGF OEPs no significant difference in the gene expression of *ATOH1* was seen between before and after hair cell media differentiation. At the end of the 14 day hair cell media differentiation phase no differences were observed between FGF-derived and Modified Protocol 3-derived OEPs.

Figure 6.1B and 6.1B' also demonstrate that in the protein expression with antibody immunolabelling at the end of hair cell media treatment, for the combinations of POU4F3/ATOH1 (42.61% ± 4.19% and 41.33% ± 5.56% double positive cells in FGF and Modified Protocol 3, respectively) and POU4F3/MYO7A (46.28% ± 4.94% and 49.20% ± 2.78% double positive cells in FGF and Modified Protocol 3, respectively), no significant differences were seen in the percentage of double positive cells between the two otic progenitor induction protocols.

In addition the H14S9 Atoh1nGFP reporter generated and discussed in Chapter 3, appeared to have a rapid downregulation of enhancer activity upon differentiating the OEPs in hair cell media. This was the case for OEPs produced in either the standard FGF or Modified Protocol 3 conditions. Enhancer-driven GFP positive cells could not be detected by fluorescent microscopy throughout the 14 days of hair cell media treatment.

### *6.2.2 Neuronal differentiation was more efficient with otic progenitors generated from manipulation of canonical Wnt signalling*

Described in greater detail in Chapter 2, an *in vitro* differentiation protocol was developed in order to promote the differentiation of the immature otic progenitors into the more mature auditory neurons. In brief the 12 day protocol consists of dissociating the manually purified otic neural progenitors (ONPs) with trypsin and then culturing the cells in DFNB media supplemented with basic FGF and Sonic hedgehog ligands for three days. On day four the media is supplemented further with the neurotrophic factors BDNF and NT-3 until day 6. From day 6 to the end of differentiation the cells are maintained in DFNB with the supplemented neurotrophic factors only (Sonic hedgehog is removed from day 6). After differentiation cells were either fixed for antibody immunolabelling or lysed for RNA extraction and QPCR analysis (Figure 6.2A). Gene expression of the sensory neural markers *POU4F1 (BRN3A), SYP (Synaptophysin), and SLC17A7 (VGLUT1)* was investigated. ONP cells prior to further neural differentiation were also used in QPCR analysis to determine the gene expression of neuronal markers at the progenitor stage. Immunolabelling was carried out using the antibody combinations POU4F1/NKAα3 (sodium/potassium-ATPase subunit 3) and β-tubulin III/Neurofilament200 (NF200). Representative images are displayed in Figure 6.2B, with quantification highlighted in Figure 6.2B'.

**Figure 6.2A: Gene expression of sensory neuronal cell markers *POU4F1*, *SYP* and *SLC17A7* following a 12 day neural differentiation protocol. H14S9 ONPs were seeded at $4x10^3/cm^2$.** Neural differentiation media (day 1-3) consists of DFNB supplemented with 20 ng/ml basic FGF and 500ng/ml Sonic hedgehog C24II; day 4 and 5 with supplemented BDNF and NT-3 at 10 ng/ml; day 6 – 12 removal of Sonic hedgehog. Gene expression is presented as relative to that of baseline DFNB control ONPs after 12 days culture. Phase 1 refers to the end of the standard 12 day FGF or Modified Protocol 3 protocol. Phase 2 NM refers to the end of neural differentiation. Bar charts denote mean and standard deviation of gene expression relative to that of the DFNB control condition (n=3 independent experiments). Statistical significance was determined by one way ANOVA with Bonferroni's multiple comparison post-test. ns = no significant difference. **P*<0.05, ***P*<0.01, ****P*<0.001, *****P*<0.0001.

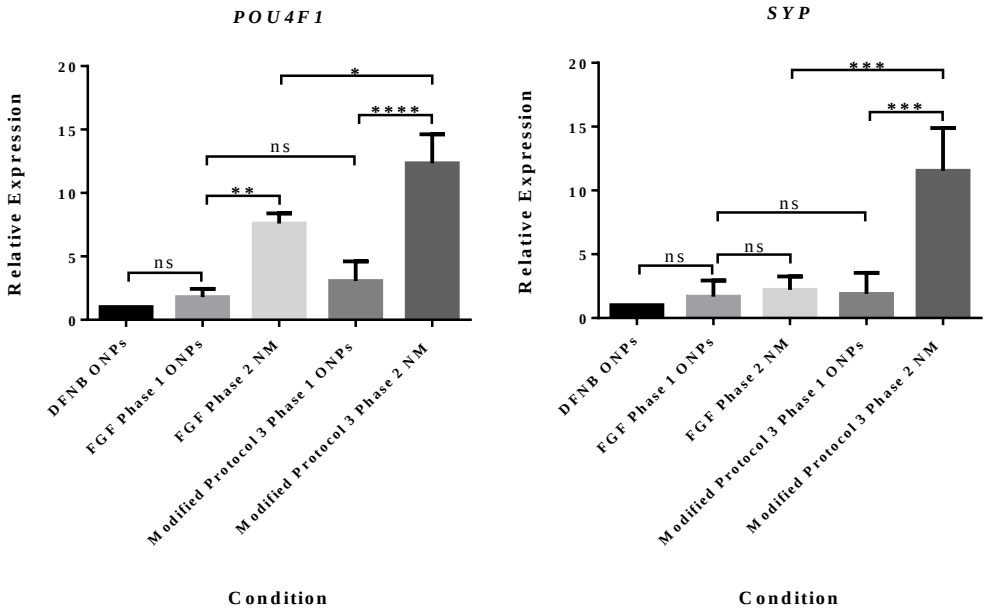

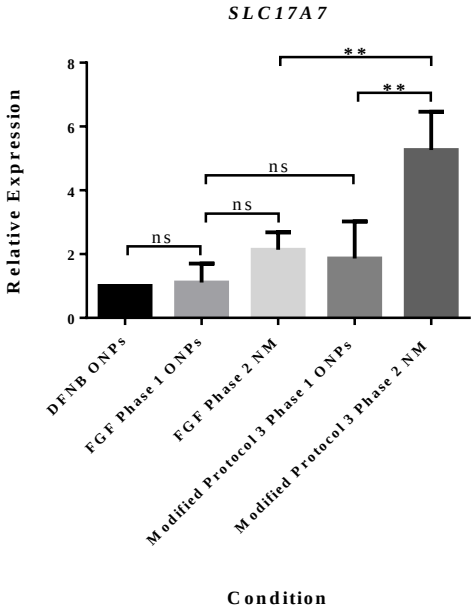
SLC17A7
Relative Expression
0
2
4
6
8
ns
ns
ns
**
**
DFNB ONPs
FGF Phase 1 ONPs
FGF Phase 2 NM
Modified Protocol 3 Phase 1 ONPs
Modified Protocol 3 Phase 2 NM
Condition

**Figure 6.2B: Immunolabelling of ONPs following the 12 day neural differentiation protocol. Cells were labelled with a combination of NKAα3 (green) and POU4F1 (red), or β-tubulin III (green) and NF200 (red). Nuclei counterstained with DAPI.** Single representative field of view, 20x magnification**.** Scale bar is 200 µM.

**NKAα3 (green)/POU4F1 (red)**

**FGF** **Modified Protocol 3**

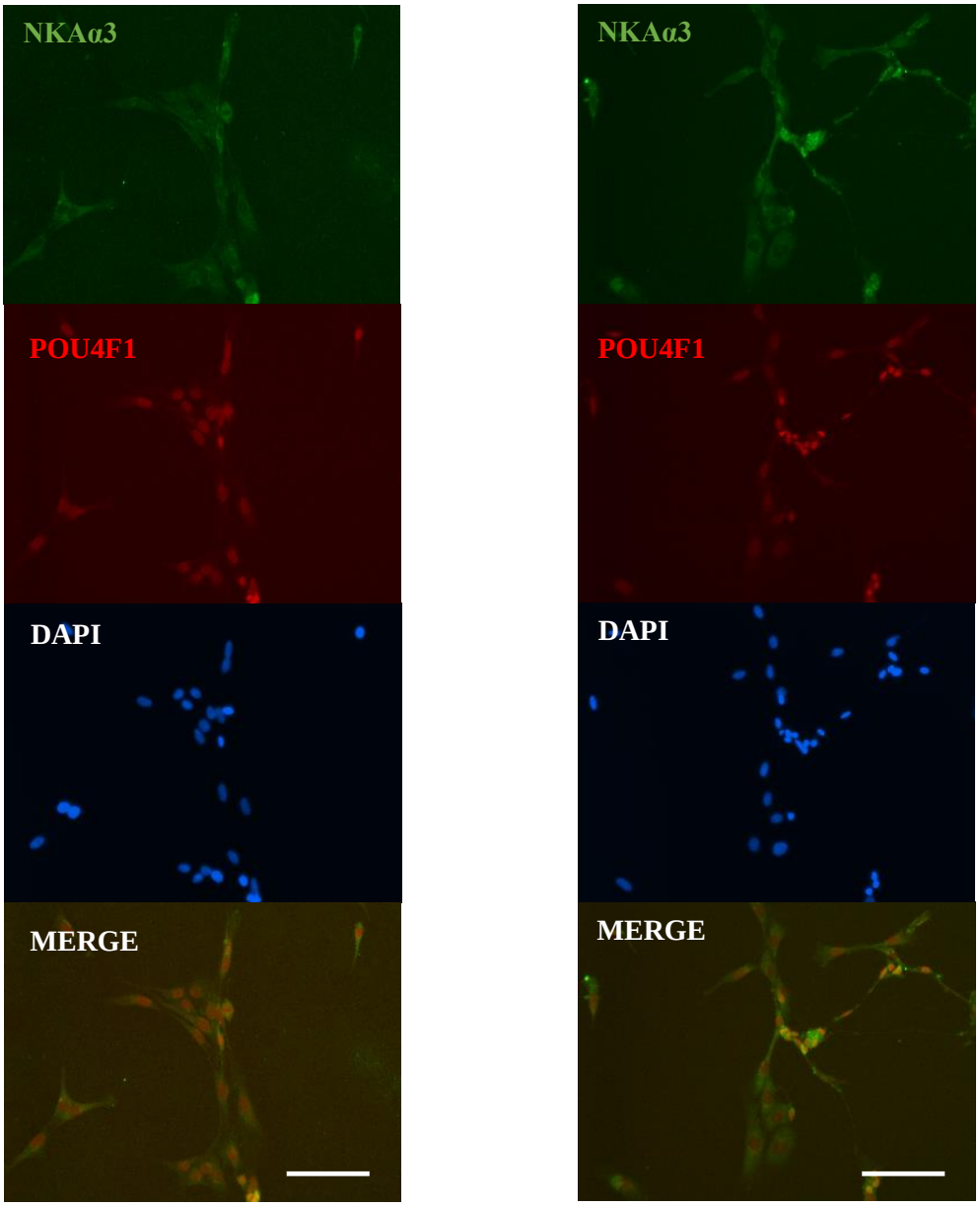

**β-tubulin III (green)/NF200 (red)**

**FGF**

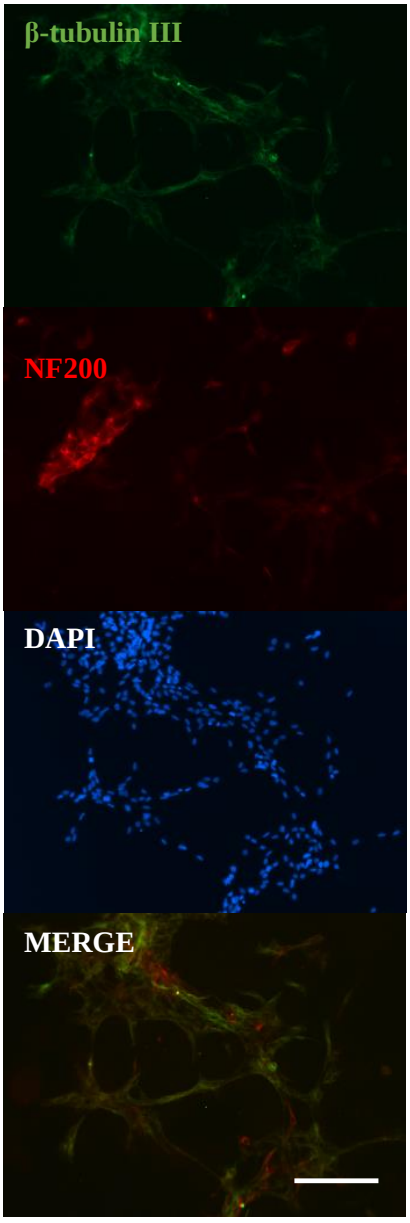


**Modified Protocol 3**

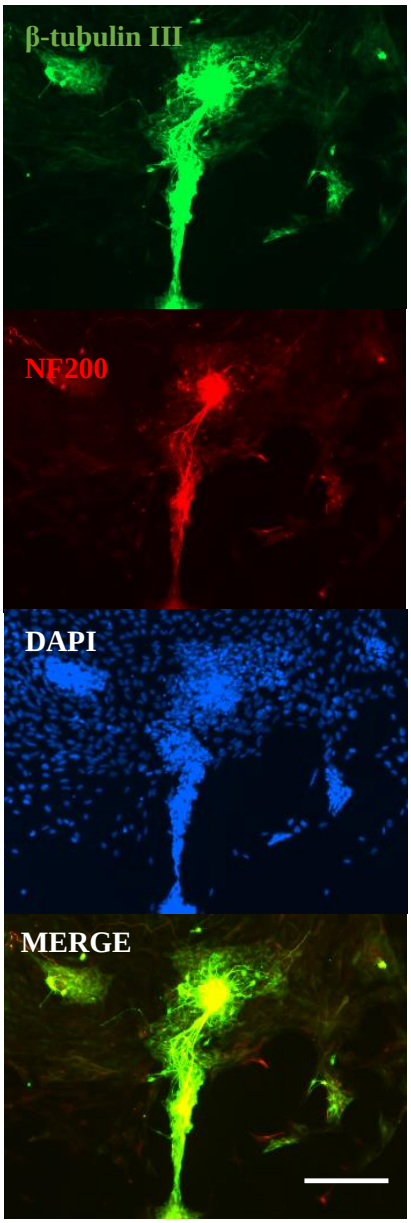

**Figure 6.2B': Quantification of neural marker immunolabelling.** Bar charts show the mean percentage of double positive cells labelled with the antibody combinations NKAα3/POU4F1 and β-tubulin III/NF200 from n=3 independent experiments. Error bars denote mean and standard deviation. Statistical significance was determined using Chi-square with Yates' continuity correction. ns = no significant difference. ****$P$<0.0001.

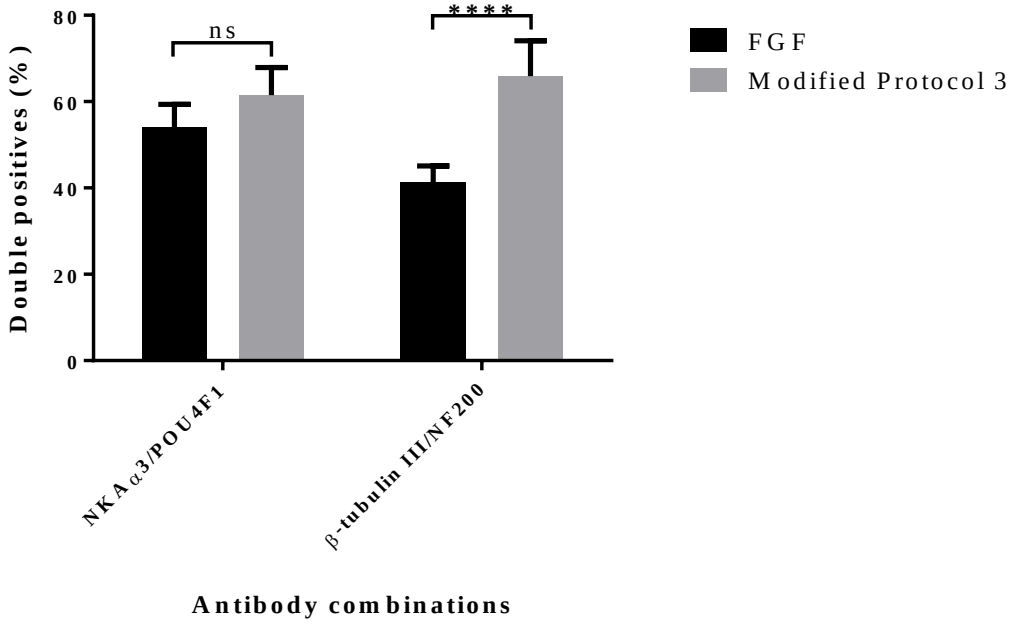

Gene expression of all three neural markers investigated by QPCR (*POU4F1*, *SYP* and *SLC17A7*) was found to be significantly upregulated in the cells generated from Modified Protocol 3 compared to the standard FGF condition following the 12 day neutralising protocol (Figure 6.2A). There was also a significant upregulation of the gene expression of all three markers between the Modified Protocol 3 progenitors pre- and post-neural differentiation. In the case of the FGF progenitors, only *POU4F1* was significantly upregulated after neural differentiation compared to the expression in the progenitor state.

The percentage of double positive cells observed by immunolabelling (Figure 6.2B and 6.2B') also highlights differences between the neural differentiation outcome of FGF and Modified Protocol 3 generated otic progenitors. Although there was no significant difference in the percentage of double positive NKAα3/POU4F1 cells between FGF and Modified Protocol 3, the fluorescent intensity of the neuralised cells from Modified Protocol 3 generally looked brighter than from the standard FGF condition. In the case of β-tubulin III/NF200 there was a highly significant increase in the percentage of double positive cells from Modified Protocol 3, and also the intensity of the immunolabelling appeared visually brighter with these cells compared to the FGF cells.

## 6.3 Discussion

### *6.3.1 OEPs obtained with Modified Protocol 3 can differentiate into hair cell-like cells at a similar level of efficiency as conventional OEPs obtained from the FGF-based protocol*

However, despite the substantial upregulation of the characteristic otic markers, *PAX2*, *PAX8*, *FOXG1* and *SOX2* (seen at both the gene transcript and protein expression levels), induced by differentiating hES cells in Modified Protocol 3 conditions, hair cell differentiation was not subsequently improved overall compared to differentiating the otic progenitors produced from the standard FGF protocol. Gene expression of *POU4F3*, *ATOH1* and *MYO7A* did not significantly alter in level when comparing the expression in the FGF-produced otic progenitors prior to and after undergoing hair cell differentiation. From Modified Protocol 3, *POU4F3* and *MYO7A* gene expression was also not significantly different between the progenitor and hair cell media treated state. Interestingly the gene expression of *ATOH1* was significantly increased in the Modified Protocol 3 progenitor state over the progenitors emanating from the FGF condition, and moreover, this increased gene expression of *ATOH1* was significantly downregulated following hair cell media treatment.

Expression of *ATOH1* has been shown to be necessary and sufficient for the induction of hair cell differentiation *in vivo*, with the Math1-null mouse failing to form inner or outer hair cells in the organ of Corti (Bermingham et al., 1999). *ATOH1* expression is known to be early and transient, rapidly being downregulated once hair cell differentiation progresses and matures. With a significant upregulation of *ATOH1* gene expression observed in the Modified Protocol 3 progenitors by day 12 of differentiation, this could suggest that the OEPs are becoming primed for differentiation into hair cells, and consequently the gene expression of *ATOH1* is downregulated by the end of the 14 day hair cell differentiation period. This downregulation is not a complete loss of *ATOH1* expression however and this could perhaps explain the presence of ATOH1-positive cells detected by immunolabelling at day 14. Studies investigating the *in vitro* generation of hair cells from mouse (Ouji et al., 2013) and human ES and IPS cells (Ronaghi et al., 2014) tend to see gene

expression of *ATOH1* peaking after hair cell differentiation, rather than at the otic progenitor stage. Ronaghi et al. (2014) for example showed downregulation of *ATOH1* expression following a phase of otic induction, with significant upregulation of *ATOH1* after hair cell differentiation. It must be noted however that the hair cell differentiation strategy used by Ronaghi et al. (2014) was very different to the one used in this work. Otic induction was carried out in an embryoid body format rather than in monolayer, and following a period of otic induction hair cell differentiation occurred via a phase of gradual serum depletion; EGF or retinoic acid were not supplemented. It is possible that hair cell induction favours a more three dimensional differentiation format rather than in monolayer.

### *6.3.2 Sensory neuronal differentiation was improved from canonical Wnt signalling-manipulated otic progenitors*

Sensory spiral ganglion neurons in the developing cochlea are crucial for the conveying of sound information from the cochlear hair cells to the brain. Important to the differentiation, survival and migration of these auditory neurons is *POU4F1* (*BRN3A*). Emphasising the importance of *POU4F1* in promoting sensory neural differentiation and survival, it was demonstrated in the *Pou4f1* knockout mouse (Huang et al., 2001) that loss of *Pou4f1* leads to subsequent downregulation of *TrkC*, the receptor for the neurotrophic factor NT-3, leading to massive neuronal cell loss within the developing cochlea.

The afferent spiral ganglion neurons innervating the inner hair cells in the organ of Corti are known as type I spiral ganglion neurons, and aid in the quick relaying of sound information to the brain. Important to these fast firing neurons is the presence of the sodium/potassium-ATPase (NKA), a membrane bound protein that maintains the hyperpolarized membrane potential of the neurons. Inhibitors of NKA, such as ouabain, have previously been shown to decrease the endocochlear potential (Konishi and Mendelsohn, 1970) and consequently reduce the rate of firing of the type I spiral ganglion neurons. A study conducted in the rat by McLean et al. (2009) identified the α3 subunit of NKA (NKAα3) is expressed only in the organ of Corti where the type I afferent neurons innervate the inner hair cells. Moreover it is restricted from the type

II spiral ganglion neurons. *SLC17A7* (*VGLUT1*) and *SYP* (*Synaptophysin*) are also found to be expressed in the developing cochlea, and are both important in the innervation of the inner hair cells of the organ of Corti by the type I spiral ganglion neurons.

The gene expression of *POU4F1*, *SYP* and *SLC17A7* in the Modified Protocol 3-produced ONPs after further differentiation in the 12 day neuralisation protocol was observed to be significantly upregulated compared to the cells in the progenitor state, and also with the ONPs produced from the standard FGF condition, pre- or post-neural differentiation (Figure 6.2A). This is suggesting that the otic progenitors produced from manipulating canonical Wnt signalling in Modified Protocol 3 differentiate more efficiently into sensory neurons than the progenitors generated under the standard FGF induction protocol. The percentage of cells co-expressing POU4F1 and NKAα3 was not significantly different between the two otic progenitor-generating conditions, however, although it could be argued that the fluorescent intensity of the immunolabelling is brighter in the Modified Protocol 3 cells, at least visually (Figure 6.2B and 6.2B'). β-tubulin III and NF200, general markers of neuronal differentiation, were also significantly upregulated in the Wnt manipulated cells than the FGF cells, as observed in both the percentage of double positive immunolabelling and in visual fluorescent intensity.

Canonical Wnt signalling-manipulated OEPs differentiated into hair cell-like cells as efficiently as the OEPs generated from the standard FGF protocol. Further enhancement of *in vitro* hair cell differentiation warrants further investigation. There are a number of more sophisticated methodologies for hair cell differentiation *in vitro* (Koehler et al., 2013; Ronaghi et al., 2014), producing a substantial improvement in hair cell generation. Thus our current hair cell differentiation protocol could be a limiting factor. Nevertheless the impact on sensory neural differentiation was significant. Generating otic progenitors with the potential to efficiently undergo neural differentiation, especially towards the more sensory neurons, could have great potential in improving cell-based transplantations to regenerate lost or damaged spiral ganglion neurons *in vivo*.

# *Chapter 7*

# CHAPTER 7: CONCLUSION

## *7.1 Conclusion and future implications*

Deafness as a consequence of sensorineural hearing loss, is a major target for regenerative medicine and potential cell-based therapies, due to the lack of conventional medical treatments. The ability to repair or replace the damaged cells of the organ of Corti and its associated neurons is currently being explored in a number of ways. Avenues of research include neurotrophic factor supplementation along with cochlear implantation to aid in the survival of the spiral ganglion neurons (Jiao et al., 2014; Zanin et al., 2014), targeting Wnt-responsive Lgr5-positive stem cells within the mature cochlea to promote hair cell generation and proliferation *in vivo* (Shi et al., 2012; Shi et al., 2013), and in our case, the exogenous production of otic progenitor cells for use in cellular transplantation to restore lost spiral ganglion neurons and improve functional hearing (Chen et al., 2012).

Human embryonic and induced pluripotent stem cells, and their differentiated derivatives, are fast approaching the clinic as sources of transplantable cells for regenerative purposes in the inner ear. The ability to efficiently direct the differentiation of human pluripotent stem cells into a differentiated progeny of choice, with minimal contamination of extraneous cell types, is the ideal outcome for stem cell based therapeutics, and will aid in the scaling up of production to meet clinical need. Based on our current differentiation protocol, otic progenitors are generated with approximately 20% efficiency as measured by the expression of *PAX2*, *PAX8*, *FOXG1* and *SOX2*. Modified Protocol 3, developed in this thesis, substantially improved this efficiency to approximately 50-60%. The basis of Modified Protocol 3 has been to incorporate the manipulation of canonical Wnt signalling into our previously established otic differentiation protocol. Canonical Wnt signalling has been shown to play a role in the induction and further expansion of the otic placode *in vivo* (Freter et al., 2008; Ohyama et al., 2006), and in combination with the crucial ligands FGF 3 and FGF 10, has helped us generate a more developmentally informed methodology.

Since the initial derivation of human embryonic stem cell lines in 1998 (Thomson et al., 1998) vast amounts of research have been undertaken attempting to efficiently produce transplantable differentiated cells. The directed differentiation into cell types of the central nervous system was one of the first target areas. Simple differentiation protocols were derived based on supplementing differentiation media with basic FGF (Zhang et al., 2001) or a modest cocktail of basic FGF and EGF (Reubinoff et al., 2001). Similarities between these studies and our otic induction protocol are apparent; differentiation of human embryonic stem cells with just one or two key ligands can generate a progenitor type of interest, but usually with limited efficacy.

Since the early differentiation studies, and as knowledge of embryonic development has widened, research into the derivation of specific cell types from human pluripotent stem cells has now begun to adopt an approach involving the manipulation of the multiple signalling pathways known to work in synchrony during development, either simultaneously or sequentially. This is being carried out in the hope that a greater proportion of the differentiating pluripotent stem cells will generate the cell type of interest by being induced through an *in vivo*-like series of events, as with Modified Protocol 3 presented in this thesis. One such example is the study conducted by Chambers et al. (2009) which set out to improve the efficiency of the differentiation of human pluripotent stem cells towards the neural lineage. Human pluripotent stem cells were exposed to inhibitors of the transforming growth factor (TGF-β) (SB413542) and BMP (Noggin) pathways, either alone or in combination. Compared to differentiation with the supplementation of SB413542 or Noggin alone, the combined treatment significantly increased the efficiency and rate of neural conversion. Using PAX6 as a positive marker for neuroectodermal differentiation, approximately 10% of the cells expressed PAX6 when treated with SB413542 or Noggin alone, compared to above 80% when the two inhibitors were exposed to the cells in combination. Another finding of the study relevant to our work was the effect of cell density on the differentiation phenotype. It was found that seeding the human embryonic stem cells into differentiation media at high density promoted the cells to almost exclusively become PAX6 positive, compared to a more SOX10 neural crest positive population at lower densities. Previous work in our laboratory has demonstrated a shift towards OEP differentiation when they the human embryonic stem cells are seeded at high densities, compared to a more ONP fate when low

densities are used. As this study also utilises a monolayer culture system, this allows for easier isolation of a cell phenotype of interest. In agreement with data presented in this thesis, a germ layer lineage bias away from endodermal and mesodermal differentiation was also promoted by inhibition of BMP and TGF-β signalling, similar to the effect of inhibition of canonical Wnt signalling highlighted in the previous chapters.

Dincer et al. (2013) expanded upon this work by Chambers et al. (2009) by investigating if this enhancement of neural lineage differentiation could be modified to produce cranial placodal precursors from the neuroectodermal progenitors initially induced by the dual inhibition with SB413542 and Noggin. BMP signalling has been implicated in the induction of the pre-placodal region of the ectoderm (Kwon et al., 2010), and it was found in this work that derepression of BMP signalling by removal of Noggin after three days of differentiation promoted a significant increase (approximately 70%) in the number of SIX1 positive cells, marking the anterior pre-placodal region. Given the correct set of signals these placodal precursors could be directed to differentiate further into pituitary, trigeminal and lens placode derivatives. These findings provide us with options to further enhance Modified Protocol 3 by incorporating the manipulation of other pathways such as BMP and TGF-β to more readily generate anterior pre-placodal ectoderm. Anteriorising the ectoderm would be beneficial for us as the otic placode is induced in the anterior ectoderm. In studies looking into retinal differentiation from human embryonic stem cells (Lamba et al., 2006) insulin-like growth factor-1 (IGF-1) has been supplemented into culture media to explore this notion of anteriorising the induced ectoderm. The effect of IGF-1 in inner ear research has been explored by Oshima et al. (2010). Inhibition of canonical Wnt and TGF-β signalling with concomitant exposure to IGF-1 caused the ectodermal differentiation of mouse pluripotent stem cells towards an anteriorised fate. Thus there is still potential for a number of factors to be manipulated, enhancing the developmental accuracy of Modified Protocol 3.

The work to restore vision is perhaps a step closer to the clinic than strategies to help restore hearing. A landmark study reported by Eiraku et al. (2011) reported using mouse embryonic stem cells in a three dimensional embryoid body assay and found a self-directed differentiation and formation of optic cup-like structures within the embryoid bodies. Taking advantage of this phenomenon Gonzalez-Cordero et al.

(2013) used this three dimensional method to isolate photoreceptor precursors for transplantation into adult mouse models of visual impairment. Following protracted differentiation in embryoid bodies, photoreceptor cells (expressing GFP driven by the *Rhodopsin* gene promoter) were isolated and transplanted into the retina of adult visually impaired mice. It was found that only 0.3% GFP positive cells had transplanted and grafted successfully, limiting the functional recovery effect provided by these cells. Within the field of inner ear research itself, a similar phenomenon of self-directed differentiation in three dimensional embryoid bodies has been reported. The work carried out by Koehler et al. (2013) aggregated mouse embryonic stem cells and using a combination of various molecules, directed the differentiation through phases of non-neural ectoderm, pre-placodal ectoderm and otic placode identities before self-directed differentiation led to the abundant formation of sensory hair cells. Non-neural ectoderm was induced by activation of BMP (with BMP 4) and inhibition of TGF-β signalling (with SB413542), followed by a phase of BMP inhibition (with LDN193189) and activation of FGF signalling (with basic FGF) to induce pre-placodal and otic placodal differentiation. This process was carried out over 8 days before the cells were left to self-differentiate until day 30. By this time aggregates were found which contained approximately 1500 sensory hair cells. I have performed a few exploratory experiments (not included in this thesis) to attempt to adapt this protocol to the use of hES cells with limited success thus far.

What is important to highlight here is that most of the studies described in the former paragraphs involve differentiating embryonic stem cells via aggregation into embryoid bodies (and the Oshima et al. (2010) and Koehler et al. (2013) are performed in mouse, and therefore still needing validation with hES cells). This differentiation approach, unlike the monolayer culture system used in the experiments of this thesis, have a number of caveats. Embryoid body differentiation protocols tend to be protracted and feature many different permutations, for example up to 30 days long as in the research by Koehler et al. (2013). Not only does this add a level of complexity to the differentiation process, the cost of such experiments is also high. Our monolayer culture system takes places over just 12 days by comparison. Embryoid bodies also take away an element of control. Despite manipulating various signalling pathways to direct differentiation, there may be cells present within the aggregates that spontaneously differentiate, or receive a lower amount of signal due to concentration

gradients imposed throughout the aggregate which will have implications on the outcome of the differentiation. A monolayer system avoids this pitfall by ensuring a much greater proportion of cells receive the same molecular signals, and this could potentially lead to a better yield of the cell derivate of choice. Following on from this, isolation of the differentiated cells in monolayer is much easier and cleaner than from embryoid bodies which usually require harsher dissociation methods to generate single cells. The low amount of engrafted cells transplanted into the mouse retinas (Gonzalez-Cordero et al., 2013) may have been a result of sub-optimal dissociation of the aggregates. Although, in fairness, the three dimensional methods appear to produce more matured phenotypes, their complexity and difficulty for purification may prevent their application for scale-up production needed for clinical application. While they remain valuable as developmental models, perhaps in the road to translation they should be adapted as an assay post-production, for testing the true potential of the progenitors obtained by simpler, two dimensional protocols.

The majority of these studies also use differentiation media and matrices which are of animal origin, for example fetal bovine serum, gelatin, mouse laminins, and matrigel. These components are essential for embryoid body formation, and as such this will hinder the translation of the research into a clinical setting (Fink, 2009). Although our culture system currently uses mouse laminin and gelatin for differentiation, and the human embryonic stem cells are cultured on mouse fibroblast feeders or on matrigel, the monolayer nature of the system will allow for easy transition to xeno-free materials. For example there are a number of newly established xeno-free substrates for human embryonic stem cell cultivation which abide by the Good Manufacturing Practice guidelines (Menasche et al., 2014), and a vast amount of research has discovered new synthetic extracellular matrices for differentiation in monolayer (Alamein et al., 2013; Rowland et al., 2013).

The generation of an otic placode-specific hES cell reporter line also has great implications for future research. It will help to provide a visual readout of otic differentiation *in vitro*, and as such, screening of compounds which may boost the differentiation process or for toxicity testing, will be made easier and potentially adaptable to a high throughput screening system. Further validation of the reporter would be required initially however.

## *7.2 Next experimental steps*

For further validation of the otic placode-specific hES cell reporter line it would be beneficial to purify a population of reporter GFP positive cells by flow cytometry and determine the gene expression levels of the various otic markers (*PAX2*, *PAX8*, *FOXG1*, *SOX2*) compared to the unpurified population of progenitors. It would be anticipated that the expression of the otic markers would be enriched in the GFP reporting cells. Following on from this, another reporter line validation experiment would be to sort the reporter GFP positive ONPs and OEPs by flow cytometry, and set these fractions of progenitors to differentiate with the mature neuronal and hair cell differentiation protocols, respectively (as described in detail in Chapters 2 and 6). If the reporter positive fractions truly represent the otic progenitors then their capacity for more mature differentiation should be greater than that of an unsorted or reporter negative fraction.

The neuronal and hair cell differentiation protocols should also be investigated further in order to improve the efficiency of our second phase of *in vitro* otic differentiation. For both of these protocols, currently gelatin is used as the growth matrix. Extensive research has been carried out in order to determine the most effective extracellular matrices for spiral ganglion neuron explant growth and survival (Aletsee et al., 2002; Brors et al., 2002; Evans et al., 2007) and the findings from such studies could be used to inform an improved neural differentiation protocol *in vitro*. As demonstrated in Chapter 6 the OEPs produced from Modified Protocol 3 were only as efficient in producing hair cells as the OEPs from the standard FGF-based protocol. As with the neuronal differentiation, this could be partly due to the matrix used in the hair cell differentiation process, or perhaps due to the inefficient and variable protocol currently being used. Studies such as those carried out by Ronaghi et al. (2014), Oshima et al. (2010) and Koehler et al. (2013) have all attempted to improve *in vitro* hair cell differentiation from pluripotent stem cells by using more sophisticated, developmentally informed protocols. It is possible, therefore, that subjecting the Modified Protocol 3 OEPs to such protocols may then lead to more robust and efficient hair cell differentiation.

## *7.3 Summary*

To summarise, canonical Wnt signalling manipulation has been utilised in order to more efficiently direct the differentiation of human embryonic stem cells into otic placodal progenitors *in vitro*, by following developmentally informed cues in a monolayer culture system. The expression level of characteristic otic markers induced by this manipulation is higher and the number of otic progenitors has been shown to be substantially greater than those obtained with the method previously reported based on FGF signalling alone (Chen et al., 2012). These improved otic progenitors are capable of further differentiating into the more mature cell types of the inner ear, especially observed in the improved efficiency of sensory neuronal differentiation. This improved generation of otic progenitors, and the human embryonic stem cell reporter lines created, will also help in future investigations, such as small molecule screening and the identification of cell surface markers for isolating progenitors of interest. The impact of the findings of this work could be crucial for improving the repair of auditory function *in vivo*, and the methodology could easily be translated to a xeno-free system to pave the way for transition into the clinic, potentially bringing a cell-based therapy for deafness one step closer.

# *Appendices*

**APPENDIX 1: Pluripotency gene expression in the parental H14S9 cell line and the H14S9 NOP-SOX2 reporter (Sarah Jacob Eshtan, PhD thesis).** Bar charts denote mean and standard deviation of gene expression (n=3 independent experiments). Statistical significance was determined by two way ANOVA. ns = no significant difference.

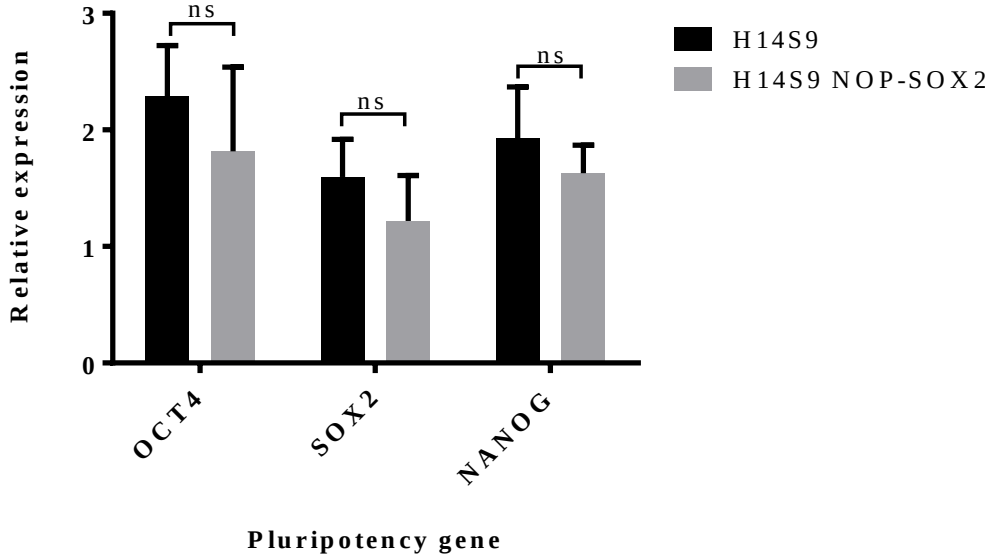

**APPENDIX 2: Gene expression of otic markers *PAX2*, *PAX8*, *FOXG1* and *SOX2* following a 12 day differentiation protocol with Shef3 hES cells, seeded at 8x10$^3$ cells/cm$^2$.** Canonical Wnt inhibition was via 10 µM IWR-1-endo and activation via 2 µM BIO. FGF 3 and FGF 10 ligands were supplemented at 50 ng/ml or 25 ng/ml where appropriate. Gene expression is presented as relative to that of the DFNB baseline control. Bar charts denote mean and standard deviation of gene expression relative to that of the DFNB control condition (n=3 independent experiments). Statistical significance was determined by one way ANOVA with Bonferroni's multiple comparison post-test. ns = no significant difference. **P*<0.05, ***P*<0.01, *****P*<0.0001.

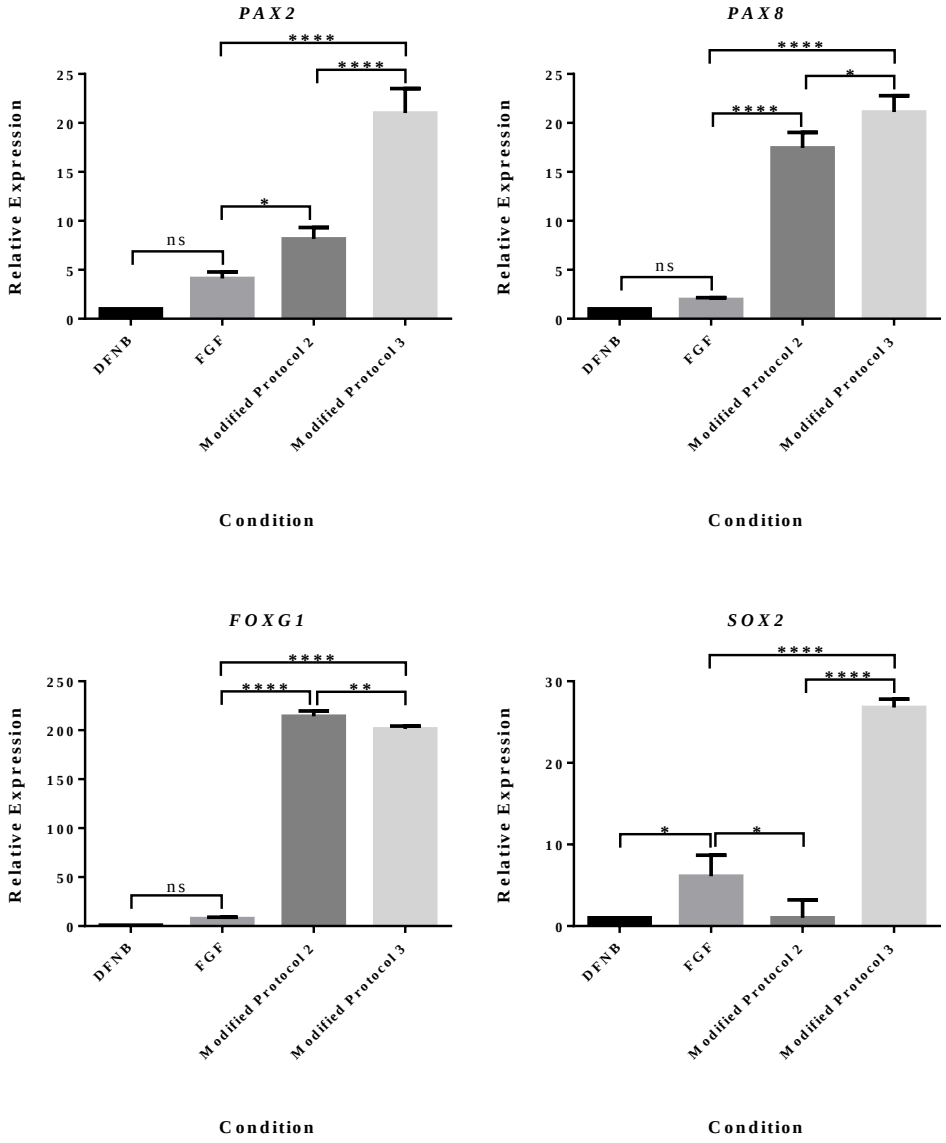

**APPENDIX 3: Single experiment results to demonstrate the variability seen in hair cell differentiation experiments. After treatment for 14 days in hair cell media Modified Protocol 3 OEPs appeared to have upregulation of *POU4F3*, *MYO7A*, and *ATOH1*.**

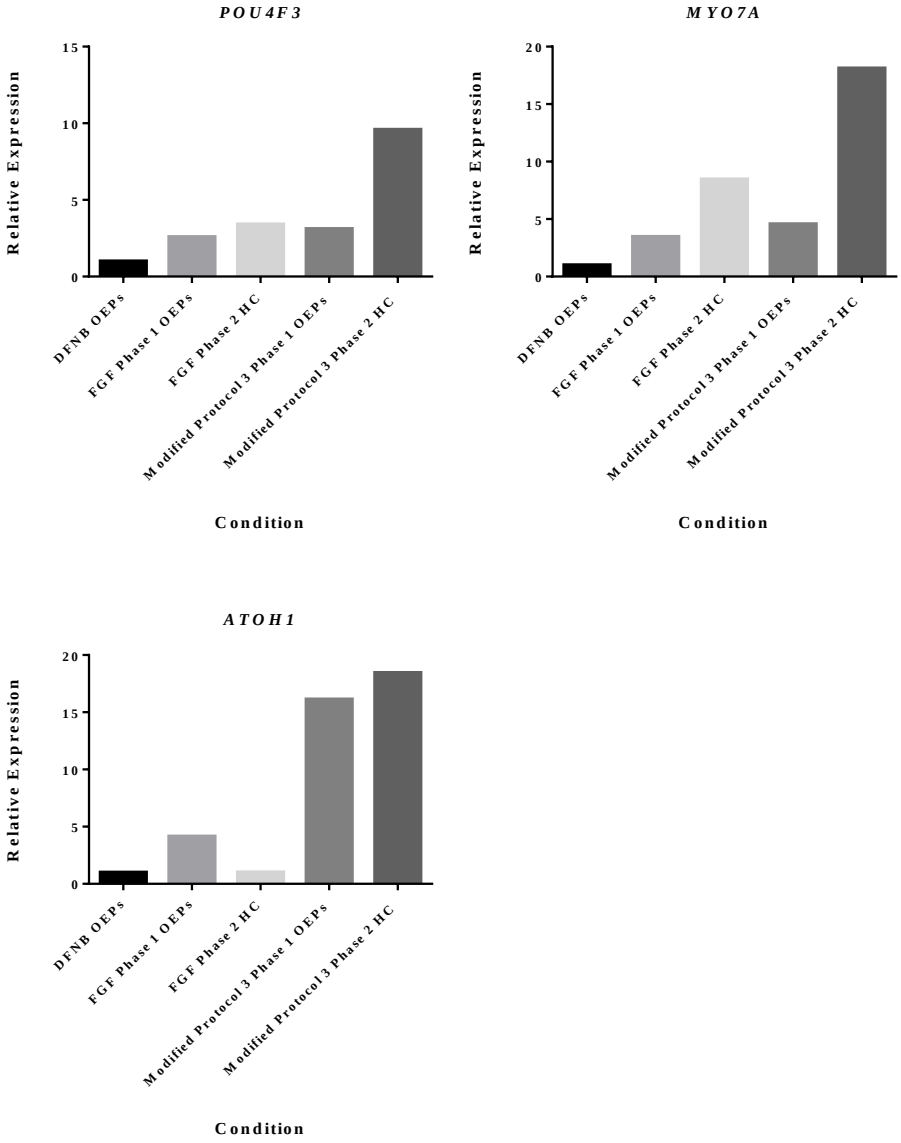

# *References*

## REFERENCES

Adachi, K., Suemori, H., Yasuda, S.Y., Nakatsuji, N., Kawase, E., 2010. Role of SOX2 in maintaining pluripotency of human embryonic stem cells. Genes to cells : devoted to molecular & cellular mechanisms 15, 455-470.

Adamson, A.D., Jackson, D., Davis, J.R., 2011. Novel approaches to in vitro transgenesis. The Journal of endocrinology 208, 193-206.

Ahrens, K., Schlosser, G., 2005. Tissues and signals involved in the induction of placodal Six1 expression in Xenopus laevis. Developmental biology 288, 40-59.

Alamein, M.A., Liu, Q., Stephens, S., Skabo, S., Warnke, F., Bourke, R., Heiner, P., Warnke, P.H., 2013. Nanospiderwebs: artificial 3D extracellular matrix from nanofibers by novel clinical grade electrospinning for stem cell delivery. Advanced healthcare materials 2, 702-717.

Alasti, F., Sanati, M.H., Behrouzifard, A.H., Sadeghi, A., de Brouwer, A.P., Kremer, H., Smith, R.J., Van Camp, G., 2008. A novel TECTA mutation confirms the recognizable phenotype among autosomal recessive hearing impairment families. International journal of pediatric otorhinolaryngology 72, 249-255.

Aletsee, C., Brors, D., Palacios, S., Pak, K., Mullen, L., Dazert, S., Ryan, A.F., 2002. The effects of laminin-1 on spiral ganglion neurons are dependent on the MEK/ERK signaling pathway and are partially independent of Ras. Hearing research 164, 1-11.

Alvarez, Y., Alonso, M.T., Vendrell, V., Zelarayan, L.C., Chamero, P., Theil, T., Bosl, M.R., Kato, S., Maconochie, M., Riethmacher, D., Schimmang, T., 2003. Requirements for FGF3 and FGF10 during inner ear formation. Development 130, 6329-6338.

Ambrosetti, D., Holmes, G., Mansukhani, A., Basilico, C., 2008. Fibroblast growth factor signaling uses multiple mechanisms to inhibit Wnt-induced transcription in osteoblasts. Molecular and cellular biology 28, 4759-4771.

Arce, L., Yokoyama, N.N., Waterman, M.L., 2006. Diversity of LEF/TCF action in development and disease. Oncogene 25, 7492-7504.

Arkell, R.M., Fossat, N., Tam, P.P., 2013. Wnt signalling in mouse gastrulation and anterior development: new players in the pathway and signal output. Current opinion in genetics & development 23, 454-460.

Atkinson, P.J., Wise, A.K., Flynn, B.O., Nayagam, B.A., Richardson, R.T., 2014. Hair cell regeneration after ATOH1 gene therapy in the cochlea of profoundly deaf adult guinea pigs. PloS one 9, e102077.

Bailey, A.P., Bhattacharyya, S., Bronner-Fraser, M., Streit, A., 2006. Lens specification is the ground state of all sensory placodes, from which FGF promotes olfactory identity. Developmental cell 11, 505-517.

Baker, C.V., Bronner-Fraser, M., 2001. Vertebrate cranial placodes I. Embryonic induction. Developmental biology 232, 1-61.

Barker, N., Clevers, H., 2010. Leucine-rich repeat-containing G-protein-coupled receptors as markers of adult stem cells. Gastroenterology 138, 1681-1696.

Barker, N., van Es, J.H., Kuipers, J., Kujala, P., van den Born, M., Cozijnsen, M., Haegebarth, A., Korving, J., Begthel, H., Peters, P.J., Clevers, H., 2007. Identification of stem cells in small intestine and colon by marker gene Lgr5. Nature 449, 1003-1007.

Baumgartner, B., Harper, J.W., 2003. Deafening cycle. Nature cell biology 5, 385-387.

Ben-Arie, N., Bellen, H.J., Armstrong, D.L., McCall, A.E., Gordadze, P.R., Guo, Q., Matzuk, M.M., Zoghbi, H.Y., 1997. Math1 is essential for genesis of cerebellar granule neurons. Nature 390, 169-172.

Bengoa-Vergniory, N., Gorrono-Etxebarria, I., Gonzalez Salazar, I., Kypta, R.M., 2014. A switch from canonical to noncanonical Wnt signaling mediates early differentiation of human neural stem cells. Stem cells.

Bermingham, N.A., Hassan, B.A., Price, S.D., Vollrath, M.A., Ben-Arie, N., Eatock, R.A., Bellen, H.J., Lysakowski, A., Zoghbi, H.Y., 1999. Math1: an essential gene for the generation of inner ear hair cells. Science 284, 1837-1841.

Bhattacharyya, S., Bronner-Fraser, M., 2008. Competence, specification and commitment to an olfactory placode fate. Development 135, 4165-4177.

Blauwkamp, T.A., Nigam, S., Ardehali, R., Weissman, I.L., Nusse, R., 2012. Endogenous Wnt signalling in human embryonic stem cells generates an equilibrium of distinct lineage-specified progenitors. Nature communications 3, 1070.

Boddy, S.L., Chen, W., Romero-Guevara, R., Kottam, L., Bellantuono, I., Rivolta, M.N., 2012. Inner ear progenitor cells can be generated in vitro from human bone marrow mesenchymal stem cells. Regenerative medicine 7, 757-767.

Bodson, M., Breuskin, I., Lefebvre, P., Malgrange, B., 2010. Hair cell progenitors: identification and regulatory genes. Acta oto-laryngologica 130, 312-317.

Bouchard, M., de Caprona, D., Busslinger, M., Xu, P., Fritzsch, B., 2010. Pax2 and Pax8 cooperate in mouse inner ear morphogenesis and innervation. BMC developmental biology 10, 89.

Brafman, D.A., Moya, N., Allen-Soltero, S., Fellner, T., Robinson, M., McMillen, Z.L., Gaasterland, T., Willert, K., 2013. Analysis of SOX2-Expressing Cell Populations Derived from Human Pluripotent Stem Cells. Stem cell reports 1, 464-478.

Brons, I.G., Smithers, L.E., Trotter, M.W., Rugg-Gunn, P., Sun, B., Chuva de Sousa Lopes, S.M., Howlett, S.K., Clarkson, A., Ahrlund-Richter, L., Pedersen, R.A., Vallier, L., 2007. Derivation of pluripotent epiblast stem cells from mammalian embryos. Nature 448, 191-195.

Brooker, R., Hozumi, K., Lewis, J., 2006. Notch ligands with contrasting functions: Jagged1 and Delta1 in the mouse inner ear. Development 133, 1277-1286.

Brors, D., Aletsee, C., Schwager, K., Mlynski, R., Hansen, S., Schafers, M., Ryan, A.F., Dazert, S., 2002. Interaction of spiral ganglion neuron processes with alloplastic materials in vitro(1). Hearing research 167, 110-121.

Brugmann, S.A., Moody, S.A., 2005. Induction and specification of the vertebrate ectodermal placodes: precursors of the cranial sensory organs. Biology of the cell / under the auspices of the European Cell Biology Organization 97, 303-319.

Brugmann, S.A., Pandur, P.D., Kenyon, K.L., Pignoni, F., Moody, S.A., 2004. Six1 promotes a placodal fate within the lateral neurogenic ectoderm by functioning as both a transcriptional activator and repressor. Development 131, 5871-5881.

Brunette, E., Stribling, R., Debs, R., 1992. Lipofection does not require the removal of serum. Nucleic acids research 20, 1151.

Cajal, M., Lawson, K.A., Hill, B., Moreau, A., Rao, J., Ross, A., Collignon, J., Camus, A., 2012. Clonal and molecular analysis of the prospective anterior neural boundary in the mouse embryo. Development 139, 423-436.

Chai, R., Kuo, B., Wang, T., Liaw, E.J., Xia, A., Jan, T.A., Liu, Z., Taketo, M.M., Oghalai, J.S., Nusse, R., Zuo, J., Cheng, A.G., 2012. Wnt signaling induces proliferation of sensory precursors in the postnatal mouse cochlea. Proceedings of the National Academy of Sciences of the United States of America 109, 8167-8172.

Chambers, S.M., Fasano, C.A., Papapetrou, E.P., Tomishima, M., Sadelain, M., Studer, L., 2009. Highly efficient neural conversion of human ES and iPS cells by dual inhibition of SMAD signaling. Nature biotechnology 27, 275-280.

Chen, B., Dodge, M.E., Tang, W., Lu, J., Ma, Z., Fan, C.W., Wei, S., Hao, W., Kilgore, J., Williams, N.S., Roth, M.G., Amatruda, J.F., Chen, C., Lum, L., 2009. Small molecule-mediated disruption of Wnt-dependent signaling in tissue regeneration and cancer. Nature chemical biology 5, 100-107.

Chen, J., Streit, A., 2013. Induction of the inner ear: stepwise specification of otic fate from multipotent progenitors. Hearing research 297, 3-12.

Chen, J., Zhao, H.B., 2014. The role of an inwardly rectifying K(+) channel (Kir4.1) in the inner ear and hearing loss. Neuroscience 265, 137-146.

Chen, P., Johnson, J.E., Zoghbi, H.Y., Segil, N., 2002. The role of Math1 in inner ear development: Uncoupling the establishment of the sensory primordium from hair cell fate determination. Development 129, 2495-2505.

Chen, W., Cacciabue-Rivolta, D.I., Moore, H.D., Rivolta, M.N., 2007. The human fetal cochlea can be a source for auditory progenitors/stem cells isolation. Hearing research 233, 23-29.

Chen, W., Johnson, S.L., Marcotti, W., Andrews, P.W., Moore, H.D., Rivolta, M.N., 2009. Human fetal auditory stem cells can be expanded in vitro and differentiate into functional auditory neurons and hair cell-like cells. Stem cells 27, 1196-1204.

Chen, W., Jongkamonwiwat, N., Abbas, L., Eshtan, S.J., Johnson, S.L., Kuhn, S., Milo, M., Thurlow, J.K., Andrews, P.W., Marcotti, W., Moore, H.D., Rivolta, M.N., 2012. Restoration of auditory evoked responses by human ES-cell-derived otic progenitors. Nature 490, 278-282.

Chien, W.W., Monzack, E.L., McDougald, D.S., Cunningham, L.L., 2015. Gene therapy for sensorineural hearing loss. Ear and hearing 36, 1-7.

Christ, S., Biebel, U.W., Hoidis, S., Friedrichsen, S., Bauer, K., Smolders, J.W., 2004. Hearing loss in athyroid pax8 knockout mice and effects of thyroxine substitution. Audiology & neuro-otology 9, 88-106.

Chuang, K.A., Lieu, C.H., Tsai, W.J., Wu, M.H., Chen, Y.C., Liao, J.F., Wang, C.C., Kuo, Y.C., 2010. Evaluation of anti-Wnt/beta-catenin signaling agents by pGL4-TOP transfected stable cells with a luciferase reporter system. Brazilian journal of medical and biological research = Revista brasileira de pesquisas medicas e biologicas / Sociedade Brasileira de Biofisica ... [et al.] 43, 931-941.

Cohen, M.A., Itsykson, P., Reubinoff, B.E., 2010. The role of FGF-signaling in early neural specification of human embryonic stem cells. Developmental biology 340, 450-458.

Collignon, J., Sockanathan, S., Hacker, A., Cohen-Tannoudji, M., Norris, D., Rastan, S., Stevanovic, M., Goodfellow, P.N., Lovell-Badge, R., 1996. A comparison of the properties of Sox-3 with Sry and two related genes, Sox-1 and Sox-2. Development 122, 509-520.

Crispino, G., Di Pasquale, G., Scimemi, P., Rodriguez, L., Galindo Ramirez, F., De Siati, R.D., Santarelli, R.M., Arslan, E., Bortolozzi, M., Chiorini, J.A., Mammano, F., 2011. BAAV mediated GJB2 gene transfer restores gap junction coupling in cochlear organotypic cultures from deaf Cx26Sox10Cre mice. PloS one 6, e23279.

Cristobal, R., Oghalai, J.S., 2008. Hearing loss in children with very low birth weight: current review of epidemiology and pathophysiology. Archives of disease in childhood. Fetal and neonatal edition 93, F462-468.

Cvekl, A., Duncan, M.K., 2007. Genetic and epigenetic mechanisms of gene regulation during lens development. Progress in retinal and eye research 26, 555-597.

Davies, J.C., Alton, E.W., Bush, A., 2007. Cystic fibrosis. Bmj 335, 1255-1259.

Dehne, N., Lautermann, J., Petrat, F., Rauen, U., de Groot, H., 2001. Cisplatin ototoxicity: involvement of iron and enhanced formation of superoxide anion radicals. Toxicology and applied pharmacology 174, 27-34.

Dincer, Z., Piao, J., Niu, L., Ganat, Y., Kriks, S., Zimmer, B., Shi, S.H., Tabar, V., Studer, L., 2013. Specification of functional cranial placode derivatives from human pluripotent stem cells. Cell reports 5, 1387-1402.

Doetzlhofer, A., White, P.M., Johnson, J.E., Segil, N., Groves, A.K., 2004. In vitro growth and differentiation of mammalian sensory hair cell progenitors: a requirement for EGF and periotic mesenchyme. Developmental biology 272, 432-447.

Draper, J.S., Pigott, C., Thomson, J.A., Andrews, P.W., 2002. Surface antigens of human embryonic stem cells: changes upon differentiation in culture. Journal of anatomy 200, 249-258.

Dravid, G., Ye, Z., Hammond, H., Chen, G., Pyle, A., Donovan, P., Yu, X., Cheng, L., 2005. Defining the role of Wnt/beta-catenin signaling in the survival, proliferation, and self-renewal of human embryonic stem cells. Stem cells 23, 1489-1501.

Duggan, C.D., DeMaria, S., Baudhuin, A., Stafford, D., Ngai, J., 2008. Foxg1 is required for development of the vertebrate olfactory system. The Journal of neuroscience : the official journal of the Society for Neuroscience 28, 5229-5239.

Duman, D., Tekin, M., 2012. Autosomal recessive nonsyndromic deafness genes: a review. Frontiers in bioscience 17, 2213-2236.

Duncan, J.S., Fritzsch, B., 2013. Continued expression of GATA3 is necessary for cochlear neurosensory development. PloS one 8, e62046.

Duran Alonso, M.B., Feijoo-Redondo, A., Conde de Felipe, M., Carnicero, E., Garcia, A.S., Garcia-Sancho, J., Rivolta, M.N., Giraldez, F., Schimmang, T., 2012. Generation of inner ear sensory cells from bone marrow-derived human mesenchymal stem cells. Regenerative medicine 7, 769-783.

Ebert, A.D., Yu, J., Rose, F.F., Jr., Mattis, V.B., Lorson, C.L., Thomson, J.A., Svendsen, C.N., 2009. Induced pluripotent stem cells from a spinal muscular atrophy patient. Nature 457, 277-280.

Economou, A., Datta, P., Georgiadis, V., Cadot, S., Frenz, D., Maconochie, M., 2013. Gata3 directly regulates early inner ear expression of Fgf10. Developmental biology 374, 210-222.

Eiraku, M., Takata, N., Ishibashi, H., Kawada, M., Sakakura, E., Okuda, S., Sekiguchi, K., Adachi, T., Sasai, Y., 2011. Self-organizing optic-cup morphogenesis in three-dimensional culture. Nature 472, 51-56.

Erkman, L., McEvilly, R.J., Luo, L., Ryan, A.K., Hooshmand, F., O'Connell, S.M., Keithley, E.M., Rapaport, D.H., Ryan, A.F., Rosenfeld, M.G., 1996. Role of transcription factors Brn-3.1 and Brn-3.2 in auditory and visual system development. Nature 381, 603-606.

Ernfors, P., Merlio, J.P., Persson, H., 1992. Cells Expressing mRNA for Neurotrophins and their Receptors During Embryonic Rat Development. The European journal of neuroscience 4, 1140-1158.

Ernfors, P., Van De Water, T., Loring, J., Jaenisch, R., 1995. Complementary roles of BDNF and NT-3 in vestibular and auditory development. Neuron 14, 1153-1164.

Evans, A.R., Euteneuer, S., Chavez, E., Mullen, L.M., Hui, E.E., Bhatia, S.N., Ryan, A.F., 2007. Laminin and fibronectin modulate inner ear spiral ganglion neurite outgrowth in an in vitro alternate choice assay. Developmental neurobiology 67, 1721-1730.

Fernandez-Garre, P., Rodriguez-Gallardo, L., Alvarez, I.S., Puelles, L., 2002. A neural plate fate map at stage HH4 in the chick: methodology and preliminary data. Brain research bulletin 57, 293-295.

Fink, D.W., Jr., 2009. FDA regulation of stem cell-based products. Science 324, 1662-1663.

Flora, A., Klisch, T.J., Schuster, G., Zoghbi, H.Y., 2009. Deletion of Atoh1 disrupts Sonic Hedgehog signaling in the developing cerebellum and prevents medulloblastoma. Science 326, 1424-1427.

Freter, S., Muta, Y., Mak, S.S., Rinkwitz, S., Ladher, R.K., 2008. Progressive restriction of otic fate: the role of FGF and Wnt in resolving inner ear potential. Development 135, 3415-3424.

Freyer, L., Aggarwal, V., Morrow, B.E., 2011. Dual embryonic origin of the mammalian otic vesicle forming the inner ear. Development 138, 5403-5414.

Freyer, L., Morrow, B.E., 2010. Canonical Wnt signaling modulates Tbx1, Eya1, and Six1 expression, restricting neurogenesis in the otic vesicle. Developmental dynamics : an official publication of the American Association of Anatomists 239, 1708-1722.

Fujimoto, C., Yamasoba, T., 2014. Oxidative stresses and mitochondrial dysfunction in age-related hearing loss. Oxidative medicine and cellular longevity 2014, 582849.

Furness, D.N., Lawton, D.M., 2003. Comparative distribution of glutamate transporters and receptors in relation to afferent innervation density in the mammalian cochlea. The Journal of neuroscience : the official journal of the Society for Neuroscience 23, 11296-11304.

Gadue, P., Huber, T.L., Paddison, P.J., Keller, G.M., 2006. Wnt and TGF-beta signaling are required for the induction of an in vitro model of primitive streak formation using embryonic stem cells. Proceedings of the National Academy of Sciences of the United States of America 103, 16806-16811.

Gibson, F., Walsh, J., Mburu, P., Varela, A., Brown, K.A., Antonio, M., Beisel, K.W., Steel, K.P., Brown, S.D., 1995. A type VII myosin encoded by the mouse deafness gene shaker-1. Nature 374, 62-64.

Giudice, A., Trounson, A., 2008. Genetic modification of human embryonic stem cells for derivation of target cells. Cell stem cell 2, 422-433.

Gonzalez-Cordero, A., West, E.L., Pearson, R.A., Duran, Y., Carvalho, L.S., Chu, C.J., Naeem, A., Blackford, S.J., Georgiadis, A., Lakowski, J., Hubank, M., Smith, A.J., Bainbridge, J.W., Sowden, J.C., Ali, R.R., 2013. Photoreceptor precursors derived from three-dimensional embryonic stem cell cultures integrate and mature within adult degenerate retina. Nature biotechnology 31, 741-747.

Gopinath, B., Rochtchina, E., Wang, J.J., Schneider, J., Leeder, S.R., Mitchell, P., 2009. Prevalence of age-related hearing loss in older adults: Blue Mountains Study. Archives of internal medicine 169, 415-416.

Graf, T., Stadtfeld, M., 2008. Heterogeneity of embryonic and adult stem cells. Cell stem cell 3, 480-483.

Greer, L.G., Roberts, S.W., Sheffield, J.S., Rogers, V.L., Hill, J.B., McIntire, D.D., Wendel, G.D., Jr., 2008. Ampicillin resistance and outcome differences in acute antepartum pyelonephritis. Infectious diseases in obstetrics and gynecology 2008, 891426.

Grindley, J.C., Davidson, D.R., Hill, R.E., 1995. The role of Pax-6 in eye and nasal development. Development 121, 1433-1442.

Haddon, C., Jiang, Y.J., Smithers, L., Lewis, J., 1998. Delta-Notch signalling and the patterning of sensory cell differentiation in the zebrafish ear: evidence from the mind bomb mutant. Development 125, 4637-4644.

He, S., Yang, J., 2011. Maturation of neurotransmission in the developing rat cochlea: immunohistochemical evidence from differential expression of synaptophysin and synaptobrevin 2. European journal of histochemistry : EJH 55, e2.

He, X., Semenov, M., Tamai, K., Zeng, X., 2004. LDL receptor-related proteins 5 and 6 in Wnt/beta-catenin signaling: arrows point the way. Development 131, 1663-1677.

Heinrich, U.R., Fischer, I., Brieger, J., Rumelin, A., Schmidtmann, I., Li, H., Mann, W.J., Helling, K., 2008. Ascorbic acid reduces noise-induced nitric oxide production in the guinea pig ear. The Laryngoscope 118, 837-842.

Helms, A.W., Abney, A.L., Ben-Arie, N., Zoghbi, H.Y., Johnson, J.E., 2000. Autoregulation and multiple enhancers control Math1 expression in the developing nervous system. Development 127, 1185-1196.

Hibino, H., Kurachi, Y., 2006. Molecular and physiological bases of the K+ circulation in the mammalian inner ear. Physiology 21, 336-345.

Hong, C.S., Saint-Jeannet, J.P., 2007. The activity of Pax3 and Zic1 regulates three distinct cell fates at the neural plate border. Molecular biology of the cell 18, 2192-2202.

Hongmiao, R., Wei, L., Bing, H., Xiong, D.D., Jihao, R., 2014. Atoh1: landscape for inner ear cell regeneration. Current gene therapy 14, 101-111.

Hu, B.H., Henderson, D., Nicotera, T.M., 2002. Involvement of apoptosis in progression of cochlear lesion following exposure to intense noise. Hearing research 166, 62-71.

Huang, E.J., Liu, W., Fritzsch, B., Bianchi, L.M., Reichardt, L.F., Xiang, M., 2001. Brn3a is a transcriptional regulator of soma size, target field innervation and axon pathfinding of inner ear sensory neurons. Development 128, 2421-2432.

Huber, I., Itzhaki, I., Caspi, O., Arbel, G., Tzukerman, M., Gepstein, A., Habib, M., Yankelson, L., Kehat, I., Gepstein, L., 2007. Identification and selection of cardiomyocytes during human embryonic stem cell differentiation. FASEB journal : official publication of the Federation of American Societies for Experimental Biology 21, 2551-2563.

Hudson, J., Titmarsh, D., Hidalgo, A., Wolvetang, E., Cooper-White, J., 2012. Primitive cardiac cells from human embryonic stem cells. Stem cells and development 21, 1513-1523.

Huelsken, J., Vogel, R., Brinkmann, V., Erdmann, B., Birchmeier, C., Birchmeier, W., 2000. Requirement for beta-catenin in anterior-posterior axis formation in mice. The Journal of cell biology 148, 567-578.

Ishikawa, T.O., Tamai, Y., Li, Q., Oshima, M., Taketo, M.M., 2003. Requirement for tumor suppressor Apc in the morphogenesis of anterior and ventral mouse embryo. Developmental biology 253, 230-246.

Itoh, N., Ohta, H., 2014. Fgf10: a paracrine-signaling molecule in development, disease, and regenerative medicine. Current molecular medicine 14, 504-509.

Jacques, B.E., Puligilla, C., Weichert, R.M., Ferrer-Vaquer, A., Hadjantonakis, A.K., Kelley, M.W., Dabdoub, A., 2012. A dual function for canonical Wnt/beta-catenin signaling in the developing mammalian cochlea. Development 139, 4395-4404.

Jayasena, C.S., Ohyama, T., Segil, N., Groves, A.K., 2008. Notch signaling augments the canonical Wnt pathway to specify the size of the otic placode. Development 135, 2251-2261.

Jeon, S.J., Fujioka, M., Kim, S.C., Edge, A.S., 2011. Notch signaling alters sensory or neuronal cell fate specification of inner ear stem cells. The Journal of neuroscience : the official journal of the Society for Neuroscience 31, 8351-8358.

Jiao, Y., Palmgren, B., Novozhilova, E., Englund Johansson, U., Spieles-Engemann, A.L., Kale, A., Stupp, S.I., Olivius, P., 2014. BDNF Increases Survival and Neuronal

Differentiation of Human Neural Precursor Cells Cotransplanted with a Nanofiber Gel to the Auditory Nerve in a Rat Model of Neuronal Damage. BioMed research international 2014, 356415.

Karakikes, I., Senyei, G.D., Hansen, J., Kong, C.W., Azeloglu, E.U., Stillitano, F., Lieu, D.K., Wang, J., Ren, L., Hulot, J.S., Iyengar, R., Li, R.A., Hajjar, R.J., 2014. Small molecule-mediated directed differentiation of human embryonic stem cells toward ventricular cardiomyocytes. Stem cells translational medicine 3, 18-31.

Kawamoto, K., Oh, S.H., Kanzaki, S., Brown, N., Raphael, Y., 2001. The functional and structural outcome of inner ear gene transfer via the vestibular and cochlear fluids in mice. Molecular therapy : the journal of the American Society of Gene Therapy 4, 575-585.

Kawashima, Y., Geleoc, G.S., Kurima, K., Labay, V., Lelli, A., Asai, Y., Makishima, T., Wu, D.K., Della Santina, C.C., Holt, J.R., Griffith, A.J., 2011. Mechanotransduction in mouse inner ear hair cells requires transmembrane channel-like genes. The Journal of clinical investigation 121, 4796-4809.

Kelley, M.W., Xu, X.M., Wagner, M.A., Warchol, M.E., Corwin, J.T., 1993. The developing organ of Corti contains retinoic acid and forms supernumerary hair cells in response to exogenous retinoic acid in culture. Development 119, 1041-1053.

Kemp, C., Willems, E., Abdo, S., Lambiv, L., Leyns, L., 2005. Expression of all Wnt genes and their secreted antagonists during mouse blastocyst and postimplantation development. Developmental dynamics : an official publication of the American Association of Anatomists 233, 1064-1075.

Khatri, S.B., Groves, A.K., 2013. Expression of the Foxi2 and Foxi3 transcription factors during development of chicken sensory placodes and pharyngeal arches. Gene expression patterns : GEP 13, 38-42.

Kiernan, A.E., Pelling, A.L., Leung, K.K., Tang, A.S., Bell, D.M., Tease, C., Lovell-Badge, R., Steel, K.P., Cheah, K.S., 2005. Sox2 is required for sensory organ development in the mammalian inner ear. Nature 434, 1031-1035.

Kikuchi, T., Kimura, R.S., Paul, D.L., Takasaka, T., Adams, J.C., 2000. Gap junction systems in the mammalian cochlea. Brain research. Brain research reviews 32, 163-166.

Kim, H., Ankamreddy, H., Lee, D.J., Kong, K.A., Ko, H.W., Kim, M.H., Bok, J., 2014. Pax3 function is required specifically for inner ear structures with melanogenic fates. Biochemical and biophysical research communications 445, 608-614.

Kim, J.H., Rodriguez-Vazquez, J.F., Verdugo-Lopez, S., Cho, K.H., Murakami, G., Cho, B.H., 2011. Early fetal development of the human cochlea. Anatomical record 294, 996-1002.

King, F.W., Ritner, C., Liszewski, W., Kwan, H.C., Pedersen, A., Leavitt, A.D., Bernstein, H.S., 2009. Subpopulations of human embryonic stem cells with distinct tissue-specific fates can be selected from pluripotent cultures. Stem cells and development 18, 1441-1450.

Klisch, T.J., Xi, Y., Flora, A., Wang, L., Li, W., Zoghbi, H.Y., 2011. In vivo Atoh1 targetome reveals how a proneural transcription factor regulates cerebellar development. Proceedings of the National Academy of Sciences of the United States of America 108, 3288-3293.

Kobayashi, M., Osanai, H., Kawakami, K., Yamamoto, M., 2000. Expression of three zebrafish Six4 genes in the cranial sensory placodes and the developing somites. Mechanisms of development 98, 151-155.

Koehler, K.R., Mikosz, A.M., Molosh, A.I., Patel, D., Hashino, E., 2013. Generation of inner ear sensory epithelia from pluripotent stem cells in 3D culture. Nature 500, 217-221.

Kofuji, P., Ceelen, P., Zahs, K.R., Surbeck, L.W., Lester, H.A., Newman, E.A., 2000. Genetic inactivation of an inwardly rectifying potassium channel (Kir4.1 subunit) in mice: phenotypic impact in retina. The Journal of neuroscience : the official journal of the Society for Neuroscience 20, 5733-5740.

Konishi, T., Mendelsohn, M., 1970. Effect of ouabain on cochlear potentials and endolymph composition in guinea pigs. Acta oto-laryngologica 69, 192-199.

Kopke, R.D., Jackson, R.L., Coleman, J.K., Liu, J., Bielefeld, E.C., Balough, B.J., 2007. NAC for noise: from the bench top to the clinic. Hearing research 226, 114-125.

Kumar, S., Deffenbacher, K., Cremers, C.W., Van Camp, G., Kimberling, W.J., 1997. Branchio-oto-renal syndrome: identification of novel mutations, molecular characterization, mutation distribution, and prospects for genetic testing. Genetic testing 1, 243-251.

Kwon, C., Arnold, J., Hsiao, E.C., Taketo, M.M., Conklin, B.R., Srivastava, D., 2007. Canonical Wnt signaling is a positive regulator of mammalian cardiac progenitors. Proceedings of the National Academy of Sciences of the United States of America 104, 10894-10899.

Kwon, H.J., Bhat, N., Sweet, E.M., Cornell, R.A., Riley, B.B., 2010. Identification of early requirements for preplacodal ectoderm and sensory organ development. PLoS genetics 6, e1001133.

Ladher, R.K., Anakwe, K.U., Gurney, A.L., Schoenwolf, G.C., Francis-West, P.H., 2000. Identification of synergistic signals initiating inner ear development. Science 290, 1965-1967.

Ladher, R.K., Wright, T.J., Moon, A.M., Mansour, S.L., Schoenwolf, G.C., 2005. FGF8 initiates inner ear induction in chick and mouse. Genes & development 19, 603-613.

Lamba, D.A., Karl, M.O., Ware, C.B., Reh, T.A., 2006. Efficient generation of retinal progenitor cells from human embryonic stem cells. Proceedings of the National Academy of Sciences of the United States of America 103, 12769-12774.

Lassiter, R.N., Stark, M.R., Zhao, T., Zhou, C.J., 2014. Signaling mechanisms controlling cranial placode neurogenesis and delamination. Developmental biology 389, 39-49.

Lawoko-Kerali, G., Rivolta, M.N., Lawlor, P., Cacciabue-Rivolta, D.I., Langton-Hewer, C., van Doorninck, J.H., Holley, M.C., 2004. GATA3 and NeuroD distinguish auditory and vestibular neurons during development of the mammalian inner ear. Mechanisms of development 121, 287-299.

Lawson, K.A., 1999. Fate mapping the mouse embryo. The International journal of developmental biology 43, 773-775.

Legan, P.K., Lukashkina, V.A., Goodyear, R.J., Kossi, M., Russell, I.J., Richardson, G.P., 2000. A targeted deletion in alpha-tectorin reveals that the tectorial membrane is required for the gain and timing of cochlear feedback. Neuron 28, 273-285.

Legan, P.K., Lukashkina, V.A., Goodyear, R.J., Lukashkin, A.N., Verhoeven, K., Van Camp, G., Russell, I.J., Richardson, G.P., 2005. A deafness mutation isolates a second role for the tectorial membrane in hearing. Nature neuroscience 8, 1035-1042.

Lenarz, T., Pau, H.W., Paasche, G., 2013. Cochlear implants. Current pharmaceutical biotechnology 14, 112-123.

Lenka, N., Lu, Z.J., Sasse, P., Hescheler, J., Fleischmann, B.K., 2002. Quantitation and functional characterization of neural cells derived from ES cells using nestin enhancer-mediated targeting in vitro. Journal of cell science 115, 1471-1485.

Levine, A.J., Brivanlou, A.H., 2007. Proposal of a model of mammalian neural induction. Developmental biology 308, 247-256.

Li, H., Roblin, G., Liu, H., Heller, S., 2003. Generation of hair cells by stepwise differentiation of embryonic stem cells. Proceedings of the National Academy of Sciences of the United States of America 100, 13495-13500.

Lian, X., Zhang, J., Azarin, S.M., Zhu, K., Hazeltine, L.B., Bao, X., Hsiao, C., Kamp, T.J., Palecek, S.P., 2013. Directed cardiomyocyte differentiation from human pluripotent stem cells by modulating Wnt/beta-catenin signaling under fully defined conditions. Nature protocols 8, 162-175.

Lindsley, R.C., Gill, J.G., Kyba, M., Murphy, T.L., Murphy, K.M., 2006. Canonical Wnt signaling is required for development of embryonic stem cell-derived mesoderm. Development 133, 3787-3796.

Litsiou, A., Hanson, S., Streit, A., 2005. A balance of FGF, BMP and WNT signalling positions the future placode territory in the head. Development 132, 4051-4062.

Liu, D., Chu, H., Maves, L., Yan, Y.L., Morcos, P.A., Postlethwait, J.H., Westerfield, M., 2003. Fgf3 and Fgf8 dependent and independent transcription factors are required for otic placode specification. Development 130, 2213-2224.

Liu, G., Bafico, A., Harris, V.K., Aaronson, S.A., 2003. A novel mechanism for Wnt activation of canonical signaling through the LRP6 receptor. Molecular and cellular biology 23, 5825-5835.

Liu, P., Wakamiya, M., Shea, M.J., Albrecht, U., Behringer, R.R., Bradley, A., 1999. Requirement for Wnt3 in vertebrate axis formation. Nature genetics 22, 361-365.

Livak, K.J., Schmittgen, T.D., 2001. Analysis of relative gene expression data using real-time quantitative PCR and the 2(-Delta Delta C(T)) Method. Methods 25, 402-408.

Lleras-Forero, L., Tambalo, M., Christophorou, N., Chambers, D., Houart, C., Streit, A., 2013. Neuropeptides: developmental signals in placode progenitor formation. Developmental cell 26, 195-203.

Loh, K.M., Ang, L.T., Zhang, J., Kumar, V., Ang, J., Auyeong, J.Q., Lee, K.L., Choo, S.H., Lim, C.Y., Nichane, M., Tan, J., Noghabi, M.S., Azzola, L., Ng, E.S., Durruthy-Durruthy, J., Sebastiano, V., Poellinger, L., Elefanty, A.G., Stanley, E.G., Chen, Q., Prabhakar, S., Weissman, I.L., Lim, B., 2014. Efficient endoderm induction from human pluripotent stem cells by logically directing signals controlling lineage bifurcations. Cell stem cell 14, 237-252.

Lumpkin, E.A., Collisson, T., Parab, P., Omer-Abdalla, A., Haeberle, H., Chen, P., Doetzlhofer, A., White, P., Groves, A., Segil, N., Johnson, J.E., 2003. Math1-driven GFP expression in the developing nervous system of transgenic mice. Gene expression patterns : GEP 3, 389-395.

Ma, Q., Anderson, D.J., Fritzsch, B., 2000. Neurogenin 1 null mutant ears develop fewer, morphologically normal hair cells in smaller sensory epithelia devoid of innervation. Journal of the Association for Research in Otolaryngology : JARO 1, 129-143.

Ma, Q., Chen, Z., del Barco Barrantes, I., de la Pompa, J.L., Anderson, D.J., 1998. neurogenin1 is essential for the determination of neuronal precursors for proximal cranial sensory ganglia. Neuron 20, 469-482.

MacDonald, B.T., Tamai, K., He, X., 2009. Wnt/beta-catenin signaling: components, mechanisms, and diseases. Developmental cell 17, 9-26.

Mahoney Rogers, A.A., Zhang, J., Shim, K., 2011. Sprouty1 and Sprouty2 limit both the size of the otic placode and hindbrain Wnt8a by antagonizing FGF signaling. Developmental biology 353, 94-104.

Mansukhani, A., Ambrosetti, D., Holmes, G., Cornivelli, L., Basilico, C., 2005. Sox2 induction by FGF and FGFR2 activating mutations inhibits Wnt signaling and osteoblast differentiation. The Journal of cell biology 168, 1065-1076.

Marchetto, M.C., Carromeu, C., Acab, A., Yu, D., Yeo, G.W., Mu, Y., Chen, G., Gage, F.H., Muotri, A.R., 2010. A model for neural development and treatment of Rett syndrome using human induced pluripotent stem cells. Cell 143, 527-539.

Marcotti, W., Erven, A., Johnson, S.L., Steel, K.P., Kros, C.J., 2006. Tmc1 is necessary for normal functional maturation and survival of inner and outer hair cells in the mouse cochlea. The Journal of physiology 574, 677-698.

Maroon, H., Walshe, J., Mahmood, R., Kiefer, P., Dickson, C., Mason, I., 2002. Fgf3 and Fgf8 are required together for formation of the otic placode and vesicle. Development 129, 2099-2108.

Martin, K., Groves, A.K., 2006. Competence of cranial ectoderm to respond to Fgf signaling suggests a two-step model of otic placode induction. Development 133, 877-887.

McLean, W.J., Smith, K.A., Glowatzki, E., Pyott, S.J., 2009. Distribution of the Na,K-ATPase alpha subunit in the rat spiral ganglion and organ of corti. Journal of the Association for Research in Otolaryngology : JARO 10, 37-49.

Meijer, L., Skaltsounis, A.L., Magiatis, P., Polychronopoulos, P., Knockaert, M., Leost, M., Ryan, X.P., Vonica, C.A., Brivanlou, A., Dajani, R., Crovace, C., Tarricone, C., Musacchio, A., Roe, S.M., Pearl, L., Greengard, P., 2003. GSK-3-selective inhibitors derived from Tyrian purple indirubins. Chemistry & biology 10, 1255-1266.

Menardo, J., Tang, Y., Ladrech, S., Lenoir, M., Casas, F., Michel, C., Bourien, J., Ruel, J., Rebillard, G., Maurice, T., Puel, J.L., Wang, J., 2012. Oxidative stress, inflammation, and autophagic stress as the key mechanisms of premature age-related hearing loss in SAMP8 mouse Cochlea. Antioxidants & redox signaling 16, 263-274.

Menasche, P., Vanneaux, V., Fabreguettes, J.R., Bel, A., Tosca, L., Garcia, S., Bellamy, V., Farouz, Y., Pouly, J., Damour, O., Perier, M.C., Desnos, M., Hagege, A., Agbulut, O., Bruneval, P., Tachdjian, G., Trouvin, J.H., Larghero, J., 2014. Towards a clinical use of human embryonic stem cell-derived cardiac progenitors: a translational experience. European heart journal.

Mendelsohn, C., Ruberte, E., LeMeur, M., Morriss-Kay, G., Chambon, P., 1991. Developmental analysis of the retinoic acid-inducible RAR-beta 2 promoter in transgenic animals. Development 113, 723-734.

Merkus, P., Di Lella, F., Di Trapani, G., Pasanisi, E., Beltrame, M.A., Zanetti, D., Negri, M., Sanna, M., 2014. Indications and contraindications of auditory brainstem implants: systematic review and illustrative cases. European archives of oto-rhino-laryngology : official journal of the European Federation of Oto-Rhino-Laryngological Societies 271, 3-13.

Mohamed, O.A., Clarke, H.J., Dufort, D., 2004. Beta-catenin signaling marks the prospective site of primitive streak formation in the mouse embryo. Developmental dynamics : an official publication of the American Association of Anatomists 231, 416-424.

Morrison, A., Hodgetts, C., Gossler, A., Hrabe de Angelis, M., Lewis, J., 1999. Expression of Delta1 and Serrate1 (Jagged1) in the mouse inner ear. Mechanisms of development 84, 169-172.

Mulvaney, J., Dabdoub, A., 2012. Atoh1, an essential transcription factor in neurogenesis and intestinal and inner ear development: function, regulation, and context dependency. Journal of the Association for Research in Otolaryngology : JARO 13, 281-293.

Narayanan, K., Schumacher, K.M., Tasnim, F., Kandasamy, K., Schumacher, A., Ni, M., Gao, S., Gopalan, B., Zink, D., Ying, J.Y., 2013. Human embryonic stem cells differentiate into functional renal proximal tubular-like cells. Kidney international 83, 593-603.

Neves, J., Vachkov, I., Giraldez, F., 2013. Sox2 regulation of hair cell development: incoherence makes sense. Hearing research 297, 20-29.

Nicoleau, C., Varela, C., Bonnefond, C., Maury, Y., Bugi, A., Aubry, L., Viegas, P., Bourgois-Rocha, F., Peschanski, M., Perrier, A.L., 2013. Embryonic stem cells neural differentiation qualifies the role of Wnt/beta-Catenin signals in human telencephalic specification and regionalization. Stem cells 31, 1763-1774.

Noisa, P., Urrutikoetxea-Uriguen, A., Li, M., Cui, W., 2010. Generation of human embryonic stem cell reporter lines expressing GFP specifically in neural progenitors. Stem cell reviews 6, 438-449.

Nyeng, P., Norgaard, G.A., Kobberup, S., Jensen, J., 2007. FGF10 signaling controls stomach morphogenesis. Developmental biology 303, 295-310.

Ohinata, Y., Yamasoba, T., Schacht, J., Miller, J.M., 2000. Glutathione limits noise-induced hearing loss. Hearing research 146, 28-34.

Ohlemiller, K.K., Wright, J.S., Dugan, L.L., 1999. Early elevation of cochlear reactive oxygen species following noise exposure. Audiology & neuro-otology 4, 229-236.

Ohyama, T., Groves, A.K., 2004. Expression of mouse Foxi class genes in early craniofacial development. Developmental dynamics : an official publication of the American Association of Anatomists 231, 640-646.

Ohyama, T., Groves, A.K., 2004. Generation of Pax2-Cre mice by modification of a Pax2 bacterial artificial chromosome. Genesis 38, 195-199.

Ohyama, T., Mohamed, O.A., Taketo, M.M., Dufort, D., Groves, A.K., 2006. Wnt signals mediate a fate decision between otic placode and epidermis. Development 133, 865-875.

Oshima, K., Grimm, C.M., Corrales, C.E., Senn, P., Martinez Monedero, R., Geleoc, G.S., Edge, A., Holt, J.R., Heller, S., 2007. Differential distribution of stem cells in the auditory and vestibular organs of the inner ear. Journal of the Association for Research in Otolaryngology : JARO 8, 18-31.

Oshima, K., Shin, K., Diensthuber, M., Peng, A.W., Ricci, A.J., Heller, S., 2010. Mechanosensitive hair cell-like cells from embryonic and induced pluripotent stem cells. Cell 141, 704-716.

Otte, J., Schunknecht, H.F., Kerr, A.G., 1978. Ganglion cell populations in normal and pathological human cochleae. Implications for cochlear implantation. The Laryngoscope 88, 1231-1246.

Ouji, Y., Ishizaka, S., Nakamura-Uchiyama, F., Wanaka, A., Yoshikawa, M., 2013. Induction of inner ear hair cell-like cells from Math1-transfected mouse ES cells. Cell death & disease 4, e700.

Ovchinnikov, D.A., Hidalgo, A., Yang, S.K., Zhang, X., Hudson, J.E., Mazzone, S.B., Chen, C., Cooper-White, J.J., Wolvetang, E.J., 2014. Isolation of the contractile cardiomyocytes from human pluripotent stem cell-derived cardiomyogenic cultures with a human NCX1-EGFP reporter. Stem cells and development.

Paige, S.L., Osugi, T., Afanasiev, O.K., Pabon, L., Reinecke, H., Murry, C.E., 2010. Endogenous Wnt/beta-catenin signaling is required for cardiac differentiation in human embryonic stem cells. PloS one 5, e11134.

Park, B.Y., Saint-Jeannet, J.P., 2008. Hindbrain-derived Wnt and Fgf signals cooperate to specify the otic placode in Xenopus. Developmental biology 324, 108-121.

Patel, A., Groppo, E., 2010. Management of temporal bone trauma. Craniomaxillofacial trauma & reconstruction 3, 105-113.

Phillips, B.T., Storch, E.M., Lekven, A.C., Riley, B.B., 2004. A direct role for Fgf but not Wnt in otic placode induction. Development 131, 923-931.

Pirvola, U., Arumae, U., Moshnyakov, M., Palgi, J., Saarma, M., Ylikoski, J., 1994. Coordinated expression and function of neurotrophins and their receptors in the rat inner ear during target innervation. Hearing research 75, 131-144.

Pirvola, U., Ylikoski, J., Palgi, J., Lehtonen, E., Arumae, U., Saarma, M., 1992. Brain-derived neurotrophic factor and neurotrophin 3 mRNAs in the peripheral target fields of developing inner ear ganglia. Proceedings of the National Academy of Sciences of the United States of America 89, 9915-9919.

Plank, J.L., Dean, A., 2014. Enhancer Function: Mechanistic and Genome-Wide Insights Come Together. Molecular cell 55, 5-14.

Praetorius, M., Baker, K., Weich, C.M., Plinkert, P.K., Staecker, H., 2003. Hearing preservation after inner ear gene therapy: the effect of vector and surgical approach. ORL; journal for oto-rhino-laryngology and its related specialties 65, 211-214.

Quinlan, G.A., Williams, E.A., Tan, S.S., Tam, P.P., 1995. Neuroectodermal fate of epiblast cells in the distal region of the mouse egg cylinder: implication for body plan organization during early embryogenesis. Development 121, 87-98.

Reiners, J., Nagel-Wolfrum, K., Jurgens, K., Marker, T., Wolfrum, U., 2006. Molecular basis of human Usher syndrome: deciphering the meshes of the Usher protein network provides insights into the pathomechanisms of the Usher disease. Experimental eye research 83, 97-119.

Reubinoff, B.E., Itsykson, P., Turetsky, T., Pera, M.F., Reinhartz, E., Itzik, A., Ben-Hur, T., 2001. Neural progenitors from human embryonic stem cells. Nature biotechnology 19, 1134-1140.

Rogers, C.D., Moody, S.A., Casey, E.S., 2009. Neural induction and factors that stabilize a neural fate. Birth defects research. Part C, Embryo today : reviews 87, 249-262.

Ronaghi, M., Nasr, M., Ealy, M., Durruthy-Durruthy, R., Waldhaus, J., Diaz, G.H., Joubert, L.M., Oshima, K., Heller, S., 2014. Inner ear hair cell-like cells from human embryonic stem cells. Stem cells and development 23, 1275-1284.

Ross, P.C., Hui, S.W., 1999. Lipoplex size is a major determinant of in vitro lipofection efficiency. Gene therapy 6, 651-659.

Rowland, T.J., Blaschke, A.J., Buchholz, D.E., Hikita, S.T., Johnson, L.V., Clegg, D.O., 2013. Differentiation of human pluripotent stem cells to retinal pigmented epithelium in defined conditions using purified extracellular matrix proteins. Journal of tissue engineering and regenerative medicine 7, 642-653.

Sala-Rabanal, M., Kucheryavykh, L.Y., Skatchkov, S.N., Eaton, M.J., Nichols, C.G., 2010. Molecular mechanisms of EAST/SeSAME syndrome mutations in Kir4.1 (KCNJ10). The Journal of biological chemistry 285, 36040-36048.

Sandell, L.L., Butler Tjaden, N.E., Barlow, A.J., Trainor, P.A., 2014. Cochleovestibular nerve development is integrated with migratory neural crest cells. Developmental biology 385, 200-210.

Schlosser, G., Ahrens, K., 2004. Molecular anatomy of placode development in Xenopus laevis. Developmental biology 271, 439-466.

Schopperle, W.M., DeWolf, W.C., 2007. The TRA-1-60 and TRA-1-81 human pluripotent stem cell markers are expressed on podocalyxin in embryonal carcinoma. Stem cells 25, 723-730.

Scott, E.L., Brann, D.W., 2013. Estrogen regulation of Dkk1 and Wnt/beta-Catenin signaling in neurodegenerative disease. Brain research 1514, 63-74.

Sehgal, R., Karcavich, R., Carlson, S., Belecky-Adams, T.L., 2008. Ectopic Pax2 expression in chick ventral optic cup phenocopies loss of Pax2 expression. Developmental biology 319, 23-33.

Self, T., Mahony, M., Fleming, J., Walsh, J., Brown, S.D., Steel, K.P., 1998. Shaker-1 mutations reveal roles for myosin VIIA in both development and function of cochlear hair cells. Development 125, 557-566.

Sharma, A., Wu, J.C., Wu, S.M., 2013. Induced pluripotent stem cell-derived cardiomyocytes for cardiovascular disease modeling and drug screening. Stem cell research & therapy 4, 150.

Shi, F., Cheng, Y.F., Wang, X.L., Edge, A.S., 2010. Beta-catenin up-regulates Atoh1 expression in neural progenitor cells by interaction with an Atoh1 3' enhancer. The Journal of biological chemistry 285, 392-400.

Shi, F., Hu, L., Edge, A.S., 2013. Generation of hair cells in neonatal mice by beta-catenin overexpression in Lgr5-positive cochlear progenitors. Proceedings of the National Academy of Sciences of the United States of America 110, 13851-13856.

Shi, F., Hu, L., Jacques, B.E., Mulvaney, J.F., Dabdoub, A., Edge, A.S., 2014. beta-Catenin is required for hair-cell differentiation in the cochlea. The Journal of neuroscience : the official journal of the Society for Neuroscience 34, 6470-6479.

Shi, F., Kempfle, J.S., Edge, A.S., 2012. Wnt-responsive Lgr5-expressing stem cells are hair cell progenitors in the cochlea. The Journal of neuroscience : the official journal of the Society for Neuroscience 32, 9639-9648.

Singh, A.M., Hamazaki, T., Hankowski, K.E., Terada, N., 2007. A heterogeneous expression pattern for Nanog in embryonic stem cells. Stem cells 25, 2534-2542.

Sokol, S.Y., 2011. Maintaining embryonic stem cell pluripotency with Wnt signaling. Development 138, 4341-4350.

Stevens, C.B., Davies, A.L., Battista, S., Lewis, J.H., Fekete, D.M., 2003. Forced activation of Wnt signaling alters morphogenesis and sensory organ identity in the chicken inner ear. Developmental biology 261, 149-164.

Steventon, B., Mayor, R., 2012. Early neural crest induction requires an initial inhibition of Wnt signals. Developmental biology 365, 196-207.

Stewart, M.H., Bosse, M., Chadwick, K., Menendez, P., Bendall, S.C., Bhatia, M., 2006. Clonal isolation of hESCs reveals heterogeneity within the pluripotent stem cell compartment. Nature methods 3, 807-815.

Streit, A., 2002. Extensive cell movements accompany formation of the otic placode. Developmental biology 249, 237-254.

Streit, A., 2007. The preplacodal region: an ectodermal domain with multipotential progenitors that contribute to sense organs and cranial sensory ganglia. The International journal of developmental biology 51, 447-461.

Sun, S.K., Dee, C.T., Tripathi, V.B., Rengifo, A., Hirst, C.S., Scotting, P.J., 2007. Epibranchial and otic placodes are induced by a common Fgf signal, but their subsequent development is independent. Developmental biology 303, 675-686.

Suzuki, M., Ushio, M., Yamasoba, T., 2008. Time course of apoptotic cell death in guinea pig cochlea following intratympanic gentamicin application. Acta oto-laryngologica 128, 724-731.

Szebenyi, K., Pentek, A., Erdei, Z., Varady, G., Orban, T.I., Sarkadi, B., Apati, A., 2014. Efficient Generation of Human Embryonic Stem Cell-Derived Cardiac Progenitors Based on Tissue-Specific EGFP Expression. Tissue engineering. Part C, Methods.

Takada, Y., Beyer, L.A., Swiderski, D.L., O'Neal, A.L., Prieskorn, D.M., Shivatzki, S., Avraham, K.B., Raphael, Y., 2014. Connexin 26 null mice exhibit spiral ganglion degeneration that can be blocked by BDNF gene therapy. Hearing research 309, 124-135.

Takahashi, K., Tanabe, K., Ohnuki, M., Narita, M., Ichisaka, T., Tomoda, K., Yamanaka, S., 2007. Induction of pluripotent stem cells from adult human fibroblasts by defined factors. Cell 131, 861-872.

Tam, P.P., Parameswaran, M., Kinder, S.J., Weinberger, R.P., 1997. The allocation of epiblast cells to the embryonic heart and other mesodermal lineages: the role of ingression and tissue movement during gastrulation. Development 124, 1631-1642.

Tamai, K., Semenov, M., Kato, Y., Spokony, R., Liu, C., Katsuyama, Y., Hess, F., Saint-Jeannet, J.P., He, X., 2000. LDL-receptor-related proteins in Wnt signal transduction. Nature 407, 530-535.

ten Berge, D., Koole, W., Fuerer, C., Fish, M., Eroglu, E., Nusse, R., 2008. Wnt signaling mediates self-organization and axis formation in embryoid bodies. Cell stem cell 3, 508-518.

Tesar, P.J., Chenoweth, J.G., Brook, F.A., Davies, T.J., Evans, E.P., Mack, D.L., Gardner, R.L., McKay, R.D., 2007. New cell lines from mouse epiblast share defining features with human embryonic stem cells. Nature 448, 196-199.

Thiede, B.R., Mann, Z.F., Chang, W., Ku, Y.C., Son, Y.K., Lovett, M., Kelley, M.W., Corwin, J.T., 2014. Retinoic acid signalling regulates the development of tonotopically patterned hair cells in the chicken cochlea. Nature communications 5, 3840.

Thompson, D.A., Feather, S., Stanescu, H.C., Freudenthal, B., Zdebik, A.A., Warth, R., Ognjanovic, M., Hulton, S.A., Wassmer, E., van't Hoff, W., Russell-Eggitt, I., Dobbie, A., Sheridan, E., Kleta, R., Bockenhauer, D., 2011. Altered electroretinograms in patients with KCNJ10 mutations and EAST syndrome. The Journal of physiology 589, 1681-1689.

Thomson, J.A., Itskovitz-Eldor, J., Shapiro, S.S., Waknitz, M.A., Swiergiel, J.J., Marshall, V.S., Jones, J.M., 1998. Embryonic stem cell lines derived from human blastocysts. Science 282, 1145-1147.

Torres, M., Gomez-Pardo, E., Gruss, P., 1996. Pax2 contributes to inner ear patterning and optic nerve trajectory. Development 122, 3381-3391.

Torres-Padilla, M.E., Chambers, I., 2014. Transcription factor heterogeneity in pluripotent stem cells: a stochastic advantage. Development 141, 2173-2181.

Trounson, A., Thakar, R.G., Lomax, G., Gibbons, D., 2011. Clinical trials for stem cell therapies. BMC medicine 9, 52.

Tsakiridis, A., Huang, Y., Blin, G., Skylaki, S., Wymeersch, F., Osorno, R., Economou, C., Karagianni, E., Zhao, S., Lowell, S., Wilson, V., 2014. Distinct Wnt-driven primitive streak-like populations reflect in vivo lineage precursors. Development 141, 1209-1221.

Tseng, A.S., Engel, F.B., Keating, M.T., 2006. The GSK-3 inhibitor BIO promotes proliferation in mammalian cardiomyocytes. Chemistry & biology 13, 957-963.

Turner, D.A., Rue, P., Mackenzie, J.P., Davies, E., Arias, A., 2014. Brachyury cooperates with Wnt/ss-Catenin signalling to elicit Primitive Streak like behaviour in differentiating mouse ES cells. BMC biology 12, 63.

Uchikawa, M., Ishida, Y., Takemoto, T., Kamachi, Y., Kondoh, H., 2003. Functional analysis of chicken Sox2 enhancers highlights an array of diverse regulatory elements that are conserved in mammals. Developmental cell 4, 509-519.

Ueno, S., Weidinger, G., Osugi, T., Kohn, A.D., Golob, J.L., Pabon, L., Reinecke, H., Moon, R.T., Murry, C.E., 2007. Biphasic role for Wnt/beta-catenin signaling in cardiac specification in zebrafish and embryonic stem cells. Proceedings of the National Academy of Sciences of the United States of America 104, 9685-9690.

Urness, L.D., Paxton, C.N., Wang, X., Schoenwolf, G.C., Mansour, S.L., 2010. FGF signaling regulates otic placode induction and refinement by controlling both ectodermal target genes and hindbrain Wnt8a. Developmental biology 340, 595-604.

Vallier, L., Touboul, T., Chng, Z., Brimpari, M., Hannan, N., Millan, E., Smithers, L.E., Trotter, M., Rugg-Gunn, P., Weber, A., Pedersen, R.A., 2009. Early cell fate

decisions of human embryonic stem cells and mouse epiblast stem cells are controlled by the same signalling pathways. PloS one 4, e6082.

Vendrell, V., Vazquez-Echeverria, C., Lopez-Hernandez, I., Alonso, B.D., Martinez, S., Pujades, C., Schimmang, T., 2013. Roles of Wnt8a during formation and patterning of the mouse inner ear. Mechanisms of development 130, 160-168.

Verani, R., Cappuccio, I., Spinsanti, P., Gradini, R., Caruso, A., Magnotti, M.C., Motolese, M., Nicoletti, F., Melchiorri, D., 2007. Expression of the Wnt inhibitor Dickkopf-1 is required for the induction of neural markers in mouse embryonic stem cells differentiating in response to retinoic acid. Journal of neurochemistry 100, 242-250.

Waldhaus, J., Cimerman, J., Gohlke, H., Ehrich, M., Muller, M., Lowenheim, H., 2012. Stemness of the organ of Corti relates to the epigenetic status of Sox2 enhancers. PloS one 7, e36066.

Wan, G., Corfas, G., Stone, J.S., 2013. Inner ear supporting cells: rethinking the silent majority. Seminars in cell & developmental biology 24, 448-459.

Wang, Q., Fang, W.H., Krupinski, J., Kumar, S., Slevin, M., Kumar, P., 2008. Pax genes in embryogenesis and oncogenesis. Journal of cellular and molecular medicine 12, 2281-2294.

Webster, M., Webster, D.B., 1981. Spiral ganglion neuron loss following organ of Corti loss: a quantitative study. Brain research 212, 17-30.

Wei, C., Liu, J., Yu, Z., Zhang, B., Gao, G., Jiao, R., 2013. TALEN or Cas9 - rapid, efficient and specific choices for genome modifications. Journal of genetics and genomics = Yi chuan xue bao 40, 281-289.

Wheeler, E.F., Bothwell, M., Schecterson, L.C., von Bartheld, C.S., 1994. Expression of BDNF and NT-3 mRNA in hair cells of the organ of Corti: quantitative analysis in developing rats. Hearing research 73, 46-56.

White, P.M., Doetzlhofer, A., Lee, Y.S., Groves, A.K., Segil, N., 2006. Mammalian cochlear supporting cells can divide and trans-differentiate into hair cells. Nature 441, 984-987.

White, P.M., Stone, J.S., Groves, A.K., Segil, N., 2012. EGFR signaling is required for regenerative proliferation in the cochlea: conservation in birds and mammals. Developmental biology 363, 191-200.

Willems, E., Spiering, S., Davidovics, H., Lanier, M., Xia, Z., Dawson, M., Cashman, J., Mercola, M., 2011. Small-molecule inhibitors of the Wnt pathway potently promote cardiomyocytes from human embryonic stem cell-derived mesoderm. Circulation research 109, 360-364.

Williams, M., Burdsal, C., Periasamy, A., Lewandoski, M., Sutherland, A., 2012. Mouse primitive streak forms in situ by initiation of epithelial to mesenchymal transition without migration of a cell population. Developmental dynamics : an official publication of the American Association of Anatomists 241, 270-283.

Wise, A.K., Hume, C.R., Flynn, B.O., Jeelall, Y.S., Suhr, C.L., Sgro, B.E., O'Leary, S.J., Shepherd, R.K., Richardson, R.T., 2010. Effects of localized neurotrophin gene expression on spiral ganglion neuron resprouting in the deafened cochlea. Molecular therapy : the journal of the American Society of Gene Therapy 18, 1111-1122.

Wright, T.J., Mansour, S.L., 2003. Fgf3 and Fgf10 are required for mouse otic placode induction. Development 130, 3379-3390.

Xia, A., Gao, S.S., Yuan, T., Osborn, A., Bress, A., Pfister, M., Maricich, S.M., Pereira, F.A., Oghalai, J.S., 2010. Deficient forward transduction and enhanced reverse transduction in the alpha tectorin C1509G human hearing loss mutation. Disease models & mechanisms 3, 209-223.

Xiang, M., Gao, W.Q., Hasson, T., Shin, J.J., 1998. Requirement for Brn-3c in maturation and survival, but not in fate determination of inner ear hair cells. Development 125, 3935-3946.

Xue, H., Wu, J., Li, S., Rao, M.S., Liu, Y., 2014. Genetic Modification in Human Pluripotent Stem Cells by Homologous Recombination and CRISPR/Cas9 System. Methods in molecular biology.

Xue, H., Wu, S., Papadeas, S.T., Spusta, S., Swistowska, A.M., MacArthur, C.C., Mattson, M.P., Maragakis, N.J., Capecchi, M.R., Rao, M.S., Zeng, X., Liu, Y., 2009.

A targeted neuroglial reporter line generated by homologous recombination in human embryonic stem cells. Stem cells 27, 1836-1846.

Yamane, H., Nakai, Y., Takayama, M., Iguchi, H., Nakagawa, T., Kojima, A., 1995. Appearance of free radicals in the guinea pig inner ear after noise-induced acoustic trauma. European archives of oto-rhino-laryngology : official journal of the European Federation of Oto-Rhino-Laryngological Societies 252, 504-508.

Yamashita, D., Jiang, H.Y., Schacht, J., Miller, J.M., 2004. Delayed production of free radicals following noise exposure. Brain research 1019, 201-209.

Yang, L., Zhang, H., Hu, G., Wang, H., Abate-Shen, C., Shen, M.M., 1998. An early phase of embryonic Dlx5 expression defines the rostral boundary of the neural plate. The Journal of neuroscience : the official journal of the Society for Neuroscience 18, 8322-8330.

Yang, S.M., Chen, W., Guo, W.W., Jia, S., Sun, J.H., Liu, H.Z., Young, W.Y., He, D.Z., 2012. Regeneration of stereocilia of hair cells by forced Atoh1 expression in the adult mammalian cochlea. PloS one 7, e46355.

Ylikoski, J., Pirvola, U., Virkkala, J., Suvanto, P., Liang, X.Q., Magal, E., Altschuler, R., Miller, J.M., Saarma, M., 1998. Guinea pig auditory neurons are protected by glial cell line-derived growth factor from degeneration after noise trauma. Hearing research 124, 17-26.

Yu, Q., Wang, Y., Chang, Q., Wang, J., Gong, S., Li, H., Lin, X., 2014. Virally expressed connexin26 restores gap junction function in the cochlea of conditional Gjb2 knockout mice. Gene therapy 21, 71-80.

Zanin, M.P., Hellstrom, M., Shepherd, R.K., Harvey, A.R., Gillespie, L.N., 2014. Development of a cell-based treatment for long-term neurotrophin expression and spiral ganglion neuron survival. Neuroscience 277, 690-699.

Zhang, S.C., Wernig, M., Duncan, I.D., Brustle, O., Thomson, J.A., 2001. In vitro differentiation of transplantable neural precursors from human embryonic stem cells. Nature biotechnology 19, 1129-1133.

Zheng, W., Huang, L., Wei, Z.B., Silvius, D., Tang, B., Xu, P.X., 2003. The role of Six1 in mammalian auditory system development. Development 130, 3989-4000.

Zheng, Z., de Iongh, R.U., Rathjen, P.D., Rathjen, J., 2010. A requirement for FGF signalling in the formation of primitive streak-like intermediates from primitive ectoderm in culture. PloS one 5, e12555.

Zilberstein, Y., Liberman, M.C., Corfas, G., 2012. Inner hair cells are not required for survival of spiral ganglion neurons in the adult cochlea. The Journal of neuroscience : the official journal of the Society for Neuroscience 32, 405-410.

Zou, D., Silvius, D., Fritzsch, B., Xu, P.X., 2004. Eya1 and Six1 are essential for early steps of sensory neurogenesis in mammalian cranial placodes. Development 131, 5561-5572.